Re-Os geochronology and geochemistry of Proterozoic sedimentary successions

ALAN ROONEY

Re-Os geochronology and geochemistry of Proterozoic sedimentary successions

Alan David Rooney

A thesis submitted in partial fulfilment of the requirements for the degree of Doctor of Philosophy at Durham University

Department of Earth Sciences, Durham University

2011

“All I am trying to do is help you understand that “The Name of the Rose” is merely a blip on an otherwise uninterrupted downward trajectory.”

Abstract

The Re-Os organic-rich sedimentary rocks (ORS) geochronometer has the potential to provide precise depositional ages and vital information on the Os isotope composition of palaeo-seawater. This thesis presents new geochronology data from Proterozoic sedimentary successions and insights into Re-Os systematics of organic-rich sedimentary rocks and petroleum products such as bitumen and oil.

New Re-Os ORS geochronology from two drill cores indicate that the Proterozoic Atar Group of the Taoudeni basin, Mauritania is ~200 Ma older than previous estimates (1107 ± 12 Ma, 1109 ± 22 Ma and 1105 ± 37 Ma). Furthermore, this data also provides precise Re-Os geochronology data from sedimentary rocks that have experienced flash pyrolysis and demonstrate that the Re-Os systematics are not disturbed by the effects of very rapid heating. Coupled with palaeomagnetic data the Re-Os geochronology suggests that a reassessment of the role of the West African craton during the assembly of Rodinia is required.

New Re-Os geochronology for the Ballachulish Slate Formation of the Dalradian Supergroup, Scotland yields a depositional age of 659.6 ± 9.6 Ma. The Re-Os age represents a maximum age for the glaciogenic Port Askaig Formation and represents the first successful application of the Re-Os geochronometer in sedimentary rocks with low Re and Os abundances (<1 ppb and <50 ppt, respectively). This new age suggests that the Port Askaig Formation may be correlative with Sturtian glaciations rather than middle Cryogenian events.

Laboratory-based hydrous pyrolysis experiments were employed to evaluate the complexation of Re and Os in ORS and their transfer behaviour into petroleum. The findings from these experiments demonstrate that the Re-Os geochronometer is not disturbed by thermal maturation of whole rocks. Furthermore, the data support the hypothesis that the isotope composition of oils and bitumens can be used to fingerprint petroleum to specific source rocks.

Declaration

I declare that this thesis, which I submit for the degree of Doctor of Philosophy at Durham University, is my own work and not substantially the same as any which has previously been submitted at this or any other university.

Alan Rooney
Durham University
2011

Acknowledgements

My two supervisors, Dave Selby at Durham and Jean-Pierre Houzay at TOTAL, conceived the initial version of my project and have both helped to modify and improve the original concept. Jean-Pierre provided positive feedback and constructive criticism during the Mauritania work and his diplomatic liaison between TOTAL and me was hugely helpful.

Dave Selby has been a fantastic mentor during my time at Durham encouraging me to develop my own research projects in line with my interests and ambitions. Dave has been an unfailing source of first-class advice and encouragement.

My thanks to all those who have offered support and guidance since October 2007: Mike Lewan; Paul Lillis; Dave Chew; Paul Renne; Chris Ottley; Geoff Nowell; Rob Strachan Francoise Champion; Valerie Aout; Jean-Bernard Berrut; Kath Liddell, Augusta Warden and many others.

While at Durham I have benefited from formal and informal discussions with many of the postgraduates and staff. In particular, Chris Mallows, Jacqueline Malarkey, Jude Coggon, Rich Walker, Mark Ireland and Jim White were all happy to help with fieldwork, lab tasks or just someone normal who is interested in football. In the labs Chris Dale, Alex Finlay, Sarah Porter, Ali Rogers, Chris Lawley and Lisa Baldini cultivated a fun and friendly atmosphere that was always welcoming.

I also want to thank Viv for everything she's taught me and the unfailing support and encouragement she gave me. Finally, I'll mention Jane and Ellie who have been constant in their support and love and I'm very proud to have them as my family.

Contents

List of Figures ..... **viii**

Chapter One – Introduction **1**

1.1 Re-Os geochronology 1

1.2 Re-Os geochronology of organic-rich sedimentary rocks (ORS) 2

1.2.1 Hydrocarbon source rocks 5

1.2.2 Hydrocarbon deposits 5

1.2.3 Stratigraphic boundaries 6

1.2.4 Re-Os in Proterozoic sedimentary rocks 7

1.2.5 Re-Os geochronology and systematics 8

1.3 Rationale of this thesis 9

Chapter Two: Re-Os geochronology of the Atar Group, Mauritania 10

Chapter Three: Re-Os geochronology of the Dalradian Supergroup, Scotland 11

Chapter Four: Evaluation of the complexation location and behaviour of Re and Os in response to laboratory simulated hydrocarbon maturation 11

Chapter Five: Conclusions and future work 12

1.4 References 12

Chapter Two – Re-Os geochronology of the Atar Group, Mauritania **18**

2.1 Introduction 18

2.2 Geological setting 20

2.2.1 Geology of the West African Craton 20

2.2.2 Stratigraphy of the Taoudeni basin 20

2.2.3 Dolerite intrusion mineralogy and petrology 22

2.3 Analytical methodology 23

2.3.1 Sampling 23

2.3.2 TOC and T_{max} analysis 24

2.3.3 Re-Os analysis 24

2.3.4 $^{40}Ar/^{39}Ar$ plagioclase geochronology 26

2.4 Results 28

2.4.1 Total Organic Carbon and T_{max} results 28

2.4.2 Immature shale Re-Os geochronology 28

2.4.3 Overmature shale Re-Os geochronology 29
2.4.4 $^{40}Ar/^{39}Ar$ geochronology 29
2.5 Discussion 31
2.5.1 Previous geochronology and Rb-Sr systematics 31
2.5.2 TOC versus Re and Os abundance 32
2.5.3 Conditions of flash pyrolysis and non-disturbance of Re-Os systematics associated with flash pyrolysis 33
2.5.4 Implications for basin correlation, craton-craton correlation and Rodinia reconstructions 37
2.6 Conclusions 39
2.7 References 40
Chapter Three – Re-Os geochronology of the Ballachulish Slate Formation, Scotland .. 48
3.1 Introduction 48
3.2 Geological Setting 50
3.2.1 The Dalradian Supergroup 50
3.2.1.1 Dalradian glaciogenic horizons and possible global correlations 54
3.2.2 Current chronological constraints for the Dalradian Supergroup 54
3.2.3 Metamorphism and deformation of the Dalradian Supergroup 55
3.3 Samples for this study 56
3.3.1 Appin Group – Ballachulish Slate Formation 56
3.3.2 Southern Highland Group – Leny Limestone 57
3.4 Sampling and analytical methods 58
3.5 Results 59
3.5.1 Ballachulish Slate Formation samples 59
3.6 Discussion 62
3.6.1 Implications for low Re and Os abundance geochronology 62
3.6.2 Age of Ballachulish Slate Formation 63
3.6.3 Implications for global correlations involving the glacial Port Askaig Formation 65
3.6.4 Os isotopic composition of seawater at 660 Ma 67
3.6.5 Systematics of Re-Os in Leny Limestone Formation 68
3.7 Conclusions 69

3.8 References 71

Chapter 4 – Hydrous Pyrolysis experiments and Re-Os systematics 80

4.1 Introduction 80

4.2 Samples 81

4.2.1 Staffin Shale and Phosphoria Formation 81

4.3 Methodology 84

4.3.1 TOC and T_{max} analysis 86

4.3.2 Bitumen extraction 86

4.3.3 Hydrous pyrolysis experiments 86

4.3.4 Re-Os analysis 87

4.4 Results 89

4.4.1 Re-Os data of the Staffin Shale and Phosphoria Formations 89

4.5 Discussion 92

4.5.1 Complexation behaviour and location of Re and Os in ORS 92

4.5.2 Re and Os elemental abundance data of whole rock, kerogen and bitumen components as a function of hydrous pyrolysis temperature 93

4.5.3 Implications of Re and Os isotopic data of pyrolysed whole rock, kerogen and bitumen 98

4.6 Conclusions 102

4.7 References 104

Chapter 5: Conclusions and future research 107

5.1 Re-Os geochronology of the Atar Group, Mauritania 107

5.2 Re-Os geochronology of the Dalradian Supergroup, Scotland 109

5.3 Hydrous pyrolysis of organic-rich sedimentary rocks and insights into Re-Os systematics 111

5.4 References 113

List of Figures

Figure 2.1 Regional geological setting for the Taoudeni basin, West Africa 21
Figure 2.2 Generalised stratigraphy for Supergroups 1 and 2 of the Taoudeni basin..... 23
Figure 2.3a Re-Os isochron diagram for the Touirist Formation of the Atar Group from the S2 core..... 30
Figure 2.3b Re-Os isochron diagram for the En Nesoar Formation of the Atar Group from the S2 core..... 30
Figure 2.3c Re-Os isochron diagram for the Touirist Formation of the Atar Group from the S1 core..... 31
Figure 2.4 Ar-Ar age spectrum from plagioclase grains of dolerite sill 32
Figure 3.1 Simplified geological map for the Dalradian Supergroup highlighting the sample locations 51
Figure 3.2 Generalised stratigraphic column for the Dalradian Supergroup 53
Figure 3.3 Re-Os isochron for the Ballachulish Slate Formation 60
Figure 3.4 Re-Os isochron for the Leny Limestone Formation 62
Figure 3.5 Re-Os geochronology and Os_i data for Late Neoproterozoic glaciations 66
Figure 4.1 Re abundance and mass of bitumen against hydrous pyrolysis temperatures for the Staffin Shale Formation 94
Figure 4.2 Os abundance and mass of bitumen against hydrous pyrolysis temperatures for the Staffin Shale Formation 95
Figure 4.3 Re abundance and mass of bitumen against hydrous pyrolysis temperatures for the Phosphoria Formation 96
Figure 4.4 Os abundance and mass of bitumen against hydrous pyrolysis temperatures for the Phosphoria Formation 96
Figure 4.5 Re abundance against Os abundance for the Phosphoria Formation hydrous pyrolysis experiments 97
Figure 4.6 $^{187}Re/^{188}Os$ for the Phosphoria Formation plotted against hydrous pyrolysis experiment temperature..... 99
Figure 4.7 $^{187}Os/^{188}Os$ for the Phosphoria Formation plotted against hydrous pyrolysis experiment temperature.....100

Chapter One – Introduction

1.1 Re-Os geochronology

The development of the rhenium-osmium (Re-Os) geochronometer began in the 1950s and 1960s. This introduction will briefly describe the major developments in analytical techniques and our improved understanding of the half-life and decay constant of ^{187}Re (λ^{187}). Use of the Re-Os isotope system has driven major advancements in our understanding of Earth science systems. The Re-Os system has been successfully applied to cosmochemistry for determining crystallisation ages of early solar system asteroids and the formation of iron meteorites (Walker and Morgan, 1989; Morgan et al., 1990; Horan et al., 1992; Morgan et al., 1992; Shen et al., 1996; Smoliar et al., 1996). The Re-Os system has also played a critical role in dating and understanding sulphide ore genesis and related tectonic events, mantle evolution, crustal growth, diamond formation, oceanic osmium isotope composition and most recently, organic-rich sedimentary rocks and hydrocarbons (Herr et al., 1964; Luck and Allègre, 1982; Hertogen, 1980; Morgan, 1986; Walker et al., 1988, Walker et al., 1989; Herzberg, 1993; Pearson et al., 1995; Foster et al., 1996; Walker et al., 1994; Suzuki et al., 1996; Markey et al., 1998; Pearson et al., 1998; Raith and Stein, 2000; Ravizza and Turekian, 1989; Cohen et al., 1999; Creaser et al., 2002; Selby and Creaser, 2003; 2005a; Kendall et al., 2004; Selby et al., 2005, 2007b). As this thesis focuses on Re-Os geochronology and geochemistry of organic-rich sedimentary rocks (ORS) I will outline and discuss some of the landmark advances in this young but rapidly evolving field.

Early workers such as Herr et al. (1954) and Hirt et al. (1963) provided ^{187}Re half-life values of $5 \times 10^{10}y^{-1}$ and $4.3 \pm 0.5 \times 10^{10}y^{-1}$, respectively. These values were calculated from chemical measurements of rhenium and osmium present in molybdenite and are considerable improvements on the value of $3 \pm 1 \times 10^{12}y^{-1}$ gained from direct counting of Re decay (Naldrett and Libby, 1948). Work by Lindner et al. (1989) provided a half life of $4.23 \pm 0.13 \times 10^{10}y^{-1}$ which was considerably more accurate and precise than previous values. Uncertainties in the decay constant remained a limiting factor in Re-Os geochronology but a landmark study by Smoliar et al. (1996) on iron meteorites reported a decay constant of $1.666 \pm 0.0017 \times 10^{-11}y^{-1}$. Uncertainty in the decay constant is the

principal factor in limiting the accuracy of age determinations from radioactive isotope systems (Begemann et al., 2001). As a result, independent confirmation of the accuracy of the λ^{187} was urgently needed. A study by Selby et al. (2007a) combined Re-Os molybdenite geochronology from magmatic ore deposits with U-Pb zircon geochronology of the related magmatic bodies yielded a λ^{187} value that was identical to that reported by Smoliar et al. (1996). These experiments were repeated on ore systems spanning 2.7 Ga of the geological record. The result increased the confidence and reliability of data calculated using the λ^{187} value of $1.666 \pm 0.0017 \times 10^{-11} y^{-1}$.

One of the constant difficulties in Re-Os isotope analysis was the inability to precisely analyse low abundances (nanogram and sub-nanogram) of these elements. This issue stems from the high ionisation potential of these metals (8.7 eV) which cannot be overcome by conventional thermal ionisation mass-spectrometry (TIMS). The analysis of Re and Os via mass spectrometry developed sporadically with the earliest studies utilising electron bombardment mass spectrometry. Later studies used secondary ionization mass spectrometry (SIMS; Allègre and Luck, 1980), resonance ionization mass spectrometry (RIMS; Walker and Fassett, 1986), accelerated mass spectrometry (AMS; Fehn et al., 1986) and more recently, inductively coupled plasma mass spectrometry (ICPMS; Russ et al., 1987). A major advancement in Re-Os isotope analysis was the successful development of negative thermal ionisation mass spectrometry (NTIMS). The primary benefit of the NTIMS method results from coating the sample with $Ba(NO_3)_2$ which results in ionization efficiencies of up to 6% for Os and >20% for Re. The application of NTIMS for measuring Re and Os isotopes resulted in greatly improved sensitivity and ionization efficiency with analytical precisions better than ± 2‰ (2σ; Creaser et al., 1991; Völkening et al. 1991).

1.2 Re-Os geochronology of organic-rich sedimentary rocks (ORS)

As Re and Os are organophilic and redox-sensitive, Re-Os ORS geochronology has the potential to provide depositional ages and vital information on the Os isotope composition of palaeo-seawater (Ravizza et al., 1991; Ravizza & Turekian 1992; Colodner et al., 1993; Crusius et al., 1996; Selby & Creaser 2003; Kendall et al., 2004; 2009a,b; Selby et al., 2005, 2009). Under suboxic, anoxic or euxinic conditions Re is removed and enriched in sediments from pore waters near the sediment-water interface (≤1 cm; Colodner et al., 1993; Crusius et al., 1996; Morford et al., 2005). Reductive capture of Re from

$Re^{VII}O_4^-$ to Re^{IV} has been suggested as the primary mechanism for the removal of Re from pore waters (Colodner et al., 1993). For Os, reductive capture has been proposed for the removal of Os into sediments. However, the presence of osmium-bearing complexes in seawater suggests that Os may be incorporated into reducing sediments through an association with organic matter (Koide et al., 1991; Levasseur et al., 1998).

There are four main assumptions associated with the Re-Os ORS geochronometer including: 1) the Re and Os in ORS are hydrogenous in origin; 2) there is rapid immobilisation of Re and Os after deposition thus Re-Os dates reflect the age of deposition and not a younger diagenetic age; 3) all samples analysed have a consistent initial Os isotope composition (Os_i) derived from seawater at the time of deposition; and 4) the samples have remained a closed system with little or no post-depositional mobilisation of Re and Os (Kendall et al., 2004, 2009c).

The results of Re-Os ORS geochronology are presented in this thesis as isochrons and thus a short note detailing the rationale underlying decisions taken in terms of data regression and interpretations is required. The data are presented with 2σ uncertainties for error propagation of uncertainties in sample-weighing, spike calibration, blank abundances, isotope compositions and reproducibility of standard Re and Os isotope values. The Re-Os isotope data, 2σ calculated uncertainties for $^{187}Os/^{188}Os$ and $^{187}Re/^{188}Os$ ratios and the associated error correlation function (rho) are regressed to generate an isochron using *Isoplot V. 3.0* with the $\lambda\ ^{187}Re$ constant of $1.666 \times 10^{-11}\ a^{-1}$ with the intercept recording the initial osmium isotope composition at the time of deposition (Ludwig, 1980; Ravizza et al., 1989; Smoliar et al., 1996; Ludwig, 2003; Selby and Creaser, 2003). By incorporating these errors and uncertainties I have compensated for sources of analytical scatter and the data produced should only reflect any geological scatter. For the interpretation of these isochrons certain principles regarding the fit of data to the isochron line were adhered to. To be confident of generating a 'true' isochron representing meaningful data, the mean square of weighted deviates (MSWD) was required to be low (<3). Additionally, the *Isoplot V.3.0* program of Ludwig, (2003), was used to regress the Re-Os isotope data thus generating isochrons with varying degrees of assigned errors e.g., Model 1, 2 or 3. The Model 1 age represents a fit of the data to a line with the assigned analytical errors representing the *only* reason that the data-points scatter from a straight line. Model 2 ages are generated by assigning equal weights and zero error-correlations to each point. This avoids weighting the points according to analytical errors when it is clear that some other

cause of scatter is involved (cf. Model 1). A Model 3 age assumes that the scatter on the isochron is due to a combination of the assigned errors plus an unknown error e.g., geological error due to variations in initial isotope ratios (Ludwig, 2003).

The application of the ^{187}Re-^{187}Os geochronometer to ORS was pioneered by Ravizza and Turekian (1989) who provided a whole rock isochron age for a Devonian/Mississippian ORS. Despite the large uncertainty associated with this work, (ca. 14%) the age was indistinguishable from the accepted age of this timescale boundary. This work highlighted many of the benefits Re-Os geochronology can provide e.g., depositional ages of sedimentary successions and valuable information on the Os isotope composition of seawater throughout geological time. The study utilised the now obsolete nickel sulphide fire assay technique and measured the isotope ratios using an ion microprobe and plotted an isochron using a York regression (York, 1966). Despite the advances in Re-Os ORS geochronology over the past two decades, the work by Ravizza and Turekian (1989) is still considered to be one of the major advances in the geochronology of sedimentary rocks. Furthermore, this study provided the foundations for Earth scientists to further exploit and improve the accuracy and precision of Re-Os geochronology.

Following this initial study, work on Jurassic age ORS yielded depositional ages that were identical, within uncertainty, of the interpolated stratigraphic ages (Cohen et al., 1999). Additionally, this study provided valuable estimates of the initial $^{187}Os/^{188}Os$ ratios (Os_i) composition of the Jurassic oceans. These values for Os_i allow us to hypothesise about the extent of continental weathering and the rate and volume of hydrothermal and volcanic activity during the Jurassic. The work also highlighted the important advances in Re-Os chemistry e.g., the use of Carius tubes for digestion using *aqua-regia* at high temperatures (200 – 260 °C; Shirey and Walker, 1995). The Carius tube method also resolved issues such as digesting phases that were resistant to low temperature (<150 °C) alkaline or acid digestion and achieving complete spike equilibration (Walker, 1988; Birck et al., 1997; Shirey and Walker, 1998 and references therein). The work presented by Cohen et al. (1999) also benefited from a more accurate value for λ^{187} Re provided by Smoliar et al. (1996) and the improved analytical techniques such as NTIMS (Creaser et al., 1991; Völkening et al. 1991).

1.2.1 Hydrocarbon source rocks

Building on the initial studies using Re-Os geochronology for ORS, Creaser et al. (2002) focused on the Exshaw Formation, an important stratigraphic marker horizon and hydrocarbon source rock of the Western Canadian Sedimentary Basin. This work provided depositional ages that were within uncertainty of established ages for the Exshaw Formation. Furthermore, there was no significant variation in the depositional ages gained from immature, mature or overmature hydrocarbon source rocks. As a result, Creaser et al. (2002) were able to demonstrate that hydrocarbon maturation and migration does not adversely affect the Re-Os systematics in ORS.

Additional work on the Exshaw Formation detailed the utilisation of CrO_3-H_2SO_4 for the digestion of ORS for Re-Os geochronology (Selby and Creaser, 2003). This technique has the benefit of incorporating predominantly hydrogenous rhenium and osmium. Previous work had shown that ORS contained non-hydrogenous Re and Os components and that the detrital components are responsible for much of the geological scatter about the line of an isochron (Ravizza et al., 1991; Ravizza and Esser, 1993; Cohen et al., 1999; Peucker-Ehrenbrink and Hannigen, 2000; Creaser et al., 2002). A further benefit of this study is the ability to gain much more accurate data on the osmium isotope composition of seawater during the deposition of the respective ORS.

1.2.2 Hydrocarbon deposits

A study by Selby and Creaser (2005a) provided accurate age data for the timing of hydrocarbon generation and vital information on the migration of hydrocarbon deposits in the Western Canadian Sedimentary Basin. The data provided an age of deposition and an Os isotope ratio or 'geological fingerprint' that ruled out generation driven by orogenic events and instead indicated that the hydrocarbons were generated from an older source rock. This study illustrated that the Re-Os isotope system has great potential for elucidating many of the thermal processes involved in the shallow crust such as hydrocarbon generation and migration.

The possibility of dating hydrocarbon maturation and migration using the Re-Os geochronometer was further illustrated by dating bitumen from the Polaris Mississippi-Valley-type deposit, Canada (Selby et al., 2005). The Re-Os geochronology data indicates

that the migration of fluids associated with sulphide mineralisation was contemporaneous with those responsible for hydrocarbon generation and migration.

Work by Selby et al. (2007b) assessed the Re and Os isotope composition and abundance of 12 oils from worldwide petroleum reservoirs. The findings indicated that the majority (>80%) of Re and Os is located in the asphaltene fraction of the oil. Furthermore, the $^{187}Re/^{188}Os$ and $^{187}Os/^{188}Os$ ratios in asphaltenes at the time of generation are similar to those from the whole oil. The study illustrates the potential for the Re-Os isotope system to act as a tracer for hydrocarbons and a correlation tool between source rock and generated hydrocarbons.

1.2.3 Stratigraphic boundaries

Sedimentary horizons such as black shales frequently demarcate geological boundaries yet often lack horizons suitable for U-Pb or Ar-Ar geochronology. Work by Selby and Creaser (2005b) highlighted the potential for using the Re-Os geochronometer to resolve issues associated with calibration of the geological timescale. Their work on the Exshaw Formation that encompasses the Devonian-Mississippian boundary provided accurate and precise age data which are in excellent agreement with the interpolated age from U-Pb zircon geochronology (Trapp et al., 2004). The Re-Os geochronology data provide a direct date without the need for interpolation of tuff horizons above and below the stratigraphic boundary.

Work on the Oxfordian-Kimmeridgian boundary provided a Re-Os age that was ~45% more precise than the established age derived from correlation of ammonite zones and the M-sequence polarity scale (Selby, 2007). The use of Re-Os geochronology in sedimentary sequences has been shown to help in constraining the rates involved in geological processes, e.g., basin dynamics and, in this case, ammonite evolution. Additionally, the calculated Os_i can provide insights into rates of weathering and the types and ages of crustal material being weathered which is ultimately the source of hydrogenous Re and Os. The Os_i calculated for the Oxfordian-Kimmeridgian suggests that the upper crust being weathered was <0.5 Ga (Selby, 2007).

Work on the Aptian / Albian and Cenomanian / Turonian boundaries provided a new U-Pb zircon age for the Aptian / Albian boundary that calls into question the suitability of the GL-O glauconite standard for geochronology (Selby, 2009; Selby et al., 2009). The Re-Os data for the stage boundaries yield accurate, but imprecise isochron ages. The lack of

precision in the Re-Os age data can be attributed to the limited spread in $^{187}Re/^{188}Os$ ratios, but still yield ages that are identical, within uncertainty, to those of the Geological Time Scale 2008 (Ogg et al., 2008). Moreover, this study presents Os_i data that can be correlated with geological processes and events occurring during the Cretaceous such as increased volcanism associated with large igneous provinces and ocean anoxia events. Furthermore, when combined with geochemical data from previous studies, this work suggests that the redox chemistry of the ocean is not the primary controlling factor in Re and Os uptake in ORS (Selby et al. 2009). Instead, other factors such as sedimentation rate, recharge of Re and Os in the water column and post-depositional processes have a combined effect on the Re and Os abundances in ORS. This is in agreement with our understanding of the enrichment of other metals such as V and Ni in ORS (Lewan and Maynard, 1982; Crusius and Thomson, 2000; Turgeon, 2007; Kendall et al., 2009a).

1.2.4 Re-Os in Proterozoic sedimentary rocks

The use of the CrO_3-H_2SO_4 solution for sample digestion and improvements in the analytical capabilities of modern TIMS machines has enabled workers to provide absolute age data for ORS with uncertainties of <1% (2σ; Selby and Creaser, 2005b; Kendall et al., 2004, 2006, 2009b). Previous studies focused on ORS with total organic carbon (TOC) contents >10% due to an apparent association between Re and Os with TOC (Ravizza and Turekian, 1989; Cohen et al., 1999; Creaser et al., 2002). Work by Kendall et al. (2004) focused on low TOC (<1%) shales of the Old Fort Point Formation associated with the Marinoan glaciation. These shales had experienced chlorite-grade metamorphism and deformation as a result of Mesozoic orogenic events that affected the Western continental margin of North America. Kendall et al. (2004) presented a precise and accurate Proterozoic depositional age for this glacially related formation. The results from this study indicate that low TOC samples and low-grade metamorphism are not hindrances for Re-Os geochronology. Furthermore, this study provided accurate and precise age data of glacially-related strata that were previously correlated using relative techniques such as lithostratigraphy and chemostratigraphy.

With the evolution of the latest "Snowball Earth" theory there was a renewed interest in the Proterozoic Eon, in particular, the sedimentary and biogeochemical record. Work by Kendall et al. (2006) focused on the glacial horizons of the Sturtian glacial event of southern Australia. This study provided accurate and precise Re-Os age constraints that

strongly suggest the Sturtian 'glaciation' was actually a series of diachronous glaciations produced at uplifted margins during the 'zipper-rift' break up of Rodinia. Additional Re-Os geochronology on glacially-related strata from Australia yielded data that strongly suggest "Sturtian-type" diamictite-cap carbonates cannot be used as chronostratigraphic marker horizons (Kendall et al., 2009b).

The Lapa Formation of the Vazante Group, Brazil is a post-glacial deposit originally considered to be of Sturtian age (~ 700 Ma) based on Sr and C-isotope profiles (Azmy et al. 2001; 2006). Using Re-Os ORS geochronology, Azmy et al. (2008) presented an age of 1100 ± 77 Ma. This work provided the first evidence of Mesoproterozoic glacial horizons and implied that glaciations may have been common throughout the Proterozoic Eon and not restricted to the triumvirate of ages that encompassed the "Snowball Earth" period.

1.2.5 Re-Os geochronology and systematics

Coupled with Mo isotope data Re-Os geochronology can yield valuable information on changes in ocean redox chemistry over time. Work by Kendall et al. (2009b) reported accurate and precise Re-Os age data for Mesoproterozoic source rocks and associated biomarkers and acritarchs from the Roper Group, Australia. The Re-Os and Mo isotope data can be used to evaluate changes in redox chemistry of the Roper basin and due to its connection with the global ocean, changes in global ocean redox chemistry during the Mesoproterozoic. This study also documented post-depositional disturbance of the Re-Os isotope system as a result of Re and Os mobilisation caused by fluid flow. This fluid flow was attributed to the formation of a Pb-Zn-Ag SEDEX ore deposit ca. 1640 Ma (Southgate et al., 2000). The disturbance in Re-Os systematics was highlighted by a very inaccurate and imprecise age of 1359 ± 150 Ma and a highly radiogenic Os_i value of 3.5 ± 1.5.

A study focusing on carbonaceous slates of the Superior Province, Canada reported Re-Os data that provided the first temporal constraints on sedimentation ages of this Archean greenstone belt (Yang et al., 2009). The age data are consistent with our understanding of the tectonic deformation and mafic volcanism associated with this Archean terrane. However, this study can also be used to highlight some issues regarding sampling procedures, the relationship between Re and Os and the meaning of the Os_i value for ORS. The material used in this study was recovered from two separate drill cores. One of the drill cores reported a Model 3 age of 2684 ± 16 Ma and an MSWD of 3.8 but an Os_i

value of -0.29 ± 0.20. The negative Os_i value was reported to be a result of addition of Re derived from nearby mafic volcanic rocks and was considered to be evidence of resetting of the Re-Os isotope system. This reasoning is debatable as it requires that the amount of Re added to be *proportional* to the amount of Os in each sample to produce an isochron. A more likely explanation is that the small amount of sample used (<1 g) does not minimise the heterogeneities in Re and Os found within ORS. This explanation is further supported by Kendall et al. (2009c) who suggest that >20 g of powder must be sampled to ensure that these heterogeneities in ORS are minimised. Furthermore, the study by Yang et al. (2009) reported an isochron with a Model 1 age and an MSWD of 0.8 that was produced from 5 data points that included 3 samples which were in fact repeats. These 3 "samples" all had varying Re and Os abundances and thus varying $^{187}Re/^{188}Os$ and $^{187}Os/^{188}Os$ ratios as a result of improper sampling procedures.

1.3 Rationale of this thesis

The research undertaken for this thesis is presented in paper-format with three main research chapters representing work carried out and written as distinct papers. The research focuses on Re-Os geochronology with three separate studies providing the opportunity to evaluate how different geological events affect Re-Os systematics.

The Taoudeni basin of Mauritania is a vast intracratonic basin covering an area in excess of 1 M km^2. The sedimentary cover of the basin has very poor geochronological constraints in part, due to a lack of horizons suitable for traditional geochronology techniques such as U-Pb or fossils suitable for relative dating (cf. Deynoux et al., 2006). The lowermost Supergroups have been ascribed as Proterozoic based upon Rb-Sr dating of clays and illites (Clauer, 1981). The Taoudeni basin has become a focus for hydrocarbon exploration as a lack of traditional, 'easy' discoveries has forced oil companies to explore new areas and new geological settings. As a result, it is imperative that we improve our geochronological knowledge of the Taoudeni basin. Gaining new and precise geochronological data for the Taoudeni basin will provide data fundamental to our understanding of the geological history of this Proterozoic sedimentary succession. Additionally, the sedimentary succession of the Taoudeni basin has been affected by a number of igneous intrusions. Use of altered and unaltered ORS from the Taoudeni basin allow the evaluation of the affect of flash pyrolysis on Re-Os systematics.

The Dalradian Supergroup of Scotland represents ~25 km of Neoproterozoic sedimentary units that have experienced polyphase metamorphism and deformation (Harris et al., 1994). At present, our understanding of the Dalradian is limited by a lack of reliable geochronological data with only two units having reliable radiometric data (Halliday et al., 1989; Dempster et al., 2002). As a result, it is very challenging to understand the rates and durations of geological events recorded in this Neoproterozoic succession. Globally, the Dalradian is very important in our understanding of past climates and the rates of climatic change during the Proterozoic (Eyles, 1993; Hoffman et al., 1998; Arnaud and Eyles, 2006). Providing accurate and precise geochronology for the Dalradian Supergroup will greatly enhance our understanding of these sedimentary units as well as their relationship to other Proterozoic successions.

At present, we have a very limited understanding of how and where Re and Os are complexed in ORS. It has been demonstrated that source rocks, oils and heavy molecular weight fractions are enriched in Re and Os. From our understanding of the speciation and bonding of metals in oils it is highly probable that Re and Os in oils are transferred from the source rock as a result of hydrocarbon maturation. The research carried out as a part of this thesis utilises hydrous pyrolysis experiments to mimic natural hydrocarbon maturation processes. These experiments provide us with the opportunity to evaluate the behaviour and location of Re and Os through various stages of hydrocarbon maturation.

Chapter Two: Re-Os geochronology of the Atar Group, Mauritania

This chapter focuses on providing new Re-Os geochronology data for the Atar Group of the Taoudeni basin, Mauritania. This second chapter also presents data on the effect of flash pyrolysis on the Re-Os geochronometer. An additional aspect of this study is the use of Ar-Ar geochronology on plagioclase grains from a dolerite intrusion. All sample preparation, laboratory work, data collection and evaluation for the Re-Os geochronology study was carried out by the author. Professor Paul R. Renne carried out the Ar-Ar laboratory work, data collection and evaluation at the Berkeley Geochronology Center, USA. Determination of total organic carbon (TOC) contents and thermal maturity parameters was carried out at the TOTAL organic geochemistry laboratory, Pau, France under the supervision of Dr Jean-Pierre Houzay. The chapter was written by the author with Drs Selby and Houzay providing editorial comments and suggestions. A version of this

chapter has been published in Earth and Planetary Science Letters, **289,** 486 – 496, 2010, co-authored by David Selby of Durham University, Jean-Pierre Houzay of the Fluids and Geochemistry Department of TOTAL and Paul R. Renne of Berkeley Geochronological Center and the Department of Earth and Planetary Science, University of California, Berkeley, USA

Chapter Three: Re-Os geochronology of the Dalradian Supergroup, Scotland

This chapter details an attempt to provide Re-Os geochronology for the metasedimentary Ballachulish Subgroup of the Appin Group and the Leny Limestone of the Southern Highland Group from the Dalradian Supergroup. This research provides Re-Os geochronology from a Neoproterozoic metasedimentary unit that has experienced regional metamorphism as a result of the Caledonian Orogeny and contact metamorphism related to a large granite intrusion. Additionally, the results from the Leny Limestone study yield valuable insights into the mechanisms of disturbance of Re-Os systematics. Dr David Chew provided samples of the Ballachulish slate. All sample preparation, Re-Os analytical work, collection and evaluation of the Re-Os data was carried out by the author. This chapter was written by the author with Drs Selby and Chew providing editorial comments and suggestions. A version of this chapter has been submitted for publication to Precambrian Research, 2010, co-authored by Dr David Selby of Durham University and Dr David Chew of Trinity College, Dublin.

Chapter Four: Evaluation of the complexation location and behaviour of Re and Os in response to laboratory simulated hydrocarbon maturation

This chapter concentrates on evaluating the complexation location in ORS and understanding the transfer of Re and Os from ORS to hydrocarbons. This study utilises hydrous pyrolysis experiments to further understand the location of Re and Os in ORS and their behaviour in response to hydrocarbon maturation. This research provides data on the geochemistry of source rocks and organic fractions from immature, mature and overmature ORS. Furthermore, this research yields fundamental information on the Re and Os abundances and isotope composition of the source rocks and organic fractions. Dr Michael

D. Lewan oversaw the hydrous pyrolysis experiments and Soxhlet extractions at the US Geological Survey, Denver, USA. Determination of total organic carbon (TOC) contents, bitumen extraction and thermal maturity parameters was carried out at the TOTAL organic geochemistry laboratory, Pau, France under the supervision of Dr Jean-Pierre Houzay. All sample preparation, laboratory work, data collection and evaluation was carried out by the author. This chapter was written by the author with Drs Selby and Lewan providing editorial comments and suggestions. A version of this chapter will be submitted for publication to Geochimica et Cosmochimica Acta, 2010, co-authored by David Selby of Durham University, Michael D. Lewan and Paul G. Lillis of the US Geological Survey and Jean-Pierre Houzay of TOTAL.

Chapter Five: Conclusions and future work

The final chapter of this thesis provides an overview and summary of the work outlined in this thesis. Additionally, this chapter provides an insight into possible future work that builds on the findings of the research carried out for this thesis.

1.4 References

Allègre, C. L. and Luck, J. M., 1980. Osmium isotopes as petrogenetic and geological tracers. *Earth and Planetary Sciences Letters* **48**, 148-154.

Arnaud, E. and Eyles, C. H., 2006. Neoproterozoic environmental change recorded in the Port Askaig Formation, Scotland: Climatic vs. tectonic controls. *Sedimentary Geology* **183**, 99-124.

Azmy, K., Kaufman, A. J., Misi, A., and de Oliveira, T. F., 2006. Isotope stratigraphy of the Lapa Formation, Sao Francisco Basin, Brazil: Implications for Late Neoproterozoic glacial events in South America. *Precambrian Research* **149**, 231-248.

Azmy, K., Kendall, B., Creaser, R. A., Heaman, L., and de Oliveira, T. F., 2008. Global correlation of the Vazante Group, Sao Francisco Basin, Brazil: Re-Os and U-Pb radiometric age constraints. *Precambrian Research* **164**, 160-172.

Azmy, K., Veizer, J., Misi, A., de Oliveira, T. F., Sanches, A. L., and Dardenne, M. A., 2001. Dolomitization and isotope stratigraphy of the Vazante Formation, Sao Francisco Basin, Brazil. *Precambrian Research* **112**, 303-329.

Begemann, F., Ludwig, K. R., Lugmair, G. W., Min, K., Nyquist, L. E., Patchett, P. J., Renne, P. R., Shih, C.-Y., Villa, I. M., and Walker, R. J., 2001. Call for an improved set of decay constants for geochronological use. *Geochimica et Cosmochimica Acta* **65**, 111-121.

Birck, J. L., RoyBarman, M., and Capmas, F., 1997. Re-Os measurements at the femtomole level in natural samples. *Geostandards Newsletter* **20**, 19-27.

Clauer, N., 1981. Rb—Sr and K—Ar dating of Precambrian clays and glauconies. *Precambrian Research* **15**, 331-352

Cohen, A. S., Coe, A. L., Bartlett, J. M., and Hawkesworth, C. J., 1999. Precise Re-Os ages of organic-rich mudrocks and the Os isotope composition of Jurassic seawater. *Earth and Planetary Science Letters* **167**, 159-173.

Colodner, D., Sachs, J., Ravizza, G.,Turekian, K.K., Edmond, J., Boyle, E., 1993. The geochemical cycles of rhenium: a reconnaissance. *Earth and Planetary Science Letters* **117,** 205-221.

Creaser, R. A., Papanastassiou, D. A., and Wasserburg, G. J., 1991. Negative thermal ion mass spectrometry of osmium, rhenium and iridium. *Geochimica et Cosmochimica et Acta* **55**, 397-401.

Creaser, R. A., Sannigrahi, P., Chacko, T., and Selby, D., 2002. Further evaluation of the Re-Os geochronometer in organic-rich sedimentary rocks: A test of hydrocarbon maturation effects in the Exshaw Formation, Western Canada Sedimentary Basin. *Geochimica et Cosmochimica Acta* **66**, 3441-3452.

Crusius, J. and Thomson, J., 2000. Comparative behavior of authigenic Re, U, and Mo during reoxidation and subsequent long-term burial in marine sediments. *Geochimica et Cosmochimica* **64**, 2233-2242.

Dempster, T. J., Rogers, G., Tanner, P. W. G., Bluck, B. J., Muir, R. J., Redwood, S. D., Ireland, T. R., and Paterson, B. A., 2002. Timing of deposition, orogenesis and glaciation within the Dalradian rocks of Scotland: constraints from U-Pb zircon ages. *Journal of the Geological Society* **159**, 83-94.

Deynoux, M., Affaton, P., Trompette, R., and Villeneuve, M., 2006. Pan-African tectonic evolution and glacial events registered in Neoproterozoic to Cambrian cratonic and foreland basins of West Africa. *Journal of African Earth Sciences* **46**, 397-426.

Eyles, N., 1993. Earths Glacial Record and Its Tectonic Setting. *Earth-Science Reviews* **35**, 1-248.

Fehn, U., Teng, R., Elmore, D., and Kubik, P. W., 1986. Isotope Composition of Osmium in Terrestrial Samples Determined by Accelerator Mass-Spectrometry. *Nature* **323**, 707-710.

Foster, J. G., Lambert, D. D., Frick, L. R., and Maas, R., 1996. Re-Os isotope evidence for genesis of Archaean nickel ores from uncontaminated komatiites. *Nature* **382**, 703-706.

Halliday, A. N., Graham, C. M., Aftalion, M., and Dymoke, P., 1989. The Depositional Age of the Dalradian Supergroup - U-Pb and Sm-Nd Isotope Studies of the Tayvallich Volcanics, Scotland. *Journal of the Geological Society* **146**, 3-6.

Harris, A. L., Haselock, P.J., Kennedy, M.J., Mendum, J.R., Long, C.B., Winchester, J.A. and Tanner, P.W.G., 1994. The Dalradian Supergroup in Scotland and Ireland. In: Gibbons, W., and Harris, A.L. (Ed.), *A Revised correlation of Precambrian rocks in the British Isles*. Geological Society, London.

Herr, W., Hintenberger, H., and Voshage, H., 1954. Half-life of rhenium. *Physics Review* **95**, 1691.

Herr, W., Wolfle, R., Eberhardt, P., and Kopp, E., 1964. Development and recent applications of the Re/Os dating method. *Radioactive Dating and Methods of Low-Level Counting: International Atomic Energy Agency*, 499-508.

Hertogen, J., Janssens, M. J., and Palme, H., 1980. Trace-Elements in Ocean Ridge Basalt Glasses - Implications for Fractionations during Mantle Evolution and Petrogenesis. *Geochimica et Cosmochimica Acta* **44**, 2125-2143.

Herzberg, C. T., 1993. Lithosphere Peridotites of the Kaapvaal Craton. *Earth and Planetary Science Letters* **120**, 13-29.

Hirt, B., Tilton, G. R., Herr, W., and Hoffmeister, W., 1963. The half-life of ^{187}Re. In: Geiss, J. and Goldberg, E. Eds.), *Earth Science and Meteoritics*. North Holland, Amsterdam.

Hoffman, P. F., Kaufman, A. J., Halverson, G. P., and Schrag, D. P., 1998. A Neoproterozoic snowball earth. *Science* **281**, 1342-1346.

Horan, M. F., Morgan, J. W., Walker, R. J., and Grossman, J. N., 1992. Rhenium-Osmium Isotope Constraints on the Age of Iron-Meteorites. *Science* **255**, 1118-1121.

Kendall, B., Creaser, R. A., Calver, C. R., Raub, T. D., and Evans, D. A. D., 2009a. Correlation of Sturtian diamictite successions in southern Australia and northwestern Tasmania by Re-Os black shale geochronology and the ambiguity of "Sturtian"-type diamictite-cap carbonate pairs as chronostratigraphic marker horizons. *Precambrian Research* **172**, 301-310.

Kendall, B., Creaser, R. A., Gordon, G. W., and Anbar, A. D., 2009b. Re-Os and Mo isotope systematics of black shales from the Middle Proterozoic Velkerri and Wollogorang Formations, McArthur Basin, northern Australia. *Geochimica et Cosmochimica Acta* **73**, 2534-2558.

Kendall, B., Creaser, R. A., and Selby, D., 2009c. ^{187}Re-^{187}Os geochronology of Precambrian organic-rich sedimentary rocks. *Geological Society, London, Special Publications* **326**, 85-107.

Kendall, B., Creaser, R. A., and Selby, D., 2006. Re-Os geochronology of postglacial black shales in Australia: Constraints on the timing of "Sturtian" glaciation. *Geology* **34**, 729-732.

Kendall, B. S., Creaser, R. A., Ross, G. M., and Selby, D., 2004. Constraints on the timing of Marinoan 'Snowball Earth' glaciation by ^{187}Re – ^{187}Os dating of a Neoproterozoic post-glacial black shale in Western Canada. *Earth and Planetary Science Letters* **222**, 729-740.

Koide, M., Goldberg, E.D., Niemeyer, S., Gerlach, D., Hodge, V., Bertine, K.K., Padova, A., 1991. Osmium in marine sediments. *Geochimica et Cosmochimica Acta* **55,** 1641-1648.

Levasseur, S., Birck, J.-L., Allègre, C.J., 1998. Direct measurement of femtomoles of osmium and the ^{187}Os/^{186}Os ratio in seawater. *Science* **282,** 272-274.

Lewan, M. D. and Maynard, J. B., 1982. Factors controlling enrichment of vanadium and nickel in the bitumen of organic sedimentary rocks. *Geochimica et Cosmochimica Acta* **46**, 2547-2560.

Lindner, M., Leich, D. A., Russ, G. P., Bazan, J. M., and Borg, R. J., 1989. Direct determination of the half-life of ^{187}Re. *Geochimica et Cosmochimica Acta* **53**, 1597-1606.

Luck, J.M., and Allègre, C.J., 1982. The study of molybdenites through the ^{187}Re-^{187}Os chronometer. *Earth and Planetary Science Letters* **61,** 291-296.

Ludwig, K.R., 1980. Calculation of uncertainties of U-Pb isotope data. *Earth and Planetary Science Letters* **46,** 212-220.

Ludwig, K.R., 2003. Isoplot/Ex, Version 3: A Geochronological Toolkit for Microsoft Excel. Geochronology Center, Berkeley.

Markey, R., Stein, H., and Morgan, J., 1998. Highly precise Re-Os dating for molybdenite using alkaline fusion and NTIMS. *Talanta* **45**, 935-946.

Morford, J.L. and Emerson, S., 1999. The geochemistry of redox sensitive trace metals in sediments. Geochimica et Cosmochimica Acta **63,** 1735-1750.

Morgan, J. W., 1986. Ultramafic Xenoliths - Clues to Earths Late Accretionary History. *Journal of Geophysical Research-Solid Earth and Planets* **91**, 2375-2387.

Morgan, J. W., Walker, R. J., and Grossman, J. N., 1992. Rhenium-Osmium Isotope Systematics in Meteorites .1. Magmatic Iron Meteorite Group-Iiab and Group-Iiiab. *Earth and Planetary Science Letters* **108**, 191-202.

Naldrett, S. N. and Libby, W. F., 1948. Natural radioactivity of rhenium. *Physics Review* **73**, 487-493.

Noble, S. R., Hyslop, E. K., and Highton, A. J., 1996. High-precision U-Pb monazite geochronology of the c.806 Ma Grampian shear zone and the implications for the evolution of the central highlands of Scotland. *Journal of the Geological Society* **153**, 511-514.

Ogg, J. G., Ogg, G. and Gradstein, F.M., 2008. *The Concise Geologic Time Scale*. Cambridge University Press, Cambridge.

Pearson, D. G., Carlson, R. W., Shirey, S. B., Boyd, F. R., and Nixon, P. H., 1995. Stabilization of Archean Lithospheric Mantle - a Re-Os Isotope Study of Peridotite Xenoliths from the Kaapvaal Craton. *Earth and Planetary Science Letters* **134**, 341-357.

Pearson, D. G., Shirey, S. B., Harris, J. W., and Carlson, R. W., 1998. Sulphide inclusions in diamonds from the Koffiefontein kimberlite, S Africa: constraints on diamond ages and mantle Re-Os systematics. *Earth and Planetary Science Letters* **160**, 311-326.

Peucker-Ehrenbrink, B. and Hannigan, R. E., 2000. Effects of black shale weathering on the mobility of rhenium and platinum group elements. *Geology* **28**, 475-478.

Raith, J. G. and Stein, H. J., 2000. Re-Os dating and sulfur isotope composition of molybdenite from W-Mo deposits in western Namaqualand, South Africa: implications for ore genesis and low-P high-grade metamorphism. *Mineralium Deposita* **35**, 741-753.

Ravizza, G. and Turekian, K. K., 1989. Application of the ^{187}Re-^{187}Os system to black shale geochronometry. *Geochimica et Cosmochimica Acta* **53**, 3257-3262.

Ravizza, G. and Turekian, K.K., 1992. The Osmium isotopic composition of organic-rich marine sediments. *Earth and Planetary Science Letters* **110,** 1-6.

Ravizza, G. and Esser, B. K., 1993. A possible link between the seawater osmium isotope record and weathering of ancient sedimentary organic matter. *Chemical Geology* **107**, 255-258.

Ravizza, G., Turekian, G. G., and Hay, B. J., 1991. The geochemistry of rhenium and osmium in recent sediments from the Black Sea. *Geochimica et Cosmochimica Acta* **55**, 3741-3752.

Russ, G. P. and Bazan, J. M., 1987. Osmium Isotope Ratio Measurements by Inductively Coupled Plasma Source-Mass Spectrometry. *Analytical Chemistry* **59**, 984-989.

Selby, D., 2007. Direct Rhenium-Osmium age of the Oxfordian-Kimmeridgian boundary, Staffin bay, Isle of Skye, U.K., and the Late Jurassic time scale. *Norwegian Journal of Geology* **87**, 9.

Selby, D., Mutterlose, J., and Condon, D.J., 2009. U-Pb and Re-Os geochronology of the Aptian / Albian and Cenomanian / Turonian stage boundaries: Implications for timescale calibration, osmium isotope seawater composition and Re-Os systematics in organic-rich sediments. *Chemical Geology* **265,** 394-409.

Selby, D., 2009. U-Pb zircon geochronology of the Aptian/Albian boundary implies that the GL-O international glauconite standard is anomalously young. *Cretaceous Research* **30**, 1263-1267.

Selby, D. and Creaser, R. A., 2003. Re-Os geochronology of organic rich sediments: an evaluation of organic matter analysis methods. *Chemical Geology* **200**, 225-240.

Selby, D. and Creaser, R. A., 2005a. Direct radiometric dating of hydrocarbon deposits using rhenium-osmium isotopes. *Science* **308**, 1293-1295.

Selby, D. and Creaser, R. A., 2005b. Direct radiometric dating of the Devonian-Mississippian time-scale boundary using the Re-Os black shale geochronometer. *Geology* **33**, 545-548.

Selby, D., Creaser, R. A., Dewing, K., and Fowler, M., 2005. Evaluation of bitumen as a $Re-^{187}-Os-^{187}$ geochronometer for hydrocarbon maturation and migration: A test case from the Polaris MVT deposit, Canada. *Earth and Planetary Science Letters* **235**, 1-15.

Selby, D., Creaser, R. A., Stein, H. J., Markey, R. J., and Hannah, J. L., 2007a. Assessment of the $Re-^{187}$ decay constant by cross calibration of Re-Os molybdenite and U-Pb zircon chronometers in magmatic ore systems. *Geochimica et Cosmochimica Acta* **71**, 1999-2013.

Selby, D., Creaser, R. A., and Fowler, M. G., 2007b. Re-Os elemental and isotope systematics in crude oils. *Geochimica et Cosmochimica Acta* **71**, 378-386.

Shen, J. J., Papanastassiou, D. A., and Wasserburg, G. J., 1996. Precise Re-Os determinations and systematics of iron meteorites. *Geochimica et Cosmochimica Acta* **60**, 2887-2900.

Shirey, S. B. and Walker, R. J., 1995. Carius tube digestion for low-blank rhenium-osmium analysis. *Anal Chem* **67**, 2136-2141.

Shirey, S. B. and Walker, R. J., 1998. The Re-Os isotope system in cosmochemistry and high temperature geochemistry. *Annual Reviews Earth and Planetary Science Letters* **26**, 423-500.

Smoliar, M. I., Walker, R. J., and Morgan, J. W., 1996. Re-Os isotope constraints on the age of Group IIA, IIIA, IVA, and IVB iron meteorites. *Science* **271**, 1099-1102.

Southgate, P. N., Bradshaw, B.E., Domagala, J., Jackson, M.J., Idnurm, M., Krassay, A.A., Page, R.W., Sami, T.T., Scott, D.L., Lidsay, J.F., McConachie, B.A. and Tarlowski, C. 2000. Chronostratigraphic basin framework for Palaeoproterozoic rocks (1730-1575 Ma) in northern Australia and implications for base-metal mineralization. *Australian Journal of Earth Sciences* **47,** 461-483.

Suzuki, K., Shimizu, H., and Masuda, A., 1996. Re-Os dating of molybdenites from ore deposits in Japan: Implications for the closure temperature of the Re-Os system for molybdenite and the cooling history of molybdenum ore deposits. *Geochimica et Cosmochimica Acta* **60**, 3151-3159.

Trapp, E., Kaufmann, B., Mezger, K., Korn, M., and Weyer, D., 2004. Numerical calibration of the Devonian-Carboniferous boundary: Two new U-Pb isotope dilution-thermal ionization mass spectrometry single-zircon ages from Hasselbachtal (Sauerland, Germany). *Geology* **32**, 857-860.

Turgeon, S. C., Creaser, R. A., and Algeo, T. J., 2007. Re-Os depositional ages and seawater Os estimates for the Frasnian-Famennian boundary: Implications for weathering rates, land plant evolution, and extinction mechanisms. *Earth and Planetary Science Letters* **261**, 649-661.

Völkening, J., Walczyk, T., and G. Heumann, K., 1991. Osmium isotope ratio determinations by negative thermal ionization mass spectrometry. *International Journal of Mass Spectrometry and Ion Processes* **105**, 147-159.

Walker, R. J., 1988. Low-blank chemical separation of rhenium and osmium from gram quantities of silicate rock for measurement by resonance ionization mass spectrometry. *Anal Chem* **60**, 1231-1234.

Walker, R. J. and Fassett, J. D., 1986. Isotope measurement of subnanogram quantities of rhenium and osmium by resonance ionization mass spectrometry. *Anal Chem* **58**, 2923-2927.

Walker, R. J. and Morgan, J. W., 1989. Rhenium-Osmium Isotope Systematics of Carbonaceous Chondrites. *Science* **243**, 519-522.

Walker, R. J., Morgan, J. W., Horan, M. F., Czamanske, G. K., Krogstad, E. J., Fedorenko, V. A., and Kunilov, V. E., 1994. Re-Os Isotope Evidence for an Enriched-Mantle Source for the Norilsk-Type, Ore-Bearing Intrusions, Siberia. *Geochimica et Cosmochimica Acta* **58**, 4179-4197.

Yang, G., Hannah, J. L., Zimmerman, A., Stein, H. J., and Bekker, A., 2009. Re-Os depositional age for Archean carbonaceous slates from the southwestern Superior Province: Challenges and insights. *Earth and Planetary Science Letters* **280**, 83-92.

York, D., 1966. Least-Squares Fitting of a Straight Line. *Canadian Journal of Physics* **44**, 1079-1086.

Chapter Two – Re-Os geochronology of the Atar Group, Mauritania

Re-Os geochronology of a Mesoproterozoic sedimentary succession, Taoudeni basin, Mauritania: Implications for basin-wide correlations and Re-Os organic-rich sediment systematics*

*A version of this chapter has been published in Earth and Planetary Science Letters, **289,** 486 – 496, 2010, co-authored by David Selby of Durham University, Jean-Pierre Houzay of the Fluids and Geochemistry Department of TOTAL and Paul R. Renne of Berkeley Geochronological Center and the Department of Earth and Planetary Science, University of California, Berkeley, USA.

2.1 Introduction

Proterozoic successions record enormous portions of geological time and yet the sedimentary units are poorly constrained in terms of chronostratigraphy. Many of the sedimentary successions lack volcanic horizons which can be targeted for U–Pb or Ar-Ar geochronology and are bereft of fossils suitable for relative age dating. As a result, accurate and precise ages are difficult to determine for these successions and thus hamper regional and worldwide correlations.

For example, the Shaler Supergroup of North America is constrained by upper and lower ages of 723 + 4 / - 2 Ma and 1077 ± 4 Ma, respectively (Heaman et al., 1992; Rainbird et al., 1994). Other examples are the Bylot Supergroup of Canada, constrained by ages of 723 ± 3 Ma and 1267 ± 2 Ma (LeCheminant and Heaman, 1989; Heaman et al., 1990), and the Dalradian Supergroup of Scotland, which is constrained by a basal age of 806 ± 3 Ma and upper ages of 595 ± 4 Ma and 601 ± 4 Ma (Halliday et al., 1989; Noble et al., 1996; Dempster et al., 2002). The focus of this study is the Proterozoic sedimentary succession of the Taoudeni basin, NW Africa, a Proterozoic basin lacking accurate and precise geochronology (Fig. 2.1). Recently, in contrast with the existing Rb-Sr geochronology, it has been suggested that the sedimentary succession is much older than

previously thought based on $\delta^{13}C$ chemostratigraphy (Mesoproterozoic vs. Neoproterozoic; Teal and Kah, 2005).

The Taoudeni basin records a discontinuous sedimentation history from the Mesoproterozoic (this study) to the Mesozoic-Cenozoic (Fig. 2.1; Trompette, 1973; Bertrand-Sarfati and Moussine-Pouchkine, 1985, 1988; Ahmed Benan and Deynoux, 1998; Deynoux et al., 2006). At present, the geochronology of the lowermost Supergroup of the basin is constrained only by Rb-Sr illite and glauconite geochronology (Fig. 2.2; Clauer, 1976, 1981). The Rb-Sr data for the basal Char Group yields a Tonian age (850 – 1000 Ma; Ogg et al., 2008) of 998 ± 34 Ma (Clauer, 1981). Unconformably overlying the Char Group, the Atar Group was proposed to be Tonian to Cryogenian based on Rb-Sr illite and glauconite ages (890 ± 37 Ma to 775 ± 54 Ma) for stratigraphically successive formations (Fig. 2.2; Clauer, 1981). However, based on identification of a distinctive negative excursion, $\delta^{13}C$ chemostratigraphy strongly suggests a Mesoproterozoic age for the Atar Group (Teal and Kah, 2005). This excursion is marked by an abrupt decrease of 5‰ over ~25 m, which is followed by a stepwise increase to initial $\delta^{13}C$ values of ca. +3‰ (Kah et al., 1999; Kah and Bartley, 2004). This excursion is very similar to C-isotope signatures identified in Mesoproterozoic strata from Arctic Canada (Kah et al., 1999) and Siberia (Bartley et al., 2001), and is distinct from more muted excursions recorded in 1200 – 1300 Ma strata (Frank et al., 2003) or the more extreme excursions noted in Neoproterozoic strata (cf. Halverson et al., 2005).

Since the pioneering work of Ravizza and Turekian (1989), studies have demonstrated the successful application of the rhenium-osmium (Re-Os) chronometer for both Phanerozoic and Proterozoic sedimentary rocks with age determinations $\leq \pm 1\%$ (2σ; Selby and Creaser, 2005; Kendall et al., 2006; Kendall et al., 2009a). This precision is limited by uncertainty in the value of the ^{187}Re decay constant (~0.31%; Smoliar et al., 1996; Selby et al., 2007). The Re-Os system also provides valuable information on the Os isotope geochemistry of the oceans that is interpreted to reflect changes in continental weathering rates and interactions between weathering rates and atmospheric O_2 and CO_2 levels (Cohen et al., 1999; Ravizza and Peucker-Ehrenbrink, 2003; Cohen, 2004; Anbar et al., 2007; Finlay et al., 2010).

This study presents Re-Os geochronology data which provide precise depositional ages for organic-rich sediments (ORS) of the Atar Group of the Taoudeni basin, Mauritania. These ORS have elevated total organic carbon (TOC; 0.8% to 22.6%) levels in

comparison with 1.2% for average shale hydrocarbon source rocks as detailed by Hunt (1961; Table 2.1). The Re-Os ages strongly suggest that basin-wide correlation of the sedimentary succession is possible and provide valuable information for evaluating the evolution of the Taoudeni basin. As such, the Re-Os ORS geochronology produces a revised sedimentation history for the West African craton. Furthermore, the Re-Os ORS geochronology provides absolute ages for the recent chemostratigraphy studies (Kah and Bartley, 2004; Teal and Kah, 2005). In addition, this study provides a further understanding of Re-Os systematics in ORS which have experienced abrupt hydrocarbon maturation (flash pyrolysis) as a result of contact metamorphism by a Mesozoic dolerite sill.

2.2 Geological setting

2.2.1 Geology of the West African Craton

The West African craton records a protracted history of crustal evolution beginning with Mesoarchean basement, which was affected by the Eburnean orogeny ca. 2000 Ma. This Palaeoproterozoic orogeny is recorded to the north of the Taoudeni basin in the Reguibat Shield and to the south in the Leo Shield (Fig. 2.1; Schofield et al., 2006; Schofield and Gillespie, 2007). The craton has been considered stable with regard to magmatic and major tectonic events since ca. 1700 Ma with the exception of extensional tectonics and intrusions related to the opening of the North Atlantic during the Late Triassic (Clauer et al., 1982; Villeneuve and Cornée, 1994; Verati et al., 2005; this study). The Taoudeni basin evolved as a result of subsidence of the lower crust triggered by the dense ferruginous quartzite material associated with aluminous gneisses of the basement (Bronner et al., 1980). The duration between craton stabilisation and the onset of sedimentation of the Taoudeni basin is advocated to have been ~1 Ga (Deynoux et al., 2006 and references therein). This timing will be discussed further based on our new Re-Os ORS geochronology data.

2.2.2 Stratigraphy of the Taoudeni basin

The sedimentary succession of the Taoudeni basin comprises Proterozoic to Palaeozoic units with a thin cover of Mesozoic-Cenozoic units in the basin centre and large areas of Quaternary sand dunes (Fig. 2.1; Clauer et al., 1982; Bertrand-Sarfati and Moussine-Pouchkine, 1988; Ahmed Benan and Deynoux, 1998; Deynoux et al., 2006). The

structural evolution of the basin suggests normal faulting created accommodation zones (Bronner et al., 1980). These normal faults delineate horsts and grabens across the basin and associated synsedimentary breccias of the basal sedimentary unit can be traced for several tens of kilometres across the basin (Ahmed Benan and Deynoux, 1998). These large-scale features imply that sedimentary deposition onto the craton was initially controlled by tectonic instability (Bronner et al., 1980; Ahmed Benan and Deynoux, 1998).

Early work on the sedimentary succession of the Taoudeni basin focused on facies analyses and stratigraphic correlations on a basin-wide scale using marker horizons of tillites and stromatolite morphologies (Bertrand-Sarfati and Trompette, 1976; Deynoux et al., 1978; Bertrand-Sarfati and Moussine-Pouchkine, 1988; Ahmed-Benan and Deynoux, 1998).

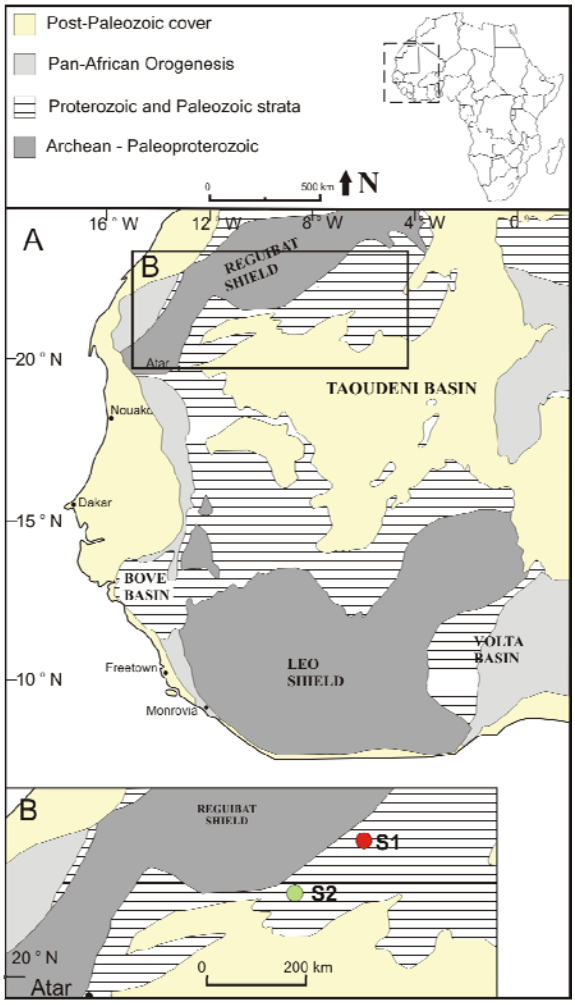

Fig. 2.1 (A) Regional geological setting for the Taoudeni basin, West Africa. (B) Inset map showing the location of drill cores S1 and S2. Modified from Deynoux et al. (2006).

The type section for the Taoudeni basin was described in the Adrar region of the Mauritanian section of the basin and in this area four Supergroups are recognized (Trompette, 1973; Deynoux et al., 2006). For practical reasons nomenclature proposed by Trompette (1973) is retained in a revised form for clarity where possible (Fig. 2.2). The first Supergroup was defined as Proterozoic based upon stromatolites that were classified as Riphean, the second; uppermost Proterozoic, the third; Upper Ordovician and Silurian and the fourth is of mainly Devonian sedimentary rocks (Trompette, 1973; Bertrand-Sarfati and Moussine-Pouchkine, 1988, Deynoux et al., 2006). This study presents Re-Os geochronology from Supergroup 1, specifically the Touirist and En Nesoar Formations of the Atar Group (Fig. 2.2).

2.2.2.1 Geology of Supergroup 1

The Atar group at ~800 m thick unconformably overlies the basal Char Group. The basin-wide unconformity between these two groups is of an unknown duration (Bronner et al., 1980; Ahmed Benan and Deynoux, 1998; Deynoux et al., 2006). The Atar Group consists of stromatolitic carbonates interbedded with siliciclastic units deposited in a marine setting (Bertrand-Sarfati and Moussine-Pouchkine, 1985). Analysis of the Atar Group shales by X-ray diffractometry reveals a mineral assemblage of, in order of decreasing abundance, quartz, kaolinite, illite, feldspar and minor amounts of pyrite/pyrrhotite (this study). This mineral assemblage suggests that the shales have not experienced regional metamorphism and based upon a cratonic geothermal gradient of 25 ^{o}C/km (Girard et al., 1989) and the stratigraphic thickness of the Atar Group (~800 m) were buried to a maximum depth of ~3 km, hence have been only subjected to post-depositional temperature of <100 ^{o}C.

Present age determinations of the Proterozoic sedimentary succession are constrained using Rb-Sr glauconite and illite geochronology (Clauer, 1976, 1981), which are discussed below.

2.2.3 Dolerite intrusion mineralogy and petrology

This study focuses on ORS retrieved from drill cores that penetrated the Atar Group in the Adrar region of the basin (Fig. 2.1b). One of the drill cores intersected ORS that had been intruded by a 30 m thick Mesozoic dolerite sill that is part of the Central Atlantic magmatic province associated with the initial stages of the opening of the Atlantic Ocean

(Verati et al., 2005). Fresh surfaces of the dolerite sill have a fine to medium grained texture and a homogenous mineralogy of plagioclase, clinopyroxene with minor amounts of quartz, biotite (~5%) and hornblende. The fine to medium grained texture of the sill in addition to the homogenous mineralogy is consistent with a shallow depth of emplacement (<1 km; Girard et al., 1989).

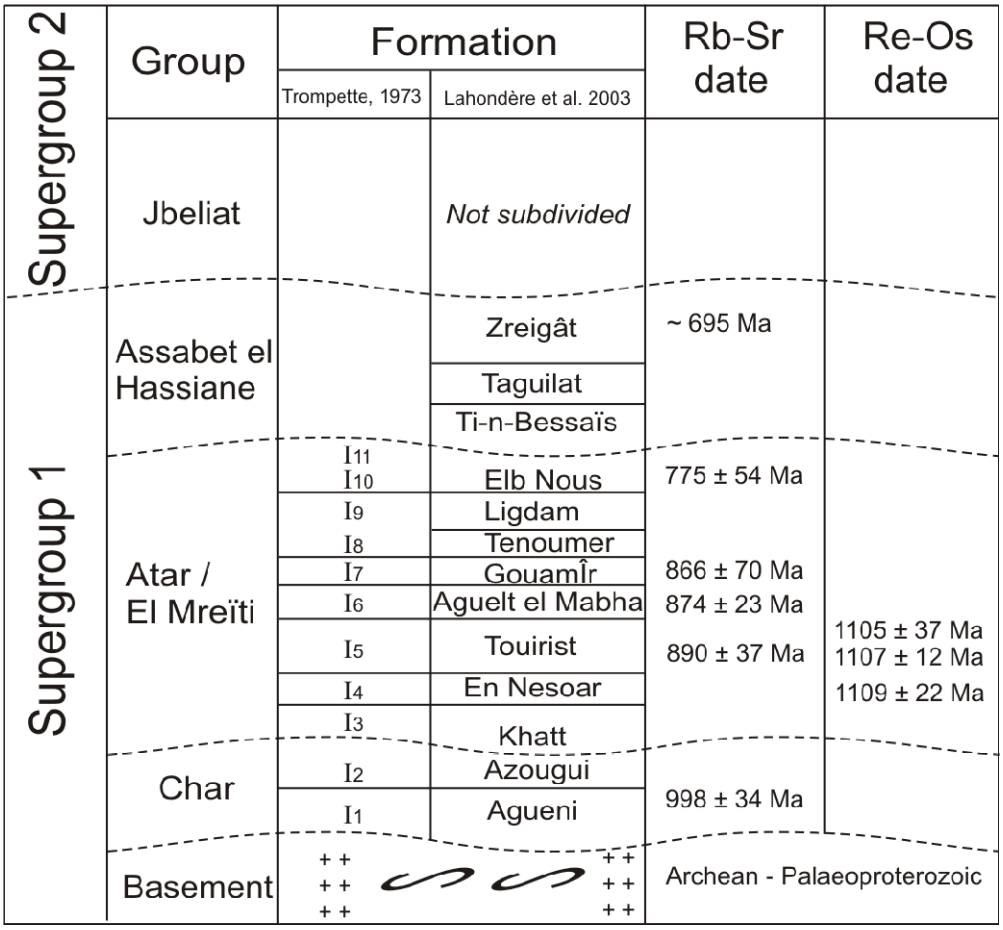

Fig. 2.2 Stratigraphy of Supergroups 1 and 2 of the Taoudeni basin. Rb-Sr geochronology data from Clauer (1981). Re-Os geochronology data (this study). Stratigraphic nomenclature after Trompette (1973) and Lahondère et al. (2003).

2.3 Analytical methodology

2.3.1 Sampling

Samples of ORS from the Atar Group were taken from two exploration wells (S1 and S2) drilled in 2004 by the petroleum company TOTAL (Fig. 2.1b). The drill cores are located; 23° 28' 60 N / 7° 52' 0 W and 22° 43'0 N / 9° 37' 0 W, respectively (Fig. 2.1b). The

Atar Group shales from these localities are massive (laminations are typically absent), non-fissile, organic-rich, black mudstones and are considered to have been deposited in a quiet marine environment representative of extensive flooding of the craton (Bertrand-Sarfati and Moussine-Pouchkine, 1988; Ahmed Benan and Deynoux, 1998; 2004; Kah et al., 2008).

Samples were collected from three intervals of the two drill cores; sample intervals were selected on the basis of TOC and T_{max} data determined at the TOTAL Geochemistry and Fluids Laboratory (Pau, France; Table 2.1). Samples were selected from the S1 core at depths between 73.15 and 89.50 m; for S2-A at depths between 139.45 and 143.82 m and S2-B, 206.70 to 207.60 m. The sampled intervals represent the Touirist and En Nesoar Formations (Fig. 2.2; Trompette, 1973; Lahondère et al., 2003). The dolerite sill, although assumed to be Mesozoic in age, was sampled for $^{40}Ar/^{39}Ar$ plagioclase geochronology.

2.3.2 TOC and T_{max} analysis

The TOC values are derived from combustion of powdered samples using a LECO 244 carbon analyser. Source rock maturity parameters are indicated by T_{max} data. The T_{max} data was generated using a VINCI Technologies Rock-Eval 6 Turbo at the TOTAL Geochemistry and Fluids Laboratory (Pau, France).

2.3.3 Re-Os analysis

Prior to crushing, all samples were polished to remove cutting and drilling marks to eliminate any contamination. The samples were dried at 60 °C for ~12 hrs and then crushed to a fine powder ~30 μm. The samples of ~100 g represent ~2 cm of stratigraphy and were broken into chips with no metal contact and powdered in a ceramic mill. Rhenium-Osmium isotope analysis was carried out at Durham University's TOTAL laboratory for source rock geochronology and geochemistry at the Northern Centre for Isotope and Elemental Tracing (NCIET) using Cr^{VI}-H_2SO_4 digestion and solvent extraction ($CHCl_3$), micro-distillation and anion chromatography methods and negative mass spectrometry as outlined by Selby and Creaser (2003), and Selby (2007). Total procedural blanks during this study were between 14.5 and 17.6 pg and 0.20 to 0.83 pg for Re and Os respectively, with an average $^{187}Os/^{188}Os$ ratio of ~0.19 ($n = 3$).

Uncertainties for $^{187}Re/^{188}Os$ and $^{187}Os/^{188}Os$ ratio are determined by error propagation of uncertainties in Re and Os mass spectrometer measurements, blank abundances and isotope compositions, spike calibrations and reproducibility of standard Re

and Os isotope values. The Re-Os isotope data, 2σ calculated uncertainties for $^{187}Re/^{188}Os$ and $^{187}Os/^{188}Os$ ratio and the associated error correlation function (rho) are regressed to yield a Re-Os date using *Isoplot V. 3.0* with the λ ^{187}Re constant of 1.666 x $10^{-11}a^{-1}$ (Ludwig, 1980; Smoliar et al., 1996; Ludwig, 2003).

Table 2.1 TOC and thermal maturity data for S1, S2-A and S2-B samples

Sample	Depth (m)	TOC % wt	T_{max} °C	S1	S2
S1 core Touirist Formation					
S1-14	73.15	7.75	517	0.15	0.32
S1-16	73.53	9.06	514	0.20	0.31
S1-18	73.70	8.84	512	0.19	0.30
S1-3	88.27	1.69	454	0.07	0.04
S1-6	88.74	2.81	304	0.13	0.10
S1-20	88.98	2.88	506	0.21	0.28
S1-22	89.33	3.69	503	0.21	0.47
S1-23	89.36	4.13	500	0.29	0.57
S1-25	89.50	0.84	522	0.10	0.02
S2-A Touirist Formation					
S2-7.2	139.45	16.48	435	10.12	114.26
S2-8	140.77	4.88	433	3.77	60.80
S2-10	141.08	8.34	431	14.57	152.36
S2-11	141.25	8.69	432	4.70	67.65
S2-12.2	141.65	22.56	437	1.79	34.21
S2-13	142.05	9.37	433	2.54	46.54
S2-15	142.90	7.41	436	3.02	53.78
S2-18	143.82	10.38	437	4.81	72.97
S2-B En Nesoar Formation					
S2-25	206.70	13.60	436	8.29	96.72
S2-26	206.80	6.49	436	2.96	46.19
S2-27	207.00	2.06	431	0.55	10.51
S2-29	207.20	7.25	436	2.90	51.47
23-30	207.40	2.46	435	0.71	14.28
S2-31	207.60	6.19	436	2.28	44.26

TOC = total organic carbon

T_{max} = temperature °C of the maximum formation of hydrocarbons by cracking of kerogen and has an uncertainty of ± 1 - 3 °C (Peters, 1986; Behar et al., 2001).

S1 = mg of hydrocarbons (free and thermovapourisable) per gram of rock.

S2 = mg of hydrocarbons (cracking of kerogen) per gram of rock (Peters, 1986).

To ensure and monitor long-term mass spectrometry reproducibility, in-house standard solutions of Re and Os (AB-2) are repeatedly analysed at NCIET. The Re standard analysed during the course of this study is made from 99.999% zone-refined Re ribbon and is considered to be identical to that of AB-1 (Creaser et al., 2002; Selby and Creaser, 2003; Kendall et al., 2004). The NCIET Re standard yields an average $^{185}Re/^{187}Re$ ratio of

0.597931 ± 0.00165 (1 SD, *n* = 94). This is in excellent agreement with the value reported for the AB-1 standard (Creaser et al., 2002). The Os standard (AB-2), made from ammonium hexachloro-osmate, yields an $^{187}Os/^{188}Os$ ratio of 0.10681 ± 0.00016 (1 SD, *n* = 89). The isotope compositions of these solutions are identical within uncertainty to that reported by Creaser et al. (2002) and Selby et al. (2009).

In addition to monitoring the AB-2 standard this paper details further use of the Durham Romil Osmium Standard (DROsS) for monitoring the mass spectrometry reproducibility of osmium isotope compositions. The DROsS values recorded during this study yield an $^{187}Os/^{188}Os$ ratio of 0.160965 ± 0.000337 (2 SD, *n* = 16), which is identical to the value of 0.160924 ± 0.000003 (2 SD, *n* = 21; Nowell et al., 2008).

2.3.4 $^{40}Ar/^{39}Ar$ plagioclase geochronology

The dolerite sill was sampled for $^{40}Ar/^{39}Ar$ analysis of plagioclase which was carried out at the Berkeley Geochronology Center. Approximately 500 g of dolerite was selected, broken into chips, powdered in a ceramic mill and sieved to grain size 210 – 74 μm, prior to magnetic separation using a Frantz isodynamic magnetic separator. The separated plagioclase grains were washed with MilliQ, rinsed in ethanol and dried overnight. The sample was then irradiated for 10 hours in the CLICIT facility of OSTR reactor along with Fish Canyon sanidine (FCs) as a neutron fluence monitor, for which an age of 28.02 Ma (Renne et al., 1998) was used for age calculations.

Approximately 30 mg of the plagioclase was analyzed by incremental heating in 31 steps with a CO_2 laser. The laser beam, of 1.1 to 30.0 W power, was directed through an integrator lens to homogenise sample temperature during heating. Heating steps were of 60 s duration, followed by 120 s of gettering and exposure to a –130 °C cold finger in the online extraction system. Mass spectrometry was performed with an MAP 215C sector mass spectrometer, by 10 cycles of peak-hopping by magnetic field switching with ion beams measured on a Balzers electron multiplier in analogue mode.

Table 2.2
Ar/Ar data and constants used in age calculations. All errors shown at 1σ

Sample: ARS1

Plagioclase grain from dolerite

Step	Laser	^{40}Ar	^{40}Ar	σ	^{39}Ar	σ	^{38}Ar	σ	^{37}Ar	σ	^{36}Ar	σ	$^{40}Ar^*/^{39}Ar_K$	σ	$\%^{40}Ar^*$	Age	σ
	(W)	(moles)	(nA)	(nA)	(nA)	(nA)	(nA)	(nA)	(nA)	(nA)	(nA)	(nA)				(Ma)	(Ma)
1	1.1	1.02E-14	0.078585	0.004412	0.000068	0.000061	0.000012	0.000012	-0.000086	0.000322	0.000016	0.000024	1078.1730	993.7075	93.87	2418.25	1227.55
2	1.4	3.27E-13	2.512140	0.005622	0.001068	0.000074	0.000220	0.000014	0.001167	0.000325	0.000818	0.000028	2127.1970	151.1847	90.38	3394.87	108.69
3	1.7	1.16E-12	8.921153	0.008955	0.010967	0.000125	0.000909	0.000021	0.013335	0.000376	0.003364	0.000039	723.5062	8.7938	88.87	1916.36	14.35
4	2.1	1.91E-12	14.699600	0.010560	0.042564	0.000286	0.002033	0.000027	0.062443	0.000881	0.007088	0.000031	296.5628	2.2553	85.78	1036.06	5.99
5	2.5	2.61E-12	20.063540	0.012781	0.077737	0.000425	0.002939	0.000031	0.142761	0.001097	0.009620	0.000054	221.9554	1.4318	85.89	826.01	4.28
6	3.0	2.89E-12	22.168400	0.015632	0.115452	0.000514	0.003677	0.000036	0.259464	0.000840	0.010829	0.000057	164.7308	0.9206	85.66	646.49	3.04
7	3.5	2.41E-12	18.503460	0.011847	0.131491	0.000190	0.003175	0.000029	0.387953	0.001098	0.007839	0.000049	123.5886	0.4144	87.65	505.42	1.48
8	3.8	1.23E-12	9.431605	0.009306	0.108954	0.000180	0.002189	0.000024	0.403379	0.001693	0.004169	0.000043	75.7427	0.2884	87.27	326.15	1.14
9	4.1	1.09E-12	8.408972	0.009749	0.098584	0.000306	0.001832	0.000023	0.422785	0.001147	0.003172	0.000029	76.3527	0.3437	89.25	328.55	1.35
10	4.4	7.42E-13	5.699587	0.012781	0.082095	0.000286	0.001420	0.000021	0.535892	0.001546	0.002444	0.000028	61.4194	0.3371	88.07	268.83	1.37
11	4.7	9.98E-13	7.665601	0.008099	0.097597	0.000316	0.001931	0.000027	0.530972	0.002147	0.003674	0.000041	68.1021	0.3368	86.38	295.80	1.35
12	5.0	9.66E-13	7.417711	0.008609	0.110280	0.000345	0.001759	0.000024	0.555941	0.002902	0.002314	0.000038	61.6734	0.2816	91.37	269.86	1.14
13	5.3	6.97E-13	5.350634	0.005215	0.093799	0.000218	0.001520	0.000024	0.530177	0.002300	0.001479	0.000034	53.0346	0.2157	92.61	234.40	0.89
14	5.6	8.13E-13	6.244852	0.007603	0.095757	0.000336	0.001524	0.000023	0.517144	0.002153	0.001616	0.000034	60.8806	0.2933	93.00	266.63	1.19
15	6.0	8.61E-13	6.609564	0.008016	0.113797	0.000228	0.001774	0.000025	0.580919	0.002456	0.001752	0.000036	54.1247	0.2054	92.86	238.92	0.85
16	6.5	9.72E-13	7.461964	0.008016	0.131862	0.000454	0.002060	0.000026	0.651150	0.002760	0.001943	0.000037	52.8026	0.2469	92.99	233.44	1.02
17	7.0	1.28E-12	9.839222	0.008353	0.164060	0.000415	0.002572	0.000023	0.790170	0.002314	0.002781	0.000035	55.5276	0.2120	92.28	244.71	0.87
18	7.5	1.76E-12	13.501710	0.010560	0.193683	0.000554	0.003171	0.000034	0.876331	0.002619	0.003832	0.000044	64.4200	0.2592	92.12	280.99	1.05
19	8.0	1.88E-12	14.473460	0.010651	0.232341	0.000773	0.003626	0.000032	0.985888	0.002772	0.003591	0.000042	58.2299	0.2505	93.20	255.81	1.03
20	9.0	3.16E-12	24.240210	0.012781	0.361598	0.000883	0.005611	0.000036	1.309444	0.003539	0.005921	0.000052	62.6385	0.2204	93.21	273.78	0.89
21	10.0	3.57E-12	27.440250	0.016594	0.432755	0.001103	0.006644	0.000038	1.494915	0.003694	0.006967	0.000049	59.0624	0.2131	92.92	259.22	0.87
22	11.0	3.20E-12	24.594250	0.015632	0.379569	0.001003	0.005914	0.000037	1.402438	0.004155	0.005706	0.000048	60.7981	0.2224	93.59	266.30	0.91
23	12.0	1.88E-12	14.418190	0.009749	0.215687	0.000763	0.003266	0.000031	1.000378	0.002784	0.003392	0.000044	62.7655	0.2797	93.59	274.29	1.13
24	14.0	2.83E-12	21.700280	0.012781	0.351197	0.000534	0.005427	0.000033	1.484613	0.004010	0.005372	0.000049	57.7697	0.1698	93.22	253.92	0.70
25	16.0	3.49E-12	26.768640	0.015632	0.421325	0.002303	0.006544	0.000080	1.849564	0.007854	0.006683	0.000051	59.3712	0.3648	93.16	260.48	1.49
26	17.0	1.23E-12	9.420756	0.009130	0.152397	0.000494	0.002371	0.000033	0.827218	0.002335	0.002364	0.000037	57.8761	0.2530	93.27	254.36	1.04
27	18.0	1.06E-12	8.108996	0.008268	0.136963	0.000336	0.002101	0.000028	0.746256	0.002337	0.001862	0.000037	55.8267	0.2140	93.94	245.94	0.88
28	19.0	7.12E-13	5.464182	0.007280	0.088174	0.000190	0.001438	0.000021	0.632153	0.002338	0.001534	0.000033	57.6767	0.2336	92.61	253.54	0.96
29	22.0	5.50E-13	4.224959	0.006294	0.065692	0.000336	0.001070	0.000021	0.555193	0.001882	0.001378	0.000033	59.1262	0.3872	91.39	259.48	1.58
30	25.0	5.30E-13	4.068485	0.005111	0.068882	0.000152	0.001125	0.000020	0.594874	0.002343	0.001223	0.000032	54.8219	0.2397	92.26	241.80	0.99
31	30.0	7.30E-13	5.605570	0.007440	0.094755	0.000375	0.001410	0.000023	0.577798	0.002344	0.001335	0.000033	55.7097	0.2906	93.77	245.46	1.20

Integrated Age = 308.9 ± 1.1 Ma

Relative abundances of Ar isotopes in nA of amplified ion beam current. Ages are model ages assuming all non-radiogenic Ar has atmospheric isotopic composition.

Calculated using J-value, interfering isotope ratios and constants below.

All uncertainties are stated at one standard deviation. Age errors do not include uncertainty in 40K decay constants or age of the standard.

J	0.0026162 ± 7.50E-06
$(^{40}Ar/^{36}Ar)_{atm}$	295.5 ± 0.5
$(^{40}Ar/^{38}Ar)_{atm}$	1575 ± 2
$(^{38}Ar/^{37}Ar)_{Ca}$	0.0000196 ± 8.16E-7
$(^{38}Ar/^{39}Ar)_{K}$	0.012200 ± 0.000027
$P(^{36}Cl/^{38}Cl)$	262.8 ± 3
Decay Constants	
$l\ ^{40}K_{\lambda e}$	(5.81 ± 1.70E-12)E-11 a^{-1}
$l\ ^{40}K_{\lambda b}$	(4.962 ± 8.600E-12)E-10 a^{-1}
$l\ ^{37}Ar$	(5.4300 ± 0.0063)E-2 a^{-1}
$l\ ^{39}Ar$	(2.58 ± 0.03)E-3 $^{a-1}$
$l\ ^{36}Cl_{\lambda\beta}$	(2.35 ± 0.02)E-6 a^{-1}

Blanks comparable to those reported by Vogel and Renne (2008) were measured between every three unknowns and average values were used for corrections. Mass discrimination (1.00892 ± 0.00179 per atomic mass unit) based on a power law correction (Renne et al., 2009) was determined from multiple air pipettes interspersed with the analyses. Argon isotope data corrected for blank, mass discrimination and radioactive decay are shown in Table 2.2. Ages shown in Table 2.2 incorporate corrections for interfering reactor-produced Ar isotopes from Ca and K (Renne et al., 2005) and Cl (Renne et al., 2008), and are based on the decay constants and isotope abundances recommended by Steiger and Jäger (1977). Age uncertainties do not include contributions from the ^{40}K decay constants or the $^{40}Ar^*/^{40}K$ of the standard.

2.4 Results

2.4.1 Total Organic Carbon and T_{max} results

The TOC content for samples from the S1 core are between 0.8 to 9.1%, the S2-A samples range from 4.9 to 22.6% and the S2-B samples between 2.1 and 13.6% (Table 2.1). Rock-Eval 6 Turbo pyrolysis data for the S1 and S2 drill cores indicate that the shales of S2 are marginally mature (431 to 437 ^oC) with respect to thermal maturity and that the S1 drill core samples are overmature (454 – 522 ^oC; Table 2.1; Peters, 1986; Behar et al., 2001). The sample S1-6 contains <0.2 mg hydrocarbons per gram of rock, which results in Rock-Eval data giving an anomalously low T_{max} value (304 ^oC; Peters, 1986). The thermal maturity data for drill core S1 suggests that the shales are overmature as a result of flash pyrolysis associated with contact metamorphism with a large (>20 m diameter) dolerite intrusion.

2.4.2 Immature shale Re-Os geochronology

The Re-Os abundances and isotope compositions for the Atar Group samples S2-A and S2-B are presented in Table 2.3. All of the S2 samples are enriched in Re (14 - 146 ppb) and Os (0.29 – 2.9 ppb), particularly in comparison with the contents of modern-day average continental crust (~1 ppb Re and 30 – 50 ppt Os; Esser and Turekian, 1993; Peucker-Ehrenbrink and Jahn, 2001; Hattori et al., 2003; Sun et al., 2003). The $^{187}Re/^{188}Os$ ratios range from 595 to 1041 and are positively correlated with the $^{187}Os/^{188}Os$ ratios of 11.3 – 19.7 (Fig. 2.3a). Linear regression of the Re-Os isotope data for the S2-A depth

interval yield a Model 1 age of 1107 ± 12 Ma (2σ, *n* = 8, Mean Squared of Weighted Deviates [MSWD] of 1.13), with an initial $^{187}Os/^{188}Os$ ratio of 0.28 ± 0.13 (Fig. 2.3a). Linear regression of the Re-Os isotope data for the S2-B depth interval yield a Model 1 age of 1109 ± 22 Ma (2σ, *n* = 6, MSWD of 0.73), with an initial $^{187}Os/^{188}Os$ ratio of 0.31 ± 0.28 (Fig. 2.3b).

2.4.3 Overmature shale Re-Os geochronology

The Re-Os abundances and isotope compositions for the ORS of the S1 drill core are presented in Table 2.3. Similar to the ORS of S2, the S1 samples are significantly enriched in Re (37 – 198 ppb) and Os (0.79 – 3.7 ppb). The $^{187}Re/^{188}Os$ ratios range from 431 to 696 and are positively correlated with the $^{187}Os/^{188}Os$ ratios of 8.4 – 13.3. Linear regression of the Re-Os isotope data for the overmature S1 drill core shale samples yield a Model 3 age of 1105 ± 37 Ma (2σ, *n* = 9, MSWD of 8.8, with an initial $^{187}Os/^{188}Os$ ratio (hereafter Os_i) of 0.31 ± 0.34; Fig. 2.3c).

2.4.4 $^{40}Ar/^{39}Ar$ geochronology

The $^{40}Ar/^{39}Ar$ age spectrum (Fig. 2.4) for plagioclase from the dolerite sill is markedly discordant, with initial low temperature steps yielding Proterozoic apparent ages, giving way in the last 80% of ^{39}Ar released to apparent ages between 230 and 300 Ma. This pattern suggests that the plagioclase contained a significant component of "excess" ^{40}Ar, mainly residing in relatively low-retentivity sites, that was probably acquired during contact metamorphism of the ORS resulting from emplacement of the sill. As a result, the analysis yields a precise, but almost certainly meaningless integrated age of 308.9 ± 1.1 Ma. The data yield no statistically valid isochron, indicating that more than one trapped (i.e., non-radiogenic) component of Ar is present. These results lead us to conclude that the Ar retention age of the plagioclase, recording cooling below 200 – 350 °C (Cassata et al., 2009) depending on the cooling rate, is less than or equal to the youngest apparent step age (233 ± 1 Ma), which is inferred to contain the lowest proportion of excess ^{40}Ar. Thus, this maximum cooling age may reflect local cooling of the sill only rather than a regional basin cooling, due to the much older ages recorded by the Rb-Sr system in low-retentivity minerals as discussed below.

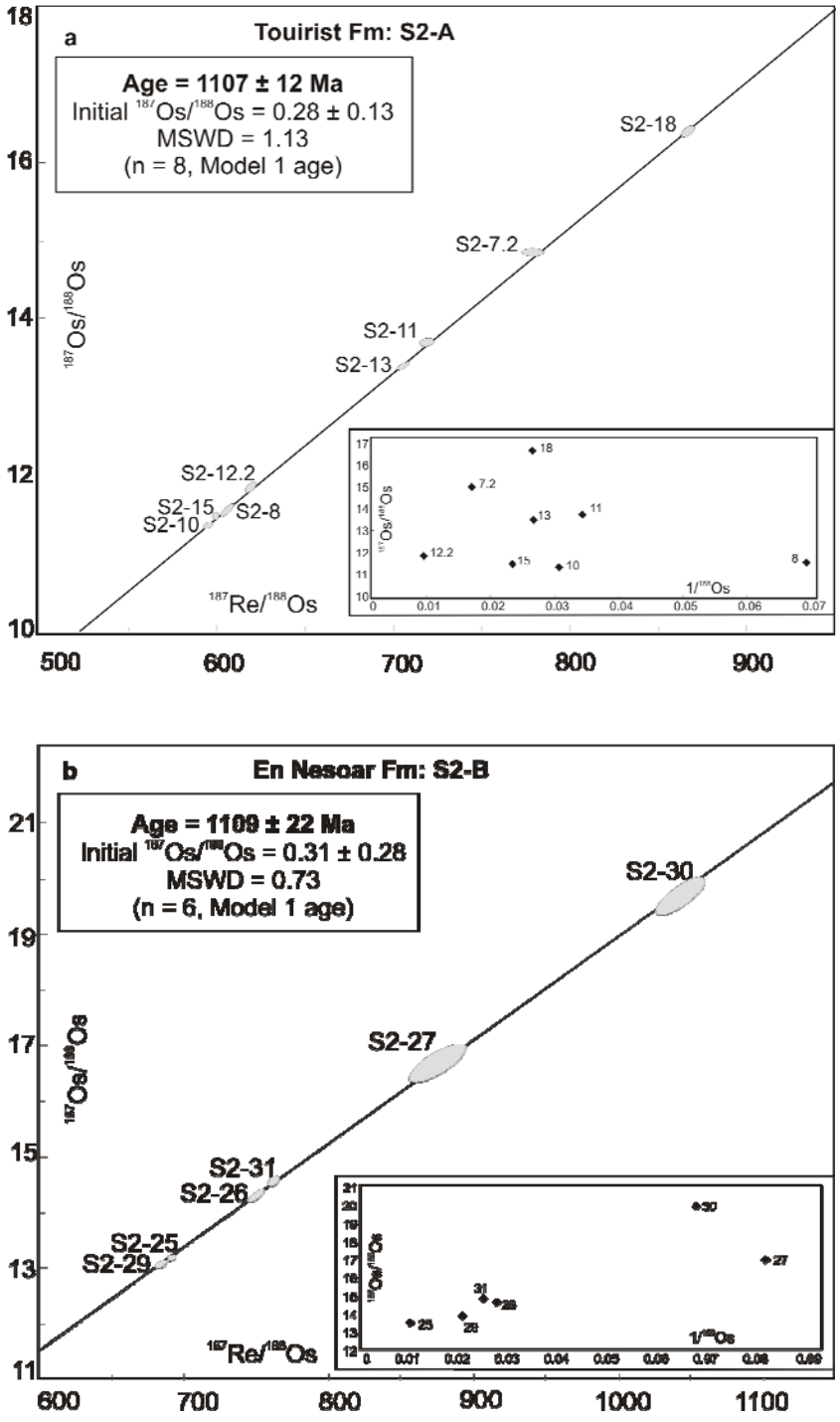

Fig. 2.3 (a) Re-Os isochron diagrams for the Atar Group ORS. S2-A horizon of the Touirist Formation (139.45 m to 143.82 m depth). The inset highlights the lack of correlation between present day $^{187}Os/^{188}Os$ and $1/^{188}Os$. (b) S2-B horizon of the En Nesoar Formation (206.7 m to 207.6 m depth). The inset highlights the lack of correlation between present day $^{187}Os/^{188}Os$ and $1/^{188}Os$.

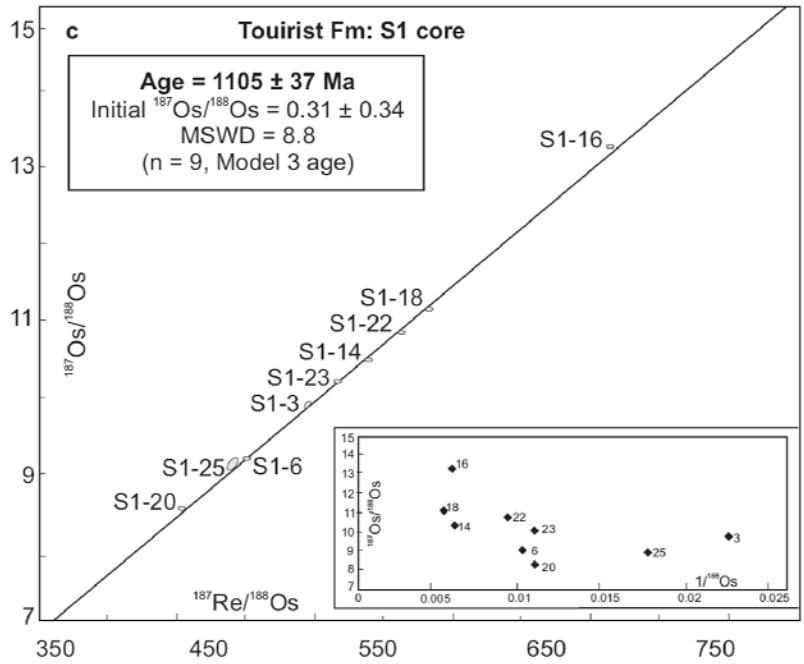

Fig. 2.3 (c) S1 horizon of the Touirist Formation (73.15 m to 89.50 m depth). The inset highlights the lack of correlation between present day $^{187}Os/^{188}Os$ and $1/^{188}Os$.

2.5 Discussion

The Re-Os data from ORS of the Atar Group yield ages of 1107 ± 12 Ma; 1109 ± 22 Ma and 1105 ± 37 Ma, respectively from two drill cores (Fig. 2.3). The 1107 ± 12 Ma and 1105 ± 37 Ma ages represent depositional ages for the Touirist Formation. The 1109 ± 22 Ma represents a depositional age for the En Nesoar Formation which conformably underlies the Touirist Formation. The Re-Os ages for these two formations provide accurate Mesoproterozoic (Stenian; 1000 – 1200 Ma; Ogg et al., 2008) ages for the deposition of the Atar Group of the Taoudeni basin. The larger uncertainty for the S1 age (± 37 Ma) is discussed below.

2.5.1 Previous geochronology and Rb-Sr systematics

The basal sedimentary units of the Taoudeni basin, including the Atar Group shales, were previously defined as Tonian, (Clauer, 1976; Clauer, 1981). For the Atar Group Rb-Sr geochronology yields an age of 890 ± 37 Ma (Clauer, 1981), which is ~200 Ma younger than the Re-Os ORS dates for this group. The clays analysed by Clauer (1976) were 1M polymorphs of illite that are characteristic of low temperature growth and re-crystallisation commonly associated with diagenesis (Bailey, 1966; Grathoff and Moore, 1996).

Although the Rb-Sr technique has been used to estimate the geochronology of the Taoudeni basin, the Rb-Sr systematics of illite and glauconite are known to be susceptible to disturbance and hence record anomalously young geological ages that are associated with diagenesis (Morton and Long, 1982; Clauer et al., 1987; Ohr et al., 1991; Awwiller, 1994; Evans, 1996; Gorokhov et al., 2001). Furthermore, previous work has highlighted the progressive genesis of glauconites over as much as 5 Ma in samples that have experienced a relatively straightforward geological history e.g., GL-O glauconite international standard (Odin and Hunziker, 1982; Smith et al., 1998; Selby, 2009).

Given the three identical, within uncertainty, Re-Os ORS dates from two locations; it can be inferred that the Rb-Sr geochronology does not record the depositional age of the Atar Group. Although it is beyond the scope of this research to fully elucidate what events the Rb-Sr data do record, known metamorphic and tectonic events associated with the Pan-African orogeny may have had a lasting effect on Rb-Sr systematics. Fundamentally, the Rb-Sr systematics are known to suffer from post-depositional events resulting in erroneously young ages.

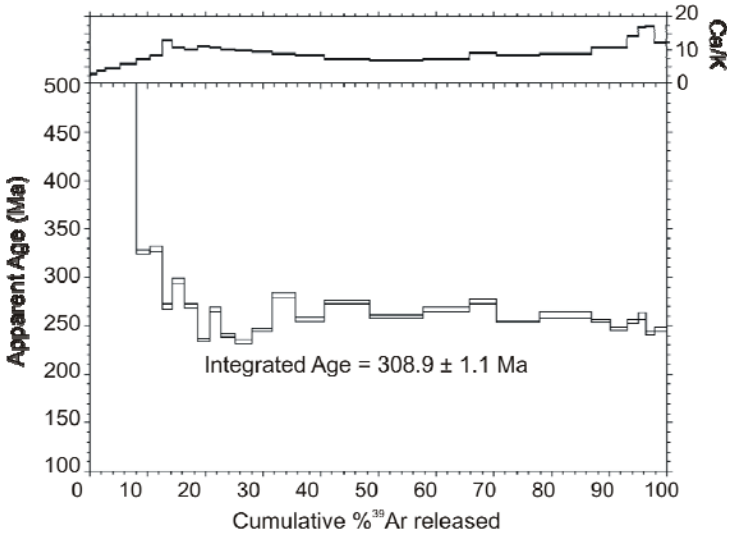

Fig. 2.4 Ar-Ar age spectrum from plagioclase grains of dolerite sill. Sampled at ~90 m depth in the S1 drill core.

2.5.2 TOC versus Re and Os abundance

At present our understanding of the mechanisms by which Re and Os are complexed into ORS is incomplete. Studies of Re and Os in marine sediments suggest the

complexation is driven by a combination of reductive capture and adsorption onto organocomplexes in seawater (Koide et al., 1991; Colodner et al., 1993; Crusius et al., 1996; Levasseur et al., 1998; Oxburgh, 1998). However, a direct link between TOC and Re and Os abundances for all ORS is unlikely as samples with low or high TOC content can have high Re/Os (0.5 – 30% and 300 to 800 units, respectively; Kendall et al., 2004; Selby et al., 2009). Other important factors include recharge of Re and Os into the water column (Turgeon et al., 2007) and post-deposition affects (Crusius and Thomson, 2000; Kendall et al., 2009b). Despite the strong correlation between Re and Os with TOC in the ORS reported in this study the relationship is not consistent. Jurassic ORS possess little or no correlation between TOC content and Re and Os abundance (Cohen et al., 1999). Furthermore, low TOC (<1%) samples of the Neoproterozoic Old Fort Point Formation contain elevated Re and Os abundances (16 ppb and 249 ppt, respectively) further indicating that Re and Os enrichment is not directly linked to TOC content (Kendall et al., 2004).

As the relationship between Re and Os with TOC content is distinct for differing ORS, their enrichment factor may be related to local factors such as: duration that the pore-water sediment interface is open; changes in the oxic-anoxic boundary of the water column; and input of Re and Os from varying sources (e.g. continental weathering, hydrothermal flux and cosmic input). Considering the behaviour and destination of other redox sensitive elements such as Ni and Mo there is a strong argument that the dominant factor controlling Re and Os enrichment in ORS is sedimentation rate (Lewan and Maynard, 1982; Kendall et al., 2009a, b).

2.5.3 Conditions of flash pyrolysis and non-disturbance of Re-Os systematics associated with flash pyrolysis

It is unlikely that the slightly larger uncertainty of the Re-Os isotope data from the S1 core compared to the uncertainties of the S2 core is caused by significant disturbance of the Re-Os systematics (1105 ± 37 Ma; 1107 ± 12 Ma and 1109 ± 22 Ma, respectively). Two studies provide evidence that the Re-Os systematics in ORS can be disturbed and/or reset (Kendall et al., 2009b; Yang et al., 2009). Work focusing on Mesoproterozoic shales from the McArthur basin, Australia reported an imprecise age, a large MSWD (86) and highly radiogenic Os_i (3.5 ± 1.5; Kendall et al., 2009b). These factors were attributed to

disturbance of the Re-Os systematics in this example, by hydrothermal fluid flow associated with ore deposition. Kendall et al. (2009b) also reported an increase in the $^{187}Os/^{188}Os$ composition as an indication of disturbance, either by mobilisation of Os relative to Re or addition of Re relative to Os.

In addition, a Re-Os data set for Archean carbonaceous slates generated a meaningful Re-Os age, but produced negative Os_i (Yang et al., 2009). These authors concluded that the Re-Os systematics had been affected by the recent addition of ^{187}Re from weathering of adjacent mafic rocks, and that the addition of ^{187}Re was proportional to the ^{187}Os concentration of each sample.

However, another explanation for the Re-Os data of the Archean carbonaceous slates may relate to the small amount of material prepared (<1 g) for the Re-Os analyses. As a result, these small aliquots do not minimise the Re-Os heterogeneity known to occur in ORS (Kendall et al., 2009a).

The $^{187}Re/^{188}Os$ ratios for the S1 core are slightly lower than those from the two S2 core analyses (Table 2.3; Fig. 2.3; 431 to 696 compared with 594 to 865 and 683 to 1041, respectively). In addition, the $^{187}Os/^{188}Os$ ratios for the S1 core are also less radiogenic (8.4 to 13.3) than those from the S2 core analyses (11.3 to 16.4 and 13.0 to 19.7; Table 2.3; Fig. 2.3). However, both cores are significantly enriched in Re and Os, particularly in comparison to average continental crust. Although the Re-Os age for the S1 core is nominally identical for those determined for the S2 core (Fig. 2.3), it possesses a larger uncertainty (± 37 Ma). This may relate to the cluster of points between 520 and 580 on the S1 isochron and not disturbance of the Re-Os systematics by hydrothermal fluid flow and/or hydrocarbon maturation and migration. Evaluation of the Re and Os isotope data can reveal whether or not Re-Os systematics have been disturbed. The scattered relationship between present day $^{187}Os/^{188}Os$ and $1/^{188}Os$ indicate that the Re-Os systematics has not been disturbed (Fig. 2.3 insets).

The Os_i of the S1 and S2 cores are identical within uncertainty (0.31 ± 0.34; 0.28 ± 0.13 and 0.31 ± 0.28, respectively) and are interpreted to record the Os isotope composition of seawater at the time of deposition (Fig. 2.3). Any disturbance of Re and/or Os isotope values would result in large variations and a radiogenic Os_i as seen in the Mesoproterozoic Velkerri Formation (Kendall et al., 2009b).

Table 2.3
Re and Os abundance and isotopic data for the Atar Group ORS.

Sample	Depth	Re (ppb)	±	Os (ppb)	±	^{192}Os (ppt)	±	^{187}Re/^{188}Os	±	^{187}Os/^{188}Os	±	rho[a]	Os$_i$[b]
S1 core													
S1-14	73.15	152.6	0.5	3.1479	0.0005	555.4	0.8	546.44	1.94	10.398	0.021	0.293	0.20
S1-16	73.53	198.1	0.6	3.7334	0.0006	566.2	0.7	696.24	2.41	13.332	0.022	0.251	0.34
S1-18	73.70	182.3	0.6	3.6546	0.0006	620.7	0.7	584.27	2.00	11.098	0.018	0.216	0.19
S1-3	88.27	36.9	0.1	0.7885	0.0001	144.1	0.5	509.37	2.29	9.785	0.044	0.485	0.28
S1-6	88.74	77.1	0.2	1.7083	0.0002	325.9	0.4	470.81	1.64	9.050	0.015	0.280	0.34
S1-20	88.98	65.2	0.2	1.5100	0.0002	300.4	0.5	431.81	1.58	8.369	0.018	0.385	0.31
S1-22	89.33	101.5	0.3	2.0630	0.0003	356.4	0.6	566.71	2.09	10.781	0.024	0.363	0.20
S1-23	89.36	79.9	0.3	1.6796	0.0003	301.4	0.5	527.55	1.95	10.099	0.022	0.395	0.25
S1-25	89.50	42.8	0.1	0.9595	0.0001	183.9	0.9	462.95	2.71	8.973	0.062	0.583	0.33
S2-A													
S2-7.2	139.45	86.9	0.5	1.5690	0.0005	222.1	0.7	778.26	4.78	14.821	0.050	0.440	0.30
S2-8	140.77	14.4	0.1	0.2851	0.0001	47.3	0.3	606.46	3.88	11.536	0.065	0.785	0.22
S2-10	141.08	33.8	0.1	0.6740	0.0001	112.9	0.3	594.88	2.44	11.349	0.033	0.529	0.25
S2-11	141.25	36.2	0.1	0.6715	0.0001	100.3	0.3	718.15	2.94	13.660	0.039	0.547	0.26
S2-12.2	141.65	146.3	0.5	2.8754	0.0005	469.9	1.2	619.13	2.51	11.827	0.038	0.454	0.27
S2-13	142.05	46.9	0.1	0.8744	0.0001	132.3	0.3	704.63	2.75	13.375	0.035	0.476	0.22
S2-15	142.90	46.3	0.2	0.9201	0.0002	153.3	0.3	600.63	2.31	11.455	0.029	0.442	0.24
S2-18	143.82	57.7	0.2	1.0007	0.0002	132.5	0.3	865.87	3.42	16.369	0.045	0.478	0.21
S2-B													
S2-25	206.70	113.6	0.4	2.1399	0.0004	327.3	0.9	690.49	2.89	13.156	0.044	0.488	0.27
S2-26	206.80	44.4	0.1	0.8127	0.0001	117.9	0.7	749.24	4.93	14.282	0.093	0.755	0.30
S2-27	207.00	17.4	0.1	0.3032	0.0001	39.7	0.7	874.08	15.12	16.641	0.309	0.889	0.33
S2-29	207.20	57.6	0.2	1.0904	0.0002	167.6	0.8	683.17	3.97	13.049	0.076	0.681	0.30
S2-30	207.40	25.0	0.1	0.4109	0.0001	47.8	0.7	1041.50	14.43	19.662	0.297	0.859	0.22
S2-31	207.60	50.2	0.2	0.9142	0.0002	131.1	0.5	761.44	3.66	14.539	0.077	0.494	0.33

Uncertainties are given as 2σ for ^{187}Re/^{188}Os and ^{187}Os/^{188}Os and ^{192}Os.

For the latter the uncertainty includes the 2 SE uncertainty for mass spectrometer analysis plus uncertainties for Os blank abundance and isotopic composition.

[a] Rho is the associated error correlation (Ludwig, 1980).

[b] Os$_i$ = initial ^{187}Os/^{188}Os isotope ratio calculated at 1105 Ma (S1, 73.15-89.50 m depth), 1107 Ma (S2-A, 139.45-143.82 m depth) and 1109 Ma (S2-B, 206.7-207.6 m depth).

Ages calculated using the λ ^{187}Re = 1.666 x $10^{-11}y^{r-1}$ (Smoliar et al., 1996).

Together, enriched levels of Re and Os, the positive correlation between $^{187}Re/^{188}Os$ and $^{187}Os/^{188}Os$ ratios and the identical Os_i values indicate that the Re-Os geochronology data of the S1 core are recording the depositional age of ORS from the Touirist Formation.

The $^{40}Ar/^{39}Ar$ dating of the dolerite sill that intersects the ORS of the S1 core yields an age of ~230 Ma indicating that the sill was intruded nearly 900 Ma after deposition of the Atar Group (Fig. 2.4). The age of the intrusion suggests that it is related to the opening of the North Atlantic during the late Triassic/early Jurassic.

The ORS of S1 are baked black 20 m above and 5 m below the contact between the S1 shales and the intrusion. Quantifying the grade of metamorphism is restricted by a lack of index minerals present in the S1 shales. Thin section and XRD analysis of the overmature S1 shales reveal compositions similar to the immature S2 shales, but with minor amounts of pyrrhotite. Pyrrhotite is a common mineral in metamorphosed graphitic rocks and generally forms under reducing conditions at temperatures >200 ^{o}C (Lambert 1973; Hall, 1986; Gillett, 2003; Pattison, 2005). The absence of extensive metamorphism can be explained by a low geothermal gradient, burial limited to ~3 km, a low country rock temperature (<100 ^{o}C) and a short duration of heat transfer due to a rapid cooling of the intrusion (Delaney and Pollard, 1982; Delaney, 1987; Raymond and Murchison, 1988; Galushkin, 1997). The overmature shales (S1) and borderline mature shales (S2) of this study both have elevated TOC (0.8 to 22.6%; Table 2.1). The TOC of overmature shales consists of a carbon-rich hydrogen-poor residue. In contrast, TOC of borderline mature shales consist of 'extractable organic matter carbon' and 'convertible carbon' (Jarvie, 1991).

Gaining a precise intrusion temperature of the sill and the extent of heating of the surrounding ORS is beyond the scope of this research. However, previous studies have modelled palaeotemperatures that sedimentary rocks experienced during intrusion of igneous bodies (Galushkin, 1997; Barker et al., 1998; Kalsbeek and Frei, 2006). From the mineralogy and petrology of the sill it can be estimated that the temperature of intrusion was between 1000 and 1200 ^{o}C and the shales of S1 were buried to depths <3 km with corresponding burial temperatures less than 100 ^{o}C (Girard et al., 1989; Deynoux et al., 2006). Using the equation ($T_{contact} = (T_{magma} + T_{host})/2$), where T = temperature (Carslaw and Jaeger, 1959), the ORS experienced temperatures between ~550 to 650 ^{o}C at the sill / ORS contact.

Mean vitrinite reflectance data can be used to estimate the maximum peak temperature experienced by the ORS. However, because of the absence of vitrinite in Proterozoic ORS, bitumen reflectance data (BRo) has been converted into vitrinite reflectance data (Ro) using Ro = 0.618BRo + 0.4 (Jacob, 1989). Two values of BRo, taken from above and below the sill, were provided by TOTAL and yield a mean vitrinite reflectance value (Rv-r) of 2.91. The mean vitrinite reflectance data is then used to estimate the maximum peak temperature (T_{peak}) experienced by the ORS by T_{peak} = (ln (Rv-r) + 1.19/0.00782; Barker and Pawlewicz, 1994). This gives a peak temperature of ~288 ^{o}C experienced by the altered S1 shales. Convective and/or conductive cooling would have lowered the temperature from ~550 to 650 ^{o}C at the contact to ~288 ^{o}C through the rest of the altered shales (Barker et al., 1998). Together the occurrence of pyrrhotite, T_{max} data, HI data and the estimated peak temperatures provide strong evidence that the shales from the S1 core have experienced maturation and expulsion of hydrocarbons as a result of flash pyrolysis. The Re-Os ORS geochronology data indicate that flash pyrolysis has not significantly affected the Re-Os ORS systematics.

2.5.4 Implications for basin correlation, craton-craton correlation and Rodinia reconstructions

The current age for the Char Group which unconformably underlies the Atar Group is from Rb-Sr illite and glauconite geochronology and gives an age of 998 ± 34 Ma (Clauer, 1981). The Atar Group Mid-Stenian Re-Os ORS ages (~1100 Ma) strongly suggest that the Char Group is also much older than previously thought. As the unconformity between the Char and Atar Groups is basin-wide in scale it is impossible to extrapolate an age for the Char Group from the depositional age of the Atar Group. However, based upon the increased age (older by 24%) the Re-Os geochronology for the Atar Group suggests that the Char Group may also be ~200 Ma older than the Rb-Sr derived age of 998 ± 34 Ma. The new geochronology data for the Atar Group enables us to provide improved models of sedimentation for the West African craton and enhance existing models of sequence stratigraphy as presented by Bertrand-Sarfati & Moussine-Pouchkine (1988).

Previous correlations of the Atar Group ORS from drill core and outcrop were based on matching high TOC horizons and using distinct stromatolite morphology as marker horizons (Bertrand-Sarfati & Moussine-Pouchkine, 1985; 1988). These methods are

unsuitable for the large distances involved in basin-wide hydrocarbon exploration because of the large range in TOC levels (0.8 to 22.6%; Table 2.1) within individual formations of the Atar Group. The Atar Group biostromes consist of juxtaposed stromatolites which record growth at different times in distinct environmental settings (Bertrand-Sarfati & Moussine-Pouchkine, 1988; Kah et al., 2008). As a consequence, the biostrome horizons cannot be used as marker horizons for correlation on a basin or craton-wide scale.

The two cores were drilled in regions separated by >200 km and the suggesting that Re-Os ORS geochronology can provide precise depositional ages for hydrocarbon source rocks and permits correlations between source rocks on a basin-wide scale.

The new Re-Os ORS geochronology provides absolute age data that supports chemostratigraphy evidence that the West African craton has a depositional history that predates 1100 Ma (Teal and Kah, 2005). From this, it can be suggested that sedimentation onto the cratonic platform began ~1.2 Ga rather than at 1 Ga which is implied by the Rb-Sr geochronology. The new geochronology data have implications for the development of sedimentation histories and basin modelling used for hydrocarbon exploration in cratonic settings.

It has been suggested that the Taoudeni basin is a vast 'super basin' consisting of a number of sub-basins (Villeneuve and Cornée, 1994; Lottaroli et al., 2009). The Re-Os geochronology is recording deposition of the Touirist Formation possibly in separate sub-basins of the Taoudeni 'super basin'. The similar Os_i values of the S1 and S2 cores are suggested to be recording the osmium isotope composition of local seawater at the time of deposition (Ravizza and Turekian, 1989; Cohen et al., 1999; Selby and Creaser, 2003). Therefore, the Os_i values for this 'super basin' may be used as a proxy for global seawater Os isotope composition at 1100 Ma.

The Re-Os geochronology for the Atar Group provides a depositional age that is consistent with sedimentation histories of other cratons involved in the formation, and subsequent break up, of the supercontinent Rodinia. However, because of the lack of available palaeomagnetic data for the West African craton its palaeogeography is poorly constrained (Li et al., 2008). Despite this, work on the West African, Amazon and Rio de la Plata cratons proposed the existence of a mega-craton that existed during the Meso- and Neoproterozoic (Onstott and Hargraves, 1981; Trompette, 1994; Zhao et al., 2006). There is strong evidence to suggest that the West Africa craton was linked with the São Francisco craton of South America during the Mesoproterozoic (Onstott et al., 1984; D'Agrella-Filho

et al., 1990; 2004; Zhao et al., 2006; Li et al., 2008). The new Re-Os geochronology data require a reassessment of the drift histories of the West African craton as discussed by Tohver et al. (2006).

The Re-Os ORS geochronology suggests that the Atar Group sedimentary rocks of the Taoudeni basin are approximately equivalent to Mesoproterozoic sedimentary rocks found on the São Francisco craton (Fairchild et al., 1996; Geboy, 2006; Zhao et al., 2006; Azmy et al., 2008; Li et al., 2008). The Vazante Group of the São Francisco craton has two Re-Os datasets that yield ages of 1126 ± 47 Ma and 1100 ± 77 Ma for the Serra do Poço Verde and Lapa Formations, respectively (Geboy, 2006; Azmy, 2008). These two formations are separated by an unconformity of unknown duration. Both of the Re-Os ages from the Vazante Group are identical, within uncertainty, to the Re-Os ages of the Atar Group (this study) and suggest that these successions were deposited coevally onto the passive margins of the São Francisco and West African cratons. The São Francisco, Amazon, Congo and West African cratons are speculated to have been separated by the Brasiliano Ocean at ~ 1100 Ma and were not involved in the formation of Rodinia at this time (Kröner and Cordani, 2003; D'Agrella-Filho et al., 2004). The Atar Group of the Taoudeni basin provides a rare record of exceptionally well-preserved sedimentary rocks that were possibly deposited in basins that existed between the West African, São Francisco and Amazon cratons during the Mesoproterozoic.

2.6 Conclusions

1. The Re-Os ORS geochronology of the Atar Group suggests that sedimentation of the Taoudeni basin began prior to 1100 Ma. This age is >200 Ma older than previous ages based upon Rb-Sr illite and glauconite geochronology (Clauer, 1976, 1981).
2. The Re-Os ages from both immature and overmature ORS strongly suggest that the Re-Os ORS systematics are not significantly affected by flash pyrolysis associated with contact metamorphism of mafic intrusions.
3. The new Re-Os ages highlight implications for supercontinent reconstructions involving the West African craton. The Re-Os data records the onset of sedimentation on the passive margin of the West African craton prior to 1100 Ma.

The new Re-Os data strongly suggest that a reassessment of the role of the West African craton in the Rodinia supercontinent configuration is required.

2.7 References

Ahmed Benan, C. A. and Deynoux, M., 1998. Facies analysis and sequence stratigraphy of Neoproterozoic platform deposits in Adrar of Mauritania, Taoudeni basin, West Africa. *Geologische Rundschau* **87**, 283-302.

Anbar, A. D., Duan, Y., Lyons, T. W., Arnold, G. L., Kendall, B., Creaser, R. A., Kaufman, A. J., Gordon, G. W., Scott, C., Garvin, J., and Buick, R., 2007. A whiff of oxygen before the great oxidation event? *Geochimica Et Cosmochimica Acta* **71**, A24-A24.

Awwiller, D. N., 1994. Geochronology and Mass-Transfer in Gulf-Coast Mudrocks (South-Central Texas, USA) - Rb-Sr, Sm-Nd and Ree Systematics. *Chemical Geology* **116**, 61-84.

Azmy, K., Kendall, B., Creaser, R. A., Heaman, L., and de Oliveira, T. F., 2008. Global correlation of the Vazante Group, Sao Francisco Basin, Brazil: Re-Os and U-Pb radiometric age constraints. *Precambrian Research* **164**, 160-172.

Bailey, S. W., 1966. The status of clay mineral structures. *Proceedings of the 14th National Conference on Clays and Clay minerals*. Pergamon, New York.

Barker, C. E., Bone, Y., and Lewan, M. D., 1998. Fluid inclusion and vitrinite-reflectance geothermometry compared to heat-flow models of maximum paleotemperature next to dikes, western onshore Gippsland Basin, Australia. *International Journal of Coal Geology* **37**, 73-111.

Barker, C. E., Pawlewicz, M.J., 1994. Calculation of vitrinite-reflectance from thermal histories and peak temperature: a comparison of methods. In: Mukhopadhyay, P. K., Dow, W.G. (Eds.), Vitrinite-Reflectance as a Maturity Parameter: Applications and Limitations, ACS Symposium Series No. 570, pp. 216-229.

Behar, F., Beaumont, V., Penteado., H.L. De B., 2001. Rock-Eval 6 Technology: Performances and Developments. *Oil and Gas Science and Technology* **56**, 111-134.

Bertrand-Sarfati, J. and Moussine-Pouchkine, A., 1985. Evolution and Environmental-Conditions of Conophyton-Jacutophyton Associations in the Atar Dolomite (Upper Proterozoic, Mauritania). *Precambrian Research* **29**, 207-234.

Bertrand-Sarfati, J. and Moussine-Pouchkine, A., 1988. Is Cratonic Sedimentation Consistent with Available Models - an Example from the Upper Proterozoic of the West-African Craton. *Sedimentary Geology* **58**, 255-276.

Bertrand-Sarfati, J., Moussine-Pouchkine, A., Amard, B., and Ahmed, A. A. K., 1995. 1st Ediacarian Fauna Found in Western Africa and Evidence for an Early Cambrian Glaciation. *Geology* **23**, 133-136.

Bertrand-Sarfati, J., Trompette, R., and Walter, M. R., 1976. Chapter 10.1 Use of Stromatolites for Intrabasinal Correlation: Example from the Late Proterozoic of the North-western Margin of the Taoudenni Basin, *Developments in Sedimentology*. Elsevier.

Bertrand-Sarfati, J. and Walter, M. R., 1981. Stromatolite Biostratigraphy. *Precambrian Research* **15**, 353-371.

Bonhomme, M. G. and Bertrand-Sarfati, J., 1982. Correlation of Proterozoic Sediments of Western and Central-Africa and South-America Based Upon Radiochronological and Paleontological Data. *Precambrian Research* **18**, 171-194.

Bronner, G., Roussel, J., Trompette, R. and Clauer, N, 1980. Genesis and geodynamic evolution of the Taoudeni Cratonic Basin (Upper Precambrian and Paleozoic), western Africa. In: Bally, A. W. (Ed.), *Dynamics of Plate Interiors, Geodyn. Series,* **1,** pp. 81-90. AGU-GSA.

Carslaw, H. S., Jaeger, J.C., 1959. *Conduction of Heat in Solids*. Oxford University Press, New York. 510 pp.

Cassata, W. S., Renne, P. R., and Shuster, D. L., 2009. Argon diffusion in plagioclase and implications for thermochronometry: A case study from the Bushveld Complex, South Africa *Geochimica Et Cosmochimica Acta* **73**, 6600-6612.

Clauer, N., 1976. Chimie isotopique du strontium des milieux sédimentaires. Application a la géochronologie de la couverture du craton ouest africain. *Mem Sci Geol* **45**, 1-256.

Clauer, N., 1981. Rb—Sr and K—Ar dating of Precambrian clays and glauconies. *Precambrian Research* **15**, 331-352

Clauer, N., Caby, R., Jeannette, D., and Trompette, R., 1982. Geochronology of Sedimentary and Meta-Sedimentary Precambrian Rocks of the West-African Craton. *Precambrian Research* **18**, 53-71.

Cohen, A. S., 2004. The rhenium-osmium isotope system: applications to geochronological and palaeoenvironmental problems. *Journal of the Geological Society* **161**, 729-734.

Cohen, A. S., Coe, A. L., Bartlett, J. M., and Hawkesworth, C. J., 1999. Precise Re-Os ages of organic-rich mudrocks and the Os isotope composition of Jurassic seawater. *Earth and Planetary Science Letters* **167**, 159-173.

Colodner, D., Sachs, J., Ravizza, G., Turekian, K., Edmond, J., and Boyle, E., 1993. The geochemical cycles of rhenium: a reconnaissance. *Earth and Planetary Science Letters* **117**, 205-221.

Creaser, R. A., Sannigrahi, P., Chacko, T., and Selby, D., 2002. Further evaluation of the Re-Os geochronometer in organic-rich sedimentary rocks: A test of hydrocarbon maturation effects in the Exshaw Formation, Western Canada Sedimentary Basin. *Geochimica et Cosmochimica Acta* **66**, 3441-3452.

Crusius, J., Calvert, S., Pedersen, T., and Sage, D., 1996. Rhenium and molybdenum enrichments in sediments as indicators of oxic, suboxic and sulfidic conditions of deposition. *Earth and Planetary Science Letters* **145**, 65-78.

Crusius, J. and Thomson, J., 2000. Comparative behavior of authigenic Re, U, and Mo during reoxidation and subsequent long-term burial in marine sediments. *Geochimica et Cosmochimica* **64**, 2233-2242.

D'Agrella-Filho, M. S., Pacca, I. G., Teixeira, W., Onstott, T. C., and Renne, P. R., 1990. Paleomagnetic evidence for the evolution of Meso- to Neo-Proterozoic glaciogenic rocks in central-eastern Brazil. *Palaeogeography, Palaeoclimatology, Palaeoecology* **80**, 255-265.

D'Agrella-Filho, M. S., Pacca, I. I. G., Trindade, R. I. F., Teixeira, W., Raposo, M. I. B., and Onstott, T. C., 2004. Paleomagnetism and 40Ar/39Ar ages of mafic dikes from Salvador (Brazil): new constraints on the São Francisco craton APW path between 1080 and 1010 Ma. *Precambrian Research* **132**, 55-77.

Delaney, P. T. and D. D. Pollard (1982). "Solidification of basaltic magma during flow in a dike." American Journal of Science **282**(6): 856-885.

Delaney, P. T., 1987. Heat transfer theory applied to mafic dike intrusions. In: Halls, H. L. and Fahrig, W. F. Eds.), *Mafic dike swarms*. Geological Association of Canada special paper; 34.

Dempster, T. J., Rogers, G., Tanner, P. W. G., Bluck, B. J., Muir, R. J., Redwood, S. D., Ireland, T. R., and Paterson, B. A., 2002. Timing of deposition, orogenesis and glaciation within the Dalradian rocks of Scotland: constraints from U-Pb zircon ages. *Journal of the Geological Society* **159**, 83-94.

Deynoux, M., Affaton, P., Trompette, R., and Villeneuve, M., 2006. Pan-African tectonic evolution and glacial events registered in Neoproterozoic to Cambrian cratonic and foreland basins of West Africa. *Journal of African Earth Sciences* **46**, 397-426.

Deynoux, M. and R. Trompette (1976). "Late Precambrian Mixtites - Glacial and/or Non-Glacial - Dealing Especially with Mixtites of West-Africa." American Journal of Science **276**(10): 1302-1315.

Esser, B. K. and Turekian, K. K., 1993. The osmium isotopic composition of the continental crust. *Geochimica Cosmochimica Acta* **57**, 3093-3104.

Evans, J. A., 1996. Dating the transition of smectite to illite in Palaeozoic mudrocks using the Rb-Sr whole-rock technique. *Journal of the Geological Society, London* **153**, 101-108.

Frank, T. D., Kah, L. C., and Lyons, T. W., 2003. Changes in organic matter production and accumulation as a mechanism for isotopic evolution in the Mesoproterozoic ocean. *Geological Magazine* **140**, 397-420.

Fairchild, T. R., Schopf, J. W., Shen-Miller, J., Guimarães, E. M., Edwards, M. D., Lagstein, A., Li, X., Pabst, M., and de Melo-Filho, L. S., 1996. Recent discoveries of Proterozoic microfossils in south-central Brazil. *Precambrian Research* **80**, 125-152.

Galushkin, Y. I., 1997. Thermal effects of igneous intrusions on maturity of organic matter: A possible mechanism of intrusion. *Organic Geochemistry* **26**, 645-658.

Geboy, N. J., 2006. Rhenium-Osmium age determinations of glaciogenic shales from the Mesoproterozoic Vazante Formation, Brazil, Masters Thesis, University of Maryland.

Gillett, S. L., 2003. Paleomagnetism of the Notch Peak contact metamorphic aureole, revisited: Pyrrhotite from magnetite plus pyrite under sub metamorphic conditions. *Journal of Geophysical Research-Solid Earth* **108**, -.

Girard, J. P., Deynoux, M., and Nahon, D., 1989. Diagenesis of the Upper Proterozoic Siliciclastic Sediments of the Taoudeni Basin (West-Africa) and Relation to Diabase Emplacement. *Journal of Sedimentary Petrology* **59**, 233-248.

Gorokhov, I. M., Siedlecka, A., Roberts, D., Melnikov, N. N., and Turchenko, T. L., 2001. Rb-Sr dating of diagenetic illite in Neoproterozoic shales, Varanger Peninsula, northern Norway. *Geological Magazine* **138**, 541-562.

Grathoff, G. H. a. M., D.M., 1996. Illite polytype quantification using WILDFIRE calculated X-ray diffraction patterns *Clays and Clay Minerals* **44**, 835 - 842.

Hall, A. J., 1986. Pyrite Pyrrhotite Redox Reactions in Nature. *Mineral Mag* **50**, 223-229.

Halliday, A. N., Graham, C. M., Aftalion, M., and Dymoke, P., 1989. The Depositional Age of the Dalradian Supergroup - U-Pb and Sm-Nd Isotopic Studies of the Tayvallich Volcanics, Scotland. *Journal of the Geological Society* **146**, 3-6.

Hattori, Y., Suzuki, K., Honda, M., and Shimizu, H., 2003. Re-Os isotope systematics of the Taklimakan Desert sands, moraines and river sediments around the Taklimakan Desert, and of Tibetan soils. *Geochimica Et Cosmochimica Acta* **67**, 1203-1213.

Heaman, L. M., LeCheminant, A. N., and Rainbird, R. H., 1992. Nature and Timing of Franklin Igneous Events, Canada - Implications for a Late Proterozoic Mantle Plume and the Break-up of Laurentia. *Earth and Planetary Science Letters* **109**, 117-131.

Heaman, L. M., LeCheminant, A.N., and Rainbird, R.H., 1990. A U-Pb baddeleyite study of Franklin igneous events. *Geological Association of Canada, Programs with Abstracts*.

Hofmann, H. J. and Jackson, G. D., 1994. Shale-Facies Microfossils from the Proterozoic Bylot Supergroup, Baffin Island, Canada. *Memoir (The Paleontological Society)* **37**, 1-39.

Hunt, J. M., 1961. Distribution of hydrocarbons in sedimentary rocks. *Geochimica Et Cosmochimica Acta* **22**, 37-49.

Jacob, H., 1989. Classification, structure, genesis and practical importance of natural solid oil bitumen ("migrabitumen"). *International Journal of Coal Geology* **11**, 65-79.

Jarvie, D. M., 1991. Total Organic Carbon (TOC) Analysis. In: Merril, R. K. (Ed.), *Source and Migration Processes and Evaluation Techniques*. The American Association of Petroleum Geologists, pp.113-118.

Kah, L. C. and Bartley, J. K., 2004. Effect of marine carbon reservoir size on the duration of carbon isotope excursions: Interpreting the Mesoproterozoic carbon isotope record. *Geological Society of America Abstracts with Programs*.

Kah, L. C., Sherman, A. G., Narbonne, G. M., Knoll, A. H., and Kaufman, A. J., 1999. delta C-13 stratigraphy of the Proterozoic Bylot Supergroup, Baffin Island, Canada: implications for regional lithostratigraphic correlations. *Canadian Journal of Earth Sciences* **36**, 313-332.

Kah, L. C., Bartley, J.K. and Stagner, A.F., 2008. Reinterpreting a Proterozoic enigma: *Conophyton-Jacutophyton* stromatolites of the Mesoproterozoic Atar Group, Mauritania. *International Association of Sedimentology Special Publication* **41**, p. 277-295.

Kalsbeek, F. and Frei, R., 2006. The Mesoproterozoic Midsommersø dolerites and associated high-silica intrusions, North Greenland: crustal melting, contamination and hydrothermal alteration. *Contrib Mineral Petr* **152**, 89-110.

Kendall, B., Creaser, R. A., and Selby, D., 2009a. 187Re-187Os geochronology of Precambrian organic-rich sedimentary rocks. *Geological Society, London, Special Publications* **326**, 85-107.

Kendall, B., Creaser, R. A., Gordon, G. W., and Anbar, A. D., 2009b. Re-Os and Mo isotope systematics of black shales from the Middle Proterozoic Velkerri and Wollogorang Formations, McArthur Basin, northern Australia. *Geochimica Et Cosmochimica Acta* **73**, 2534-2558.

Kendall, B., Creaser, R. A., and Selby, D., 2006. Re-Os geochronology of postglacial black shales in Australia: Constraints on the timing of "Sturtian" glaciation. *Geology* **34**, 729-732.

Kendall, B. S., Creaser, R. A., Ross, G. M., and Selby, D., 2004. Constraints on the timing of Marinoan 'Snowball Earth' glaciation by 187Re – 187Os dating of a Neoproterozoic post-glacial black shale in Western Canada. *Earth and Planetary Science Letters* **222**, 729-740.

Koide, M., Goldberg, E. D., Niemeyer, S., Gerlach, D., Hodge, V., Bertine, K. K., and Padova, A., 1991. Osmium in marine sediments. *Geochimica et Cosmochimica Acta* **55**, 1641-1648.

Kröner, A. and Cordani, U., 2003. African, southern Indian and South American cratons were not part of the Rodinia supercontinent: evidence from field relationships and geochronology. *Tectonophysics* **375**, 325-352.

Lahondère D., Thieblemont D., Goujou J.C., Roger J., Moussine-Pouchkine A., Le Metour J., Cocherie A., Guerrot C. 2003 - Notice explicative des cartes géologiques et gîtologiques à 1/200 000 et 1/500 000 du Nord de la Mauritanie. Volume 1. DMG, Ministère des Mines et de l'Industrie, Nouakchott.

Lambert, I. B., 1973. Post-depositional availability of sulphur and metals and formation of secondary textures and structures in stratiform sedimentary sulphide deposits. *Australian Journal of Earth Sciences: An International Geoscience Journal of the Geological Society of Australia* **20**, 205 - 215.

LeCheminant, A. N. and Heaman, L. M., 1989. Mackenzie Igneous Events, Canada - Middle Proterozoic Hotspot Magmatism Associated with Ocean Opening. *Earth and Planetary Science Letters* **96**, 38-48.

Levasseur, S., Birck, J., and J, A. C., 1998. Direct measurement of femtomoles of osmium and the 187Os/186Os ratio in seawater. *Science* **282**, 272-274.

Li, Z. X., Bogdanova, S. V., Collins, A. S., Davidson, A., De Waele, B., Ernst, R. E., Fitzsimons, I. C. W., Fuck, R. A., Gladkochub, D. P., Jacobs, J., Karlstrom, K. E., Lu, S., Natapov, L. M., Pease, V., Pisarevsky, S. A., Thrane, K., and Vernikovsky, V., 2008. Assembly, configuration, and break-up history of Rodinia: A synthesis. *Precambrian Research* **160**, 179-210.

Lottaroli, F., Craig, J. and Thusu, B, 2009. Neoproterozoic-Early Cambrian (Infracambrian) Hydrocarbon Prospectivity of North Africa: a synthesis. In: Craig, J., Thurow, J., Thusu, B., Whitham, A. & Abutarruma, Y. (Ed.), *Global Neoproterozoic Petroleum Systems: The emerging potential in North Africa*. Geological Society of London, London. **326,** 137-156.

Ludwig, K., 2003. Isoplot/Ex, version 3: a geochronological toolkit for Microsoft Excel. *Geochronology Center Berkeley*.

Ludwig, K. R., 1980. Calculation of uncertainties of U-Pb isotope data. *Earth and Planetary Science Letters* **46**, 212-220.

Morton, J. P. and Long, L. E., 1982. Rb-Sr Dating of Illite Diagenesis. *AAPG Bulletin-American Association of Petroleum Geologists* **66**, 610-610.

Moussine-Pouchkine, A. and Bertrand-Sarfati, J., 1997. Tectonosedimentary subdivisions in the Neoproterozoic to Early Cambrian cover of the Taoudenni Basin (Algeria-Mauritania-Mali). *Journal of African Earth Sciences* **24**, 425-443.

Noble, S. R., Hyslop, E. K., and Highton, A. J., 1996. High-precision U-Pb monazite geochronology of the c.806 Ma Grampian shear zone and the implications for the evolution of the central highlands of Scotland. *Journal of the Geological Society* **153**, 511-514.

Nowell, G. M., Luguet, A., Pearson, D. G., and Horstwood, M. S. A., 2008. Precise and accurate 186Os/188Os and 187Os/188Os measurements by multi-collector plasma ionisation mass spectrometry (MC-ICP-MS) part I: Solution analyses. *Chemical Geology* **248**, 363-393.

Odin, G. S., Hunziker, J.C., 1982. Radiometric Dating of the Albian-Cenomanian. In: Odin, G. S. (Ed.), *Numerical Dating in Stratigraphy Part 1*. John Wiley & Sons, pp. 537-557.

Ogg, J. G., Ogg, G. and Gradstein, F.M., 2008. *The Concise Geologic Time Scale*. Cambridge University Press, Cambridge.

Ohr, M., Halliday, A. N., and Peacor, D. R., 1991. Sr and Nd Isotopic Evidence for Punctuated Clay Diagenesis, Texas Gulf-Coast. *Earth and Planetary Science Letters* **105**, 110-126.

Onstott, T. C. and Hargraves, R. B., 1981. Proterozoic Transcurrent Tectonics - Paleomagnetic Evidence from Venezuela and Africa. *Nature* **289**, 131-136.

Oxburgh, R., 1998. Variations in the osmium isotope composition of seawater over the past 200,000 years. *Earth and Planetary Science Letters* **159**, 183-191.

Pattison, D. R. M., 2006. The fate of graphite in prograde metamorphism of pelites: An example from the Ballachulish aureole, Scotland. *Lithos* **88**, 85-99.

Peters, K. E., 1986. Guidelines for evaluating programmed pyrolysis. *American Association of Petroleum Geologists Bulletin* **70**, 318-329.

Peucker-Ehrenbrink, B. and Jahn, B.-m., 2001. Rhenium-osmium isotope systematics and platinum group element concentrations: Loess and the upper continental crust. *Geochem. Geophys. Geosyst.* **2**.

Rainbird, R. H., McNicoll, V. J., and Heaman, L. M., 1994. Detrital zircon studies of Neoproterozoic quartzarenites from north-western Canada: Additional support for an extensive river system originating from Grenville orogen *Eighth International Conference on Geochronology*. U.S. Geological Survey Circular, Berkeley, California, p.258.

Ravizza, G. and Peucker-Ehrenbrink, B., 2003. Chemostratigraphic evidence of Deccan volcanism from the marine osmium isotope record. *Science* **302**, 1392-1395.

Ravizza, G. and Turekian, K. K., 1989. Application of the 187Re-187Os system to black shale geochronometry. *Geochimica et Cosmochimica Acta* **53**, 3257-3262.

Raymond, A. C. and Murchison, D. G., 1988. Development of organic maturation in the thermal aureoles of sills and its relation to sediment compaction. *Fuel* **67**, 1599-1608.

Renne, P. R., Cassata, W. S., and Morgan, L. E., 2009. The isotopic composition of atmospheric argon and 40Ar/39Ar geochronology: Time for a change? *Quat Geochronol* **4**, 288-298.

Renne, P. R., Knight, K. B., Nomade, S., Leung, K.-N., and Lou, T.-P., 2005. Application of deuteron-deuteron (D-D) fusion neutrons to 40Ar/39Ar geochronology. *Appl Radiat Isotopes* **62**, 25-32.

Renne, P. R., Sharp, Z. D., and Heizler, M. T., 2008. Cl-derived argon isotope production in the CLICIT facility of OSTR reactor and the effects of the Cl-correction in 40Ar/39Ar geochronology. *Chemical Geology* **255**, 463-466.

Renne, P. R., Swisher, C. C., Deino, A. L., Karner, D. B., Owens, T. L., and DePaolo, D. J., 1998. Intercalibration of standards, absolute ages and uncertainties in 40Ar/39Ar dating. *Chemical Geology* **145**, 117-152.

Rocci, G., Bronner, G. & Deschamps, M., 1991. Crystalline Basement of the West African Craton, in: Dallmeyer, R. D. L., J.P. (Ed.), *The West African Orogens and Circum-Atlantic Correlatives*. Springer, Berlin, pp. 31-65.

Schofield, D. I. and Gillespie, M. R., 2007. A tectonic interpretation of "Eburnean terrane" outliers in the Reguibat Shield, Mauritania. *Journal of African Earth Sciences* **49**, 179-186.

Schofield, D. I., Horstwood, M. S. A., Pitfield, P. E. J., Crowley, Q. G., Wilkinson, A. F., and Sidaty, H. C. O., 2006. Timing and kinematics of Eburnean tectonics in the central Reguibat Shield, Mauritania. *Journal of the Geological Society* **163**, 549-560.

Selby, D., 2007. Direct Rhenium-Osmium age of the Oxfordian-Kimmeridgian boundary, Staffin bay, Isle of Skye, U.K., and the Late Jurassic time scale. *Norwegian Journal of Geology* **87**, 9.

Selby, D. and Creaser, R. A., 2003. Re-Os geochronology of organic rich sediments: an evaluation of organic matter analysis methods. *Chemical Geology* **200**, 225-240.

Selby, D. and Creaser, R. A., 2005. Direct radiometric dating of the Devonian-Mississippian time-scale boundary using the Re-Os black shale geochronometer. *Geology* **33**, 545-548.

Selby, D., Mutterlose, J., and Condon, D. J., 2009. U-Pb and Re-Os geochronology of the Aptian/Albian and Cenomanian/Turonian stage boundaries: Implications for timescale calibration, osmium isotope seawater composition and Re-Os systematics in organic-rich sediments. *Chemical Geology* **265**, 394-409.

Selby, D., 2009. U-Pb zircon geochronology of the Aptian/Albian boundary implies that the GL-O international glauconite standard is anomalously young. *Cretaceous Research* **30**, 1263-1267.

Smith, P. E., Evensen, N. M., York, D., and Odin, G. S., 1998. Single-Grain 40Ar-39Ar Ages of Glauconies: Implications for the Geologic Time Scale and Global Sea Level Variations. *Science* **279**, 1517-1519.

Smoliar, M. I., Walker, R. J., and Morgan, J. W., 1996. Re-Os isotope constraints on the age of Group IIA, IIIA, IVA, and IVB iron meteorites. *Science* **271**, 1099-1102.

Steiger, R. H. and Jager, E., 1977. Subcommission on Geochronology - Convention on Use of Decay Constants in Geochronology and Cosmochronology. *Earth and Planetary Science Letters* **36**, 359-362.

Sun, W., Arculus, R. J., Bennett, V. C., Eggins, S. M., and Binns, R. A., 2003a. Evidence for rhenium enrichment in the mantle wedge from submarine arc-like volcanic glasses (Papua New Guinea). *Geology* **31**, 845-848.

Teal, D. A. J., Kah, L.C., 2005. Using C-isotopes to constrain intrabasinal stratigraphic correlations: Mesoproterozoic Atar Group, Mauritania. *Geological Society of America Abstracts with Programs*. **37,** 45.

Trompette, R., 1973. Le Précambrien supérieur et le Paléozoïque inferieur de l'Adrar de Mauritanie (bordure occidentale de Bassin de Taoudeni, Afrique de l'Oust). Un exemple de sédimentation de craton. Etude stratigraphique et sédimentologique.

Trompette, R., 1994. *Geology of Western Gondwana (2000 - 500 Ma).* Balkema, Rotterdam. pp. 350.

Turgeon, S. C., Creaser, R. A., and Algeo, T. J., 2007. Re-Os depositional ages and seawater Os estimates for the Frasnian-Famennian boundary: Implications for weathering rates, land plant evolution, and extinction mechanisms. *Earth and Planetary Science Letters* **261**, 649-661.

Verati, C., Bertrand, H., and Féraud, G., 2005. The farthest record of the Central Atlantic Magmatic Province into West Africa craton: Precise 40Ar/39Ar dating and geochemistry of Taoudenni basin intrusives (northern Mali). *Earth and Planetary Science Letters* **235**, 391-407.

Villeneuve, M. and Cornée, J. J., 1994. Structure, evolution and paleogeography of the West African craton and bordering belts during the Neoproterozoic. *Precambrian Research* **69**, 307-326.

Vogel, N. and Renne, P. R., 2008. Ar-40-Ar-39 dating of plagioclase grain size separates from silicate inclusions in IAB iron meteorites and implications for the thermochronological evolution of the IAB parent body. *Geochimica Et Cosmochimica Acta* **72**, 1231-1255.

Yang, G., Hannah, J. L., Zimmerman, A., Stein, H. J., and Bekker, A., 2009. Re-Os depositional age for Archean carbonaceous slates from the south-western Superior Province: Challenges and insights. *Earth and Planetary Science Letters* **280**, 83-92.

Zhao, G., Sun, M., Wilde, S. A., Li, S., and Zhang, J., 2006. Some key issues in reconstructions of Proterozoic supercontinents. *Journal of Asian Earth Sciences* **28**, 3-19.

Chapter Three –Re-Os geochronology of the Neoproterozoic - Cambrian Dalradian Supergroup of Scotland and Ireland: Implications for Neoproterozoic stratigraphy, glaciations and Re-Os systematics

Re-Os geochronology of the Neoproterozoic – Cambrian Dalradian Supergroup of Scotland and Ireland: Implications for Neoproterozoic stratigraphy, glaciations and Re-Os systematics*

*A version of this chapter has been submitted for publication in Precambrian Research, co-authored by David Chew of Trinity College, Dublin and David Selby of Durham University.

3.1 Introduction

Neoproterozoic strata record a number of significant events such as the transition from stratified Proterozoic oceans with oxic surface waters and anoxic deep waters to a more-or-less fully oxygenated ocean (Anbar and Knoll, 2002; Knoll, 2003; Fike et al., 2006; Halverson and Hurtgen, 2007; Canfield et al., 2008). Major changes in biological systems and evolutionary developments occurred towards the end of the Proterozoic including the evolution of metazoans (Logan et al., 1995, 1997; Vidal and Moczydlowska-Vidal, 1997; Jensen et al., 2000; Martin et al., 2000; Narbonne and Gehling, 2003; Knoll et al., 2006; Macdonald, 2010a,b). Additionally, the Neoproterozoic was a time of major climatic fluctuation with a number of extreme glacial events recorded in the rock record (e.g., the "Snowball Earth" of Kirschvink, 1992; Hoffman et al., 1998; Hoffman and Schrag, 2002 or the "Slushball Earth" of Hyde et al., 2000). However, there is, at present, no consensus as to the cause, extent, duration or number of these glacial events (Kennedy et al., 1998; Evans, 2000; Fairchild and Kennedy, 2007). The lack of precise and accurate geochronological data has severely hindered attempts to develop a chronological framework for the Neoproterozoic. In particular, understanding and constraining the extent

and duration of these glacial events has relied upon lithostratigraphy and chemostratigraphy with only a few glaciogenic successions constrained by robust geochronological data (Hoffmann et al., 2004; Zhou et al., 2004; Kendall et al., 2004; 2006; 2009a; Condon et al., 2005; Bowring et al., 2007; Macdonald et al., 2010a).

During the Neoproterozoic, the continental masses of Laurentia, Baltica and Amazonia were juxtaposed as a result of various orogenic events to form the supercontinent Rodinia (Li et al., 2008 and references therein). During the break-up of Rodinia which commenced ca. 750 Ma there was a period of intracontinental extension and basin genesis along the eastern margin of Laurentia (Harris et al., 1994; Soper, 1994; Cawood et al., 2007). Scotland occupied a unique position within the Rodinia supercontinent lying close to the junction of the Laurentian, Baltica and Amazonian continental blocks (Dalziel, 1994). The sedimentary basins that formed during the formation and breakup of Rodinia are preserved in Scotland as the Torridonian, Moine and Dalradian Supergroups (Anderton, 1982, 1985; Rainbird et al., 2001; Strachan et al., 2002; Cawood et al., 2003, 2004, 2007).

The Dalradian Supergroup of Scotland and Ireland is a metasedimentary succession which records deposition on the eastern margin of Laurentia during the late Neoproterozoic and Early Cambrian (existing constraints imply the base is younger than 800 Ma and it extends to at least 510 Ma; Harris et al., 1994; Smith et al., 1999; Prave et al., 2009a). Despite its importance in regional and global studies of the Proterozoic, our understanding of the Dalradian suffers from a lack of absolute radiometric ages (Halliday et al., 1989; Dempster et al., 2002). In an attempt to improve the chronostratigraphy of the Dalradian, several workers have applied lithostratigraphic and chemostratigraphic tools with varying levels of success (Prave, 1999; Brasier and Shields, 2000; Condon and Prave, 2000; Thomas et al., 2004; McCay et al., 2006; Prave et al., 2009a; Sawaki et al., 2010). These studies have improved our knowledge of the Proterozoic ocean chemistry and the environmental conditions of deposition within the Dalradian sedimentary basins. However, chemostratigraphic tools cannot provide absolute age data and ultimately rely upon correlation with sequences which have robust radiometric and / or biostratigraphic age constraints (Melezhik et al., 2001, 2007; Fairchild and Kennedy, 2007; Jiang et al., 2007; Meert, 2007; Giddings and Wallace, 2009; Frimmel, 2010). As a result, obtaining precise and accurate radiometric ages remain a priority for resolving many of the issues regarding global correlations of Proterozoic sedimentary successions.

The rhenium-osmium (Re-Os) geochronometer has been shown to provide robust depositional ages even for sedimentary rocks that have experienced hydrocarbon maturation, greenschist metamorphism and flash pyrolysis associated with igneous intrusions (Creaser et al., 2002; Kendall et al., 2004, 2006, 2009a,b; Selby and Creaser, 2005; Rooney et al., 2010). Thus, the Re-Os system represents an accurate, precise and reliable geochronometer for providing depositional age data for the Dalradian metasediments and constructing a chronostratigraphic framework for existing and future chemostratigraphic, tectonostratigraphic and lithostratigraphic datasets.

Presented here are new Re-Os data that constrain the depositional age of a sedimentary unit from the Dalradian Supergroup. These Re-Os data provide an estimate for the osmium isotope composition of seawater in the Dalradian basin during the Neoproterozoic and ultimately provide a maximum depositional age for a key Neoproterozoic glacial horizon. A further aspect of this study involves the application of Re-Os geochronology to sedimentary units with low Re and Os abundances (≤2 ppb Re and ≤50 ppt Os) to provide accurate and precise geochronology data. Additionally, this work presents results from a sedimentary unit (Leny Limestone Formation) in which the Re-Os geochronometer has been disturbed as a result of post-depositional fluid flow. The results from this study provide us with new insights into the robustness of the Re-Os geochronometer.

3.2 Geological Setting

3.2.1 The Dalradian Supergroup

The Dalradian Supergroup of Scotland and Ireland consists of a thick (~25 km) metasedimentary succession and minor mafic volcanics deposited on the eastern margin of the Laurentian craton during the Neoproterozoic to early Cambrian (Fig. 3.1; Harris et al., 1994 and references therein). This quoted thickness of the Dalradian Supergroup is a cumulative thickness from all subgroups and is not a true reflection of sediment thickness. Deposition of the Dalradian Supergroup occurred along the eastern margin of Laurentia, close to the triple junction of Baltica, Laurentia and Amazonia (Soper, 1994; Dalziel, 1994).

Many aspects of basin genesis have proved controversial, with little consensus apparent even after more than a century of study. Most models for Dalradian deposition invoke a

large (10^6 km^2), shallow-marine, ensialic basin which underwent prolonged extension during the late Neoproterozoic, resulting in the eventual separation of Laurentia from western Gondwana at ca. 550 Ma (Hoffman, 1991; Soper, 1994; Dalziel and Soper, 2001). An alternative model proposes that the lower portions of the Dalradian represented a rapidly formed foredeep basin associated with the mid-Neoproterozoic (840 – 730 Ma) Knoydartian Orogeny (Prave, 1999). In both models extensional tectonics played a major role in the genesis of the upper portions of the Dalradian basin during the latest Neoproterozoic to Early Cambrian.

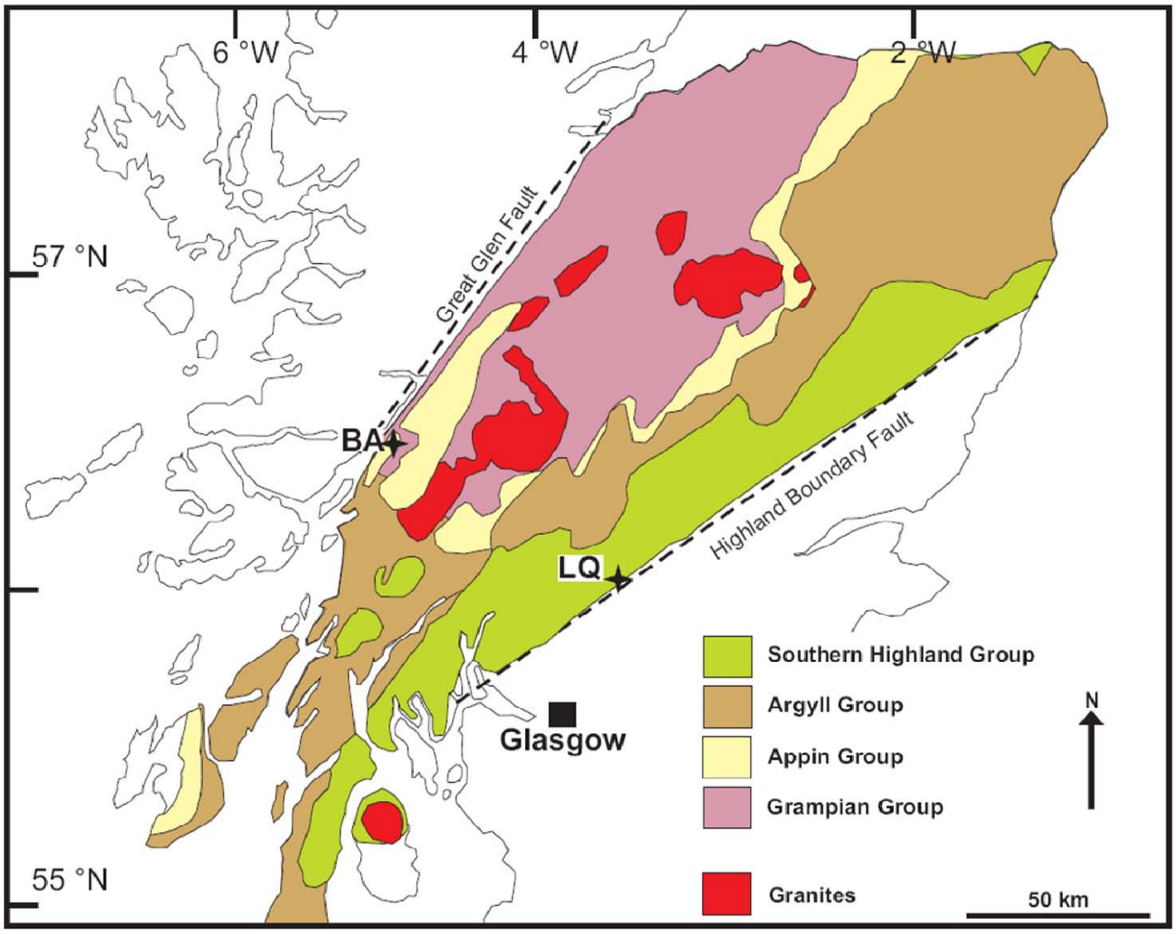

Fig. 3.1 Simplified geological and location map highlighting the fourfold division of the Dalradian Supergroup of the Grampian Terrane (modified from Harris et al., 1994; Thomas et al., 2004). Abbreviations of sampling locations: BA – Ballachulish Slate quarry; LQ - Leny Limestone quarry.

Lithostratigraphic correlation of the Dalradian Supergroup is hampered by the paucity of volcanic horizons suitable for U-Pb geochronology and the lack of biostratigraphically diagnostic fossils (Fig. 3.2). Additionally, many portions of the Dalradian sequence exhibit extreme facies variability along strike having experienced complex polyphase deformation and metamorphism (Harris et al., 1994, Strachan et al.,

2002 and references therein). Despite these issues, a coherent lithostratigraphy has been established from western Ireland to the Shetland Islands, 200 km north of mainland Scotland (Harris et al., 1994). The Dalradian Supergroup consists of four groups which are from oldest to youngest; the Grampian, Appin, Argyll and Southern Highland Groups (Figs. 3.1 and 3.2).

The basal Grampian Group crops out primarily in the Central Highlands although possible correlatives exist on the north Grampian coast and on the Shetland Islands (Strachan et al., 2002). The Grampian Group consists of up to 7 km of predominantly marine, quartzo-feldspathic psammites and semi-pelites (Glover and Winchester, 1989; Harris et al., 1994). This sedimentary succession displays sharp lateral variations typical of a synrift origin (Soper and England, 1995; Banks et al., 2007). The overlying Appin Group is exposed in a broad zone throughout Scotland and Ireland as far north as the Shetland Islands. The Appin Group consists of up to 4 km of quartzite, semi-pelites and phyllites deposited as a post-rift, thermal subsidence sequence (Litherland, 1980; Glover et al., 1995; Soper and England, 1995; Glover and McKie, 1996). The overlying Argyll Group records rapid deepening of the basin following the shallow marine conditions of the Appin Group (Anderton, 1985). The Argyll Group consists of a thick heterogeneous succession of shelf sediments up to 9 km thick which passes upwards into deep water turbidite and basinal facies and associated mafic volcanics (Anderton, 1982). The marked change from a shelf setting to deep water sedimentation is widely ascribed to the onset of syn-depositional rifting. The basal Subgroup (Islay Subgroup) of the Argyll Group is marked by a distinctive and persistent tillite horizon; the Port Askaig Formation, correlatives of which are traceable from Connemara in western Ireland to Banffshire in NE Scotland (Anderton, 1985; Harris et al., 1994). The Southern Highland Group (along with the newly defined Trossachs Group of Tanner and Sutherland, 2007) marks the top of the Dalradian succession and consists of ca. 4 km of coarse-grained turbiditic clastics and volcaniclastic strata (Anderton, 1985; Soper and England, 1995). The Southern Highland Group is considered to represent the change from a period of continental rifting and rupture to that of a thermally subsiding margin (Anderton, 1985).

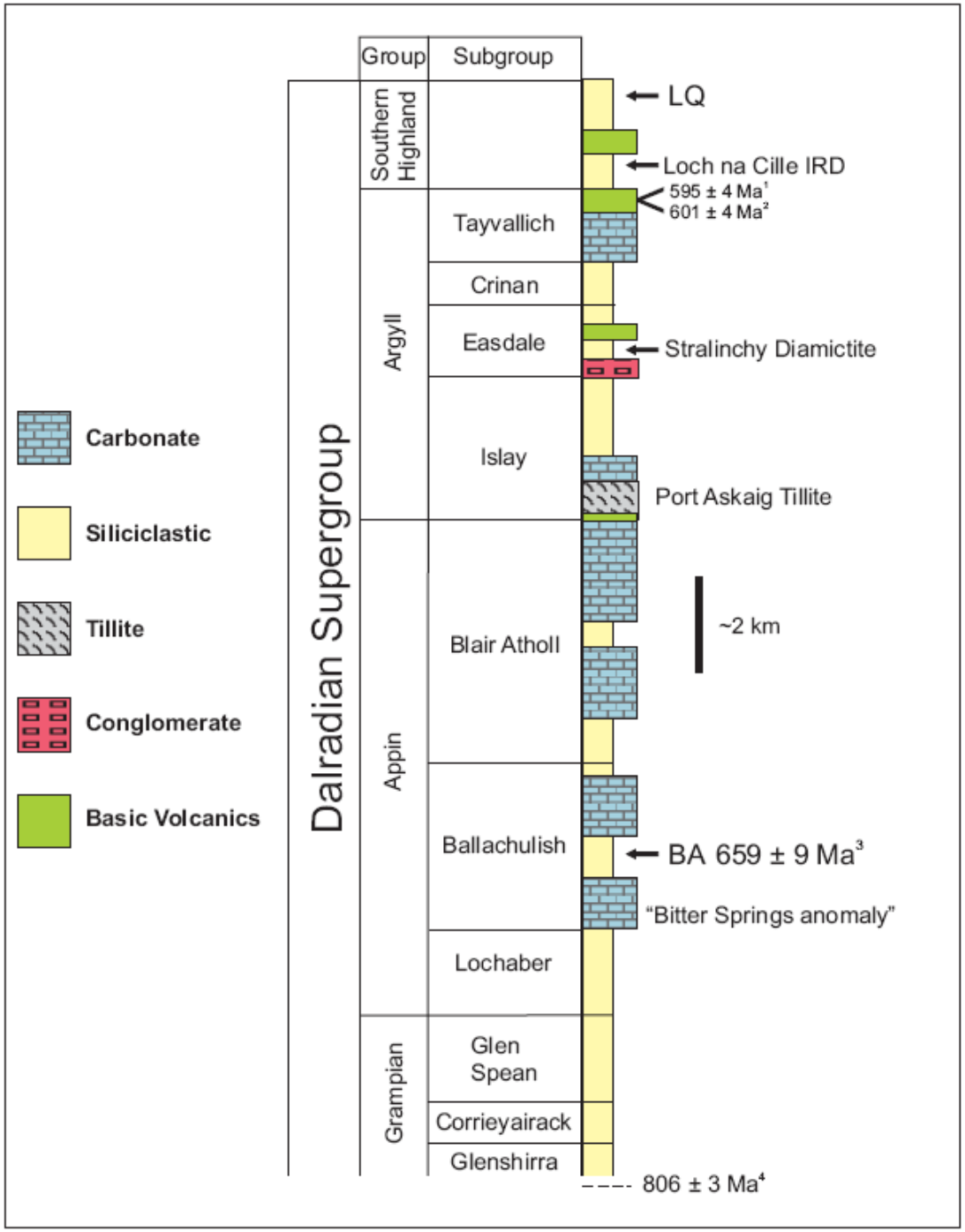

Fig. 3.2 Generalised stratigraphy of the Dalradian Supergroup with glaciogenic horizons and the purported Bitter Springs anomaly suggested by Prave et al., (2009a) but refuted by the new Re-Os geochronology data. See text for details. BA – Ballachulish Slate Formation; LQ – Leny Limestone Formation. ([1]Halliday et al., 1989; [2]Dempster et al., 2002; [3]This study; [4] Noble et al., 1996). Modified from Prave et al. (2009a)

3.2.1.1 Dalradian glaciogenic horizons and possible global correlations

The Port Askaig Formation of the Argyll Group is a thick (~900 m) succession of diamictites interbedded with sandstone, conglomerate and mudstone (Kilburn et al., 1965; Spencer, 1971; Eyles, 1988; Arnaud and Eyles, 2002). The formation represents the most persistent and distinctive glaciogenic horizon within the Dalradian Supergroup (Fig. 3.2). A glaciogenic origin was first recognised in the late nineteenth century (Thomson, 1871; 1877), and the formation is described in detail in the classic memoir of Spencer (1971). The most extensive outcrops of the Port Askaig Formation consists of ~400 m of coarse grained and poorly sorted diamictite interbedded with sandstone, mudstone and conglomerate with some megaclasts in the diamictite exceeding 100 m in size (e.g., the Great Breccia of Eileach an Naoimh; Spencer, 1971; Arnaud, 2004). Recent studies identified $\delta^{13}C$ values as high as +11.7‰ and $^{87}Sr/^{86}Sr$ values as low as 0.7067 in carbonate units above and below the Port Askaig Formation (Brasier and Shields, 2000; Sawaki et al., 2010). These data were used to correlate this glaciogenic horizon with the ca. 750 – 690 Ma global Sturtian glaciation (Brasier and Shields, 2000; Fanning and Link, 2004; McCay et al., 2006; Macdonald et al., 2010a). Two other stratigraphically younger and limited glaciogenic units within the Dalradian Supergroup have also been identified; the Stralinchy "Boulder Bed" Formation and the Inishowen - Loch na Cille Ice Rafted Debris (IRD) Formations (Fig. 3.2; Condon and Prave, 2000; McCay et al., 2006). The Stralinchy Formation occurs in the Easdale Subgroup in Donegal in NW Ireland and has been correlated with the ~635 Ma global Marinoan glaciation (Hoffmann et al., 2004; Condon et al., 2005; McCay et al., 2006). The Loch na Cille and Inishowen glaciogenic formations occur within the uppermost Argyll Group and basal Southern Highland Group respectively, and have been correlated with the 580 Ma Laurentian Gaskiers glacial event (Condon and Prave, 2000; Bowring et al., 2003).

3.2.2 Current chronological constraints for the Dalradian Supergroup

With the exception of *Bonnia-Ollenellus* Zone Early Cambrian trilobites and inarticulate brachiopods of the upper Southern Highland Group, the Dalradian Supergroup is almost entirely devoid of fossils (Pringle, 1939; Fletcher and Rushton, 2007). In addition,

absolute chronological constraints on the age of Dalradian sedimentation are also very sparse (Fig. 3.2). The oldest phase of volcanic activity in the Dalradian Supergroup occurs within correlatives of the Port Askaig Formation in NE Scotland (Chew et al., 2010). However, this thin tholeiitic pillow basalt has not been dated thus far. The lower part of the Southern Highland Group in SW Scotland is characterised by ca. 2 km of tholeiitic mafic volcanic rocks and sills (Tayvallich Volcanic Formation). The Tayvallich Formation is cross cut by a 595 ± 4 Ma (U-Pb SHIRIMP) keratophyre intrusion and a felsic tuff from this formation has yielded a U-Pb zircon age of 601 ± 4 Ma (Halliday et al., 1989; Dempster et al., 2002). Pegmatites from the Central Scottish Highlands provide a U-Pb monazite age of 806 ± 3 Ma although the stratigraphic position of these pegmatites remains controversial (Noble et al., 1996). These pegmatites have been suggested to intrude into the Grampian Group thus providing a minimum age for these sediments (Noble et al., 1996; Highton et al., 1999). However, more recent work proposes that the pegmatites intrude into the Dava and Glen Banchor successions which lie unconformably below the Grampian Group and thus the Grampian Group is younger than 806 Ma (Smith et al., 1999; Strachan et al., 2002).

Numerous studies have utilised $\delta^{13}C$, $\delta^{18}O$ and $^{87}Sr/^{86}Sr$ data from several different carbonate units of the Dalradian Supergroup with the aim of correlation with global chemostratigraphic curves (Brasier and Shields, 2000; Thomas et al., 2004; McCay et al., 2006; Halverson et al., 2007a,b; Prave et al., 2009a; Sawaki et al., 2010). A composite C-isotope profile for the Dalradian Supergroup has been used to tentatively correlate the Ballachulish Limestone of the Appin Group with the ca. 800 Ma Bitter Springs anomaly (Prave et al., 2009a; Fig. 3.2). Additional correlations include the pre-Marinoan Trezona anomaly and ca. 635 Ma Marinoan-equivalent cap carbonate sequence with units of the middle Easdale Subgroup and the terminal Proterozoic (ca. 600 – 551 Ma) Shuram-Wonoka anomaly in the Girlsta Limestone on Shetland (Melezhik et al., 2008; Prave et al., 2009a,b).

3.2.3 Metamorphism and deformation of the Dalradian Supergroup

The Dalradian Supergroup of Scotland is one of the classic areas for the study of regional and contact metamorphism (e.g., Barrow, 1893; Tilley, 1925; Baker, 1985; Voll et al., 1991; Dempster et al., 1992; Pattison and Harte, 1997). The main phases of regional metamorphism took place during the Grampian Orogeny. The Grampian Orogeny is

understood to be related to the collision of Laurentia with an oceanic arc during the Early Ordovician and can be considered broadly equivalent to the Taconic Orogeny of the Appalachians (Dewey and Mange, 1999; Soper et al., 1999). Geochronological constraints for the Grampian Orogeny include U-Pb zircon ages of 475 – 468 Ma and Sm-Nd garnet crystallisation ages of 473 – 465 Ma for the age of peak metamorphism (Friedrich et al., 1999; Baxter et al., 2002).

The Dalradian sedimentary succession also experienced contact metamorphism associated with the intrusion of numerous Late Caledonian (ca. 430 – 390 Ma; Oliver, 2001) granites throughout the Grampian Terrane of Scotland (Fig. 3.1). In addition to the granites there are also a number of minor Late Palaeozoic intrusive suites recorded in the Dalradian (Neilson et al., 2009 and references therein).

3.3 Samples for this study

Two localities were chosen for Re-Os geochronology analyses; the Ballachulish Slate Formation from the Ballachulish Subgroup of the Appin Group and the Leny Limestone Formation of the Southern Highland Group (Figs. 3.1 and 3.2). The Ballachulish Slate was chosen to provide a maximum age constraint on the depositional age of the Port Askaig Formation (Fig. 3.2). The Leny Limestone Formation was chosen as it contains the only biostratigraphically diagnostic fauna found in the Dalradian Supergroup (Pringle, 1939; Fletcher and Rushton, 2007). Additionally, the metasediments of the Dalradian Supergroup represent an opportunity to further our understanding of the effects of regional and contact metamorphism on the Re-Os geochronometer.

3.3.1 Appin Group – Ballachulish Slate Formation

The Appin Group consists of three Subgroups, the Lochaber, Ballachulish and Blair Atholl (Fig. 3.2). The Ballachulish Slate Formation consists of ca. 400 m of pyritiferous black slates and graphitic phyllites. Samples were collected on the eastern foreshore of Loch Linnhe at the entrance to Loch Leven (56° 42. 1’ N, 5° 11. 6’ W; Fig. 3.1). In this area, the top of the Ballachulish Slate Formation is estimated to be ca. 1 km below the equivalent of the Port Askaig Formation (Harris et al., 1994). Regional metamorphic grade associated with the Grampian Orogeny varies from chlorite grade in the NW to garnet grade in the SE. Estimates of P-T conditions range from ca. 450 - 550° C from NW to SE, at ca. 6 kbar (Pattison and Voll, 1991). In addition to Grampian regional metamorphism,

the Ballachulish Slates also experienced Late Caledonian (ca. 430 Ma) igneous activity and contact metamorphism primarily associated with the well-documented Ballachulish Igneous Complex (Pattison and Harte, 1997; Pattison, 2006). The metamorphic aureole varies in width from ca. 400 to 1700 m, based upon the first appearance of cordierite in metapelites (Pattison, 2006). Regional P-T conditions at the time of intrusion are estimated at ca. 250 – 300° C at ca. 3 kbar. The age of the Ballachulish Igneous Complex is constrained by Re-Os molybdenite and U-Pb zircon ages of 433.5 ± 1.8 Ma and 428 ± 9.8, respectively (Conliffe et al., 2010; Rogers and Dunning, 1991, recalculated by Neilson et al., 2009). Fluid flow between the intrusion and the aureole was limited and there is no evidence for a large-scale hydrothermal circulation system or associated mineralogical changes connected to the intrusion (Harte et al., 1991; Pattison, 2006).

The slates analysed in this study were sampled ca. 2 km NNW of the NW contact of the Ballachulish Igneous complex and are hence outside the aureole. The slates sampled are of chlorite metamorphic grade and are black and massive with bedding occasionally still discernible and predominantly orientated parallel to cleavage. X-ray diffractometry (XRD) studies indicate that the Ballachulish Slates have a composition of quartz, mica, chlorite and feldspars (albite and occasionally orthoclase), typical of an argillaceous slate. The samples of Ballachulish slate used in this study are similar to those described in greater detail by Walsh (2007).

3.3.2 Southern Highland Group – Leny Limestone

The Leny Limestone forms part of the Keltie Water Grit Formation of the Southern Highland Group. The formation consists of pale grey to white, siliceous grits, black graphitic slates and rare locally fossiliferous limestones (Tanner and Pringle, 1999). The limestones of this formation yield a fauna including polymerid and miomerid trilobites, brachiopods, sponges, hyoliths and bradoriids (Fletcher and Rushton, 2007). The miomerid trilobites indicate a stratigraphical age equivalent to the base of the paradoxidid Amgan Stage of Siberia traditionally regarded as Middle Cambrian (511 – 506 Ma, Landing et al., 1998). However, the polymerid trilobites e.g., *Pagetides*, are forms from the *Bonnia-Ollenellus* Zone and are thus Lower Cambrian (516.5 – 512 Ma; Blaker and Peel, 1997; Fletcher et al., 2005). An age of ca. 512 Ma has been adopted here as the age of the Leny Limestone Formation (Fletcher and Rushton, 2007).

Black graphitic slates of the Leny Limestone Formation were sampled on the south-easterly face of the Western Quarry (56° 15.5' N, 4° 13.1 W; Fig. 3.1). The formation was only weakly affected by the metamorphism of the Grampian Orogeny, for example temperatures are suggested to have not exceeded 270˚C and detrital biotite is preserved, albeit commonly partially altered to chlorite (Tanner and Pringle, 1999). The locality is also the locus of several phases of igneous activity such as intrusions of Devonian quartz felsite dykes and a Permo-Carboniferous quartz dolerite dykes (British Geological Survey, 2005; Fletcher and Rushton, 2007). The Devonian intrusion exhibits a 70 m fault offset, though this faulting is not seen in the Permo-Carboniferous dyke suggesting faulting occurred prior to this younger intrusive episode. Results from XRD on powders of the Leny Slate reveal a composition of quartz, micas (mainly muscovite), kaolinite and a serpentine-group mineral with the chemical formula of $Fe_3Si_2O_5(OH)_4$ suggested to represent berthierine (Brindley, 1982).

3.4 Sampling and analytical methods

Sampling of the Ballachulish Slate and Leny Limestone formations was limited to a stratigraphic interval of ca. 50 cm across a lateral interval of several tens of metres. Weathered material was removed from the outcrop prior to sampling of fresh surfaces. Large (~100 g) samples were selected to ensure homogenisation of Re-Os abundances in the samples (Kendall et al., 2009b). All samples were polished to remove cutting and drilling marks to eliminate any contamination. The samples were dried at 60 °C for ~12 hrs and then crushed to a fine powder of ~30 μm. The samples were broken into chips with no metal contact and powdered in a ceramic dish using a shatterbox.

Rhenium-osmium isotope analysis was carried out at Durham University's TOTAL laboratory for source rock geochronology and geochemistry at the Northern Centre for Isotopic and Elemental Tracing (NCIET). Approximately 1 g of sample powder was digested together with a mixed tracer (spike) solution of ^{190}Os and ^{185}Re in a Cr^{VI}-H_2SO_4 solution in a sealed carius tube at 220 °C for ~48 h (Selby and Creaser, 2003; Kendall et al., 2004). Through the use of the Cr^{VI}-H_2SO_4 digestion media it is possible to preferentially liberate the hydrogenous Re and Os components from the samples thus limiting any detrital component (Selby and Creaser, 2003; Kendall et al., 2004). Rhenium and Os were purified from the acid solution using solvent extraction ($CHCl_3$), micro-distillation and anion

chromatography methods and analysed by negative thermal ionisation mass spectrometry as outlined by Selby and Creaser (2003), and Selby (2007). The purified Re and Os fractions were loaded onto Ni and Pt filaments, respectively, (Selby et al., 2007), with the isotopic measurements conducted using a ThermoElectron TRITON mass spectrometer via static Faraday collection for Re and ion-counting using a secondary electron multiplier in peak-hopping mode for Os. Total procedural blanks during this study were 16.8 ± 0.06 pg and 0.43 ± 0.06 pg (1σ S.D. n = 3) for Re and Os respectively, with an average $^{187}Os/^{188}Os$ value of ~0.25 ± 0.11 (n = 3).

Uncertainties for $^{187}Re/^{188}Os$ and $^{187}Os/^{188}Os$ are determined by error propagation of uncertainties in Re and Os mass spectrometer measurements, blank abundances and isotopic compositions, spike calibrations and reproducibility of standard Re and Os isotopic values. The Re-Os isotopic data, 2σ calculated uncertainties for $^{187}Re/^{188}Os$ and $^{187}Os/^{188}Os$ and the associated error correlation function (rho) are regressed to yield a Re-Os date using *Isoplot V. 3.0* with a λ ^{187}Re constant of 1.666 x $10^{-11}a^{-1}$ (Ludwig, 1980; Smoliar et al., 1996; Ludwig, 2003).

To ensure and monitor long-term mass spectrometry reproducibility, in-house standard solutions of Re and Os (Durham Romil Osmium Standard [DROsS]) are repeatedly analysed at NCIET. The Re standard analysed during the course of this study is made from 99.999% zone-refined Re ribbon and is considered to have an identical Re isotopic composition to that of the AB-1 Re standard (Creaser et al., 2002; Selby and Creaser, 2003; Kendall et al., 2004). The NCIET Re standard yields an average $^{185}Re/^{187}Re$ ratio of 0.597719 ± 0.00172 (1 SD, n = 114). This is in excellent agreement with the value reported for the AB-1 standard (0.59874 ± 0.00051; Creaser et al., 2002). The Os isotope reference material (DROsS) yields an $^{187}Os/^{188}Os$ ratio of 0.10609 ± 0.00015 (1 SD, n = 36). The isotopic compositions of these solutions are identical within uncertainty to those reported by Rooney et al. (2010 and references therein).

3.5 Results

3.5.1 Ballachulish Slate Formation samples

The Ballachulish Slate samples have Re (0.29 – 1.85 ppb) and Os (25.49 – 52.20 ppt) abundances that are close to or less than that of average continental crustal values of ~1 ppb and 50 ppt, respectively (Table 3.1; Esser and Turekian, 1993; Peucker-Ehrenbrink and

Jahn, 2001; Hattori et al., 2003; Sun et al., 2003). The $^{187}Re/^{188}Os$ ratios range from 56.5 to 311.7 and the $^{187}Os/^{188}Os$ ratios range from 1.660 – 4.478 (Table 3.1). Regression of the Re-Os isotope data yields a Re-Os age of 659.6 ± 9.6 Ma (2σ, *n* = 5, Model 1, Mean Square of Weighted Deviates [MSWD] = 0.01, initial $^{187}Os/^{188}Os$ = 1.04 ± 0.03; Fig. 3.3).

3.5.1 Leny Limestone slate samples

The Leny Limestone slates are enriched in Re (46.2 – 66.1 ppb) and Os (419 – 633 ppt) in comparison to average continental crustal values of ~1 ppb and 50 ppt, respectively (Table 1). The $^{187}Re/^{188}Os$ ratios range from 898.4 to 1228.0 and the $^{187}Os/^{188}Os$ ratios range from 6.162 – 8.075 (Table 1). Regression of the Re-Os isotope data yields a Re-Os age of 310 ± 110 Ma (2σ, *n* = 9, Model 3, MSWD = 388, initial $^{187}Os/^{188}Os$ = 1.7 ± 2.0; Fig. 3.4).

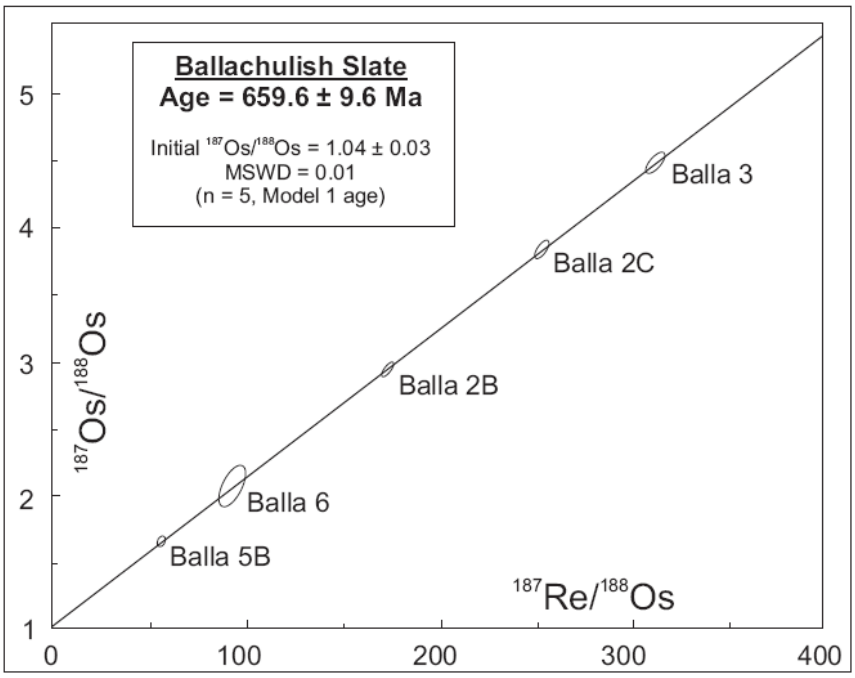

Fig. 3.3 Re-Os isochron diagram for the Ballachulish Slate Formation. A Model 1 isochron is accomplished by assuming scatter along the regression line is derived only from the input 2σ uncertainties for $^{187}Re/^{188}Os$ and $^{187}Os/^{188}Os$, and ρ (rho)

Table 3.1
Re-Os isotope data for the Ballachulish Slate and Leny Limestone Formations

Sample	Re (ppb)	±	Os (ppt)	±	^{192}Os (ppt)	±	^{187}Re/^{188}Os	±	^{187}Os/^{188}Os	±	rho[a]	Os$_i$[b]
Ballachulish Slate samples												
BA 2B	1.20	0.007	45.99	0.46	13.89	0.17	172.6	2.3	2.9440	0.0442	0.731	1.038
BA 2C	1.85	0.008	52.20	0.54	14.52	0.17	253.8	3.2	3.8413	0.0552	0.758	1.040
BA 3	1.69	0.008	40.95	0.47	10.78	0.15	311.7	4.6	4.4783	0.0723	0.813	1.038
BA 5B	0.29	0.006	29.23	0.28	10.06	0.15	56.5	1.4	1.6600	0.0286	0.482	1.036
BA 6	0.39	0.016	25.49	0.69	8.40	0.46	93.3	6.4	2.0602	0.1417	0.645	1.030
Leny Slate Samples												
LQ1	55.8	0.2	487.7	3.1	107.1	0.5	1036.8	5.6	6.874	0.033	0.716	-1.97
LQ2	55.4	0.2	431.0	3.0	89.8	0.4	1228.0	7.2	7.649	0.041	0.756	-2.83
LQ3	49.4	0.2	430.6	3.0	92.2	0.5	1065.8	6.2	7.239	0.038	0.759	-1.85
LQ4	50.9	0.2	419.2	3.0	85.0	0.4	1192.4	7.2	8.075	0.045	0.778	-2.10
LQ5	49.6	0.2	424.1	3.0	88.4	0.5	1117.0	6.7	7.642	0.042	0.771	-1.89
LQ6	51.2	0.2	443.0	3.0	92.1	0.4	1107.2	6.3	7.691	0.039	0.755	-1.76
LQ7	66.1	0.2	633.1	4.1	146.3	0.6	898.4	4.5	6.162	0.031	0.583	-1.50
LQ8	46.2	0.2	447.0	3.2	99.7	0.5	921.5	5.4	6.650	0.040	0.682	-1.21
LQ9	57.7	0.2	515.9	3.3	114.5	0.5	1001.9	5.2	6.716	0.031	0.680	-1.83

[a] Rho is the associated error correlation (Ludwig, 1980).
[b] Os_i = initial $^{187}Os/^{188}Os$ isotope ratio calculated at 659 Ma for the Ballachulish Slate samples and at 512 Ma for the Leny Slate samples

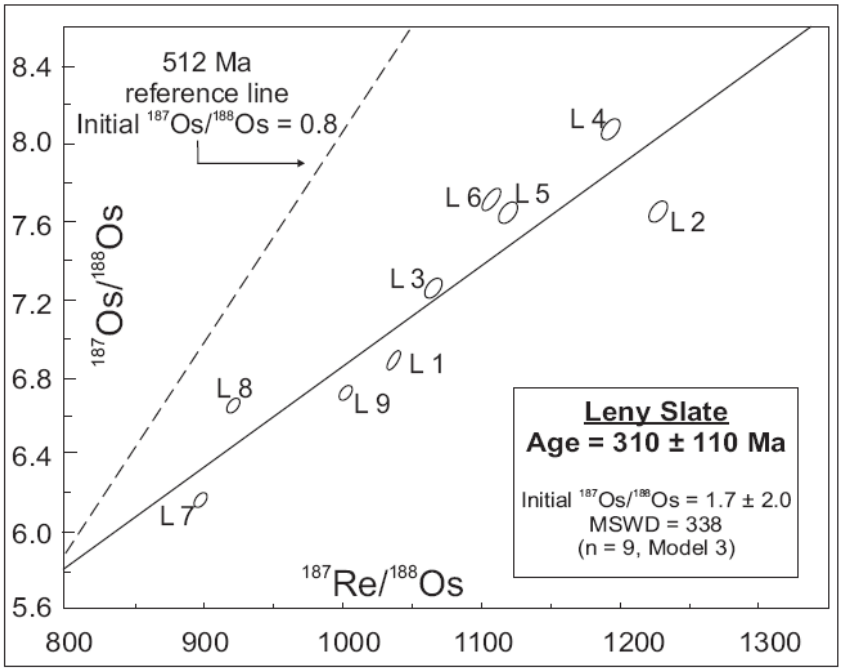

Fig. 3.4 Re-Os isochron diagram for the Leny Slate Member. The dashed line represents a 512 Ma reference line with the Osi value of 0.8 representing Cambrian seawater (Mao et al., 2002; Jiang et al., 2003). The 512 Ma age assigned for the Leny Limestone is based on a trilobite fauna (Fletcher and Rushton, 2007). See text for discussion.

3.6 Discussion

3.6.1 Implications for low Re and Os abundance geochronology

The Re-Os data for the Ballachulish Slate Formation indicate that samples with low Re and Os abundances (<2 ppb Re and <50 ppt Os) can be used to provide absolute age data (Fig. 3.3; Table 3.1). These values are similar to abundances in average continental crust which range from 0.2 – 2 ppb and 30 – 50 ppt, respectively (Esser and Turekian, 1993; Peucker-Ehrenbrink and Jahn, 2001; Hattori et al., 2003; Sun et al., 2003).

Previous work on Re-Os geochronology has focused on sedimentary units greatly enriched in Re and Os with abundances >20 ppb and 500 ppt, respectively (Ravizza et al., 1989; Cohen et al., 1999, Creaser et al., 2002; Selby and Creaser, 2005; Selby, 2007; Rooney et al., 2010). However, some recent studies have successfully applied the Re-Os geochronometer to sediments with low to moderate enrichments of Re and Os (1.7 – 50 ppb and 82 – 250 ppt, respectively; Kendall et al., 2004; 2006; 2009a,b; Selby et al., 2009; Yang et al., 2009). The Re-Os geochronology data for the Ballachulish Slate Formation

represent successful application of the Re-Os system in samples with low Re and Os abundances provided that the system has not been disturbed as discussed below.

The low Re and Os abundances do not appear to impair the robustness of the Re-Os system as the Ballachulish samples all have similar $^{187}Os/^{188}Os$ (Os_i) values, yield a large spread in present-day $^{187}Re/^{188}Os$ values (~260 units) and display positively correlative, radiogenic $^{187}Os/^{188}Os$ values indicative of a closed system (Table 3.1). This positive correlation indicates that the 659.6 ± 9.6 Ma age for the Ballachulish Slate Formation does not represent a mixing line. Additionally, if the systematics had been disturbed, any detrital Os component in these samples would represent a significant cause of geological uncertainty, resulting in an imprecise and geologically meaningless age. The highly precise age coupled with the low degree of scatter in the data, (659.6 ± 9.6 Ma and MSWD = 0.01), suggests that this is a depositional age and the Os_i value of 1.04 represents the Os isotope composition of local seawater at the time of deposition. The results from the Ballachulish Slate Formation strongly suggest that the system can be applied to sedimentary units that have low Re and Os abundances. From this it can be proposed that the system is significantly robust to provide depositional ages for strata that have experienced complex and polyphase metamorphic histories.

3.6.2 Age of Ballachulish Slate Formation

The Re-Os isotope data from the Ballachulish slates yield an age of 659.6 ± 9.6 Ma which represents the depositional age of the Ballachulish Slate Formation (Fig. 3.3). Accordingly, this Re-Os age defines a maximum age constraint for the glaciogenic Port Askaig Formation (Fig. 3.2). Taken in the context of the previous geochronological constraints for the Dalradian, the Re-Os age for the Ballachulish Slate Formation strongly suggests that the Argyll Group was deposited within ~60 Ma, prior to the eruption of the Tayvallich volcanics at ca. 600 Ma. From these two geochronological constraints, combined with the possibility that correlatives of the ca. 635 Ma Marinoan cap carbonate sequence are found within units of the Easdale Subgroup (McCay et al., 2006) it is likely that the Port Askaig Formation records a low-latitude glacial event that occurred at ca. 650 Ma.

Much of the recent work relating to the Dalradian Supergroup has focused on $\delta^{13}C$ carbonate and $^{87}Sr/^{86}Sr$ chemostratigraphy of the various carbonate units (Prave et al., 2009a and references therein; Sawaki et al., 2010). This focus on chemostratigraphy

coupled with the lack of reliable geochronology data has resulted in several attempts at correlation of the Dalradian Supergroup with better constrained Neoproterozoic strata (McCay et al., 2006; Prave et al., 2009a; Sawaki et al., 2010). The Ballachulish Limestone is ca. 200 m in thickness and passes upwards into the Ballachulish Slate (Anderton, 1982; Prave et al., 2009a). Work by Prave et al. (2009a) reported $\delta^{13}C_{carbonate}$ values as low as -7‰ for the Ballachulish Limestone and tentatively correlated this horizon with the ca. 800 Ma Bitter Springs anomaly of central Australia (Hill and Walter, 2000; Halverson et al., 2007a). However, the Re-Os data of 659.6 ± 9.6 Ma for the Ballachulish Slate Formation negates the possibility of this correlation (Fig. 3.2).

As the Dalradian basin dynamics changed from deposition on a slowly subsiding continental margin to rapid deposition within fault-bounded rift basins there is a corresponding large shift in $^{87}Sr/^{86}Sr$ of the limestones from the Appin and Argyll Groups (0.7064 – 0.7096; Thomas et al., 2004). This considerable shift in $^{87}Sr/^{86}Sr$ has been explained by a rapid rise in global seawater $^{87}Sr/^{86}Sr$ between 600 and 535 Ma that resulted from increased continental input associated with the Pan-African collision (Jacobsen and Kaufman, 1999). The upper Argyll Group was deposited over a period of up to 60 Ma in fault-bounded sub-basins as the Dalradian basin experienced increasing tectonic instability and syn-depositional faulting (Anderton, 1982; 1985). This duration of sedimentation for the Argyll Group is geologically more probable given the dynamic tectonic regime than the ca. 120 Ma required by chemostratigraphic and lithostratigraphic correlations of the Port Askaig Formation with various glaciogenic units of 715 Ma "Sturtian" age (Prave, 1999; Brasier and Shields, 2000; Prave et al., 2009a). Additionally, the Re-Os age data here negates the need for any putative unconformity within the Argyll Group which has been suggested many times although never convincingly documented despite more than a century of rigorous research (cf. Hutton and Alsop, 2004 and Tanner et al., 2005).

The new Re-Os geochronology data provide a more precise chronostratigraphic framework for understanding the tectonic evolution of the Dalradian basin and the onset of sedimentation within the basin. Furthermore, the Re-Os geochronology helps refine Neoproterozoic palaeogeographies related to the formation and breakup of the Rodinia supercontinent (e.g., Li et al., 2008).

3.6.3 Implications for global correlations involving the glacial Port Askaig Formation

At present, global correlation schemes for Neoproterozoic glaciogenic deposits are largely dependent on correlation of two distinctive types of diamictite cap-carbonate pairs. These have been designated as "Sturtian" and "Marinoan" events after the type localities in southern Australia (Kennedy et al., 1998; Hoffman and Schrag, 2002; Halverson et al., 2005; Corsetti and Lorentz, 2006). The "Sturtian" term however, is also used to define much older glacial events than the Sturtian *sensu stricto* of the Adelaide Rift Complex which has geochronological constraints for deglaciation of ca. 650 – 660 Ma (Preiss, 2000; Kendall et al., 2009a and references therein). These older glacial events assigned to the "Sturtian" have geochronological constraints which indicate low-latitude global glaciation at ca. 715 Ma based on U-Pb zircon data (Bowring et al., 2007; Macdonald et al., 2010a). In this summary, they are referred to as middle Cryogenian (ca. 715 Ma; Plumb, 1991) deposits to distinguish them from younger Sturtian (*sensu stricto)* glacial deposits on the Australian craton at ca. 650 – 660 Ma.

Early work on correlation of the Port Askaig Formation (Fig. 3.2) suggested a possible correlation with North Atlantic Varangerian tillite sequences based on Rb-Sr diagenetic illite ages of ca. 630 Ma (Hambrey, 1983; Fairchild and Hambrey, 1995; Gorokhov et al., 2001). Correlation of the Port Askaig Formation with the Varangerian tillite was supported by $^{87}Sr/^{86}Sr$ chemostratigraphy of Dalradian limestones that indicate that the base of the Dalradian Supergroup is younger than ca. 800 Ma and may be as young as ca. 700 Ma (Thomas et al., 2004). This correlation is difficult to support as the geochronological constraints for the Varangerian glaciation are based upon Rb-Sr illite geochronology which may not represent a depositional age (Morton and Long, 1982; Ohr et al., 1991; Awwiller, 1994; Evans, 1996; Gorokhov et al., 2001; Selby, 2009).

Recent work has rejected the correlation of the Port Askaig Formation and the Varangerian glaciation. Instead, $\delta^{13}C$ and $^{87}Sr/^{86}Sr$ profiles from the underlying Islay Limestone and overlying Bonahaven Formation have been used to suggest a middle Cryogenian (ca. 715 Ma) age for the Port Askaig Formation (Brasier and Shields, 2000; Prave et al., 2009a). Further 'evidence' for a 715 Ma middle Cryogenian age for the Port Askaig Formation is the presence of younger glaciogenic units in the Dalradian, namely the Stralinchy-Reelan (a possible Marinoan correlative) and the Inishowen-Loch na Cille Formations (a possible Gaskiers correlative; Condon and Prave, 2000; McCay et al., 2006).

However, the Re-Os date of 659.6 ± 9.6 Ma for the Ballachulish Slate Formation refutes the notion that the Port Askaig Formation is a component of a middle Cryogenian (ca. 715 Ma) glaciation. As reported above, the Re-Os geochronology data, coupled with existing age constraints on the Tayvallich volcanics strongly suggest that the Port Askaig Formation records a glacial event on the eastern margin of Laurentia at ~650 Ma (Fig. 3.5).

Palaeomagnetic constraints from Laurentia during the Neoproterozoic indicate that Laurentia (and hence the Port Askaig Formation) was at low latitudes from 723 – 614 Ma (see Trinidade and Macouin, 2007 and references therein). Similarly, the Sturtian (*sensu stricto*) glaciations on the Australian craton were also at low latitude and Re-Os geochronology of post-glacial rocks indicates an age of ~650 Ma for these glacial deposits. The Ballachulish Slate Formation Re-Os geochronology implies that the Port Askaig Formation could be correlated with the ~650 Ma Sturtian (*sensu stricto*) deposits of the Adelaide Rift Complex (Preiss, 2000; Kendall et al., 2006; 2009a). This suggestion is also supported by the Os_i data for the Ballachulish Slate, Upper Black River Dolomite and Tapley Hill formations as discussed below (Fig. 3.5; Kendall et al., 2006; 2009a; This study).

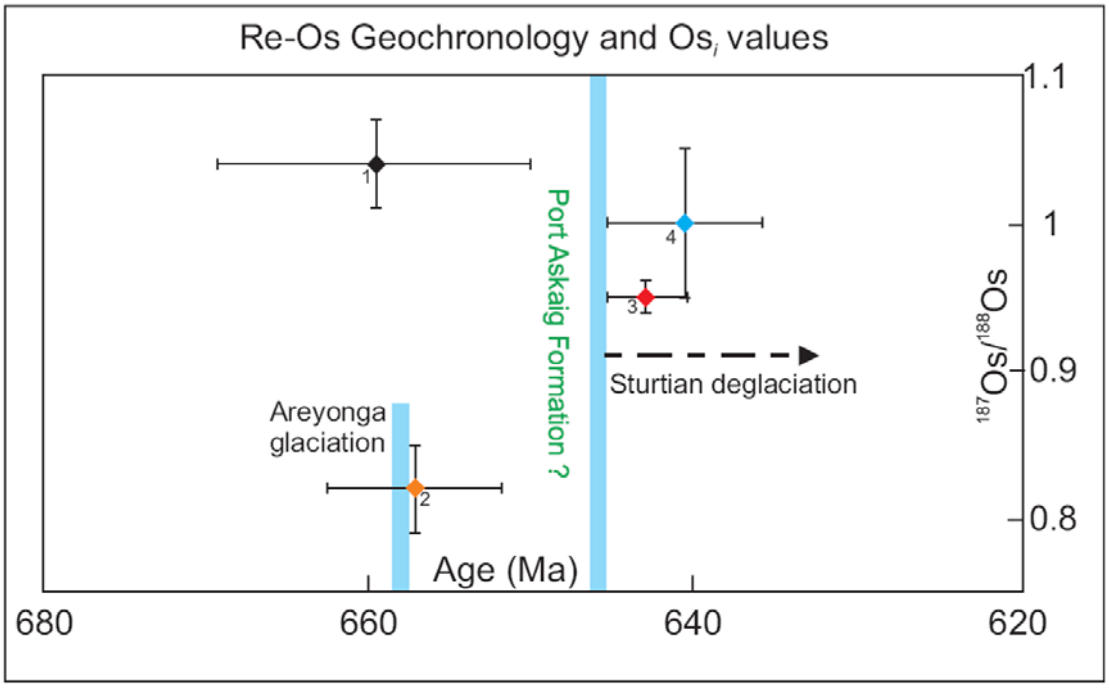

Fig. 3.5 Graphic illustration of Re-Os geochronology data and Os_i values for Cryogenian and Sturtian (*sensu stricto*) pre- and post-glacial horizons. See text for discussion. Data from 1 = Ballachulish Slate Formation (this study); 2 = Aralka Formation (Kendall et al., 2006); 3 = Tapley Hill Formation (Kendall et al., 2006); 4 = Black River Dolomite (Kendall et al., 2009a)

3.6.4 Os isotopic composition of seawater at 660 Ma

The initial Os_i values determined from the regression of the Re-Os isotope data (Table 3.1; Figs. 3.3 and 3.4) are interpreted to reflect the Os isotope composition of seawater at the time of deposition (Ravizza and Turekian, 1989; Cohen et al., 1999; Selby and Creaser, 2003). The Os isotope composition for seawater at the time of deposition of the Ballachulish Slate (1.04 ± 0.03) is identical, within uncertainty, to that of the present day Os isotopic composition of seawater (~1.06; Peucker-Ehrenbrink and Ravizza, 2000 and references therein). The radiogenic Os_i value from the Ballachulish Slate Formation demonstrates that the contribution of radiogenic Os from riverine inputs and weathering of upper continental crustal material (present-day riverine inputs of $^{187}Os/^{188}Os$ ~1.5; Levasseur et al., 1999) dominated over the influx of unradiogenic Os from cosmic dust and hydrothermal alteration of oceanic crust and peridotites (present-day $^{187}Os/^{188}Os$ ~ 0.13; Walker et al., 2002a, b).

The radiogenic values for the Os_i of the Ballachulish Slate Formation closely match values for the post-glacial Upper Black River Dolomite, Aralka and Tapley Hill Formations of southern Australia (1.04; 1.00; 0.82; 0.95, respectively; Kendall et al., 2006; 2009a). Although there are many contrasting palaeomagnetic reconstructions of the Laurentian and Australian cratons, most models indicate that during the Neoproterozoic these two cratons were both located at low latitude and were separated by oceanic basins that formed as a result of rifting associated with the breakup of Rodinia (Li et al., 2008 and references therein). Consequently, the very similar Os_i values reported from the pre-glacial Ballachulish and post-glacial Upper Black River Dolomite, Aralka and Tapley Hill Formations possibly represent a global Os isotope composition for the 660 – 640 Ma time interval (Kendall et al., 2006, 2009a). Additionally, this 'global' isotope composition for this interval is significantly more radiogenic than values for Mesoproterozoic seawater Os isotope composition (1.04 compared to 0.33 and 0.29; Rooney et al., 2010 and Kendall et al., 2009c). This increase in the Os isotope composition of Neoproterozoic seawater may be a result of the continental crust (the dominant source of hydrogenous Os) becoming more radiogenic over time. Additionally, falling sea levels and the exposure of rifted margins associated with the breakup of Rodinia would expose older more radiogenic continental crust to weathering associated with the Neoproterozoic glaciations. A further possibility for this increase in $^{187}Os/^{188}Os$ isotope composition for Neoproterozoic concerns the increased

oxygenation of subsurface waters during the late Neoproterozoic (Canfield and Teske, 1996; Anbar and Knoll, 2002; Canfield et al., 2007; 2008). This oxygenation of the oceans and atmosphere would result in increased chemical weathering of continental crust which, coupled with the breakup of Rodinia may result in an increase in seawater Os as seen for the Sr isotope composition of Neoproterozoic seawater (Jacobsen and Kaufman, 1999; Halverson et al., 2007b).

3.6.5 Systematics of Re-Os in Leny Limestone Formation

Although the Ballachulish Slate Formation experienced complex and polyphase metamorphism these samples yield a precise depositional age with a low degree of scatter about the linear regression of the Re-Os data (659.6 ± 9.6 Ma, MSWD = 0.01). The results for the Ballachulish Slate samples imply that anhydrous metamorphism and dehydration reactions do not adversely affect Re-Os systematics. In contrast, the Leny Limestone Formation which has also experienced regional Grampian metamorphic events has been disturbed. This suggests that this Re-Os isotope disturbance is probably related to hydration and fluid-flow events associated with Carboniferous / Permian contact metamorphism as discussed below.

The Re-Os isotope data for the Leny Limestone Formation yield a highly imprecise age of 310 ± 110 Ma (MSWD = 338) that is significantly younger than the accepted age of ca. 512 Ma based upon the trilobite fauna found in the Leny Limestone (Fletcher and Rushton, 2007). In addition, the Os_i value of 1.7 ± 2.0 is much more radiogenic than known values for Cambrian seawater (~0.8; Mao et al., 2002) and all of the Phanerozoic. The Re-Os geochronometer has been shown to be robust following hydrocarbon maturation events, greenschist facies metamorphism and flash pyrolysis thus suggesting the system is robust even after temperatures as high as 650 °C and pressures as high as 3 kbar (Creaser et al., 2002; Kendall et al., 2004, 2006, 2009; Rooney et al., 2010). Disturbance of the Re-Os systematics by chemical weathering has been identified from outcrop studies on the Ohio Shale (Jaffe et al., 2002). The Leny Limestone Formation outcrop is not significantly weathered and the samples were taken in such a way as to avoid the effects of recent chemical weathering on the outcrop. The measures undertaken to ensure that fresh samples were used for Re-Os geochronology include; removal of surficial weathering prior to collecting of large (~200 g) samples extracted from the outcrop prior to cutting which meant that any evidence of weathering e.g., iron-staining or leaching and features such as

quartz veins could be scrupulously avoided. Thus these factors are unlikely to have played a role in the Re-Os analysis of the Leny Limestone Formation.

Recent work has shown that the Re-Os geochronometer is susceptible to disturbance caused by hydrothermal fluid interaction with sedimentary units associated with the formation of a SEDEX deposit (Kendall et al., 2009c). The proximity of the Leny Limestone exposures to the Devonian and Permo-Carboniferous intrusions and associated interactions with hydrothermal fluids are likely causes of disturbance of the Re-Os systematics. In agreement with work by Kendall et al. (2009c) this study suggests that the Re-Os age for the Leny Limestone represents a disturbed dataset. The negative Os_i values calculated at 512 Ma and anomalously low age can be best explained by post-depositional mobilisation of Re and Os resulting from hydrothermal fluid flow driven by the igneous intrusions found within the Leny Quarry (Table 3.1). Possibly oxidising fluids generated by the intrusions may have leached Re and/or Os from the Leny Slate samples. The Leny Limestone slate samples all have $^{187}Re/^{188}Os$ values that plot to the right of the 512 Ma reference line suggestive of either Re gain or Os loss (Fig. 3.5). The occurrence of kaolinite, muscovite and berthierine from XRD analysis of the Leny Limestone slates suggests that these minerals are the products of retrograde reactions involving chlorite, muscovite and an Fe-rich phase such as cordierite that was driven by reactions with hydrothermal fluids (Slack et al., 1992; Abad et al., 2010).

The lack of documented mineralisation (small [<1 cm thick] dolomite veins in the limestones notwithstanding) and identifiable accessory or index minerals renders it extremely challenging to gain a full understanding of the P-T conditions of contact metamorphism in the Leny Limestone Formation. However, given that the Grampian Orogeny would have generated greenschist facies conditions it is likely that hydrothermal fluid flow driven by the Palaeozoic igneous intrusions hydrated the Leny Limestone slates resulting in retrograde reactions and the disturbance of the Re-Os geochronometer.

3.7 Conclusions

New Re-Os geochronology for the Ballachulish Slate Formation yields a depositional age of 659.6 ± 9.6 Ma providing a maximum age constraint for the overlying glaciogenic Port Askaig Formation. The relatively precise age coupled with the excellent linear fit of the Re-Os isotope data for the Ballachulish Slate Formation represents the first successful

application of the Re-Os system in samples with Re and Os abundances comparable with, or lower than, average continental crustal values. Additionally, these results strongly suggest that meaningful Re-Os geochronology data can be obtained from sedimentary successions that have experienced polyphase contact and regional metamorphism provided that thermal alteration was anhydrous.

The Re-Os geochronology presented here indicates that the Port Askaig Formation is younger than the middle Cryogenian glacial horizons bracketed at ca. 750 – 690 Ma, with which it was previously correlated. The new geochronology data for the Ballachulish Slate Formation also refutes a correlation of the underlying Ballachulish Limestone Formation with the ca. 800 Ma Bitter Springs anomaly of Australia (Hill and Walter, 2000; Halverson et al., 2007a; Prave et al., 2009a). The Re-Os geochronology provides a chronostratigraphic framework that indicates deposition of the Argyll Group occurred within a ~60 Ma interval prior to eruption of the Tayvallich Volcanics. The Re-Os data provides further support for the argument that Re-Os and U-Pb zircon geochronology are fundamental if we are to use chemostratigraphy to evaluate Neoproterozoic environments.

The Os_i value for seawater at the time of deposition of the Ballachulish Slate Formation is similar to that of the present-day value indicating that the dominant input of Os to seawater was radiogenic input from the weathering of the continental crust. Additionally, the close similarity of Os_i values from the Ballachulish Slate Formation with Sturtian (*sensu stricto*) deposits from the Australian craton indicates that the dominant source of Os to the oceans was from weathering of upper continental crust, suggesting a consistent weathering regime despite numerous glaciations.

Disturbance of Re-Os systematics in the Leny Limestone Formation is evident by a very imprecise and inaccurate age along with a negative value for the Os_i value (calculated at 512 Ma) for seawater in this biostratigraphically constrained Cambrian unit. These factors strongly suggest that the Re-Os system was disturbed in response to hydrothermal fluid flow associated with the intrusion of a number of igneous bodies during the Palaeozoic. The circulation of fluids through the Leny Limestone Formation is suggested to be the cause for the gain of Re and / or the loss of Os thus generating an imprecise age younger than the known depositional age.

3.8 References

Abad, I., Murphy, B., Nieto, F., Guiterrez-Alonso, G., 2010. Diagenesis to metamorphism transition in an episutural basin: the late Paleozoic St. Mary's Basin, Nova Scotia, Canada. *Canadian Journal of Earth Sciences*, **47,** 121-135.

Anbar, A. D., Knoll, A. H., 2002. Proterozoic ocean chemistry and evolution: A bioinorganic bridge? *Science* **297**, 1137-1142.

Anderton, R., 1982. Dalradian deposition and the late Precambrian-Cambrian history of the N Atlantic region: a review of the early evolution of the Iapetus Ocean. *Journal of the Geological Society* **139**, 421-431.

Anderton, R., 1985. Sedimentation and tectonics in the Scottish Dalradian. *Scot J Geol* **21**, 407-436.

Arnaud, E., Eyles, C. H., 2002. Catastrophic mass failure of a Neoproterozoic glacially influenced continental margin, the Great Breccia, Port Askaig Formation, Scotland. *Sedimentary Geology* **151**, 313-333.

Arnaud, E., 2004. Giant cross-beds in the Neoproterozoic Port Askaig Formation, Scotland: implications for snowball Earth. *Sedimentary Geology* **165,** 155-174.

Awwiller, D.N., 1994 Geochronology and Mass-Transfer in Gulf-Coast Mudrocks (South-Central Texas, USA) - Rb-Sr, Sm-Nd and Ree Systematics. *Chemical Geology*, **116**, 61-84.

Baker, A. J., 1985. Pressures and temperatures of metamorphism in the eastern Dalradian. *Journal of the Geological Society* **142**, 137-148.

Banks, C.J., Smith, M., Winchester, J.A., Horstwood, M.S.A., Noble, S.R., Ottley, C.J., 2007. Provenance of intra-Rodinian basin-fills: The Lower Dalradian Supergroup, Scotland. *Precambrian Research* **153,** 46-64.

Barrow, G., 1893. On an intrusion of muscovite-biotite gneiss in the southeast Highlands of Scotland and its accompanying metamorphism. *Quarterly Journal of the Geological Society of London* **19**, 330-358.

Baxter, E. F., Ague, J. J., Depaolo, D. J., 2002. Prograde temperature-time evolution in the Barrovian type-locality constrained by Sm/Nd garnet ages from Glen Clova, Scotland. *Journal of the Geological Society* **159**, 71-82.

Blaker, M.R., and Peel, J.S., 1997. Lower Cambrian trilobites from North Greenland. *Meddeleser om Grønland, Geoscience* **35,** 1-145.

Bowring, S. A., Grotzinger, J. P., Condon, D. J., Ramezani, J., Newall, M. J., Allen, P. A., 2007. Geochronologic constraints on the chronostratigraphic framework of the Neoproterozoic Huqf Supergroup, Sultanate of Oman. *Am J Sci* **307**, 1097-1145.

Brasier, M. D., Shields, G., 2000. Neoproterozoic chemostratigraphy and correlation of the Port Askaig glaciation, Dalradian Supergroup of Scotland. *Journal of the Geological Society* **157**, 909-914.

British Geological Survey, 2005. Aberfoyle. Scotland Sheet 38E. Bedrock and Superficial geology. 1:50 000. Geology Series. British Geological Survey, Keyworth, Nottingham

Brindley, G.W., 1982. Chemical compositions of berthierines, a review. *Clays and Clay Minerals,* **30,** 153-155.

Canfield, D.E., Teske, A., 1996. Late Proterozoic rise in atmospheric oxygen concentration inferred from phylogenetic and sulphur-isotope studies. *Nature* **382,** 127-132.

Canfield, D.E., Poulton, S.W. Narbonne, G.M., 2007. Late-Neoproterozoic Deep-Ocean Oxygenation and the Rise of Animal Life. *Science* **315,** 92-95.

Canfield, D. E., Poulton, S. W., Knoll, A. H., Narbonne, G. M., Ross, G., Goldberg, T., Strauss, H., 2008. Ferruginous Conditions Dominated Later Neoproterozoic Deep-Water Chemistry. *Science* **321**, 949-952.

Cawood, P. A., Nemchin, A. A., Smith, M., Loewy, S., 2003. Source of the Dalradian Supergroup constrained by U-Pb dating of detrital zircon and implications for the East Laurentian margin. *Journal of the Geological Society* **160**, 231-246.

Cawood, P. A., Nemchin, A. A., Strachan, R., Prave, T., Krabbendam, M., 2007. Sedimentary basin and detrital zircon record along East Laurentia and Baltica during assembly and breakup of Rodinia. *Journal of the Geological Society* **164**, 257-275.

Cawood, P. A., Nemchin, A. A., Strachan, R. A., Kinny, P. D., Loewy, S., 2004. Laurentian provenance and an intracratonic tectonic setting for the Moine Supergroup, Scotland, constrained by detrital zircons from the Loch Eil and Glen Urquhart successions. *Journal of the Geological Society* **161**, 861-874.

Chew, D. M., Fallon, N., Kennelly, C., Crowley, Q., Pointon, M., 2010. Basic volcanism contemporaneous with the Sturtian glacial episode in NE Scotland. *T Roy Soc Edin-Earth*.

Cohen, A. S., Coe, A. L., Bartlett, J. M., Hawkesworth, C. J., 1999. Precise Re-Os ages of organic-rich mudrocks and the Os isotope composition of Jurassic seawater. *Earth and Planetary Science Letters* **167**, 159-173.

Condon, D. J., Prave, A. R., 2000. Two from Donegal: Neoproterozoic glacial episodes on the northeast margin of Laurentia. *Geology* **28**, 951-954.

Condon, D., Zhu, M., Bowring, S., Wang, W., Yang, A., Jin, Y., 2005. U-Pb Ages from the Neoproterozoic Doushantuo Formation, China. Science, **308,** 95-98.

Conliffe, J., Selby, D., Porter, S. J., Feely, M., 2010. Re-Os molybdenite dates from the Ballachulish and Kilmelford Igneous Complexes (Scottish Highlands): age constraints for late Caledonian magmatism. *Journal of the Geological Society* **167**, 297-302.

Corsetti, F. A., Lorentz, N. J., 2006. On Neoproterozoic Cap Carbonates as Chronostratigraphic Markers.

Creaser, R. A., Sannigrahi, P., Chacko, T., Selby, D., 2002. Further evaluation of the Re-Os geochronometer in organic-rich sedimentary rocks: A test of hydrocarbon maturation effects in the Exshaw Formation, Western Canada Sedimentary Basin. *Geochimica et Cosmochimica Acta* **66**, 3441-3452.

Dalziel, I. W. D., 1994. Precambrian Scotland as a Laurentia-Gondwana Link - Origin and Significance of Cratonic Promontories. *Geology* **22**, 589-592.

Dalziel, I. W. D., Soper, N. J., 2001. Neoproterozoic Extension on the Scottish Promontory of Laurentia: Paleogeographic and Tectonic Implications. *The Journal of Geology* **109**, 299-317.

Dempster, T. J., 1992. Zoning and recrystallization of phengitic micas: implications for metamorphic equilibration. *Contrib. Mineral Petr.* **109**, 526-537.

Dempster, T. J., Rogers, G., Tanner, P. W. G., Bluck, B. J., Muir, R. J., Redwood, S. D., Ireland, T. R., Paterson, B. A., 2002. Timing of deposition, orogenesis and glaciation within the Dalradian rocks of Scotland: constraints from U-Pb zircon ages. *Journal of the Geological Society* **159**, 83-94.

Dewey, J., Mange, M., 1999. Petrography of Ordovician and Silurian sediments in the western Irish Caledonides: tracers of a short-lived Ordovician continent-arc collision orogeny and the evolution of the Laurentian Appalachian-Caledonian margin. *Geological Society, London, Special Publications* **164**, 55-107.

Esser, B. K., Turekian, K. K., 1993. The osmium isotopic composition of the continental crust. *Geochimica Cosmochimica Acta* **57**, 3093-3104.

Evans, D. A. D., 2000. Stratigraphic, geochronological, and paleomagnetic constraints upon the Neoproterozoic climatic paradox. *Am J Sci* **300**, 347-433.

Eyles, C. H., 1988. Glacially-Influenced and Tidally-Influenced Shallow Marine Sedimentation of the Late Precambrian Port Askaig Formation, Scotland. *Palaeogeography Palaeoclimatology Palaeoecology* **68**, 1-25.

Fairchild, I. J. Hambrey, M. J., 1995. Vendian basin evolution in East Greenland and NE Svalbard. *Precambrian Research* **73**, 217-233.

Fairchild, I. J., Kennedy, M. J., 2007. Neoproterozoic glaciation in the Earth System. *Journal of the Geological Society* **164**, 895-921.

Fanning, C.M., Link, P.K., 2004. U-Pb SHRIMP ages of Neoproterozoic (Sturtian) glaciogenic Pocatello Formation, southeastern Idaho. *Geology*, **32,** 881-884.

Fike, D. A., Grotzinger, J. P., Pratt, L. M., Summons, R. E., 2006. Oxidation of the Ediacaran Ocean. *Nature* **444**, 744-747.

Fletcher, T.P., Theokritoff, G., Lord, G.S., and Zeoli, G. 2005. The early paradoxidid *harlani* Fauna of Massachusetts and its correlatives in Newfoundland, Morocco and Spain. *Journal of Paleontology* **79,** 312-336.

Fletcher, T. P., Rushton, A. W. A., 2007. The Cambrian Fauna of the Leny Limestone, Perthshire, Scotland. *Earth Env. Sci. T. R. So.* **98**, 199-218.

Friedrich, A. M., Hodges, K. V., Bowring, S. A., Martin, M. W., 1999. Geochronological constraints on the magmatic, metamorphic and thermal evolution of the Connemara Caledonides, western Ireland. *Journal of the Geological Society* **156**, 1217-1230.

Frimmel, H. E., On the reliability of stable carbon isotopes for Neoproterozoic chemostratigraphic correlation. *Precambrian Research* **In Press, Corrected Proof**.

Giddings, J. A., Wallace, M. W., 2009. Facies-dependent [delta]13C variation from a Cryogenian platform margin, South Australia: Evidence for stratified Neoproterozoic oceans? *Palaeogeography, Palaeoclimatology, Palaeoecology* **271**, 196-214.

Glover, B. W., McKie, T., 1996. A sequence stratigraphical approach to the understanding of basin history in orogenic Neoproterozoic successions: an example from the central Highlands of Scotland. *Geological Society, London, Special Publications* **103**, 257-269.

Glover, B. W., Winchester, J. A., 1989. The Grampian Group: a major Late Proterozoic clastic sequence in the Central Highlands of Scotland. *Journal of the Geological Society* **146**, 85-96.

Gorokhov, I. M., Semikhatov, M. A., Mel'nikov, N. N., Turchenko, T. L., Konstantinova, G. V., Kutyavin, E. P., 2001. Rb-Sr geochronology of middle Riphean shales, the Yusmastakh Formation of the Anabar Massif, northern Siberia. *Stratigr Geo Correl+* **9**, 213-231.

Halliday, A. N., Graham, C. M., Aftalion, M., Dymoke, P., 1989. The Depositional Age of the Dalradian Supergroup - U-Pb and Sm-Nd Isotopic Studies of the Tayvallich Volcanics, Scotland. *Journal of the Geological Society* **146**, 3-6.

Halverson, G. P., Hoffman, P. F., Schrag, D. P., Maloof, A. C., Rice, A. H. N., 2005. Toward a Neoproterozoic composite carbon-isotope record. *Geological Society of America Bulletin* **117**, 1181-1207.

Halverson, G. P., Hurtgen, M. T., 2007. Ediacaran growth of the marine sulfate reservoir. *Earth and Planetary Science Letters* **263**, 32-44.

Halverson, G. P., Maloof, A. C., Schrag, D. P., Dudás, F. Ö., Hurtgen, M., 2007a. Stratigraphy and geochemistry of a ca 800 Ma negative carbon isotope interval in northeastern Svalbard. *Chemical Geology* **237**, 5-27.

Halverson, G.P., Dudás, F.Ö., Maloof, A.C., Bowring, S.A., 2007b. Evolution of the $^{87}Sr/^{86}Sr$ composition of Neoproterozoic seawater. *Palaeogeography, Palaeoclimatology, Palaeoecology* **256,** 103-129.

Hambrey, M. J., 1983. Correlation of Late Proterozoic tillites in the North Atlantic region and Europe. *Geological Magazine* **120**, 209-232.

Harris, A. L., Haselock, P.J., Kennedy, M.J., Mendum, J.R., Long, C.B., Winchester, J.A. Tanner, P.W.G., 1994. The Dalradian Supergroup in Scotland and Ireland. In: Gibbons, W., Harris, A.L. (Ed.), *A Revised correlation of Precambrian rocks in the British Isles*. Geological Society, London.

Harte, B., Pattison, D.R.M., Heuss-Assbichler, S., Hoernes, S., Masch, L., Strong, D.F., 1991. Evidence of fluid phase behaviour and controls in the intrusive complex and its aureole. In: Voll, G., Topel, J., Pattison, D.R.M., Seifert, F. (Ed.), *Equilibrium and Kinetics in Contact Metamorphism: the Ballachulish Igneous Complex and its Thermal Aureole*. Springer Verlag, Heidelberg.

Hattori, Y., Suzuki, K., Honda, M., Shimizu, H., 2003. Re-Os isotope systematics of the Taklimakan Desert sands, moraines and river sediments around the taklimakan desert, and of Tibetan soils. *Geochimica Et Cosmochimica Acta* **67**, 1203-1213.

Highton, A.J., Hyslop, E.K., Noble, S.R., 1999. U-Pb zircon geochronology of migmatization in the northern Central Highlands: evidence for pre-Caledonian (Neoproterozoic) tectonometamorphism in the Grampian block, Scotland. *Journal of the Geological Society* **156,** 1195-1204.

Hill, A. C., Walter, M. R., 2000. Mid-Neoproterozoic (~830-750 Ma) isotope stratigraphy of Australia and global correlation. *Precambrian Research* **100**, 181-211.

Hoffman, P. F., 1991. Did the Breakout of Laurentia Turn Gondwanaland Inside-Out? *Science* **252**, 1409-1412.

Hoffman, P. F., Kaufman, A. J., Halverson, G. P., Schrag, D. P., 1998. A Neoproterozoic snowball earth. *Science* **281**, 1342-1346.

Hoffman, P. F., Schrag, D. P., 2002. The snowball Earth hypothesis: testing the limits of global change. *Terra Nova* **14**, 129-155.

Hoffmann, K. H., Condon, D. J., Bowring, S. A., Crowley, J. L., 2004. U-Pb zircon date from the Neoproterozoic Ghaub Formation, Namibia: Constraints on Marinoan glaciation. *Geology* **32**, 817-820.

Hutton, D. H. W., Alsop, G. I., 2004. Evidence for a major Neoproterozoic orogenic unconformity within the Dalradian Supergroup of NW Ireland. *Journal of the Geological Society* **161**, 629-640.

Hyde, W. T., Crowley, T. J., Baum, S. K., Peltier, W. R., 2000. Neoproterozoic/snowball Earth/simulations with a coupled climate/ice-sheet model. *Nature* **405**, 425-429.

Jacobsen, S.B., Kaufman, A.J., 1999. The Sr, C and O isotopic evolution of Neoproterozoic seawater. *Chemical Geology* **161,** 37-57.

Jaffe, L. A., Peucker-Ehrenbrink, B., Petsch, S. T., 2002. Mobility of rhenium, platinum group elements and organic carbon during black shale weathering. *Earth and Planetary Science Letters* **198**, 339-353.

Jensen, S., Saylor, B. Z., Gehling, J. G., Germs, G. J. B., 2000. Complex trace fossils from the terminal Proterozoic of Namibia. *Geology* **28**, 143-146.

Jiang, G., Kaufman, A. J., Christie-Blick, N., Zhang, S., Wu, H., 2007. Carbon isotope variability across the Ediacaran Yangtze platform in South China: Implications for a

large surface-to-deep ocean [delta]13C gradient. *Earth and Planetary Science Letters* **261**, 303-320.

Kendall, B., Creaser, R. A., Calver, C. R., Raub, T. D., Evans, D. A. D., 2009a. Correlation of Sturtian diamictite successions in southern Australia and northwestern Tasmania by Re-Os black shale geochronology and the ambiguity of "Sturtian"-type diamictite-cap carbonate pairs as chronostratigraphic marker horizons. *Precambrian Research* **172**, 301-310.

Kendall, B., Creaser, R. A., Selby, D., 2009b. ^{187}Re-^{187}Os geochronology of Precambrian organic-rich sedimentary rocks. *Geological Society, London, Special Publications* **326**, 85-107.

Kendall, B., Creaser, R. A., Gordon, G. W., Anbar, A. D., 2009c. Re-Os and Mo isotope systematics of black shales from the Middle Proterozoic Velkerri and Wollogorang Formations, McArthur Basin, northern Australia. *Geochimica Et Cosmochimica Acta* **73**, 2534-2558.

Kendall, B., Creaser, R. A., Selby, D., 2006. Re-Os geochronology of postglacial black shales in Australia: Constraints on the timing of "Sturtian" glaciation. *Geology* **34**, 729-732.

Kendall, B. S., Creaser, R. A., Ross, G. M., Selby, D., 2004. Constraints on the timing of Marinoan 'Snowball Earth' glaciation by ^{187}Re – ^{187}Os dating of a Neoproterozoic post-glacial black shale in Western Canada. *Earth and Planetary Science Letters* **222**, 729-740.

Kennedy, M. J., Runnegar, B., Prave, A. R., Hoffmann, K. H., Arthur, M. A., 1998. Two or four Neoproterozoic glaciations? *Geology* **26**, 1059-1063.

Kilburn, C., Shackleton, R. M., Pitcher, W. S., 1965. The stratigraphy and origin of the Port Askaig boulder bed series (Dalradian). *Geol J* **4**, 343-360.

Kirschvink, J. L., 1992. Late Proterozoic low-latitude global glaciation: the snow ball earth. In: Schopf, J. W. a. K., C (Ed.), *The Proterozoic Biosphere*. Cambridge University Press, Cambridge.

Knoll, A. H., 2003. The geological consequences of evolution. *Geobiology* **1**, 3-14.

Knoll, A. H., Javaux, E. J., Hewitt, D., Cohen, P., 2006. Eukaryotic organisms in Proterozoic oceans. *Philosophical Transactions of the Royal Society B-Biological Sciences* **361**, 1023-1038.

Landing, E., Bowring, S.A., Davidek, K.L., Westrop, S.R., Geyer, G., Heldmaier, W., 1998. Duration of the Early Cambrian: U-Pb ages of volcanic ashes from Avalon and Gondwana. *Canadian Journal of Earth Sciences* **35,** 329-338.

Levasseur, S., Birck, J., Allègre, C.J., 1999. The osmium riverine flux and oceanic mass balance of osmium. *Earth and Planetary Science Letters,* **174,** 7-23.

Li, Z. X., Bogdanova, S. V., Collins, A. S., Davidson, A., De Waele, B., Ernst, R. E., Fitzsimons, I. C. W., Fuck, R. A., Gladkochub, D. P., Jacobs, J., Karlstrom, K. E., Lu, S., Natapov, L. M., Pease, V., Pisarevsky, S. A., Thrane, K., Vernikovsky, V., 2008. Assembly, configuration, and break-up history of Rodinia: A synthesis. *Precambrian Research* **160**, 179-210.

Litherland, M., 1980. The Stratigraphy of the Dalradian Rocks around Loch Creran, Argyll. *Scot J Geol* **16**, 105-123.

Logan, G. A., Hayes, J. M., Hieshima, G. B., Summons, R. E., 1995. Terminal Proterozoic reorganization of biogeochemical cycles. *Nature* **376**, 53-56.

Logan, G. A., Summons, R. E., Hayes, J. M., 1997. An isotopic biogeochemical study of Neoproterozoic and Early Cambrian sediments from the Centralian Superbasin, Australia. *Geochimica Et Cosmochimica Acta* **61**, 5391-5409.

Ludwig, K., 2003. Isoplot/Ex, version 3: a geochronological toolkit for Microsoft Excel. *Geochronology Center Berkeley*.

Ludwig, K. R., 1980. Calculation of uncertainties of U-Pb isotope data. *Earth and Planetary Science Letters* **46**, 212-220.

Macdonald, F.A., Schmitz, M.D., Crowley, J.L., Roots, C.F., Jones, D.S., Maloof, A.C., Strauss, J.V., Cohen, P.A., Johnston, D.T., Schrag, D.P., 2010a. Calibrating the Cryogenian. *Science* **327,** 1241-1243.

Macdonald, F. A., Cohen, P. A., Dudas, F. O., Schrag, D. P., 2010b. Early Neoproterozoic scale microfossils in the Lower Tindir Group of Alaska and the Yukon Territory. *Geology* **38**, 143-146.

Mao, J., Lehmann, B., Du, A., Zhang, G., Ma, D., Wang, Y., Zeng, M., Kerrich, R., 2002. Re-Os Dating of Polymetallic Ni-Mo-PGE-Au Mineralization in Lower Cambrian Black Shales of South China and its geological significance. *Economic Geology* **97,** 1051-1061.

Martin, M. W., Grazhdankin, D. V., Bowring, S. A., Evans, D. A.,D., Fedonkin, M. A., Kirschvink, J. L., 2000. Age of Neoproterozoic Bilatarian Body and Trace Fossils, White Sea, Russia: Implications for Metazoan Evolution. *Science* **288**, 841-845.

McCay, G. A., Prave, A. R., Alsop, G. I., Fallick, A. E., 2006. Glacial trinity: Neoproterozoic Earth history within the British-Irish Caledonides. *Geology* **34**, 909-912.

Meert, J. G., 2007. Testing the Neoproterozoic glacial models. *Gondwana Research* **11**, 573-574.

Melezhik, V. A., Gorokhov, I. M., Kuznetsov, A. B., Fallick, A. E., 2001. Chemostratigraphy of Neoproterozoic carbonates: implications for 'blind dating'. *Terra Nova* **13**, 1-11.

Melezhik, V. A., Roberts, D., Fallick, A. E., Gorokhov, I. M., 2008. The Shuram-Wonoka event recorded in a high-grade metamorphic terrane: insight from the Scandinavian Caledonides. *Geological Magazine* **145**, 161-172.

Morton, J.P., Long, L.E., 1982. Rb-Sr Ages of Precambrian Sedimentary-Rocks in the USA. *Precambrian Research*, **18,** (1-2), 133-138.

Narbonne, G. M., Gehling, J. G., 2003. Life after snowball: The oldest complex Ediacaran fossils. *Geology* **31**, 27-30.

Neilson, J. C., Kokelaar, B. P., Crowley, Q. G., 2009. Timing, relations and cause of plutonic and volcanic activity of the Siluro-Devonian post-collision magmatic episode in the Grampian Terrane, Scotland. *Journal of the Geological Society* **166**, 545-561.

Ohr, M., Halliday, A.N., Peacor, D.R., 1991 Sr and Nd Isotopic Evidence for Punctuated Clay Diagenesis, Texas Gulf-Coast. *Earth and Planetary Science Letters*, **105**, 110-126.

Oliver, G. J. H., 2001. Reconstruction of the Grampian episode in Scotland: its place in the Caledonian Orogeny. *Tectonophysics* **332**, 23-49.

Pattison, D. R. M., 2006. The fate of graphite in prograde metamorphism of pelites: An example from the Ballachulish aureole, Scotland. *Lithos* **88**, 85-99.

Pattison, D. R. M., Harte, B., 1997. The geology and evolution of the Ballachulish Igneous Complex and Aureole. *Scot J Geol* **33**, 1-29.

Peucker-Ehrenbrink, B., Jahn, B.-m., 2001. Rhenium-osmium isotope systematics and platinum group element concentrations: Loess and the upper continental crust. *Geochem. Geophys. Geosyst.* **2**.

Piasecki, M. A. J., 1980. New light on the Moine rocks of the Central Highlands of Scotland. *Journal of the Geological Society* **137**, 41-59.

Plumb, K.A., New Precambrian time scale. *Episodes* **14,** 139-140.

Prave, A. R., 1999. The Neoproterozoic Dalradian Supergroup of Scotland: an alternative hypothesis. *Geological Magazine* **136**, 609-617.

Prave, A. R., Fallick, A. E., Thomas, C. W., Graham, C. M., 2009a. A composite C-isotope profile for the Neoproterozoic Dalradian Supergroup of Scotland and Ireland. *Journal of the Geological Society* **166**, 845-857.

Prave, A. R., Strachan, R. A., Fallick, A. E., 2009b. Global C cycle perturbations recorded in marbles: a record of Neoproterozoic Earth history within the Dalradian succession of the Shetland Islands, Scotland. *Journal of the Geological Society* **166**, 129-135.

Preiss, W. V., 2000. The Adelaide Geosyncline of South Australia and its significance in Neoproterozoic continental reconstruction. *Precambrian Research* **100**, 21-63.

Pringle, J., 1939. The discovery of Cambrian trilobites in the Highland Border rocks near Callander, Perthshire. *Report of the British Association for the Advancement of Science* **252**.

Rainbird, R.H., Hamilton, M.A., Young, G.M., 2001. Detrital zircon geochronology and provenance of the Torridonian, NW, Scotland: *Journal of the Geological Society*, **158,** 15-27

Ravizza, G., Turekian, K. K., 1989. Application of the ^{187}Re-^{187}Os system to black shale geochronometry. *Geochimica et Cosmochimica Acta* **53**, 3257-3262.

Rogers, G., Dunning, G. R., 1991. Geochronology of appinitic and related granitic magmatism in the W Highlands of Scotland: constraints on the timing of transcurrent fault movement. *Journal of the Geological Society* **148**, 17-27.

Rooney, A. D., Selby, D., Houzay, J.-P., Renne, P. R., 2010. Re-Os geochronology of a Mesoproterozoic sedimentary succession, Taoudeni basin, Mauritania: Implications for basin-wide correlations and Re-Os organic-rich sediments systematics. *Earth and Planetary Science Letters* **289**, 486-496.

Sawaki, Y., Kawai, T., Shibuya, T., Tahata, M., Omori, S., Komiya, T., Yoshida, N., Hirata, T., Ohno, T., Windley, B. F., Maruyama, S., 2010. ^{87}Sr/^{86}Sr chemostratigraphy of Neoproterozoic Dalradian carbonates below the Port Askaig Glaciogenic Formation, Scotland. *Precambrian Research* **179**, 150-164.

Selby, D., 2007. Direct Rhenium-Osmium age of the Oxfordian-Kimmeridgian boundary, Staffin bay, Isle of Skye, U.K., and the Late Jurassic time scale. *Norwegian Journal of Geology* **87**, 9.

Selby, D., 2009. U-Pb zircon geochronology of the Aptian/Albian boundary implies that the GL-O international glauconite standard is anomalously young. *Cretaceous Research*, **30**, 1263-1267.

Selby, D., Creaser, R. A., 2003. Re-Os geochronology of organic rich sediments: an evaluation of organic matter analysis methods. *Chemical Geology* **200**, 225-240.

Selby, D., Creaser, R. A., 2005. Direct radiometric dating of the Devonian-Mississippian time-scale boundary using the Re-Os black shale geochronometer. *Geology* **33**, 545-548.

Selby, D., Creaser, R. A., Stein, H. J., Markey, R. J., Hannah, J. L., 2007. Assessment of the Re-^{187} decay constant by cross calibration of Re-Os molybdenite and U-Pb zircon chronometers in magmatic ore systems. *Geochimica Et Cosmochimica Acta* **71**, 1999-2013.

Slack, J.F., Jiang, W.T., Peacor, D.R., Okita, P.M., 1992. Hydrothermal and metamorphic berthierine from the Kidd Creek Volcanogenic Massive Sulfide Deposit, Timmins, Ontario. *Canadian Mineralogist.* **30,** 1127-1142.

Smith, M., Robertson, S., Rollin, K. E., 1999. Rift basin architecture and stratigraphical implications for basement-cover relationships in the Neoproterozoic Grampian Group of the Scottish Caledonides. *Journal of the Geological Society* **156**, 1163-1173.

Smoliar, M. I., Walker, R. J., Morgan, J. W., 1996. Re-Os isotope constraints on the age of Group IIA, IIIA, IVA, and IVB iron meteorites. *Science* **271**, 1099-1102.

Soper, N. J., 1994. Neoproterozoic sedimentation on the northeast margin of Laurentia and the opening of Iapetus *Geological Magazine* **131**, 291-299.

Soper, N. J., England, R. W., 1995. Vendian and Riphean rifting in NW Scotland. *Journal of the Geological Society* **152**, 11-14.

Soper, N. J., Ryan, P. D., Dewey, J. F., 1999. Age of the Grampian orogeny in Scotland and Ireland. *Journal of the Geological Society* **156**, 1231-1236.

Spencer, A. M., 1971. Late Precambrian glaciation in Scotland. *Memoirs of the Geological Society of London* **6**, 1-100.

Strachan, R. A., Smith, M., Harris, A.L., Fettes, D.J.,, 2002. The Northern Highland and Grampian terranes. In: Trewin, N. H. (Ed.), *The Geology of Scotland*. The Geological Society, London.

Sun, W., Arculus, R. J., Bennett, V. C., Eggins, S. M., Binns, R. A., 2003. Evidence for rhenium enrichment in the mantle wedge from submarine arc-like volcanic glasses (Papua New Guinea). *Geology* **31**, 845-848.

Tanner, P. W. G., Alsop, G. I., Hutton, D. H. W., 2005. Discussion on evidence for a major Neoproterozoic orogenic unconformity within the Dalradian Supergroup of NW Ireland. *Journal of the Geological Society* **162**, 221-224.

Tanner, P. W. G., Evans, J. A., 2003. Late Precambrian U-Pb titanite age for peak regional metamorphism and deformation (Knoydartian orogeny) in the western Moine, Scotland. *Journal of the Geological Society* **160**, 555-564.

Tanner, P. W. G., Pringle, M. S., 1999. Testing for the presence of a terrane boundary within Neoproterozoic (Dalradian) to Cambrian siliceous turbidites at Callander, Perthshire, Scotland. *Journal of the Geological Society* **156**, 1205-1216.

Tanner, P. W. G., Sutherland, S., 2007. The Highland Border Complex, Scotland: a paradox resolved. *Journal of the Geological Society* **164**, 111-116.

Thomas, C., Graham, C., Ellam, R., Fallick, A., 2004. $^{87}Sr/^{86}Sr$ chemostratigraphy of Neoproterozoic Dalradian limestones of Scotland and Ireland: constraints on depositional ages and time scales. *Journal of the Geological Society* **161**, 229-242.

Thomson, J., 1871. On the occurrence of pebbles and boulders of granite in schistose rocks on Islay, Scotland *Report of the 40th Meeting of the British Association for the Advancement of Science*, Liverpool.

Thomson, J., 1877. On the geology of the island of Islay. *Transactions of the Geological Society of Glasgow* **5**, 200-222.

Tilley, C. E., 1925. A preliminary survey of metamorphic zones in the southern Highlands of Scotland. *Quarterly Journal of the Geological Society of London* **81**.

Trindade, R. I. F., Macouin, M., 2007. Palaeolatitude of glacial deposits and palaeogeography of Neoproterozoic ice ages. *Comptes Rendus Geosciences* **339**, 200-211.

Vidal, G., Moczydlowska-Vidal, M., 1997. Biodiversity, Speciation, and Extinction Trends of Proterozoic and Cambrian Phytoplankton. *Paleobiology* **23**, 230-246.

Voll, G., Topel, J., Pattison, D.R.M., Seifert, F., 1991. Equilibrium and Kinetics in Contact Metamorphism: The Ballachulish Igneous Complex and its Aureole. . Springer Verlag, Heidelberg.

Walker, R. J., Horan, M. F., Morgan, J. W., Becker, H., Grossman, J. N., Rubin, A. E., 2002a. Comparative ^{187}Re-^{187}Os systematics of chondrites: Implications regarding early solar system processes. *Geochimica Et Cosmochimica Acta* **66**, 4187-4201.

Walker, R. J., Prichard, H. M., Ishiwatari, A., Pimentel, M., 2002b. The osmium isotopic composition of convecting upper mantle deduced from ophiolite chromites. *Geochimica Et Cosmochimica Acta* **66**, 329-345.

Walsh, J. A., 2007. The use of the scanning electron microscope in the determination of the mineral composition of Ballachulish slate. *Materials Characterization* **58**, 1095-1103.

Yang, G., Hannah, J. L., Zimmerman, A., Stein, H. J., Bekker, A., 2009. Re-Os depositional age for Archean carbonaceous slates from the southwestern Superior Province: Challenges and insights. *Earth and Planetary Science Letters* **280**, 83-92.

Zhou, C., Tucker, R., Xiao, S., Peng, Z., Yuan, X., Chen, Z., 2004. New constraints on the ages of Neoproterozoic glaciations in south China. *Geology* **32,** 437-440.

Chapter 4 – Hydrous Pyrolysis experiments and Re-Os systematics

4.1 Introduction

The application and analytical advancements of the rhenium-osmium (Re-Os) geochronometer has permitted the determination of accurate and precise (≤±1 %) depositional ages for organic-rich sedimentary rocks (ORS; Ravizza and Turekian, 1989; Cohen et al., 1999; Selby and Creaser, 2003; Kendall et al., 2004; 2006; Selby and Creaser, 2005a; Anbar et al., 2007). As a result, the Re-Os ORS geochronometer has provided accurate and precise dates for timescale calibration and sedimentary horizons lacking tuff horizons and biostratigraphy (Selby and Creaser 2005a; Selby, 2007; Turgeon et al., 2008; Kendall et al., 2009a,b; Yang et al. 2009; Rooney et al., 2010).

Depositional ages obtained from ORS affected by petroleum maturation, flash pyrolysis and/or polyphase metamorphism indicate that these processes do not significantly affect the ORS Re-Os systematics (Creaser et al., 2002; Selby and Creaser, 2005a; Kendall et al., 2004; Rooney et al., 2010). Specifically, the Re-Os ORS systematics are known to remain undisturbed at pressures up to 6 kbar and temperatures >650 °C resulting from contact and regional metamorphism (Rooney et al., 2010). However, interactions with low temperature (~100 °C) hydrothermal fluids have been shown to disturb Re-Os ORS systematics (Cooke et al., 1988; Kendall et al., 2009b).

Natural petroleum generated from ORS through the maturation of organic matter is enriched in Re and Os, which has been transferred from source rocks (Barre et al., 1995; Woodland et al., 2001; Selby and Creaser, 2005b; Selby et al., 2007; Finlay et al., 2010). It has been shown that the Re-Os systematics of petroleum may yield the timing of oil generation (Selby and Creaser, 2005a; Selby et al., 2005; Finlay et al., 2010). Our present understanding suggests that Re and Os may be bound in petroleum by heteroatomic ligands and other metallo-organic complexes (Selby et al., 2007). However, the elemental and isotopic behaviour of Re and Os in the ORS – petroleum system is poorly understood. Specifically, we have a limited understanding of the complexation and transfer of Re and

Os and the Re-Os isotope systematics in and from ORS to petroleum as a result of petroleum maturation.

To improve our understanding of Re and Os complexation in ORS and their transfer behaviour and the Re-Os isotope systematics from ORS to petroleum it is crucial to fully understand Re-Os systematics during the generation of petroleum. Laboratory-based hydrous pyrolysis experiments allow us to mimic natural petroleum maturation of source rocks on a suitable timescale. Herein this technique is used to evaluate the complexation of Re and Os in ORS and their transfer behaviour from ORS to petroleum.

Hydrous pyrolysis is an experimental technique that simulates the maturation, generation and expulsion of immiscible oil that is physically and chemically similar to natural crude oils (Lewan et al., 1979; Lewan, 1985; 1997; Ruble et al., 2001; Lewan and Ruble, 2002). Hydrous pyrolysis experiments provide the most realistic conditions for the generation of immiscible oil under laboratory conditions primarily because it involves the generation of an intermediate bitumen component during maturation (Lewan and Ruble, 2002). The generation of this intermediate bitumen component permits the separation and expulsion of oil from the polar-rich, water-saturated bitumen. The experiments result in the generation of three organic phases; bitumen, immiscible oil and gas (Ruble et al., 2001).

This paper presents results from a series of hydrous pyrolysis experiments on Phanerozoic petroleum immature ORS, designed to mimic natural petroleum maturation in an effort to evaluate Re and Os location in ORS and the transfer mechanisms of Re and Os in ORS to petroleum. Furthermore, this work enables us to enhance our understanding of the Re-Os isotope systematics of petroleum, in particular, the use of the Re-Os isotope system for fingerprinting oils.

4.2 Samples

4.2.1 Staffin Shale and Phosphoria Formation

The Jurassic Staffin Shale and Permian Phosphoria Formations were selected for hydrous pyrolysis experiments as each formation is composed of a distinct kerogen type (Type III and IIS, respectively), have elevated total organic carbon (TOC) values and are immature with respect to petroleum maturation (Table 4.1). These two samples provide an ideal opportunity to evaluate the location of Re and Os in a petroleum immature ORS and the effect of petroleum maturation on Re-Os systematics in ORS.

Table 4.1
Samples used for hydrous pyrolysis experiments

Sample	TOC % wt	T_{max} °C	S1	S2	Bitumen %	Asphaltene %
Staffin Shale	2.5	431	0.03	4.05	0.01	7.9
Phosphoria	17.4	418	2.46	101.42	1.60	34

TOC = total organic carbon

Tmax = temperature °C of the maximum formation of hydrocarbons by cracking of kerogen and has an uncertainty of ± 1 - 3 °C (Peters, 1986; Behar et al., 2001).

S1 = mg of hydrocarbons (free and thermovapourisable) per gram of rock.

S2 = mg of hydrocarbons (cracking of kerogen) per gram of rock (Peters, 1986).

4.2.1.1 Jurassic Staffin Shale Formation

Approximately 6 kg of the Jurassic Staffin Shale Formation was sampled from Staffin Bay, Skye, Scotland (57° 39' 42.00" N, 6° 14' 45.26" W). The sample consists of dark grey and black clays and silty-shales from Bed 35 of the Flodigarry Shale Member (Matyja et al., 2006; Selby, 2007). In addition to the 6 kg sample 4 other samples from Bed 35 were taken along its strike (Staffin 182-5, 226-5; Staffin DSa, DSb). A Re-Os age of 154.1 ± 2.2 Ma provides accurate and precise geochronology for the Oxfordian-Kimmeridgian boundary marked by the Flodigarry Shale Member (Selby, 2007). The thermal maturity, TOC and hydrogen and oxygen index values were determined by this study (see methodology). The samples are thermally immature with respect to petroleum maturation with a T_{max} value of 431 °C (Table 4.1). The samples have TOC values of approximately 2.5% and extractable organic matter (bitumen) constituting 0.01% (Table 4.1). The hydrogen and oxygen index values of 176 and 23, respectively, indicate that the Staffin Shale Formation is a gas-prone Type III kerogen (Tissot and Welte, 1984; Vandenbroucke, 2003). The Staffin samples are enriched in Re and Os ~14 ng/g and ~200 pg/g, respectively, relative to average continental crust (~0.2 – 2 ng/g Re and 30 – 50 pg/g Os; Esser and Turekian, 1993; Peucker-Ehrenbrink and Jahn, 2001; Hattori et al., 2003; Sun et al., 2003). Bed 35 has $^{187}Re/^{188}Os$ ratios of ~355 and radiogenic $^{187}Os/^{188}Os$ ratios of ~1.477 (Table 4.2; Selby, 2007; this study).

Table 4.2
Re and Os abundance data from Staffin Shale Formation hydrous pyrolysis experiments and control samples

Sample	Re (ng/g orig. rock)	±	Os (pg/g orig. rock)	±	Re (ng/g)	±	Os (pg/g)	±	$^{187}Re/^{188}Os$	±	$^{187}Os/^{188}Os$	±
Staffin 182-5					14.9	0.05	189.8	1.1	465.53	2.86	1.8840	0.0135
Staffin 226-5					13.8	0.05	219.4	1.1	355.18	2.09	1.4771	0.0091
Staffin Dsa					13.4	0.08	193.9	0.6	393.42	2.30	1.5440	0.0039
Staffin DSb					13.2	0.04	199.1	0.8	376.41	1.69	1.4904	0.0064
Non-pyrolysed rock												
Whole rock	13.75	0.05	219.4	1.1					355.18	2.09	1.4771	0.0091
Kerogen	14.01	0.05	224.4	1.1					353.50	2.06	1.4702	0.0089
Bitumen					3.8	0.31	194.9	10.4	116.42	17.46	2.0014	0.3032
250 °C Pyrolysis												
Whole rock	13.03	0.04	204.7	1.1					359.80	2.14	1.4538	0.0091
Kerogen	12.89	0.04	205.3	1.1					354.50	2.14	1.4434	0.0091
Bitumen					1.1	0.18	8.2	3.9	815.48	1119.19	2.4053	3.3387
300 °C Pyrolysis												
Whole rock	12.58	0.04	208.2	1.1					342.12	1.99	1.4702	0.0088
Kerogen	12.50	0.04	214.4	1.1					330.07	1.91	1.4655	0.0087
Bitumen					1.4	0.07	2.0	1.6	4150.57	9232.62	1.9203	4.3845
325 °C Pyrolysis												
Whole rock	12.52	0.04	207.0	1.1					341.18	1.99	1.4525	0.0088
Kerogen	13.03	0.06	211.1	1.1					347.96	2.23	1.4294	0.0087
Bitumen					2.1	0.06	3.8	1.3	2891.80	2352.55	0.89	0.8094
350 °C Pyrolysis												
Whole rock	12.20	0.04	206.9	1.1					333.17	1.96	1.4499	0.0090
Kerogen	13.25	0.05	203.0	1.1					369.58	2.16	1.4729	0.0089
Bitumen					0.4	0.07	0.3	1.7	10072.74	149295.42	2.7386	41.1209

Staffin 182-5 and 226-5 are from Bed 35 of Matyja et al., 2006; Selby, 2007; Dsa and b are from Selby, 2007

4.2.1.2 Permian Phosphoria Formation

Approximately 20 kg of the Permian Phosphoria Formation was sampled from Retort Mountain quarry, Beaverhead, Montana, U.S.A. (Lewan, 1978; Lewan et al., 1986; Piper and Link, 2002; Hein et al., 2004). The Phosphoria Formation is a fine-grained argillaceous phosphatic claystone with minor amounts of pyrite (Lewan et al., 1986). The Phosphoria samples have elevated TOC values of 17.4% and extractable bitumen constituting 1.6%, of which 34% is asphaltene (this study; Table 4.1). The samples are thermally immature with respect to petroleum maturation with a T_{max} value of 418 °C (this study; Table 4.1). The kerogen of the Phosphoria Formation is predominantly amorphous organic matter with a sulphur content of 1.8 wt%, and hydrogen and oxygen index values of 582 and 9 (Lewan et al., 1986). These values indicate the Phosphoria Formation possesses an oil-prone Type IIS kerogen (Tissot and Welte, 1984; Lewan et al., 1986; Reynolds and Burnham, 1995; Vandenbroucke, 2003). The Phosphoria samples are also greatly enriched in Re and Os with abundances of ~470 ng/g and ~3300 pg/g, respectively (this study; Table 4.3) and possess elevated $^{187}Re/^{188}Os$ ratios of ~988 and radiogenic $^{187}Os/^{188}Os$ ratios of ~3.314 (Table 4.3).

4.3 Methodology

The entire Staffin and Phosphoria Formation sample sets were crushed, without metal contact, to small rock fragments (~1 x 1 x 1cm to 2 x 2 x 1cm), with any weathered surface material removed. Randomly selected 400 g aliquots of the rock fragments (and for Staffin samples Staffin 182-5, 226-5, DSa, DSb) were taken for each sample to establish the variation in Re and Os abundance and isotope compositions of the non-pyrolysed rock and for the hydrous pyrolysis experiments. The pyrolysed samples were also analysed for their Re and Os abundances and isotope compositions. In addition, the samples were analysed for TOC and Tmax parameters. The bitumen fraction of the Staffin and Phosphoria pyrolysed and non-pyrolysed samples was extracted for Re-Os analysis.

Table 4.3
Re and Os abundance data from Phosphoria Formation hydrous pyrolysis experiments and control samples

Sample	Re (ng/g orig. rock)	±	Os (pg/g orig. rock)	±	Re (ng/g)	±	Os (pg/g)	±	$^{187}Re/^{188}Os$	±	$^{187}Os/^{188}Os$	±
Phosphoria bag					504.91	1.6	3376.7	16.0	1013.18	4.12	3.2409	0.0123
Phosphoria large tub					469.77	1.5	3267.2	12.4	981.76	3.58	3.3239	0.0081
Phosphoria small tub					452.57	1.5	3122.0	9.4	978.46	3.36	3.1997	0.0051
Non-pyrolysed rock												
Whole rock	477.08	1.50	3295.3	11.0					987.99	3.35	3.3144	0.0045
Kerogen	478.70	1.48	3065.4	10.8					1113.58	3.87	3.1637	0.0056
Bitumen					60.87	0.201	144.8	2.17	3571.44	83.87	5.9785	0.1428
Asphaltene					236.77	0.8	443.2	7.5	4218.29	85.46	5.0242	0.1401
250 °C Pyrolysis												
Whole rock	427.10	1.46	3119.1	10.7					924.96	3.15	3.2079	0.0048
Kerogen	380.46	1.42	2691.7	10.4					952.11	3.24	3.1776	0.0046
Bitumen					115.00	0.38	227.9	2.4	3573.92	51.08	3.7299	0.0543
Asphaltene					265.89	0.9	498.6	3.7	3798.89	29.08	3.7941	0.0302
300 °C Pyrolysis												
Whole rock	434.50	1.43	3048.7	10.5					959.18	3.24	3.1690	0.0042
Kerogen	374.70	1.27	2890.5	9.3					883.69	3.17	3.3102	0.0061
Bitumen					133.86	0.44	313.7	3.1	3045.74	39.78	3.8185	0.0512
Asphaltene					252.67	0.8	574.6	5.1	3158.76	33.80	3.8900	0.0433
325 °C Pyrolysis												
Whole rock	504.03	1.36	3178.3	10.0					1070.21	3.69	3.1987	0.0048
Kerogen	396.56	1.23	2922.1	9.0					912.02	3.08	3.1562	0.0043
Bitumen					93.69	0.31	187.7	2.4	3465.67	72.67	3.5101	0.0741
Asphaltene					225.60	0.8	421.8	4.3	3745.73	54.11	3.6021	0.0526
350 °C Pyrolysis												
Whole rock	477.99	1.31	3331.1	9.6					974.77	3.28	3.2690	0.0042
Kerogen	413.29	1.24	2835.1	9.1					988.76	3.35	3.2556	0.0047
Bitumen					3.86	0.040	34.3	1.3	780.58	70.88	3.5017	0.3477
Asphaltene					11.75	0.10	131.3	1.4	578.02	8.94	2.7354	0.0481
Asphaltene of oil					0.13	0.002	5.6	0.7	163.40	59.01	3.5954	1.3598

4.3.1 TOC and T_{max} analysis

TOC values and thermal maturity data for the Phosphoria Formation were determined using Rock-Eval pyrolysis (Peters, 1986; Hunt, 1996) at the TOTAL Geochemistry and Fluids Laboratory (Pau, France). The TOC values and thermal maturity data for the Staffin samples were generated using a LECO SR Analyser machine by Weatherford (Houston, USA). For Rock-Eval pyrolysis, T_{max} is a laboratory temperature that represents the temperature of peak petroleum release by kerogen cracking in the Rock-Eval pyrolyzer (Peters, 1986; Behar, 2001).

4.3.2 Bitumen extraction

Bitumen (the soluble extractable organic matter extracted from ORS) was extracted from both the non-pyrolysed and pyrolysed Staffin samples (~100 g) using Soxhlet apparatus for 24 h with chloroform. The refluxed solvent was filtered through a 0.45 μm PTFE filter and the bitumen was concentrated by rotary vacuum evaporation. Bitumen from the Phosphoria non-pyrolysed and pyrolysed samples was extracted using an ASE 200 at the TOTAL Laboratory for Fluids and Geochemistry (Pau, France) with dichloromethane using 15 g of sample at 100°C and 100 bars.

4.3.3 Hydrous pyrolysis experiments

Randomly selected rock fragments (~400 g) of the Phosphoria and Staffin samples were matured through progressive stages of petroleum generation by isothermal hydrous pyrolysis (Lewan, 1985). Hydrous pyrolysis experiments were conducted in Hastelloy C-276 reactors with carburised surfaces. The rock fragments from the Staffin and Phosphoria sample sets were immersed in 400 ml distilled water. The reactors are sealed and filled with ~6.9 MPa of He and leak checked using a thermal conductivity leak detector. Temperatures were monitored with Type J thermocouples which are calibrated against national standards and remain within ± 0.5°C of the desired temperature. The hydrous pyrolysis experiments were carried out at 250°, 300°, 325° and 350 °C for 72 h. These temperatures were selected as they represent various stages of oil generation: 1) pre-oil generation, 2) the onset of primary generation, 3) primary oil generation and 4) post-oil generation of a Type II source rock (Lewan, 1985).

After the experiments had cooled to room temperature, pressure and temperature values were recorded and a sample of head-space gas was collected in an evacuated 30 cm^{-3} stainless-steel cylinder. Expelled oil generated in the hydrous pyrolysis experiments was collected in three steps. First, any expelled oil was collected from the surface of the water in the reactor with a Pasteur pipettete. Second, the water and minor amounts of expelled oil not collected with the pipettete were decanted into a glass separatory funnel. The separated oil was concentrated at the funnel stop cock, where it was collected with the same Pasteur pipette used to collect the oil on the water surface. Third, the thin film of expelled oil on the reactor walls, separatory funnel, Pasteur pipette, and rock fragments were rinsed with benzene at room temperature. This benzene rinse was filtered through a 0.45 μm polytetrafluoroethylene (PTFE) filter and the expelled oil was concentrated by rotary vacuum evaporation of the benzene. The decanted water was filtered through a 0.45 μm cellulose-acetate/nitrate filter. Rock fragments were removed from the reactor and dried at room temperature (~20°C) in a HEPA hood until their weight was constant (<1% change).

4.3.4 Re-Os analysis

Rhenium-osmium isotope analysis was carried out at Durham University's TOTAL Laboratory for Source Rock Geochronology and Geochemistry at the Northern Centre for Isotopic and Elemental Tracing (NCIET). In this study Re-Os analysis were conducted on the non-pyrolysed and recovered pyrolysed rock fragments. For clarity the term 'non-pyrolysed' rock refers to the original rock that has not experienced hydrous pyrolysis. Rhenium-Os analysis was conducted on an aliquot (~0.2 to 0.5 g) from the powdered rock fragments (~50 g) of both the non-pyrolysed and recovered pyrolysed samples. These whole rock analyses reflect the total organic matter within the rock matrix, which constitutes the kerogen and bitumen fractions. Analysis was also conducted on solvent-extracted (or bitumen free) rock. This rock analysis is termed 'kerogen' and does not refer to an isolated kerogen. The isolated bitumen and separated asphaltene fractions, hydrous pyrolysis generated petroleum and water used in the pyrolysis experiments were also analysed.

For whole rock and kerogen analyses, between 0.2 g and 0.5 g of sample material was placed into a Carius tube with a known amount of a tracer solution of ^{185}Re – ^{190}Os, plus 8 ml of a Cr^{VI}-H_2SO_4 solution (made from 0.25 g of CrO_3 per 1 ml of 4N H_2SO_4) and heated to 220°C for ~48 h (Selby and Creaser, 2003). For analysis of bitumen and

asphaltene, fractions and organic precipitates between 0.1 g and 0.2 g together with a known amount of ^{185}Re – ^{190}Os mixed tracer solution were dissolved in inverse *aqua regia* (8 ml ~14N HNO_3 and 3 ml ~10N HCl) in Carius tubes at 220 °C for ~48 h (Selby et al., 2007).

Osmium was extracted from the Cr^{VI}-H_2SO_4 and *aqua regia* solutions using solvent extraction ($CHCl_3$) and purified by micro-distillation, with the Re fraction purified using anion column chromatography (Selby and Creaser, 2003). Determination of Re-Os isotope composition and abundances was achieved using isotope dilution negative thermal ionisations mass spectrometry (ID-NTIMS) (Creaser et al., 1991; Völkening et al., 1991; Walczyk et al., 1991; Selby and Creaser, 2003).

Procedural blanks during this study were 2 ± 0.12 pg Re and 0.2 ± 0.08 pg Os (1 SD, n = 3, *aqua regia*), and 16.8 ± 0.4 pg Re and 0.4 ± 0.1 pg Os (1 SD, n = 4, Cr^{VI}-H_2SO_4 solution). The blank $^{187}Os/^{188}Os$ isotope composition for *aqua regia* are 0.27 ± 0.51 (1 SD, n = 3) and 0.25 ± 0.21 (1 SD, n = 4) for the Cr^{VI}-H_2SO_4 solution.

Uncertainties for $^{187}Re/^{188}Os$ and $^{187}Os/^{188}Os$ ratios are determined by error propagation of uncertainties in Re and Os mass spectrometer measurements, blank abundances and isotope compositions, spike calibrations and reproducibility of standard Re and Os isotope values.

To ensure and monitor long-term mass spectrometry reproducibility, in-house standard solutions of Re and Os are repeatedly analysed at NCIET. The Re standard analysed during the course of this study is made from 99.999% zone-refined Re ribbon and is considered to be identical to that of AB-1 (Creaser et al., 2002; Selby and Creaser, 2003; Kendall et al., 2004). The NCIET Re standard yields an average $^{185}Re/^{187}Re$ of 0.59772 ± 0.00172 (1 SD, n = 114). This is in excellent agreement with the ratio reported for the AB-1 standard (Creaser et al., 2002). This paper details further use of the Durham Romil Osmium Standard (DROsS) for monitoring the mass spectrometry reproducibility of osmium isotope compositions. The DROsS recorded during this study yield an average $^{187}Os/^{188}Os$ ratio of 0.16093 ± 0.00015 (2 SD, n = 36), which is identical to ratios reported by Rooney et al. (2010 and references therein).

4.4 Results

4.4.1 Re-Os data of the Staffin Shale and Phosphoria Formations

Data for Re and Os of the Staffin and Phosphoria Formation non-pyrolysed and pyrolysed samples are presented in Table 4.2 and 4.3, respectively. Rhenium and Os abundance data from the hydrous pyrolysis experiments were mass-balanced and are reported as ng/g of original rock and pg/g of original rock, respectively using the equation:

$$\{M_i\} = [(A_i * g_i)/1000]/G \qquad \textbf{(1)}$$

Where the subscript "i" refers to the material, (non-pyrolysed / pyrolysed rock, kerogen, bitumen etc.,) being analysed, A is abundance in ppb or ppt; g is weight of material in grams and G is weight of starting rock in grams. Presenting the data in this format allows the evaluation of the Re and Os abundances located in the various fractions and to more accurately interpret the transfer behaviour and mechanisms of Re and Os in the ORS and petroleum system.

The Re and Os abundance (13.8 ng/g and 219 pg/g of original rock, respectively) in the Staffin Formation non-pyrolysed rock taken from the 6 kg sample are very similar to other sections of Bed 35 from the Staffin Formation (Re = 12.2 to 13.0 ng/g; Os = 205 to 208 pg/g of original rock). The Re and Os abundances for the pyrolysed rock samples range from 12.2 to 13.0 ng/g and 204 to 208 pg/g of original rock, respectively (Table 4.2).

The Re and Os abundance in the kerogen from the non-pyrolysed Staffin sample are 14.0 ng/g and 224 pg/g of original rock, respectively. These abundances are similar to kerogen of pyrolysed samples at all temperatures (Re =12.5 to 13.3 ng/g; Os = 203 to 214 pg/g of original rock; Table 4.2).

The non-pyrolysed rock contains 0.01% of bitumen or 0.03 g of the whole rock. This bitumen contains Re and Os abundances of 3.8 ng/g and 194.9 pg/g, respectively (Table 4.2). The hydrous pyrolysis of the Staffin shales generated 0.05 g, 0.13 g, 0.14 g and 0.23 g of bitumen for the 250°, 300°, 325° and 350°C experiments, respectively (Table 4.4). Bitumen from the pyrolysed rock possess a Re abundance (0.4 – 2.1 ng/g) that is lower than that of the non-pyrolysed sample. Conversely, Os for the bitumen of non-pyrolysed samples (0.3 pg/g to 8.2 pg/g) are lower than that of the bitumen from the pyrolysed sample.

Table 4.4 details of Hydrous Pyrolysis Experiments

Sample	Rock at start (g)	Water in reactor (g)	Recovered rock (g)	Oil recovered (g)	Bitumen (g)	Bitumen %
Staffin experiments						
Non-pyrolysed	400.1	-	390.3	-	0.03	0.026
250 °C Hydrous pyrolysis	400.2	410.3	373.5	-	0.05	0.052
300 °C Hydrous pyrolysis	400.1	410.3	370.7	-	0.13	0.120
325 °C Hydrous pyrolysis	400.1	410.3	368.6	-	0.14	0.129
350 °C Hydrous pyrolysis	400.1	410.3	365.7	-	0.23	0.221
Phosphoria experiments						
Non-pyrolysed	400.1	-	400	-	0.80	1.606
250 °C Hydrous pyrolysis	400.4	375.1	388.5	-	1.13	2.253
300 °C Hydrous pyrolysis	400.4	375.8	380.4	0.50	5.50	11.006
325 °C Hydrous pyrolysis	400.6	375.0	364.2	4.45	4.96	9.927
350 °C Hydrous pyrolysis	400.4	375.4	349.7	12.35	2.84	5.682

The $^{187}Re/^{188}Os$ ratios of the Staffin non-pyrolysed whole rock, kerogen and bitumen are ~355, 353 and 116, respectively. The pyrolysed samples have $^{187}Re/^{188}Os$ ratios of, 333 to 360 for whole rock, 330 to 370 for the kerogen and 816 to 10073 for the bitumen (Table 4.2). It must be noted that many of the bitumen samples have large uncertainties (± >1000) associated with them. The large uncertainties also reflect the blank correction associated with measuring these small (<0.05 g) samples and the minor abundance of Re and Os in the bitumen. The $^{187}Os/^{188}Os$ ratios of the non-pyrolysed whole rock, kerogen and bitumen are 1.477, 1.470 and 2.001, respectively. The pyrolysed samples have $^{187}Os/^{188}Os$ ratios of, 1.450 to 1.470 for whole rock, 1.429 to 1.473 for the kerogen and 0.889 to 2.739 for the bitumens (Table 4.2). As with the $^{187}Re/^{188}Os$ ratios many of the bitumen $^{187}Os/^{188}Os$ ratios have large uncertainties (± 3.3 – 41.1) associated with them related to the small (<0.05 g) sample size and minute Os abundance in the bitumen fraction.

The hydrous pyrolysis experiments on the Staffin Shale Formation did not generate any free oil although an equipment rinse did provide a small quantity (<0.05 g) of pyrolysate at 350°C. This material does not contain any measurable amounts of Re or Os and was not included in the mass balance calculations.

The non-pyrolysed Phosphoria Formation whole rock sample contains 477 ng/g and 3295 pg/g of original rock, of Re and Os, respectively (Table 4.3). There are significant variations in the Phosphoria Shale Re and Os abundances with values ranging from 453 to 504 ng/g and 3122 to 3377 pg/g, respectively (Table 4.3). The slight variations in Re and Os abundances seen in the Phosphoria pyrolysed samples may be related to these variations in the non-pyrolysed samples and the nature of the Phosphoria outcrop. The Phosphoria

samples are taken from a much larger outcrop sample than the Staffin samples which are all taken from one bed and show a much smaller range in elemental abundances whereas the Phosphoria is from >20 kg and has a considerable range in elemental abundances.

The pyrolysed whole rock samples have Re and Os abundances ranging from 427 ng/g to 504 ng/g and from 3049 pg/g to 3331 pg/g of original rock, respectively. The non-pyrolysed kerogen fraction contains 479 ng/g and 3065 pg/g of original rock, respectively of Re and Os, in comparison with pyrolysed sample abundances that range from 375 ng/g to 413 ng/g and from 2692 pg/g to 2922 pg/g of original rock, respectively.

The non-pyrolysed Phosphoria bitumen has Re and Os abundances of 60.9 ng/g and 144.8 pg/g, respectively. In comparison, the pyrolysed bitumen samples have Re and Os abundances ranging from 3.9 ng/g to 133.9 ng/g and 34.3 pg/g and 313.7 pg/g rock, respectively. The higher TOC value of the Phosphoria samples (17.4% vs. 2.5% for the Staffin Shale) permits the extraction of an asphaltene fraction from the bitumen component. The extracted maltene fraction was not analysed as the small (<0.01 g) amounts inhibit precise ID-NTIMS analysis and previous work has shown that the maltene contains only minor amounts of Re and Os (<14%; Selby et al., 2007). The asphaltene abundance is not mass balanced as together with the maltene it represents 100% of the bitumen and contains 237 ng of Re and 443 pg of Os in the non-pyrolysed sample (Table 4.3). The pyrolysis-generated asphaltene has Re and Os abundances ranging from 12 to 266 ng and 131 to 575 pg, respectively.

The $^{187}Re/^{188}Os$ ratios for the non-pyrolysed Phosphoria whole rock, kerogen and bitumen samples are 988, 1114 and 3571, respectively. The $^{187}Os/^{188}Os$ ratios for these fractions are 3.314, 3.164 and 5.979, respectively. The $^{187}Re/^{188}Os$ ratios for the whole rock, kerogen and bitumen fractions of the pyrolysed Phosphoria Shale samples range from 925 to 1070, 884 to 1114 and 781 to 3574, respectively (Table 4.3). The $^{187}Os/^{188}Os$ ratios for the whole rock, kerogen and bitumen fractions of the pyrolysed Phosphoria Shale samples range from 3.17 to 3.31, 3.16 to 3.30 and 3.50 to 5.98, respectively (Table 4.3).

The organic precipitates from the decanted hydrous pyrolysis waters are only slightly enriched in Re and Os (0.1 – 10 ppb and 1 – 224 ppt, respectively) though these abundances do have significant uncertainties (>10%) associated with the blank correction. As a result, these precipitates are not considered in the discussions concerning Re and Os transfer in maturing ORS.

The hydrous pyrolysis experiments on the Phosphoria Shale at 300°, 325° and 350°C yielded small quantities of free oil (0.5, 4.45 and 12.35 g, respectively; Table 4.4). However, the generated oils from the 300° and 325˚C experiments do not contain significant amounts of Re or Os and are not considered in the mass balance calculations. In contrast, the asphaltene component of the 350°C oil was analysed for Re and Os abundance and isotope composition and contains very minor abundances although the isotope ratios are pertinent to the discussion below. The asphaltene component of the oil contains 130 ppt of Re and 5.6 ppt of Os with a $^{187}Re/^{188}Os$ ratio of 163 and a radiogenic $^{187}Os/^{188}Os$ ratio of 3.59.

4.5 Discussion

4.5.1 Complexation behaviour and location of Re and Os in ORS

Aliquots of whole rock, kerogen and naturally occurring petroleum fractions from Phanerozoic sedimentary rocks (Permian and Jurassic) were analysed for Re and Os abundance and isotope compositions (Tables 4.2 and 4.3). These Re-Os data provide us with crucial information regarding the complexation of Re and Os in ORS and the Re-Os systematics of the ORS – Petroleum system.

Analyses of the thermally immature Staffin and Phosphoria samples indicate that the kerogens are enriched in Re and Os with abundances that are identical, within uncertainty, to those of the whole rocks (Tables 4.2 and 4.3). These data alone suggest that the vast majority of the Re and Os budget in ORS is complexed within the kerogen fraction (Tables 4.2 and 4.3). However, the ORS used in this study have experienced burial resulting in the generation of an extractable bitumen fraction, although the samples are still considered thermally immature based on a laboratory thermal maturation analysis (T_{max}; Table 4.1). The Staffin sample contains very small amounts of bitumen (0.01%), in comparison to the Phosphoria sample (1.6%). This is a direct result of the higher TOC content (17.4% [Phosphoria] vs. 2.5% [Staffin]) and earlier bitumen generation from a Type IIS kerogen to that of a Type III kerogen (Lewan et al., 2006).

The bitumen fractions from the non-pyrolysed Staffin and Phosphoria samples contain considerable abundances of Re (3.8 and 61 ng/g, respectively). This represents a significant percentage of the whole rock Re content (Staffin = 28% and Phosphoria = 13%; Tables 4.2 and 4.3). For Os the bitumen of the Staffin and Phosphoria samples contain 195

and 145 pg/g, respectively. These abundances represent a significant percentage of the whole rock Os content, especially for the Staffin sample (Staffin = 89% and Phosphoria = 4%). However, if we assume that Re and Os in ORS are associated entirely with the organic matter then the whole rock value of ~480 ng/g is a considerable underestimate of the true Re abundance for the Phosphoria sample. A more realistic Re and Os abundance (T_A) can be calculated using the equation:

T_A = (100/TOC) * Re content of whole rock (2)

Based upon a TOC of 17.4% and a whole rock Re content of 477 ng/g the true abundance (T_A) for Re of the Phosphoria Formation is closer to 2742 ng/g. This equation is equally valid for the Os component and the true Os abundance of the Phosphoria is 18939 pg/g. Thus, the bitumen component represents only 2.2% of total Re and 0.8% of total Os found in the immature Phosphoria sample. This further illustrates that >95% of the Re and Os budget is housed within the kerogen fraction. Likewise, the Staffin samples also show that the Re and Os content of the bitumen is only a minor component of the whole rock Re and Os budget. For example, the Staffin bitumen contains 3.8 ng/g of Re from a T_A of 550 ng/g and for Os the bitumen has 195 pg/g from a T_A of 8760 pg/g thus representing 0.7% of total Re and 2.2% of total Os found in this sample.

4.5.2 Re and Os elemental abundance data of whole rock, kerogen and bitumen components as a function of hydrous pyrolysis temperature

Previous studies have shown that the Re-Os geochronometer is not adversely disturbed by thermal events such hydrocarbon maturation, flash pyrolysis or metamorphism (Creaser et al., 2002; Kendall et al., 2004; Selby and Creaser, 2005a; Rooney et al., 2010). As such, the Re-Os ORS geochronometer records the timing of sediment deposition and not the age of post-depositional events. Although current evidence suggests that the Re-Os system is not adversely affected by these events, it has been shown that natural crude oils are enriched in Re and Os that have been transferred from the source rock (Selby and Creaser, 2005b; Selby et al., 2005; Selby et al., 2007, Finlay et al., 2010). However, there is a very limited understanding of the mechanisms and magnitude of elemental transfer from a source rock to the generated petroleum.

The Staffin whole rock pyrolysed samples display a constant but small (6%) decrease in Re abundance throughout the hydrous pyrolysis temperature range although the

Re abundance is identical, within uncertainty, to several whole rock non-pyrolysed samples from the same stratigraphic horizon (Bed 35; Table 4.2). Similarly, the Os abundance in the pyrolysed whole rock displays a small (5%) decrease through the range of hydrous pyrolysis temperatures, but again this range is similar to the Os abundance variability within Bed 35 (Table 4.2).

The kerogen Re and Os abundance data for the Staffin pyrolysed samples are similar across the range of hydrous pyrolysis temperatures (4% variation for both Re and Os). The Staffin bitumens show an extremely minor increase in Re abundance peaking at 300°C although this value is still lower than the Re abundance of the non-pyrolysed rock (Fig. 4.1). The Os abundance in the Staffin bitumen decreases from the non-pyrolysed sample value of 195 pg/g (Fig. 4.2).

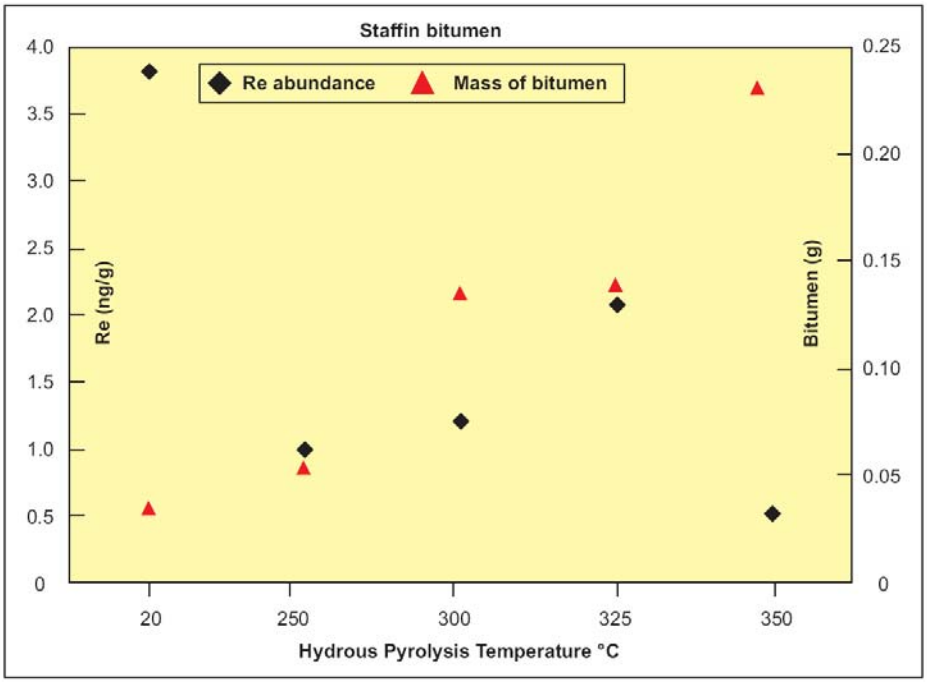

Fig. 4.1 Re abundance and amount of bitumen for the Staffin bitumens against temperature of hydrous pyrolysis experiments.

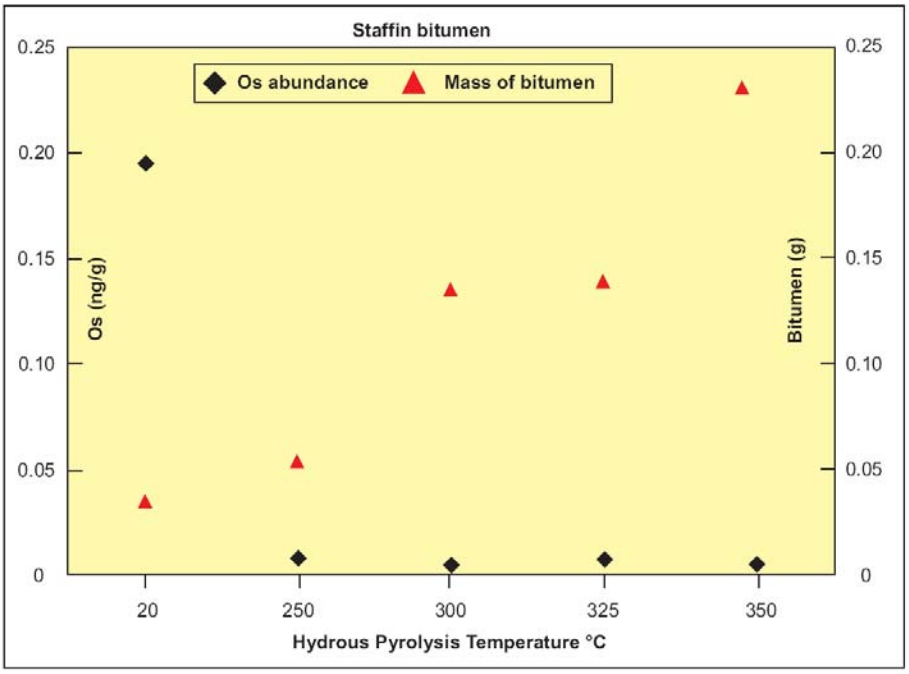

Fig. 4.2 Os abundance and amount of bitumen for the Staffin bitumens against temperature of hydrous pyrolysis experiments.

The generated bitumen from the Staffin samples do not contain significant concentrations of Re or Os (0.4 – 2.1 ng/g and 0.3 – 8.2 pg/g, respectively) suggesting that these metals are very tightly bound in the Type III kerogen molecules. As the thermal parameters of the hydrous pyrolysis experiments were identical for the Staffin and Phosphoria samples it can be proposed that kerogen type is a controlling factor for the transfer of Re and Os from kerogen into bitumen. This would agree with experimental and natural data which predicts greater thermal stress is required to crack Type III kerogens in comparison with Type II/IIS (Lewan, 1985; Lewan and Ruble, 2002).

The results from hydrous pyrolysis experiments on the Phosphoria Shale define small variations in Re and Os abundance (8% and 3%, respectively) of the whole rock fractions. These variations can be attributed to the natural variations inherent in the Phosphoria Shale Formation as seen in the non-pyrolysed samples (Table 4.3). Likewise, the Re-Os data from the Phosphoria kerogen samples reveals only small increases or decreases in Re or Os abundance (10% and 5%, respectively). The Phosphoria bitumen samples display an enrichment in Re and Os that is correlative with the peak bitumen generation temperature for a Type IIS kerogen (300°C; Table 4.3; Figs. 4.3 and 4.4; Lewan, 1985).

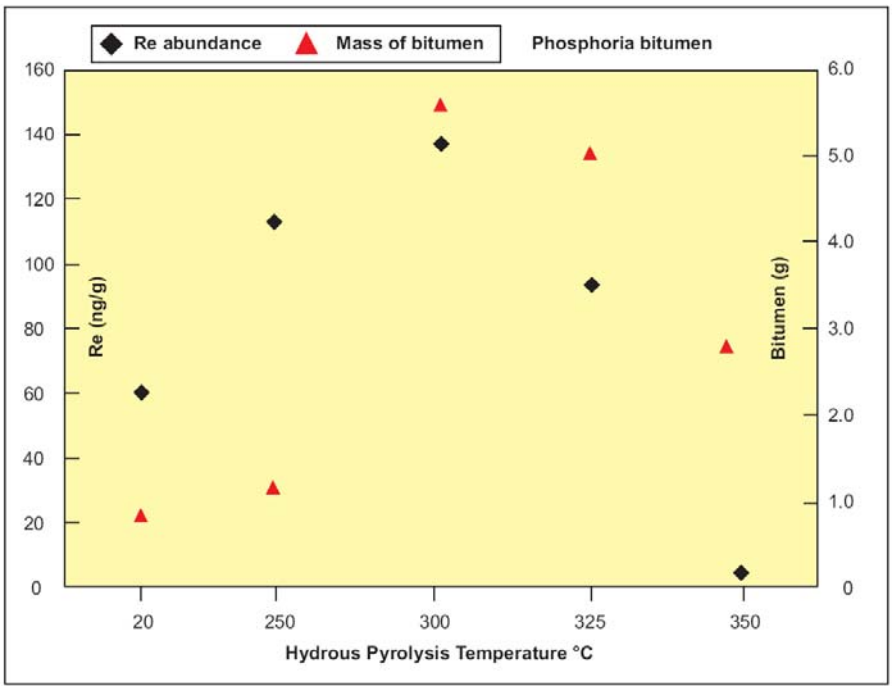

Fig. 4.3 Re abundance and amount of bitumen for the Phosphoria bitumens against temperature of hydrous pyrolysis experiments. The graph illustrates the agreement between peak Re abundance in the bitumen and peak bitumen generation temperature for this Type IIS kerogen

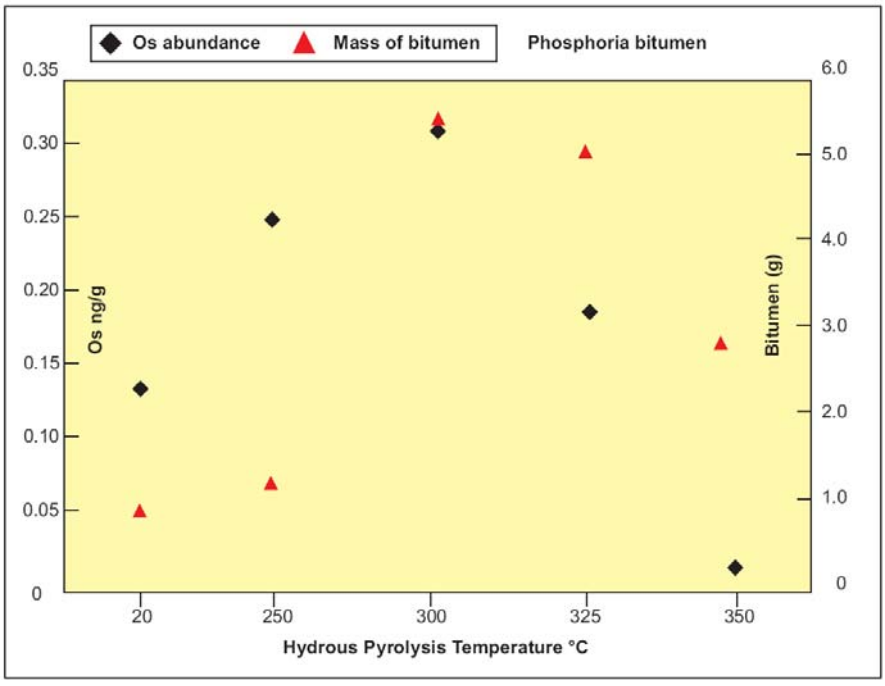

Fig. 4.4 Os abundance and amount of bitumen for the Phosphoria bitumens against temperature of hydrous pyrolysis experiments. The graph illustrates the agreement between peak Os abundance in the bitumen and peak bitumen generation temperature for this Type IIS kerogen.

Additionally, the Re and Os abundances for the Phosphoria bitumen illustrate an excellent linear relationship (r = 0.96; Fig. 4.5). This would suggest that these metals reside

in similar organic hosts within the bitumen and are transferred consistently in terms of amount and the destination throughout natural maturation.

The Re and Os present in the pyrolysed bitumen represents only 2.2% and 0.7%, respectively, of that within the whole rock. This reveals minimal transfer of Re and Os from the kerogen to the bitumen resulting from hydrous pyrolysis experiments. Ultimately, this strongly suggests that hydrous pyrolysis and by inference natural thermal maturation, does not result in any significant mobilisation of Re and Os from the ORS.

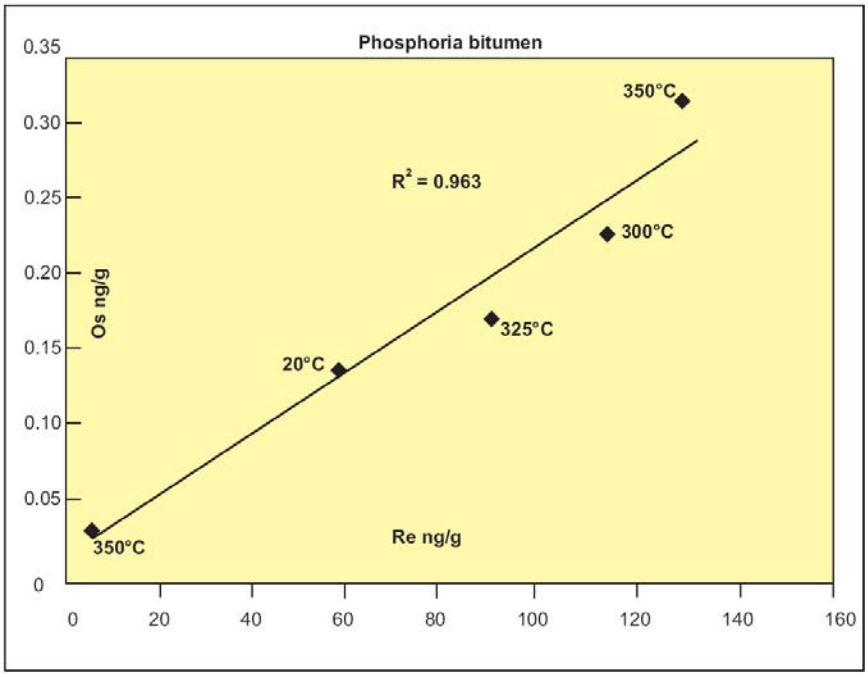

Fig. 4.5 Re abundance vs. Os abundance for the Phosphoria bitumens. Graph illustrates the linear relationship between Re and Os abundance in bitumens generated from hydrous pyrolysis experiments and naturally-occurring bitumen suggesting that Re and Os are transferred to similar organic sites for this Type IIS kerogen.

Analysis of the Staffin and Phosphoria bitumen and asphaltene fractions from both non-pyrolysed and pyrolysed samples indicate that the asphaltene contains >90% of the bitumen Re and Os budget. These findings are in agreement with studies on asphaltene fractions of whole oils suggesting that Re and Os in natural and pyrolysis generated bitumens are bound in heteroatomic ligands, preferentially found in asphaltenes (Selby et al., 2007).

This research demonstrates that in both natural and pyrolysis generated bitumen, Re and Os is present, which originated from the alteration of kerogen. In contrast to natural oils, the oils generated from hydrous pyrolysis on the Staffin and Phosphoria samples do

not contain any Re or Os above blank levels (Selby et al., 2007; this study). Only the asphaltene of the 350˚C oil contained enough Re and Os to provide precise abundance and isotope composition data.

The lack of Re and Os transfer from the bitumens to the oils indicates that hydrous pyrolysis may not completely mimic natural petroleum generation with respect to Re and Os transfer from source rocks to oils. However, there are two major differences between natural systems and the hydrous pyrolysis experiments. Principally, the temperatures of hydrous pyrolysis are much greater than that of natural generation. The higher temperatures involved in hydrous pyrolysis may induce the transfer of Re and Os from the kerogen into an insoluble phase such as pyrobitumen. Pyrobitumen is impossible to distinguish or isolate from kerogen without using HF. The latter process results in artificially disturbing the Re-Os systematics by leaching Re preferentially over Os (Selby and Creaser, 2003). The Re and Os have not been transferred to the oil despite reaching the peak oil generation temperature and they are not found in the water used in the hydrous pyrolysis or the precipitate. From this it is plausible to hypothesise that the Re has been taken up into the kerogen as a form of pyrobitumen which is insoluble and cannot be analysed without adversely affecting the Re-Os systematics. Secondly, the distinct time differences for maturation in natural systems in contrast with hydrous pyrolysis experiments may be vital to transfer of Re and Os from bitumen to oil (10^6 to 10^8 years and hours and days, respectively).

These two major differences, time and temperature, lead us to suggest that the transfer of Re and Os from kerogens to bitumens and into oils is kinetically controlled. The kinetic parameters of hydrous pyrolysis, namely high temperatures over short periods of time are not conducive to the transfer of Re and Os from source rock kerogens to bitumens and into oils. Thus, it can be postulated that these metals reside in very stable functional groups that, despite the elevated temperatures, do not undergo significant transfer on a short timescale.

4.5.3 Implications of Re and Os isotopic data of pyrolysed whole rock, kerogen and bitumen

Whole rock and kerogen $^{187}Re/^{188}Os$ ratios across the temperature range of the hydrous pyrolysis experiments are broadly similar for the Staffin and Phosphoria samples

(Fig. 4.6). Similarly, the $^{187}Os/^{188}Os$ ratios show only minor variations for the Staffin and Phosphoria whole rock and kerogen samples (Fig. 4.6). These isotope data strongly suggest that petroleum generation through hydrous pyrolysis experiments does not disturb the Re-Os systematics in ORS as supported by various studies on natural systems (Creaser et al., 2002; Selby and Creaser, 2005a; Rooney et al., 2010). This lack of disturbance in the isotope ratios suggests that Re-Os geochronology of overmature ORS is viable because Re and Os are not significantly removed from the kerogen fraction of the source rock during petroleum maturation. As a result, the $^{187}Re/^{188}Os$ and $^{187}Os/^{188}Os$ ratios of overmature ORS are broadly similar to those of the immature ORS counterpart. Minute variations in $^{187}Re/^{188}Os$ and $^{187}Os/^{188}Os$ ratios in ORS of varying maturity and any fractionation that occurs during this process may result from the minor transfer of Re and Os from kerogen to bitumen to petroleum. These very minor variations and any associated fractionation could be one of the factors that control the uncertainties presented for Re-Os ORS geochronology.

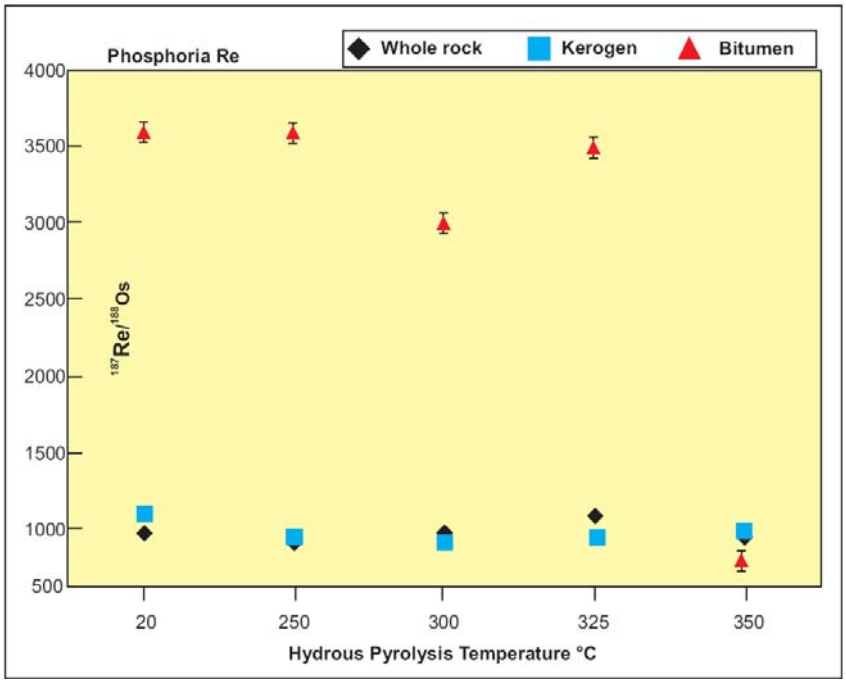

Fig. 4.6 $^{187}Re/^{188}Os$ ratios for the three organic components of the Phosphoria source rocks plotted against hydrous pyrolysis temperatures.

The Staffin bitumen samples have very large uncertainties associated with the $^{187}Re/^{188}Os$ and $^{187}Os/^{188}Os$ ratios related to the blank correction on these very small (<0.05 g) samples bearing minor Re and Os (0.4 – 2.1 ng/g and 0.3 – 8.2 pg/, respectively) that are not conducive to precise analysis. As a result, it is extremely difficult to evaluate the Re-Os isotope data for the pyrolysed Staffin bitumen fractions with any confidence so these

findings will not be discussed further. The non-pyrolysed Staffin bitumen sample does provide precise $^{187}Re/^{188}Os$ and $^{187}Os/^{188}Os$ data. This bitumen fraction possesses a much lower $^{187}Re/^{188}Os$ ratio compared with the whole rock. The significance of these results will be discussed more fully with respect to the Phosphoria results.

The bitumen components for the Phosphoria samples yield precise data that allow the discussion of the isotope composition and transfer of Re and Os from kerogen to bitumen. Bitumen generated from pyrolysis at 250°, 300° and 325˚C have broadly similar $^{187}Re/^{188}Os$ ratios (~3200 – 3800). In contrast the bitumen from the 350˚C experiment has a much lower $^{187}Re/^{188}Os$ ratio (781; Fig. 4.6). This is due to the significantly lower Re abundance in comparison with the Os abundance in the 350˚C generated bitumen. The $^{187}Os/^{188}Os$ ratios of the Phosphoria bitumens also display a considerable variation (26%). The majority of this variation is centred on the contrast in $^{187}Os/^{188}Os$ ratios from the non-pyrolysed bitumen sample to the pyrolysed bitumen samples (5.979 vs. 3.640, respectively). All the pyrolysed bitumen samples possess similar $^{187}Os/^{188}Os$ ratios (4% variation) across the range of hydrous pyrolysis temperatures (Fig. 4.7).

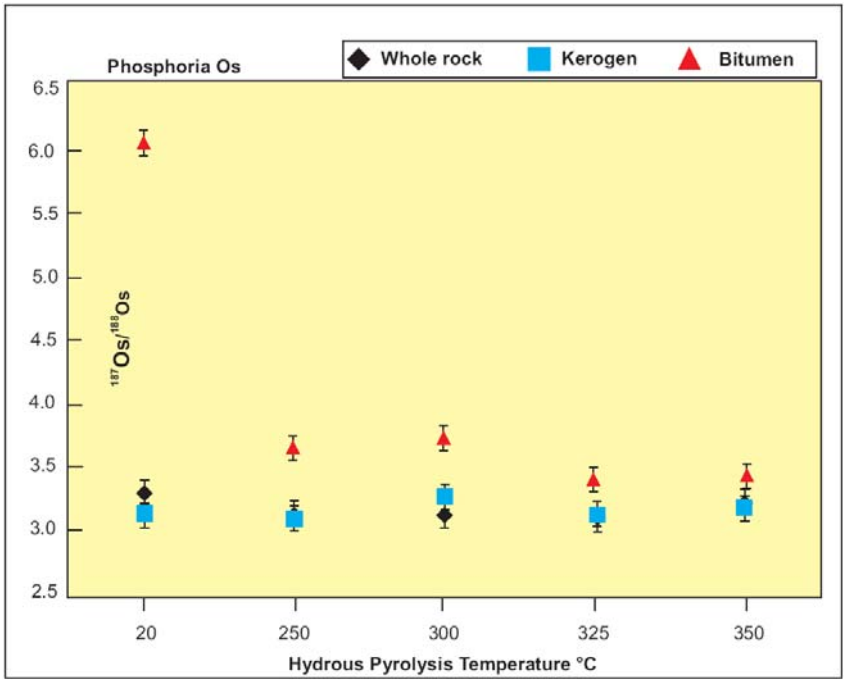

Fig. 4.7 $^{187}Os/^{188}Os$ ratios for the three organic components of the Phosphoria source rocks plotted against hydrous pyrolysis temperatures.

The bitumen of the non-pyrolysed rock was generated as a result of burial of the Permian Phosphoria Formation. This bitumen contains significant enrichment of Re (0.98 ng/g) over Os (2.3 pg/g), which is reflected in the very high $^{187}Re/^{188}Os$ ratio (>3500). Due

to the in-growth of radiogenic ^{187}Os, this natural bitumen has a much more radiogenic ratio than that of the whole rock. In contrast, the pyrolysed rock has no time to produce radiogenic ^{187}Os thus the $^{187}Os/^{188}Os$ ratio is much lower, and reflects that of the whole rock and kerogen ratios (Table 4.3). There is a general trend in the relationship between the $^{187}Os/^{188}Os$ ratio and the temperature of bitumen generation through hydrous pyrolysis with the lower temperature bitumens having a more radiogenic $^{187}Os/^{188}Os$ ratio than the higher temperature bitumens. Our understanding behind this trend is that the bitumen containing the $^{187}Os/^{188}Os$ ratio inherited from the kerogen from the experiments is overwhelmed by the more radiogenic $^{187}Os/^{188}Os$ ratio of the pre-existing bitumen. Conversely, the higher temperature experiments e.g., 300°C bitumen have generated a greater amount of bitumen and thus the $^{187}Os/^{188}Os$ ratio is slightly less radiogenic and is closer, in this regard, to the whole rock value (Tables 4.3 and 4.4).

In contrast, the Staffin samples strongly suggest that there is greater transfer of Os than Re into the bitumen. This suggests that Os transfer in contrast with Re transfer from a Type III kerogen occurs more readily. Furthermore, the differing kinetic conditions involved in natural maturation in contrast with hydrous pyrolysis may play a role as discussed in section 5.2. The $^{187}Os/^{188}Os$ ratio of the natural Staffin bitumen is more radiogenic than the whole rock component reflecting the in-growth of radiogenic ^{187}Os from the decay of ^{187}Re coupled with the Os abundance (2.2% of whole rock content) which was transferred during burial.

Analysis of the asphaltene from the oil generated from the Phosphoria 350°C experiment yields a $^{187}Os/^{188}Os$ ratio that is comparable with that of the bitumen for the pyrolysed samples (3.5954 and 3.5017, respectively; Table 4.3). Although this is only one analysis and the small amount of asphaltene only provided imprecise data the results do agree with previous studies which show the $^{187}Os/^{188}Os$ ratio of oils and asphaltenes can be used as a technique for correlating an oil to its source. The variation in $^{187}Os/^{188}Os$ ratios between the non-pyrolysed rock bitumen and pyrolysed rock bitumens could have implications for employing the Re-Os system as a tool for fingerprinting oils within petroleum systems (e.g., Selby and Creaser, 2005b; Selby et al., 2007).

The Phosphoria samples illustrate an excellent relationship between $^{187}Os/^{188}Os$ ratios for hydrous pyrolysis bitumens and whole rock $^{187}Os/^{188}Os$ ratios (Table 4.3; Figs. 4.6 and 4.7). This strongly suggests that generated bitumens from hydrous pyrolysis reflect or inherit the $^{187}Os/^{188}Os$ ratios of the source rock and that any fractionation is extremely

minor (Fig. 4.7). Additionally, some oils generated in natural systems have high $^{187}Re/^{188}Os$ ratios relative to the source rock while other oils have low $^{187}Re/^{188}Os$ ratios but both have $^{187}Os/^{188}Os$ ratios that are comparable to the source rock (Selby and Creaser, 2005a; Selby et al., 2007; Finlay, 2010). These findings suggest that kerogen type is a critical factor in the transfer behaviour of Re and Os from ORS into oils. Consequently, these data support earlier studies which suggest that it is possible to relate the $^{187}Os/^{188}Os$ ratio of petroleum to a source rock thus fingerprinting petroleum deposits to a particular source rock (Selby and Creaser, 2005a; Selby et al., 2007; Finlay et al., 2010). This dataset potentially suggests that the Re-Os ORS-petroleum system has the ability to date a source, date the timing of petroleum generation and also fingerprint the source of petroleum. The deployment of the Re-Os system to date and fingerprint petroleum generation will enable geoscientists to more fully understand the geological history of a petroleum system. In particular, this technique will aid in elucidating the timing and rates of generation, the role of fluid flow in sedimentary basins and ultimately increase the accuracy and decrease the risk of exploration programmes.

4.6 Conclusions

Hydrous pyrolysis experiments were employed to improve our understanding of how Re and Os in ORS are affected by hydrocarbon maturation and gain an improved insight to the Re-Os systematics of the ORS – petroleum system. The experiments were designed to allow us to evaluate how Re and Os are transferred from source rock kerogen to bitumen and into oils. The experiments provide the results on Re and Os isotope abundance and isotope data from the first attempt to monitor the transfer of Re and Os from source rocks into oils on a laboratory timescale.

Following extraction of bitumen from two immature Phanerozoic source rocks Re-Os isotope analyses indicate that the kerogen component has Re and Os abundances that are broadly similar of the whole rock values. Thus Re and Os are predominantly bound in the kerogen. In addition, the $^{187}Re/^{188}Os$ and $^{187}Os/^{188}Os$ ratios of the kerogen and whole rock components of these immature source rocks are very similar.

Although there are significant (up to 27%) variations in Re and Os abundances between the pyrolysed whole rock and kerogen components, the $^{187}Re/^{188}Os$ and $^{187}Os/^{188}Os$ ratios of the kerogens and whole rock components display much smaller

variations. Importantly, the non-pyrolysed and pyrolysed whole rocks and kerogen $^{187}Re/^{188}Os$ and $^{187}Os/^{188}Os$ ratios vary less than the abundances (17% and 4%, respectively). These results suggest minimal transfer of Re-Os from kerogen to the bitumen fraction. The dataset from these hydrous pyrolysis experiments allow us to conclude that Re and Os remain complexed in kerogen even after hydrocarbon maturation and / or polyphase metamorphism. This is probably a result of the Re and Os being complexed within very stable functional groups that are associated with insoluble organic matter. Furthermore, it can be hypothesised that the hydrocarbon maturation process does not adversely upset the Re-Os system. This has been observed for natural systems and thus further demonstrates that Re-Os geochronology is feasible on petroleum overmature and metamorphosed ORS.

The peak bitumen generation temperature of Type IIS kerogens occurs at 300°C and correlates with the peak Re and Os abundance of this bitumen. This suggests that as the kerogen cracks to bitumen, Re and Os are mobilised and transferred from the complexation site in kerogen to the related site in Type IIS bitumens.

The Phosphoria bitumens from the non-pyrolysed samples have $^{187}Os/^{188}Os$ ratios that are much more radiogenic than those of the non-pyrolysed whole rocks. In contrast, the pyrolysis-generated bitumens have $^{187}Os/^{188}Os$ ratios which are closer to the value for the whole rock ratio (44% and up to 17% variation, respectively). These results are in agreement with studies on natural crude oils and suggest that when oils / bitumen / asphaltene are generated they take on the $^{187}Os/^{188}Os$ ratios of the source rock at the time of generation and could possibly be used as a "finger-printing" tool in petroleum systems.

After bitumen generation, the source rocks produce immiscible oil with generation peaking at 355° and 350°C for Type IIS and III, respectively. Natural Phosphoria oils contain up to 17 ppb Re and 102 ppt Os however, in contrast, the oils generated by hydrous pyrolysis contain less than 0.2 ppb Re and 0.5 ppt Os. This lack of transfer from the bitumen to the oils demonstrates that hydrous pyrolysis experiments do not fully mimic natural systems with respect to Re and Os transfer from source rocks to oils. This lack of transfer of Re and Os to the oils from bitumens in the experiments may be a result of the high experimental temperatures and short time frames resulting in the formation of inorganic phase such as pyrobitumen. This pyrobitumen phase is insoluble and impossible to isolate without disturbing Re-Os systematics. This lack of Re and Os in the oils from these experiments strongly suggests that the transfer of Re and Os is kinetically controlled with time possibly being the most important factor.

4.7 References

Anbar, A. D., Duan, Y., Lyons, T. W., Arnold, G. L., Kendall, B., Creaser, R. A., Kaufman, A. J., Gordon, G. W., Scott, C., Garvin, J., and Buick, R., 2007. A whiff of oxygen before the great oxidation event? *Science* **317**, 1903 -1906.

Barre, A. B., Prinzhofer, A., and Allegre, C. J., 1995. Osmium isotopes in the organic matter of crude oil and asphaltenes. *Terra Abstracts* **7**, 199.

Behar, F., Beaumont, V., Penteado., H.L. De B., 2001. Rock-Eval 6 Technology: Performances and Developments. *Oil and Gas Science and Technology* **56**, 111-134.

Cohen, A. S., Coe, A. L., Bartlett, J. M., and Hawkesworth, C. J., 1999. Precise Re-Os ages of organic-rich mudrocks and the Os isotope composition of Jurassic seawater. *Earth and Planetary Science Letters* **167**, 159-173.

Cohen, A. S., Coe, A. L., Harding, M. S., and Schwark, L., 2004. Osmium isotope evidence for the regulation of atmospheric CO2 by continental weathering. *Geology* **32**, 157-160.

Cooke, D. R., Bull, S. W., Donovan, S., and Rogers, J. R., 1998. K-Metasomatism and base metal depletion in volcanic rocks from the McArthur Basin, Northern Territory - Implications for base metal mineralization. *Economic Geology* **93**, 1237-1263.

Creaser, R. A., Papanastassiou, D. A., and Wasserburg, G. J., 1991. Negative thermal ion mass spectrometry of osmium, rhenium and iridium. *Geochimica et Cosmochimica et Acta* **55**, 397-401.

Creaser, R. A., Sannigrahi, P., Chacko, T., and Selby, D., 2002. Further evaluation of the Re-Os geochronometer in organic-rich sedimentary rocks: A test of hydrocarbon maturation effects in the Exshaw Formation, Western Canada Sedimentary Basin. *Geochimica et Cosmochimica Acta* **66**, 3441-3452.

Esser, B. K. and Turekian, K. K., 1993. The osmium isotopic composition of the continental crust. *Geochimica Cosmochimica Acta* **57**, 3093-3104.

Finlay, A. J., Selby, D., Osborne, M., and Finucane, D., 2010. Fault-charged mantle-fluid contamination of United Kingdom North Sea oils: Insights from Re-Os isotopes. *Geology* **38**, 979-982.

Hattori, Y., Suzuki, K., Honda, M., and Shimizu, H., 2003. Re-Os isotope systematics of the Taklimakan Desert sands, moraines and river sediments around the taklimakan desert, and of Tibetan soils. *Geochimica Et Cosmochimica Acta* **67**, 1203-1213.

Hein, J. R., Perkins, R. B., and McIntyre, B. R., 2004. Evolution of thought concerning the origin of the Phosphoria Formation, Western US phosphate Field. In: Hein, J. R. (Ed.), *Life Cycle of the Phosphoria Formation: From deposition to post-mining environment*. Elsevier.

Hunt, J. M., 1996. *Petroleum Geochemistry and Geology*. W.H. Freeman and Comapny, New York.

Kendall, B., Creaser, R. A., Calver, C. R., Raub, T. D., and Evans, D. A. D., 2009a. Correlation of Sturtian diamictite successions in southern Australia and northwestern Tasmania by Re-Os black shale geochronology and the ambiguity of "Sturtian"-type diamictite-cap carbonate pairs as chronostratigraphic marker horizons. *Precambrian Research* **172**, 301-310.

Kendall, B., Creaser, R. A., Gordon, G. W., and Anbar, A. D., 2009b. Re-Os and Mo isotope systematics of black shales from the Middle Proterozoic Velkerri and

Wollogorang Formations, McArthur Basin, northern Australia. *Geochimica Et Cosmochimica Acta* **73**, 2534-2558.

Kendall, B. S. and Creaser, R. A., 2006. Re-Os systematics of the Proterozoic Velkerri and Wollogorang black shales, McArthur basin, Northern Australia. *Geochimica Et Cosmochimica Acta* **70**, A314-A314.

Kendall, B. S., Creaser, R. A., Ross, G. M., and Selby, D., 2004. Constraints on the timing of Marinoan 'Snowball Earth' glaciation by $^{187}Re - ^{187}Os$ dating of a Neoproterozoic post-glacial black shale in Western Canada. *Earth and Planetary Science Letters* **222**, 729-740.

Lewan, M. D., 1978. Laboratory Classification of Very Fine-Grained Sedimentary-Rocks. *Geology* **6**, 745-748.

Lewan, M. D., 1979. Generation of oil-like pyrolyzates from organic-rich shales. *Science* **203**, 897-899.

Lewan, M. D., 1985. Evaluation of petroleum generation by hydrous pyrolysis experimentation. *Philosophical Transactions of the Royal Society A: Mathematical and Physical Sciences* **315**, 123-134.

Lewan, M. D., 1986. Stable carbon isotopes of amorphous kerogens from Phanerozoic sedimentary rocks. *Geochimica et Cosmochimica Acta* **50**, 1583-1591.

Lewan, M. D., 1997. Experiments on the role of water in petroleum formation. *Geochimica Et Cosmochimica Acta* **61**, 3691-3723.

Lewan, M. D., Kotarba, M. J., Curtis, J. B., Wieclaw, D., and Kosakowski, P., 2006. Oil-generation kinetics for organic facies with Type-II and -IIS kerogen in the Menilite Shales of the Polish Carpathians. *Geochimica Et Cosmochimica Acta* **70**, 3351-3368.

Lewan, M. D. and Ruble, T. E., 2002. Comparison of petroleum generation kinetics by isothermal hydrous and nonisothermal open-system pyrolysis. *Organic Geochemistry* **33**, 1457-1475.

Matyja, B. A., Wierzbowski, A., and Wright, J. K., 2006. The Subboreal/Boreal ammonite succession at the Oxfordian/Kimmeridgian boundary at Flodigarry, Staffin Bay (Isle of Skye), Scotland. *Transactions of Royal Society of Edinburgh, Earth Sciences* **96**, in press.

Peters, K. E., 1986. Guidelines for evaluating programmed pyrolysis. *American Association of Petroleum Geologists Bulletin* **70**, 318-329.

Peucker-Ehrenbrink, B. and Jahn, B.-m., 2001. Rhenium-osmium isotope systematics and platinum group element concentrations: Loess and the upper continental crust. *Geochem. Geophys. Geosyst.* **2**.

Piper, D. Z. and Link, P. K., 2002. An upwelling model for the Phosphoria sea: A Permian, ocean-margin sea in the northwest United States. *AAPG Bulletin* **86**, 1217-1235.

Ravizza, G. and Turekian, K. K., 1989. Application of the ^{187}Re-^{187}Os system to black shale geochronometry. *Geochimica et Cosmochimica Acta* **53**, 3257-3262.

Reynolds, J. G. and Burnham, A. K., 1995. Comparison of Kinetic-Analysis of Source Rocks and Kerogen Concentrates. *Organic Geochemistry* **23**, 11-19.

Rooney, A. D., Selby, D., Houzay, J.-P., and Renne, P. R., 2010. Re-Os geochronology of a Mesoproterozoic sedimentary succession, Taoudeni basin, Mauritania: Implications for basin-wide correlations and Re-Os organic-rich sediments systematics. *Earth and Planetary Science Letters* **289**, 486-496.

Ruble, T. E., Lewan, M. D., and Philp, R. P., 2001. New insights on the Green River petroleum system in the Uinta basin from hydrous pyrolysis experiments. *Aapg Bulletin* **85**, 1333-1371.

Selby, D., 2007. Direct Rhenium-Osmium age of the Oxfordian-Kimmeridgian boundary, Staffin bay, Isle of Skye, U.K., and the Late Jurassic time scale. *Norwegian Journal of Geology* **87**, 9.

Selby, D. and Creaser, R. A., 2003. Re-Os geochronology of organic rich sediments: an evaluation of organic matter analysis methods. *Chemical Geology* **200**, 225-240.

Selby, D. and Creaser, R. A., 2005a. Direct radiometric dating of hydrocarbon deposits using rhenium-osmium isotopes. *Science* **308**, 1293-1295.

Selby, D. and Creaser, R. A., 2005b. Direct radiometric dating of the Devonian-Mississippian time-scale boundary using the Re-Os black shale geochronometer. *Geology* **33**, 545-548.

Selby, D., Creaser, R. A., Dewing, K., and Fowler, M., 2005. Evaluation of bitumen as a Re-187-Os-187 geochronometer for hydrocarbon maturation and migration: A test case from the Polaris MVT deposit, Canada. *Earth and Planetary Science Letters* **235**, 1-15.

Selby, D., Creaser, R. A., and Fowler, M. G., 2007. Re-Os elemental and isotopic systematics in crude oils. *Geochimica Et Cosmochimica Acta* **71**, 378-386.

Sun, W., Arculus, R. J., Bennett, V. C., Eggins, S. M., and Binns, R. A., 2003. Evidence for rhenium enrichment in the mantle wedge from submarine arc-like volcanic glasses (Papua New Guinea). *Geology* **31**, 845-848.

Tissot, B. P. and Welte, D. H., 1984. *Petroleum formation and occurrence*. Springer, Berlin. P.143. 538 pp.

Turgeon, S. C., Creaser, R. A., and Algeo, T. J., 2007. Re-Os depositional ages and seawater Os estimates for the Frasnian-Famennian boundary: Implications for weathering rates, land plant evolution, and extinction mechanisms. *Earth and Planetary Science Letters* **261**, 649-661.

Vandenbroucke, M., 2003. Kerogen: from types to models of chemical structure. *Oil & Gas Science and Technology-Revue De L Institut Francais Du Petrole* **58**, 243-269.

Völkening, J., Walczyk, T., and G. Heumann, K., 1991. Osmium isotope ratio determinations by negative thermal ionization mass spectrometry. *International Journal of Mass Spectrometry and Ion Processes* **105**, 147-159.

Walczyk, T., Hebeda, E. H., and Heumann, K. G., 1991. Osmium isotope ratio measurements by negative thermal ionization mass spectrometry (NTI-MS). Improvement in precision and enhancement in emission by introducing oxygen or Freon into the ion source. *Fresenius' Journal of Analytical Chemistry* **341**, 537-541.

Woodland, S. J., Ottley, C. J., Pearson, D. G., and Swarbrick, R. E., 2001. Microwave digestion of oils for analysis of platinum group and rare earth elements by ICP-MS, *Plasma Source Mass Spectrometry*. Special Publication Royal Society of Chemistry, London.

Yang, G., Hannah, J. L., Zimmerman, A., Stein, H. J., and Bekker, A., 2009. Re-Os depositional age for Archean carbonaceous slates from the southwestern Superior Province: Challenges and insights. *Earth and Planetary Science Letters* **280**, 83-92.

Chapter 5: Conclusions and future research

This thesis addresses two aspects of Re-Os geochronology; use of Re-Os geochronology in Proterozoic successions and the effects of various geological processes on Re-Os systematics. As this thesis was written as a series of papers each chapter has its own specific conclusion section. This concluding chapter briefly draws together the key aspects of each chapter and suggests possible directions for future research.

5.1 Re-Os geochronology of the Atar Group, Mauritania

The Atar Group of the Taoudeni basin is a sedimentary succession which includes potential source rocks for a hydrocarbon system of considerable size (~ 1M km^2). Our understanding of the basin's stratigraphy had hitherto suffered from a lack of biostratigraphically useful fossils and accurate radiometric age constraints. Previous geochronological constraints from Rb-Sr clay ages were brought into question by preliminary $\delta^{13}C_{carbonate}$ chemostratigraphy studies which suggest the Atar Group rocks were much older.

The new Re-Os geochronology provides three precise Mesoproterozoic ages which are identical, within uncertainty, from 2 drill cores. These drill cores are separated by >200 km. The Re-Os data indicates that the Atar Group rocks are >200 Ma older than previously thought. Additionally, the identical Re-Os ages derived from samples of both drill cores indicate that Re-Os geochronology provides geoscientists with a technique for accurately correlating source rocks on a basin-wide scale. The new Re-Os age data infer that the Rb-Sr ages record a diagenetic event, possibly associated with the Pan African orogeny ca. 700 Ma.

The shales from the S1 drill core have experienced flash pyrolysis and offer an opportunity to evaluate the effects of very rapid heating of source rocks on Re-Os systematics. The age for the S1 core is identical, within uncertainty, to the immature shales indicating that the Re-Os system is not adversely affected by this type of thermal alteration. Identification of pyrrhotite and the mineralogical composition of the intrusive body enable us to place loose constraints on the temperatures experienced during 'flash pyrolysis'. The presence of pyrrhotite coupled with calculations based on bitumen reflectance data suggests that the S1 shales experienced temperatures of up to 650°C. These temperature data provide

vital information on the robustness of the Re-Os system in this geological setting and strongly suggest that accurate and precise Re-Os geochronology is possible in sedimentary rocks that have experienced contact metamorphism.

The Re-Os ages for the Atar Group of the Taoudeni basin have profound implications for basin-basin and craton-craton correlations as well as new insights into the formation and break-up of the Rodinia supercontinent. The Re-Os geochronology enables us to enhance our understanding of the Taoudeni basin's geological evolution through improved sequence-stratigraphy and the coupling of chemostratigraphic profiles to precise geochronological data.

The Re-Os ages for the Atar Group shales are approximately equivalent to ages for Mesoproterozoic sedimentary rocks found on the São Francisco craton. Additionally, the similar Os_i for the shales on these two cratons suggest that the sediments were deposited in basins of the Brasiliano Ocean that existed between the West African and São Francisco cratons during the Mesoproterozoic. Although reliable palaeomagnetic data are limited, it has been suggested that the São Francisco and West African cratons were separated by the Brasiliano Ocean and thus not involved in the initial formation of Rodinia. The new Re-Os geochronology data suggest a reassessment of the drift history of the West African craton and its role in the formation of Rodinia is required.

Use of the Re-Os ORS technique has yielded new geochronology data that are vital to fully understanding the geological history of the Taoudeni basin of Mauritania. However, the Taoudeni basin is still a largely unexplored region and the data presented here offers a basis upon which future work may be planned. The size of the Taoudeni basin (>1 M km^2), the harsh desert environment and an unstable geopolitical context are principle reasons why the geological history of the basin is so poorly understood.

Future work that may redress gaps in our knowledge include building a more complete chronostratigraphy for the Touirist and En Nesoar Formations of the Atar Group and also of the Char Group, which unconformably underlies the Atar Group. Furthermore, additional Re-Os studies will also provide a more complete understanding of the Os_i of seawater throughout the Mesoproterozoic and will enable us to assess whether the sub-basins of the Taoudeni basin were well connected.

Much of this proposed future work is reliant on material being provided from further exploration programmes of oil companies or national geology surveys such as the BGS or BRGM.

5.2 Re-Os geochronology of the Dalradian Supergroup, Scotland

Application of the Re-Os geochronometer to the Ballachulish Slate Formation of the Dalradian Supergroup yields a depositional age of 659.6 ± 9.6 Ma. The samples used in this study have low Re and Os abundances (~1 ppb and ~50 ppt, respectively). The excellent fit of the data and low MSWD indicate that it is possible to gain accurate and precise ages from samples with low Re and Os abundances as well as samples with higher abundances.

The depositional age for the Ballachulish Slate provides a maximum age constraint for the glaciogenic Port Askaig Formation. Additionally, the Re-Os age enables us to improve our current understanding of glaciations during the late Neoproterozoic and refine the $\delta^{13}C$ and $^{87}Sr/^{86}Sr$ chemostratigraphy of the Dalradian. The Re-Os age of 659.6 ± 9.6 Ma for the Ballachulish Slate Formation suggests that the Port Askaig Formation may record a low latitude glaciation at ca. 650 Ma. This glacial event may be correlative with the Sturtian events recorded in the Adelaide Rift Complex. The Re-Os age presented here rules out a correlation of the Port Askaig Formation with the middle Cryogenian (715 Ma) glaciations.

The Re-Os age enables us to better understand the dynamics of the Dalradian basin during the Neoproterozoic. The geochronology coupled with sedimentological interpretations of the middle Dalradian indicate that, as the environment of deposition evolved from a slowly subsiding margin to rapid deposition in rift basins, the Argyll Group was deposited in ca. 60 Ma.

In addition to the new age, the Ballachulish study provides essential new data on the Os_i of Neoproterozoic seawater. The Os_i value for the Ballachulish slate of 1.04 is radiogenic and very similar to that of present day seawater (1.06). This indicates that the input of radiogenic Os from weathering of the continental crust dominated over the influx of unradiogenic Os from hydrothermal sources and alteration of oceanic crusts. The radiogenic values for the Ballachulish Slate Formation are also similar to those from Sturtian age (*sensu stricto*) post-glacial shales. From this it can be suggested that together these Os_i values represent a global Os isotope composition for the 660 – 640 Ma interval. The Neoproterozoic values for Os_i are much more radiogenic than values from Mesoproterozoic seawater. Possible causes for this rise in Os_i may be a) that as the

continental crust became more radiogenic over time the Os isotope composition of seawater became more radiogenic in the late Neoproterozoic and b) the increased oxygenation of subsurface waters during the late Neoproterozoic (Canfield and Teske, 1996; Anbar and Knoll, 2002; Canfield et al., 2007). This 'global' radiogenic Neoproterozoic Os isotope composition of seawater is suggestive of an evolved continental crust shedding radiogenic Os into oceans that were well connected.

The successful application of the Re-Os system to the Ballachulish Slate Formation samples illustrate that low Re and Os abundances or polyphase metamorphism do not adversely affect the Re-Os systematics. In contrast, the study on the Leny Limestone samples did not yield a meaningful age despite the enriched levels of Re and Os. Evaluation of these samples, the geological history of the Leny Quarry and the Os isotope composition suggests that hydration and fluid-flow events associated with contact metamorphism have resulted in open-system behaviour. The plotting of the Re-Os isotope data reveals that the Leny Limestone samples have $^{187}Re/^{188}Os$ ratios which plot to the right of the 512 Ma reference line and imply that samples experienced either Re gain or Os loss. Use of XRD analysis reveals a composition including kaolinite, muscovite and berthierine. The disturbed Re-Os isotope data and the presence of igneous intrusions would suggest that these minerals are the products of retrograde reactions driven by hydrothermal fluids. The results of the Leny Limestone study strongly suggest that the Re-Os system in these samples was disturbed by hydrothermal fluid flow associated with the intrusion of numerous igneous bodies during the Palaeozoic.

While the Re-Os data for the Ballachulish Slate Formation provides a maximum age constraint for the Port Askaig Formation there is no upper constraint for this formation, although the Tayvallich Volcanics do provide an age constraint of 600 Ma for the Argyll Group. Future Re-Os work on the Dalradian has the potential to greatly enhance our understanding of the Port Askaig Formation and its role as a Neoproterozoic glacial unit. Reliable, high-precision geochronology is essential for our efforts to elucidate more of the geological history of the Dalradian and its role in the formation and break up of the Rodinia supercontinent. Furthermore, the application of Re-Os geochronology will aid in more fully understanding the stable isotope data that already exist for the Dalradian. In particular, sedimentary units such as the Easdale Slate and Cuil Bay slates may provide new geochronological constraints and insights into the rates of geological processes during deposition of the Dalradian Supergroup. Gaining reliable depositional age data for the

Easdale Slate Formation will also provide a more accurate minimum age constraint for the Port Askaig Formation. The successful application of the Re-Os geochronometer to samples with very low Re and Os abundances raises the possibility of directly dating a glaciogenic horizon. The sedimentary succession of the Port Askaig Formation includes mudstones that may be possible to date despite the lack of a thick black mudstone horizon. Gaining a depositional age for the Port Askaig Formation would be the first dating of a glacial unit and would end more than a century's debate regarding the age of this glaciogenic horizon.

5.3 Hydrous pyrolysis of organic-rich sedimentary rocks and insights into Re-Os systematics

The hydrous pyrolysis experiments were designed to improve our current knowledge of the Re-Os systematics in ORS. The experiments provided useful insights into the location and transfer mechanisms of Re and Os in ORS during maturation of hydrocarbons. This study provides the first Re and Os data from Type IIS and III kerogens and represents a novel way of exploring the effects of thermal maturation on Re-Os systematics.

Analysis of Phanerozoic source rocks and kerogen show that the Re and Os abundances of the kerogen component are within ~15% of whole rock values despite reaching peak bitumen generation temperature. The $^{187}Re/^{188}Os$ and $^{187}Os/^{188}Os$ ratios for both source rocks are similar (within ~15%) for the whole rock and kerogen components. These results suggest that the kerogen component is host to >90% of the Re and Os budget in immature source rocks.

The high levels of enrichment of the kerogen in comparison to the generated pyrolysates and bitumen suggest that there is limited disturbance of the Re-Os systematics from the cracking of kerogen. This also suggests that Re and Os are located in very stable organic sites that are associated with insoluble organic matter (kerogen) and remain in these sites even after hydrocarbon generation.

The results from these experiments strongly suggest that the lack of disturbance to the kerogen Re-Os systematics is *why* thermal stress alone does not result in disturbance to the Re-Os systematics. These data support previous studies that have demonstrated that the

Re-Os geochronometer can provide meaningful geological dates even from ORS that have experienced hydrocarbon maturation and / or polyphase metamorphism (Creaser et al., 2002; Kendall et al., 2009; Rooney et al., 2010).

The isotope composition data from the Staffin bitumens cannot be assessed with any degree of confidence due to the large uncertainties associated with the small sample size and the minor Re and Os abundances of the bitumen. In contrast, the bitumens from the Phosphoria Formation do provide precise Re and Os abundance and isotope composition data. The Re and Os abundances for the Phosphoria Formation peak at 300°C which is the temperature of peak bitumen generation for a Type IIS kerogen (Lewan, 1985). The excellent linear relationship ($R^2 = 0.963$) between Re and Os abundance in the bitumens is likely to be due to these metals being transferred consistently from the kerogen to similar sites within the bitumen. Further analysis of the bitumen components reveals that >90% of the Re and Os is hosted in the asphaltene component of the bitumen, as identified by Selby et al. (2007) in natural petroleum.

The non-pyrolysed bitumen for the Phosphoria sample has a $^{187}Os/^{188}Os$ composition that is much more radiogenic than that of the pyrolysed samples. This is likely to be caused by the significant in-growth of radiogenic ^{187}Os from the decay of ^{187}Re added to the $^{187}Os/^{188}Os$ ratio of the source rock at the time of bitumen generation. In contrast, the pyrolysed bitumens $^{187}Os/^{188}Os$ ratios are closer in value to whole rock values. Although the hydrous pyrolysis experiments do result in the generation of immiscible oil only one of these oils contains measureable Re and Os abundances. This general lack of Re and Os enrichment in the oils is in stark contrast to natural oils (Barre et al., 1995; Woodland et al., 2001; Selby and Creaser, 2005; Selby et al., 2007; Finlay et al., 2010). The oil from the 350°C Phosphoria experiment does produce an oil with sufficient quantities of Re and Os for analysis of the asphaltene component of the oil. The $^{187}Os/^{188}Os$ ratio of this asphaltene is very similar (2% variation) to that of the bitumens generated from the Phosphoria sample. This is in agreement with previous studies which established that natural oils / bitumens / asphaltenes take on the $^{187}Os/^{188}Os$ ratio of the whole rock at the time of generation and can be used as a tool for fingerprinting oils to source rocks

Explanations for the limited transfer of Re and Os from kerogens to bitumens and finally to oils may centre on the kinetics involved in hydrous pyrolysis experiments and the very stable location of Re and Os in functional groups located in the kerogens. The very short timescale of the hydrous pyrolysis experiments, coupled with the very high

temperatures are not conducive to Re and Os transfer possibly result in the generation of pyrobitumen. The generation of this pyrobitumen may result in Re and Os being retained within the matrix of the kerogen and not released as part of the soluble organic matter.

This research has enabled us to refine our understanding of the Re-Os system and its limitations with respect to thermally altered ORS. Further studies will build upon this research and expand current ideas concerning the deployment of the Re-Os geochronometer in sedimentary rocks and petroleum systems. In particular, hydrous pyrolysis of Type I kerogens will provide new information on the Re-Os systematics in these source rocks which are principally lacustrine rocks although some Proterozoic source rocks are also Type I. As seen from the experiments on the Phosphoria and Staffin shales, the transfer of Re and Os from kerogen to bitumen and then oil may be controlled by kinetics. Thus, longer duration experiments on these source rocks may yield more insights into Re-Os behaviour. Durations of 168 h, 30 days and 90 days are suitable for the laboratory and a research plan that would allow for extraction of bitumen and asphaltene separation and full Re-Os isotope composition analyses.

5.4 References

Anbar, A. D., Knoll, A. H., 2002. Proterozoic ocean chemistry and evolution: A bioinorganic bridge? *Science* **297**, 1137-1142.

Barre, A. B., Prinzhofer, A., and Allegre, C. J., 1995. Osmium isotopes in the organic matter of crude oil and asphaltenes. *Terra Abstracts* **7**, 199.

Canfield, D.E., Teske, A., 1996. Late Proterozoic rise in atmospheric oxygen concentration inferred from phylogenetic and sulphur-isotope studies. *Nature* **382,** 127-132.

Canfield, D.E., Poulton, S.W. Narbonne, G.M., 2007. Late-Neoproterozoic Deep-Ocean Oxygenation and the Rise of Animal Life. *Science* **315,** 92-95.

Creaser, R. A., Sannigrahi, P., Chacko, T., Selby, D., 2002. Further evaluation of the Re-Os geochronometer in organic-rich sedimentary rocks: A test of hydrocarbon maturation effects in the Exshaw Formation, Western Canada Sedimentary Basin. *Geochimica et Cosmochimica Acta* **66**, 3441-3452.

Finlay, A. J., Selby, D., Osborne, M., and Finucane, D., 2010. Fault-charged mantle-fluid contamination of United Kingdom North Sea oils: Insights from Re-Os isotopes. *Geology* **38**, 979-982.

Kendall, B., Creaser, R. A., Gordon, G. W., Anbar, A. D., 2009. Re-Os and Mo isotope systematics of black shales from the Middle Proterozoic Velkerri and Wollogorang Formations, McArthur Basin, northern Australia. *Geochimica Et Cosmochimica Acta* **73**, 2534-2558.

Rooney, A. D., Selby, D., Houzay, J.-P., Renne, P. R., 2010. Re-Os geochronology of a Mesoproterozoic sedimentary succession, Taoudeni basin, Mauritania: Implications for basin-wide correlations and Re-Os organic-rich sediments systematics. *Earth and Planetary Science Letters* **289**, 486-496.

Selby, D. and Creaser, R. A., 2005a. Direct radiometric dating of hydrocarbon deposits using rhenium-osmium isotopes. *Science* **308**, 1293-1295.

Selby, D., Creaser, R. A., and Fowler, M. G., 2007. Re-Os elemental and isotopic systematics in crude oils. *Geochimica Et Cosmochimica Acta* **71**, 378-386.

Woodland, S. J., Ottley, C. J., Pearson, D. G., and Swarbrick, R. E., 2001. Microwave digestion of oils for analysis of platinum group and rare earth elements by ICP-MS, *Plasma Source Mass Spectrometry*. Special Publication Royal Society of Chemistry, London.

Earth and Planetary Science Letters 289 (2010) 486–496

Contents lists available at ScienceDirect

Earth and Planetary Science Letters

journal homepage: www.elsevier.com/locate/epsl

Re–Os geochronology of a Mesoproterozoic sedimentary succession, Taoudeni basin, Mauritania: Implications for basin-wide correlations and Re–Os organic-rich sediments systematics

Alan D. Rooney [a,*], David Selby [a], Jean-Pierre Houzay [b], Paul R. Renne [c,d]

[a] Department of Earth Sciences, University of Durham, Durham, DH1 3LE, UK
[b] Fluids and Geochemistry Department, Total, Avenue Larribau, 64018, Pau Cedex, France
[c] Berkeley Geochronology Center, 2455 Ridge Road, Berkeley, CA 94709, USA
[d] Department of Earth and Planetary Science, University of California, Berkeley, CA 94720, USA

ARTICLE INFO

Article history:
Received 2 September 2009
Received in revised form 17 November 2009
Accepted 17 November 2009
Available online 11 December 2009

Editor: R.W. Carlson

Keywords:
Re–Os geochronology
Mesoproterozoic
Mauritania
Atar Group
Taoudeni basin

ABSTRACT

The exceptionally well-preserved sedimentary rocks of the Taoudeni basin, NW Africa represent one of the world's most widespread (>1 M km^2) Proterozoic successions. Hitherto, the sedimentary rocks were considered to be Mid Tonian based on Rb–Sr illite and glauconite geochronology of the Atar Group. However, new Re–Os organic-rich sediment (ORS) geochronology from two drill cores indicates that the Proterozoic Atar Group is ~200 Ma older (1107 ± 12 Ma, 1109 ± 22 Ma and 1105 ± 37 Ma). The Re–Os geochronology suggests that the Rb–Sr geochronology records the age of diagenetic events possibly associated with the Pan African collision.

The new Re–Os geochronology data provide absolute age constraints for recent carbon isotope chemostratigraphy which suggests that the Atar Group is Mesoproterozoic and not Neoproterozoic.

The new Re–Os ORS geochronology supports previous studies that suggest that rapid hydrocarbon generation (flash pyrolysis) from contact metamorphism of a dolerite sill does not significantly disturb the Re–Os ORS systematics. Modelled contact conditions suggest that the Re–Os ORS systematics remain undisturbed at ~650 °C at the sill/shale contact and ≥280 °C 20 m from the sill/shale contact.

Moreover, the Re–Os geochronology indicates that the West African craton has a depositional history that predates 1100 Ma and that ORS can be correlated on a basin-wide scale. In addition, the Re–Os depositional ages for the ORS of the Taoudeni basin are comparable to those of ORS from the São Francisco craton, suggesting that these cratons are correlatable. This postulate is further supported by identical Os_i values for the Atar Group and the Vazante Group of the São Francisco craton.

1. Introduction

Proterozoic successions record enormous portions of geological time and yet the sedimentary units are poorly constrained in terms of chronostratigraphy. Many of the sedimentary successions lack volcanic horizons that can be targeted for U–Pb or Ar–Ar geochronology and are bereft of fossils suitable for relative age dating. As a result, accurate and precise ages are difficult to determine for these successions and thus hamper regional and worldwide correlations.

For example, the Shaler Supergroup of North America is constrained by upper and lower ages of 723 + 4/−2 Ma and 1077 ± 4 Ma, respectively (Heaman et al., 1992; Rainbird et al., 1994). Other examples are the Bylot Supergroup of Canada, constrained by ages of 723 ± 3 Ma and 1267 ± 2 Ma (LeCheminant and Heaman, 1989; Heaman et al., 1990), and the Dalradian Supergroup of Scotland, which is constrained by a basal age of 806 ± 3 Ma and upper ages of 595 ± 4 Ma and 601 ± 4 Ma (Halliday et al., 1989; Noble et al., 1996; Dempster et al., 2002). The focus of this study is the Proterozoic sedimentary succession of the Taoudeni basin, NW Africa, a Proterozoic basin lacking accurate and precise geochronology (Fig. 1). Recently, in contrast with the existing Rb–Sr geochronology, it has been suggested that the sedimentary succession is much older than previously thought (Mesoproterozoic vs. Neoproterozoic) based on $\delta^{13}C$ chemostratigraphy (Teal and Kah, 2005).

The Taoudeni basin records a discontinuous sedimentation history from the Mesoproterozoic (this study) to the Mesozoic–Cenozoic (Fig. 1; Trompette, 1973; Bertrand-Sarfati and Moussine-Pouchkine, 1985, 1988; Ahmed Benan and Deynoux, 1998; Deynoux et al., 2006). At present, the geochronology of the lowermost Supergroup of the basin is constrained only by Rb–Sr illite and glauconite geochronology (Fig. 2; Clauer, 1976, 1981). The Rb–Sr data for the basal Char Group yields a Tonian age (850–1000 Ma; Ogg et al., 2008) of 998 ± 34 Ma

* Corresponding author. Tel.: +44 0191 334 2300; fax: +44 0191 334 2301.
E-mail address: alan.rooney@durham.ac.uk (A.D. Rooney).

0012-821X/$ – see front matter © 2009 Elsevier B.V. All rights reserved.
doi:10.1016/j.epsl.2009.11.039

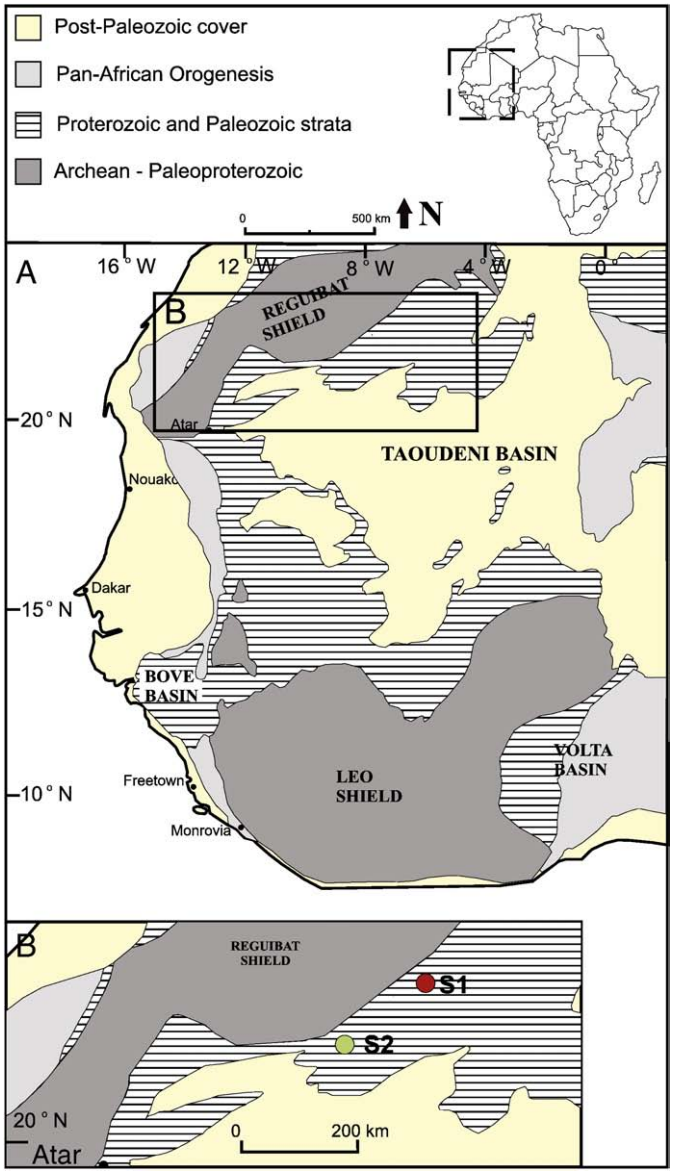

Fig. 1. (A) Regional geological setting for the Taoudeni basin, West Africa. (B) Inset map showing the location of drill cores S1 and S2.
Modified from Deynoux et al. (2006).

(Clauer, 1981). Unconformably overlying the Char Group, the Atar Group is proposed to be Tonian to Cryogenian based on Rb–Sr illite and glauconite ages (890 ± 37 Ma to 775 ± 54 Ma) for stratigraphically successive formations (Fig. 2; Clauer, 1981). However, based on identification of a distinctive negative excursion, $\delta^{13}C$ chemostratigraphy strongly suggests a Mesoproterozoic age for the Atar Group (Teal and Kah, 2005). This excursion is marked by an abrupt decrease of 5‰ over ~25 m, which is followed by a stepwise increase to initial $\delta^{13}C$ values of ca. + 3‰ (Kah et al., 1999; Kah and Bartley, 2004). This excursion is very similar to C-isotope signatures identified in Mesoproterozoic strata from Arctic Canada (Kah et al., 1999) and Siberia (Bartley et al., 2001), and is distinct from more muted excursions recorded in 1200–1300 Ma strata (Frank et al., 2003) or the more extreme excursions noted in Neoproterozoic strata (cf. Halverson et al., 2005).

Since the pioneering work of Ravizza and Turekian (1989), studies have demonstrated the successful application of the rhenium–osmium (Re–Os) chronometer for both Phanerozoic and Proterozoic sedimentary rocks with age determinations $\leq \pm 1\%$ (2σ; Selby and Creaser, 2005; Kendall et al., 2006; Selby, 2007; Kendall et al., 2009a).

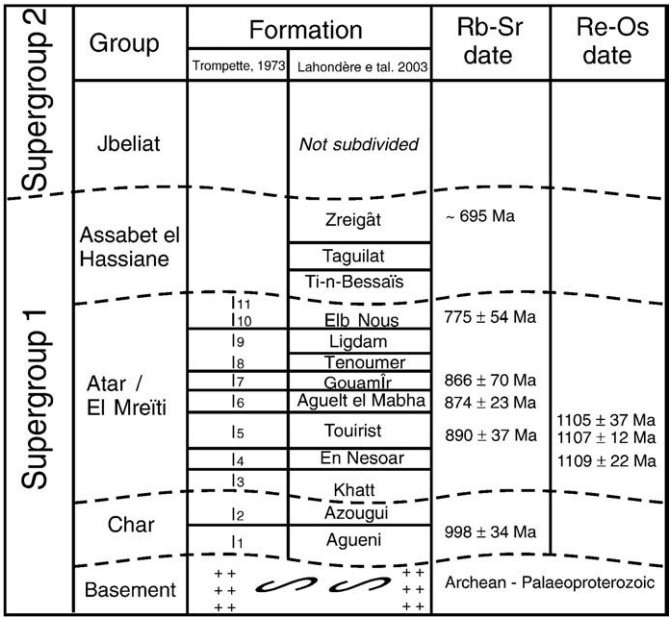

Fig. 2. Stratigraphy of Supergroups 1 and 2 of the Taoudeni basin. Rb–Sr geochronology data from Clauer (1981). Re–Os geochronology data (this study). Stratigraphic nomenclature after Trompette (1973) and Lahondère et al. (2003).

This precision is limited by uncertainty in the value of the ^{187}Re decay constant (~0.31%; Smoliar et al., 1996; Selby, 2007). The Re–Os system also provides valuable information on the Os isotope geochemistry of the oceans that is interpreted to reflect changes in continental weathering rates and interactions between weathering rates and atmospheric O_2 and CO_2 levels (Cohen et al., 1999; Ravizza and Peucker-Ehrenbrink, 2003; Cohen, 2004; Anbar et al., 2007).

We present Re–Os geochronology data which provide precise depositional ages for organic-rich sediments (ORS) of the Atar Group of the Taoudeni basin, Mauritania. These ORS are sediments with elevated total organic carbon (TOC; 0.8% to 22.6%) levels in comparison with 1.2% for average shale hydrocarbon source rocks as detailed by Hunt (1961; Table 1). The Re–Os ages strongly suggest that basin-wide correlation of the sedimentary succession is possible and provide valuable information for evaluating the evolution of the Taoudeni basin. As such, the Re–Os ORS geochronology produces a revised sedimentation history for the West African craton. Furthermore, the Re–Os ORS geochronology provides absolute ages for the recent chemostratigraphy studies (Kah and Bartley, 2004; Teal and Kah, 2005). In addition, we provide a further understanding of the Re–Os systematics in ORS that have experienced abrupt hydrocarbon maturation (flash pyrolysis) as a result of contact metamorphism by a Mesozoic dolerite sill.

2. Geological setting

2.1. Geology of the West African craton

The West African craton records a protracted history of crustal evolution beginning with Mesoarchean basement, which was affected by the Eburnean orogeny ca. 2000 Ma. This Palaeoproterozoic orogeny is recorded to the north of the Taoudeni basin in the Reguibat shield and to the south in the Leo shield (Fig. 1; Schofield et al., 2006; Schofield and Gillespie, 2007). The craton has been considered stable with regard to magmatic and major tectonic events since ca. 1700 Ma with the exception of extensional tectonics and intrusions related to the opening of the North Atlantic during the Late Triassic (Clauer et al., 1982; Villeneuve and Cornée, 1994; Verati et al., 2005; this study). The Taoudeni basin evolved as a result of subsidence of the lower crust

Table 1
TOC and thermal maturity data for S1, S2-A and S2-B samples.

Sample	Depth (m)	TOC (wt.%)	T_{max} (°C)	S1	S2
S1 core					
S1-14	73.15	7.75	517	0.15	0.32
S1-16	73.53	9.06	514	0.20	0.31
S1-18	73.70	8.84	512	0.19	0.30
S1-3	88.27	1.69	454	0.07	0.04
S1-6r	88.74	2.81	304	0.13	0.10
S1-20	88.98	2.88	506	0.21	0.28
S1-22	89.33	3.69	503	0.21	0.47
S1-23	89.36	4.13	500	0.29	0.57
S1-25	89.50	0.84	522	0.10	0.02
S2-A					
S2-7.2	139.45	16.48	435	10.12	114.26
S2-8	140.77	4.88	433	3.77	60.80
S2-10	141.08	8.34	431	14.57	152.36
S2-11	141.25	8.69	432	4.70	67.65
S2-12.2	141.65	22.56	437	1.79	34.21
S2-13	142.05	9.37	433	2.54	46.54
S2-15	142.90	7.41	436	3.02	53.78
S2-18	143.82	10.38	437	4.81	72.97
S2-B					
S2-25	206.70	13.60	436	8.29	96.72
S2-26	206.80	6.49	436	2.96	46.19
S2-27	207.00	2.06	431	0.55	10.51
S2-29	207.20	7.25	436	2.90	51.47
23-30	207.40	2.46	435	0.71	14.28
S2-31	207.60	6.19	436	2.28	44.26

TOC = total organic carbon.
T_{max} = temperature oC of the maximum formation of hydrocarbons by cracking of kerogen and has an uncertainty of ±1–3 °C (Peters, 1986; Behar et al., 2001).
S1 = mg of hydrocarbons (free and thermovapourisable) per gram of rock.
S2 = mg of hydrocarbons (cracking of kerogen) per gram of rock (Peters, 1986).

triggered by the dense ferruginous quartzite material associated with aluminous gneisses of the basement (Bronner et al., 1980). The duration between craton stabilization and the onset of sedimentation of the Taoudeni basin is advocated to have been ~1 Ga (Deynoux et al., 2006 and references therein). This timing will be discussed further based on our new Re–Os ORS geochronology data.

2.2. Stratigraphy of the Taoudeni basin

The sedimentary succession of the Taoudeni basin comprises Proterozoic to Palaeozoic units with a thin cover of Mesozoic–Cenozoic units in the basin centre and large areas of Quaternary sand dunes (Fig. 1; Clauer et al., 1982; Bertrand-Sarfati and Moussine-Pouchkine, 1988; Ahmed Benan and Deynoux, 1998; Deynoux et al., 2006). The structural evolution of the basin suggests normal faulting created accommodation zones (Bronner et al., 1980). These normal faults delineate horsts and grabens across the basin and associated synsedimentary breccias of the basal sedimentary unit can be traced for several tens of kilometres across the basin (Ahmed Benan and Deynoux, 1998). These large scale features imply that sedimentary deposition onto the craton was initially controlled by tectonic instability (Bronner et al., 1980; Ahmed Benan and Deynoux, 1998).

Early work on the sedimentary succession of the Taoudeni basin focused on facies analyses and stratigraphic correlations on a basin-wide scale using marker horizons of tillites and stromatolite morphologies (Bertrand-Sarfati et al., 1976; Deynoux et al., 1976; Bertrand-Sarfati and Moussine-Pouchkine, 1988; Ahmed Benan and Deynoux, 1998). The type section for the Taoudeni basin was described in the Adrar region of the Mauritanian section of the basin and in this area four Supergroups are recognized (Trompette, 1973; Deynoux et al., 2006). For practical reasons nomenclature proposed by Trompette (1973) is retained in a revised form for clarity where possible (Fig. 2). The first Supergroup was defined as Proterozoic based upon stromatolites that were classified as Riphean, the second; uppermost Proterozoic, the third; Upper Ordovician and Silurian and the fourth is of mainly Devonian sedimentary rocks (Trompette, 1973; Bertrand-Sarfati and Moussine-Pouchkine, 1988; Deynoux et al., 2006). This study presents Re–Os ORS geochronology from Supergroup 1, specifically the Touirist and En Nesoar Formations of the Atar Group (Fig. 2).

2.2.1. Geology of Supergroup 1

The Atar Group at ~800 m thick unconformably overlies the basal Char Group. The basin-wide unconformity between these two groups is of an unknown duration (Bronner et al., 1980; Ahmed Benan and Deynoux, 1998; Deynoux et al., 2006). The Atar Group consists of stromatolitic carbonates interbedded with siliciclastic units deposited in a marine setting (Bertrand-Sarfati and Moussine-Pouchkine, 1985). Analysis of the Atar Group shales by X-ray diffractometry reveals a mineral assemblage of, in order of decreasing abundance, quartz, kaolinite, illite, feldspar and minor amounts of pyrite/pyrrhotite (this study). This mineral assemblage suggests that the shales have not experienced regional metamorphism and based upon a cratonic geothermal gradient of 25 °C/km (Girard et al., 1989) and the stratigraphic thickness of the Atar Group (~800 m) were buried to a maximum depth of ~3 km, hence have been only subjected to post-depositional temperature of <100 °C.

Present age determinations of the Proterozoic sedimentary succession are constrained using Rb–Sr glauconite and illite geochronology (Clauer, 1976, 1981), which are discussed below.

2.3. Dolerite intrusion mineralogy and petrology

This study focuses on ORS retrieved from drill cores that penetrated the Atar Group in the Adrar region of the basin (Fig. 1B). One of the drill cores intersected ORS that had been intruded by a 30 m thick Mesozoic dolerite sill that is part of the Central Atlantic magmatic province associated with the initial stages of the opening of the Atlantic Ocean (Verati et al., 2005). Fresh surfaces of the dolerite sill have a fine to medium grained texture and a homogenous mineralogy of plagioclase, clinopyroxene with minor amounts of quartz, biotite (~5%) and hornblende. The fine to medium grained texture of the sill in addition to the homogenous mineralogy is consistent with a shallow depth of emplacement (<1 km; Girard et al., 1989).

3. Analytical methodology

3.1. Sampling

Samples of ORS from the Atar Group were taken from two exploration wells (S1 and S2) drilled in 2004 by the petroleum company Total (Fig. 1B). The drill cores are located; 23° 28′ 60 N/7° 52′ 0 W and 22° 43′ 0 N/9° 37′ 0 W, respectively (Fig. 1B). The Atar Group shales from these localities are massive (laminations are typically absent), non-fissile, organic-rich, black mudstones and are considered to have been deposited in a quiet marine environment representative of extensive flooding of the craton (Bertrand-Sarfati and Moussine-Pouchkine, 1988; Ahmed Benan and Deynoux, 1998; Kah et al., 2008).

Samples were collected from three intervals of the two drill cores; sample intervals were selected on the basis of TOC and T_{max} data determined at the Total Geochemistry and Fluids Laboratory (Pau, France; Table 1). Samples were selected from the S1 core at depths between 73.15 and 89.50 m; for S2-A at depths between 139.45 and 143.82 m and S2-B, 206.70 to 207.60 m. The sampled intervals represent the Touirist and En Nesoar Formations (Fig. 2; Trompette, 1973; Lahondère et al., 2003). The dolerite sill, although assumed to be Mesozoic in age, was sampled for $^{40}Ar/^{39}Ar$ plagioclase geochronology.

Table 2
Ar/Ar data and constants used in age calculations. All errors shown at 1σ.

Sample: ARS1																	
Plagioclase grains from dolerite																	
Step	Laser (W)	^{40}Ar (moles)	^{40}Ar (nA)	σ (nA)	^{39}Ar (nA)	σ (nA)	^{38}Ar (nA)	σ (nA)	^{37}Ar (nA)	σ (nA)	^{36}Ar (nA)	σ (nA)	^{40}Ar*/^{39}Ar$_K$	σ	%^{40}Ar*	Age (Ma)	σ (Ma)
1	1.1	1.02E−14	0.078585	0.004412	0.000068	0.000061	0.000012	0.000012	−0.000086	0.000322	0.000016	0.000024	1078.1730	993.7075	93.87	2418.25	1227.55
2	1.4	3.27E−13	2.512140	0.005622	0.001068	0.000074	0.000220	0.000014	0.001167	0.000325	0.000818	0.000028	2127.1970	151.1847	90.38	3394.87	108.69
3	1.7	1.16E−12	8.921153	0.008955	0.010967	0.000125	0.000909	0.000021	0.013335	0.000376	0.003364	0.000039	723.5062	8.7938	88.87	1916.36	14.35
4	2.1	1.91E−12	14.699600	0.010560	0.042564	0.000286	0.002033	0.000027	0.062443	0.000881	0.007088	0.000031	296.5628	2.2553	85.78	1036.06	5.99
5	2.5	2.61E−12	20.063540	0.012781	0.077737	0.000425	0.002939	0.000031	0.142761	0.001097	0.009620	0.000054	221.9554	1.4318	85.89	826.01	4.28
6	3.0	2.89E−12	22.168400	0.015632	0.115452	0.000514	0.003677	0.000036	0.259464	0.000840	0.010829	0.000057	164.7308	0.9206	85.66	646.49	3.04
7	3.5	2.41E−12	18.503460	0.011847	0.131491	0.000190	0.003175	0.000029	0.387953	0.001098	0.007839	0.000049	123.5886	0.4144	87.65	505.42	1.48
8	3.8	1.23E−12	9.431605	0.009306	0.108954	0.000180	0.002189	0.000024	0.403379	0.001693	0.004169	0.000043	75.7427	0.2884	87.27	326.15	1.14
9	4.1	1.09E−12	8.408972	0.009749	0.098584	0.000306	0.001832	0.000023	0.422785	0.001147	0.003172	0.000029	76.3527	0.3437	89.25	328.55	1.35
10	4.4	7.42E−13	5.699587	0.012781	0.082095	0.000286	0.001420	0.000021	0.535892	0.001546	0.002444	0.000028	61.4194	0.3371	88.07	268.83	1.37
11	4.7	9.98E−13	7.665601	0.008099	0.097597	0.000316	0.001931	0.000027	0.530972	0.002147	0.003674	0.000041	68.1021	0.3368	86.38	295.80	1.35
12	5.0	9.66E−13	7.417711	0.008609	0.110280	0.000345	0.001759	0.000024	0.555941	0.002902	0.002314	0.000038	61.6734	0.2816	91.37	269.86	1.14
13	5.3	6.97E−13	5.350634	0.005215	0.093799	0.000218	0.001520	0.000024	0.530177	0.002300	0.001479	0.000034	53.0346	0.2157	92.61	234.40	0.89
14	5.6	8.13E−13	6.244852	0.007603	0.095757	0.000336	0.001524	0.000023	0.517144	0.002153	0.001616	0.000034	60.8806	0.2933	93.00	266.63	1.19
15	6.0	8.61E−13	6.609564	0.008016	0.113797	0.000228	0.001774	0.000025	0.580919	0.002456	0.001752	0.000036	54.1247	0.2054	92.86	238.92	0.85
16	6.5	9.72E−13	7.461964	0.008016	0.131862	0.000454	0.002060	0.000026	0.651150	0.002760	0.001943	0.000037	52.8026	0.2469	92.99	233.44	1.02
17	7.0	1.28E−12	9.839222	0.008353	0.164060	0.000415	0.002572	0.000023	0.790170	0.002314	0.002781	0.000035	55.5276	0.2120	92.28	244.71	0.87
18	7.5	1.76E−12	13.501710	0.010560	0.193683	0.000554	0.003171	0.000034	0.876331	0.002619	0.003832	0.000044	64.4200	0.2592	92.12	280.99	1.05
19	8.0	1.88E−12	14.473460	0.010651	0.232341	0.000773	0.003626	0.000032	0.985888	0.002772	0.003591	0.000042	58.2299	0.2505	93.20	255.81	1.03
20	9.0	3.16E−12	24.240210	0.012781	0.361598	0.000883	0.005611	0.000036	1.309444	0.003539	0.005921	0.000052	62.6385	0.2204	93.21	273.78	0.89
21	10.0	3.57E−12	27.440250	0.016594	0.432755	0.001103	0.006644	0.000038	1.494915	0.003694	0.006967	0.000049	59.0624	0.2131	92.92	259.22	0.87
22	11.0	3.20E−12	24.594250	0.015632	0.379569	0.001003	0.005914	0.000037	1.402438	0.004155	0.005706	0.000048	60.7981	0.2224	93.59	266.30	0.91
23	12.0	1.88E−12	14.418190	0.009749	0.215687	0.000763	0.003266	0.000031	1.000378	0.002784	0.003392	0.000044	62.7655	0.2797	93.59	274.29	1.13
24	14.0	2.83E−12	21.700280	0.012781	0.351197	0.000534	0.005427	0.000033	1.484613	0.004010	0.005372	0.000049	57.7697	0.1698	93.22	253.92	0.70
25	16.0	3.49E−12	26.768640	0.015632	0.421325	0.002303	0.006544	0.000080	1.849564	0.007854	0.006683	0.000051	59.3712	0.3648	93.16	260.48	1.49
26	17.0	1.23E−12	9.420756	0.009130	0.152397	0.000494	0.002371	0.000033	0.827218	0.002335	0.002364	0.000037	57.8761	0.2530	93.27	254.36	1.04
27	18.0	1.06E−12	8.108996	0.008268	0.136963	0.000336	0.002101	0.000028	0.746256	0.002337	0.001862	0.000037	55.8267	0.2140	93.94	245.94	0.88
28	19.0	7.12E−13	5.464182	0.007280	0.088174	0.000190	0.001438	0.000021	0.632153	0.002338	0.001534	0.000033	57.6767	0.2336	92.61	253.54	0.96
29	22.0	5.50E−13	4.224959	0.006294	0.065692	0.000336	0.001070	0.000021	0.555193	0.001882	0.001378	0.000033	59.1262	0.3872	91.39	259.48	1.58
30	25.0	5.30E−13	4.068485	0.005111	0.068882	0.000152	0.001125	0.000020	0.594874	0.002343	0.001223	0.000032	54.8219	0.2397	92.26	241.80	0.99
31	30.0	7.30E−13	5.605570	0.007440	0.094755	0.000375	0.001410	0.000023	0.577798	0.002344	0.001335	0.000033	55.7097	0.2906	93.77	245.46	1.20
Integrated Age = 308.9 ± 1.1 Ma																	

Relative abundances of Ar isotopes in nA of amplified ion beam current. Ages are model ages assuming all non-radiogenic Ar has atmospheric isotopic composition.
Calculated using *J*-value, interfering isotope ratios and constants below.
All uncertainties are stated at one standard deviation. Age errors do not include uncertainty in 40 K decay constants or age of the standard.
$J = 0.0026162 \pm 7.50E{-}06$.
$(^{40}Ar/^{36}Ar)_{atm} = 295.5 \pm 0.5$.
$(^{40}Ar/^{38}Ar)_{atm} = 1575 \pm 2$.
$(^{38}Ar/^{37}Ar)_{Ca} = 0.0000196 \pm 8.16E{-}7$.
$(^{38}Ar/^{39}Ar)_K = 0.012200 \pm 0.000027$.
$P(^{36}Cl/^{38}Cl) = 262.8 \pm 3$.
Decay constants: $l\ ^{40}K_{Ae} = 5.81E{-}11\ a^{-1}$; $l\ ^{40}K_{A\beta} = 4.962E{-}10\ a^{-1}$; $l\ ^{37}Ar = 5.4300E{-}2\ a^{-1}$; $l\ ^{39}Ar = 2.58E{-}3\ a^{-1}$; $l\ ^{36}Cl_{A\beta} = 2.35E{-}6\ a^{-1}$.

3.2. TOC and T_{max} analysis

The TOC values are derived from combustion of powdered samples using a LECO 244 carbon analyser. Source rock maturity parameters are indicated by T_{max} data. The T_{max} data was generated using a VINCI Technologies Rock-Eval 6 Turbo at the TOTAL Geochemistry and Fluids Laboratory (Pau, France).

3.3. Re–Os analysis

Prior to crushing, all samples were polished to remove cutting and drilling marks to eliminate any contamination. The samples were dried at 60 °C for ~12 h and then crushed to a fine powder ~30 μm. The samples of ~100 g represent ~2 cm of stratigraphy and were broken into chips with no metal contact and powdered in a ceramic mill. Rhenium–osmium isotope analysis was carried out at Durham University's TOTAL laboratory for source rock geochronology and geochemistry at the Northern Centre for Isotopic and Elemental Tracing (NCIET) using Cr^{VI}–H_2SO_4 digestion and solvent extraction ($CHCl_3$), micro-distillation and anion chromatography methods and negative mass spectrometry as outlined by Selby and Creaser (2003), and Selby (2007). Total procedural blanks during this study were between 14.5 and 17.6 pg and 0.20 to 0.83 pg for Re and Os respectively, with an average $^{187}Os/^{188}Os$ value of ~0.19 ($n=3$).

Uncertainties for $^{187}Re/^{188}Os$ and $^{187}Os/^{188}Os$ are determined by error propagation of uncertainties in Re and Os mass spectrometer measurements, blank abundances and isotopic compositions, spike calibrations and reproducibility of standard Re and Os isotopic values. The Re–Os isotopic data, 2σ calculated uncertainties for $^{187}Re/^{188}Os$ and $^{187}Os/^{188}Os$ and the associated error correlation function (rho) are regressed to yield a Re–Os date using *Isoplot V. 3.0* with the λ ^{187}Re constant of 1.666×10^{-11} a^{-1} (Ludwig, 1980; Smoliar et al., 1996; Ludwig, 2003).

To ensure and monitor long-term mass spectrometry reproducibility, in-house standard solutions of Re and Os (AB-2) are repeatedly analysed at NCIET to monitor long-term mass spectrometer reproducibility. The Re standard analysed during the course of this study is made from 99.999% zone-refined Re ribbon and is considered to be identical to that of AB-1 (Creaser et al., 2002; Selby and Creaser, 2003; Kendall et al., 2004). The NCIET Re standard yields an average $^{185}Re/^{187}Re$ ratio of 0.597931 ± 0.00165 (1 SD, $n=94$). This is in excellent agreement with the value reported for the AB-1 standard (Creaser et al., 2002). The Os standard (AB-2), made from ammonium hexachloro-osmate, yields an $^{187}Os/^{188}Os$ ratio of 0.10681 ± 0.00016 (1 SD, $n=89$). The isotopic compositions of these solutions are identical within uncertainty to that reported by Creaser et al. (2002) and Selby et al. (2009).

In addition to monitoring the AB-2 standard this paper details further use of the Durham Romil Osmium Standard (DROsS) for monitoring the mass spectrometry reproducibility of osmium isotope compositions. The DROsS values recorded during this study yield an $^{187}Os/^{188}Os$ ratio of 0.160965 ± 0.000337 (2 SD, $n=16$), which is identical to the value of 0.160924 ± 0.000003 (2 SD, $n=21$; Nowell et al., 2008).

3.4. $^{40}Ar/^{39}Ar$ plagioclase geochronology

The dolerite sill was sampled for $^{40}Ar/^{39}Ar$ analysis of plagioclase carried out at the Berkeley Geochronology Center. Approximately 500 g of dolerite was selected, broken into chips, powdered in a ceramic mill and sieved to grain size 210–74 μm, prior to magnetic separation using a Frantz isodynamic magnetic separator. The separated plagioclase grains were washed with MilliQ, rinsed in ethanol and dried overnight. The sample was then irradiated for 10 h in the CLICIT facility of OSTR reactor along with Fish Canyon sanidine (FCs) as a neutron fluence monitor, for which an age of 28.02 Ma (Renne et al., 1998) was used for age calculations.

Approximately 30 mg of the plagioclase was analysed by incremental heating in 31 steps with a CO_2 laser. The laser beam, of 1.1 to 30.0 W power, was directed through an integrator lens to homogenize sample temperature during heating. Heating steps were of 60 s duration, followed by 120 s of gettering and exposure to a −130 °C cold finger in the online extraction system. Mass spectrometry was performed with an MAP 215C sector mass spectrometer, by 10 cycles of peak-hopping by magnetic field switching with ion beams measured on a Balzers electron multiplier in analogue mode.

Blanks comparable to those reported by Vogel and Renne (2008) were measured between every three unknowns and average values were used for corrections. Mass discrimination (1.00892 ± 0.00179 per atomic mass unit) based on a power law correction (Renne et al., 2009) was determined from multiple air pipettes interspersed with the analyses. Argon isotope data corrected for blank, mass discrimination and radioactive decay are shown in Table 2. Ages shown in Table 2 incorporate corrections for interfering reactor-produced Ar isotopes from Ca and K (Renne et al., 2005) and Cl (Renne et al., 2008), and are based on the decay constants and isotope abundances recommended by Steiger and Jager (1977). Age uncertainties do not include contributions from the ^{40}K decay constants or the $^{40}Ar^*/^{40}K$ of the standard.

4. Results

4.1. Total organic carbon and T_{max} results

The total organic carbon (TOC) content for samples from the S1 core are between 0.8 and 9.1%, the S2-A samples range from 4.9 to 22.6% and the S2-B samples between 2.1 and 13.6% (Table 1). Rock-Eval 6 Turbo pyrolysis data for the S1 and S2 drill cores indicate that the shales of S2 are marginally mature (431 to 437 °C) with respect to thermal maturity and that the S1 drill core samples are overmature (454–522 °C; Table 1; Peters, 1986; Behar et al., 2001). The sample S1-6r contains <0.2 mg hydrocarbons per gram of rock, which results in Rock-Eval data giving an anomalously low T_{max} value (304 °C; Peters, 1986). The thermal maturity data for drill core S1 suggests that the shales are overmature as a result of flash pyrolysis associated with contact metamorphism with a large (>20 m diameter) dolerite intrusion.

4.2. Immature shale Re–Os geochronology

The Re–Os abundances and isotope compositions for the Atar Group samples S2-A and S2-B are presented in Table 3. All of the S2 samples are enriched in Re (14–146 ppb) and Os (0.29–2.9 ppb), particularly in comparison with the contents of modern-day average continental crust (~1 ppb Re and 30–50 ppt Os; Esser and Turekian, 1993; Peucker-Ehrenbrink and Jahn, 2001; Hattori et al., 2003; Sun et al., 2003). The $^{187}Re/^{188}Os$ ratios range from 595 to 1041 and are positively correlated with the $^{187}Os/^{188}Os$ compositions of 11.3–19.7 (Fig. 3a). Linear regression of the Re–Os isotope data for the S2-A depth interval yield a Model 1 age of 1107 ± 12 Ma (2σ, $n=8$, Mean Squared of Weighted Deviates [MSWDs] of 1.13), with an initial $^{187}Os/^{188}Os$ of 0.28 ± 0.13 (Fig. 3a). Linear regression of the Re–Os isotope data for the S2-B depth interval yield a Model 1 age of 1109 ± 22 Ma (2σ, $n=6$, MSWD of 0.73), with an initial $^{187}Os/^{188}Os$ of 0.31 ± 0.28 (Fig. 3b).

4.3. Overmature shale Re–Os geochronology

The Re–Os abundances and isotope compositions for the ORS of the S1 drill core are presented in Table 3. Similar to the ORS of S2, the S1 samples are significantly enriched in Re (37–198 ppb) and Os (0.79–3.7 ppb). The $^{187}Re/^{188}Os$ ratios range from 431 to 696 and are positively correlated with the $^{187}Os/^{188}Os$ compositions of 8.4–13.3. Linear regression of the Re–Os isotope data for the overmature S1 drill core shale samples yield a Model 3 age of 1105 ± 37 Ma (2σ, $n=9$, MSWD of 8.8, with an initial $^{187}Os/^{188}Os$ (hereafter Os_i) of 0.31 ± 0.34; Fig. 3c).

Table 3
Re and Os abundance and isotopic data for the Atar Group ORS.

Sample	Depth	Re (ppb)	±	Os (ppb)	±	^{192}Os (ppt)	±	^{187}Re/^{188}Os	±	^{187}Os/^{188}Os	±	rho[a]	Os$_i$[b]
S1 core													
S1-14	73.15	152.6	0.5	3.1479	0.0005	555.4	0.8	546.44	1.94	10.398	0.021	0.293	0.20
S1-16	73.53	198.1	0.6	3.7334	0.0006	566.2	0.7	696.24	2.41	13.332	0.022	0.251	0.34
S1-18	73.70	182.3	0.6	3.6546	0.0006	620.7	0.7	584.27	2.00	11.098	0.018	0.216	0.19
S1-3	88.27	36.9	0.1	0.7885	0.0001	144.1	0.5	509.37	2.29	9.785	0.044	0.485	0.28
S1-6r	88.74	77.1	0.2	1.7083	0.0002	325.9	0.4	470.81	1.64	9.050	0.015	0.280	0.34
S1-20	88.98	65.2	0.2	1.5100	0.0002	300.4	0.5	431.81	1.58	8.369	0.018	0.385	0.31
S1-22	89.33	101.5	0.3	2.0630	0.0003	356.4	0.6	566.71	2.09	10.781	0.024	0.363	0.20
S1-23	89.36	79.9	0.3	1.6796	0.0003	301.4	0.5	527.55	1.95	10.099	0.022	0.395	0.25
S1-25	89.50	42.8	0.1	0.9595	0.0001	183.9	0.9	462.95	2.71	8.973	0.062	0.583	0.33
S2-A													
S2-7.2	139.45	86.9	0.5	1.5690	0.0005	222.1	0.7	778.26	4.78	14.821	0.050	0.440	0.30
S2-8	140.77	14.4	0.1	0.2851	0.0001	47.3	0.3	606.46	3.88	11.536	0.065	0.785	0.22
S2-10	141.08	33.8	0.1	0.6740	0.0001	112.9	0.3	594.88	2.44	11.349	0.033	0.529	0.25
S2-11	141.25	36.2	0.1	0.6715	0.0001	100.3	0.3	718.15	2.94	13.660	0.039	0.547	0.26
S2-12.2	141.65	146.3	0.5	2.8754	0.0005	469.9	1.2	619.13	2.51	11.827	0.038	0.454	0.27
S2-13	142.05	46.9	0.1	0.8744	0.0001	132.3	0.3	704.63	2.75	13.375	0.035	0.476	0.22
S2-15	142.90	46.3	0.2	0.9201	0.0002	153.3	0.3	600.63	2.31	11.455	0.029	0.442	0.24
S2-18	143.82	57.7	0.2	1.0007	0.0002	132.5	0.3	865.87	3.42	16.369	0.045	0.478	0.21
S2-B													
S2-25	206.70	113.6	0.4	2.1399	0.0004	327.3	0.9	690.49	2.89	13.156	0.044	0.488	0.27
S2-26	206.80	44.4	0.1	0.8127	0.0001	117.9	0.7	749.24	4.93	14.282	0.093	0.755	0.30
S2-27	207.00	17.4	0.1	0.3032	0.0001	39.7	0.7	874.08	15.12	16.641	0.309	0.889	0.33
S2-29	207.20	57.6	0.2	1.0904	0.0002	167.6	0.8	683.17	3.97	13.049	0.076	0.681	0.30
S2-30	207.40	25.0	0.1	0.4109	0.0001	47.8	0.7	1041.50	14.43	19.662	0.297	0.859	0.22
S2-31	207.60	50.2	0.2	0.9142	0.0002	131.1	0.5	761.44	3.66	14.539	0.077	0.494	0.33

Uncertainties are given as 2σ for ^{187}Re/^{188}Os and ^{187}Os/^{188}Os and ^{192}Os.
For the latter the uncertainty includes the 2 SE uncertainty for mass spectrometer analysis plus uncertainties for Os blank abundance and isotopic composition.
Ages calculated using the $\lambda\ ^{187}\mathrm{Re} = 1.666\times10^{-11}\mathrm{y}^{r-1}$ (Smoliar et al., 1996).
[a] Rho is the associated error correlation (Ludwig, 1980).
[b] Os$_i$ = initial ^{187}Os/^{188}Os isotope ratio calculated at 1105 Ma (S1, 73.15–89.50 m depth), 1107 Ma (S2-A, 139.45–143.82 m depth) and 1109 Ma (S2-B, 206.7–207.6 m depth).

4.4. ^{40}Ar/^{39}Ar geochronology

The ^{40}Ar/^{39}Ar age spectrum (Fig. 4) for plagioclase from the dolerite sill is markedly discordant, with initial low temperature steps yielding Proterozoic apparent ages, giving way in the last 80% of ^{39}Ar released to apparent ages between 230 and 300 Ma. This pattern suggests that the plagioclase contained a significant component of "excess" ^{40}Ar, mainly residing in relatively low-retentivity sites, that was probably acquired during contact metamorphism of the ORS resulting from emplacement of the sill. As a result, the analysis yields a precise, but almost certainly meaningless integrated age of 308.9 ± 1.1 Ma. The data yield no statistically valid isochron, indicating that more than one trapped (i.e., non-radiogenic) component of Ar is present. These results lead us to conclude that the Ar retention age of the plagioclase, recording cooling below 200–350 °C (Cassata et al., 2009) depending on the cooling rate, is less than or equal to the youngest apparent step age (233 ± 1 Ma), which is inferred to contain the lowest proportion of excess ^{40}Ar. We further conclude that this maximum cooling age reflects local cooling of the sill only rather than a regional basin cooling, due to the much older ages recorded by the Rb–Sr system in low-retentivity minerals as discussed below.

5. Discussion

The Re–Os data from ORS of the Atar Group yield ages of 1107 ± 12 Ma; 1109 ± 22 Ma and 1105 ± 37 Ma, respectively from two drill cores (Fig. 3). The 1107 ± 12 Ma and 1105 ± 37 Ma ages represent depositional ages for the Touirist Formation. The 1109 ± 22 Ma represents a depositional age for the En Nesoar Formation that conformably underlies the Touirist Formation. The Re–Os ages for these two formations provide accurate Mesoproterozoic (Stenian; 1000–1200 Ma; Ogg et al., 2008) ages for the deposition of the Atar Group of the Taoudeni basin. The larger uncertainty for the S1 age (± 37 Ma) is discussed below.

5.1. Previous geochronology and Rb–Sr systematics

The basal sedimentary units of the Taoudeni basin, including the Atar Group shales, were previously defined as being Tonian, (Clauer, 1976, 1981). For the Atar Group Rb–Sr geochronology yields an age of 890 ± 37 Ma (Clauer, 1981), which is ~200 m.y younger than the Re–Os ORS dates for this group. The clays analysed by Clauer (1976) were 1 M polymorphs of illite that are characteristic of low temperature growth and re-crystallisation commonly associated with diagenesis (Bailey, 1966; Grathoff and Moore, 1996).

Although the Rb–Sr technique has been used to estimate the geochronology of the Taoudeni basin, the Rb–Sr systematics of illite and glauconite are known to be susceptible to disturbance and hence record anomalously young geological ages that are associated with diagenesis (Morton and Long, 1982; Ohr et al., 1991; Awwiller, 1994; Evans, 1996; Gorokhov et al., 2001). Furthermore, previous work has highlighted the progressive genesis of glauconites over as much as 5 Ma in samples that have experienced a relatively straightforward geological history e.g., GL-O glauconite international standard (Odin and Hunziker, 1982; Smith et al., 1998; Selby, 2009).

Given the three identical, within uncertainty, Re–Os ORS dates from two locations; we suggest that the Rb–Sr geochronology does not record the depositional age of the Atar Group.

5.2. TOC versus Re and Os abundance

At present our understanding of the mechanisms by which Re and Os are complexed into ORS is incomplete. Studies of Re and Os in marine sediments suggest the complexation is driven by a combination

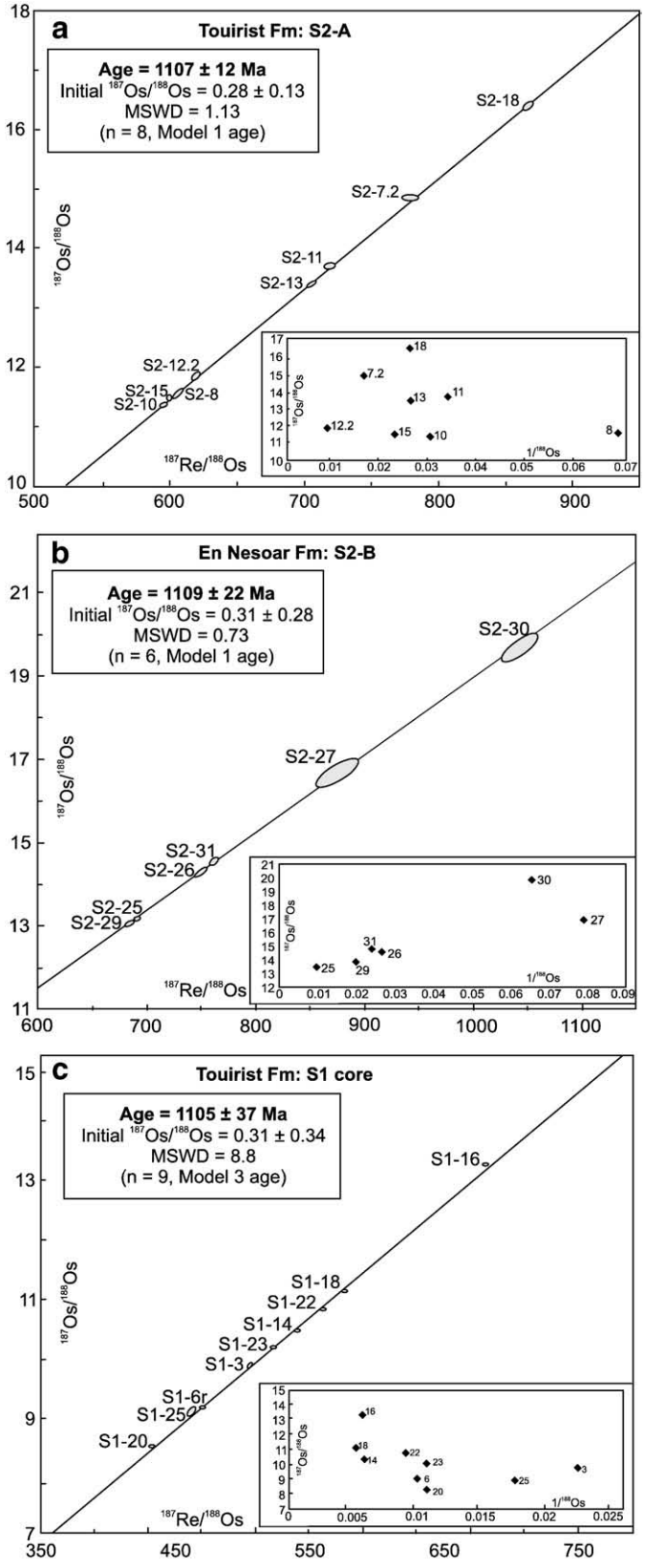

Fig. 3. Re–Os isochron diagrams for the Atar Group ORS. (a) S2-A horizon of the Touirist Formation (139.45 m to 143.82 m depth). (b) S2-B horizon of the En Nesoar Formation (206.7 m to 207.6 m depth). (c) S1 horizon of the Touirist Formation (73.15 m to 89.50 m depth). The insets highlight the lack of correlation between present day $^{187}Os/^{188}Os$ and $1/^{188}Os$.

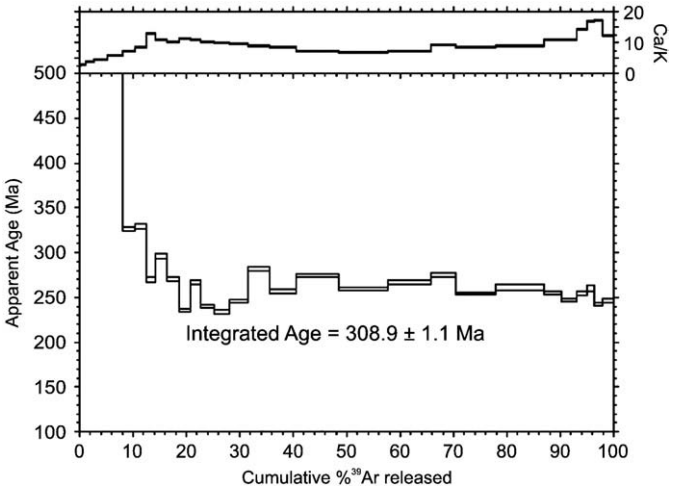

Fig. 4. Ar–Ar age spectrum from plagioclase grains of dolerite sill. Sampled at ~90 m depth in the S1 drill core.

of reductive capture and adsorption onto organocomplexes in seawater (Koide et al., 1991; Colodner et al., 1993; Crusius et al., 1996; Levasseur et al., 1998; Oxbugh, 1998). However, a direct link between TOC and Re and Os abundances for all ORS is unlikely as samples with low or high TOC content can have high Re/Os (0.5–30% and 300 to 800 units, respectively; Kendall et al., 2004; Selby et al., 2009). Other important factors include recharge of Re and Os into the water column (Turgeon et al., 2007) and post-deposition affects (Crusius and Thomson, 2000; Kendall et al., 2009b). Despite the strong correlation between Re and Os with TOC in the ORS reported in this study the relationship is not consistent. Jurassic ORS possess little or no correlation between TOC content and Re and Os abundance (Cohen et al., 1999). Furthermore, the low TOC (<1%) Neoproterozoic Old Fort Point Formation contains elevated Re and Os abundances (16 ppb and 249 ppt, respectively) further indicating that Re and Os enrichment is not directly linked to TOC content (Kendall et al., 2004).

As the relationship between Re and Os with TOC content is distinct for differing ORS, their enrichment factor may be related to local factors such as; duration the pore-water sediment interface is open, changes in the oxic–anoxic boundary of the water column and input of Re and Os from varying sources e.g. continental weathering, hydrothermal flux and cosmic input. Considering the behaviour and destination of other redox sensitive elements such as Ni and Mo there is a strong argument that the dominant factor controlling Re and Os enrichment in ORS is sedimentation rate (Lewan and Maynard, 1982; Kendall et al., 2009a,b).

5.3. Conditions of flash pyrolysis and non-disturbance of Re–Os systematics associated with flash pyrolysis

It is unlikely that the slightly larger uncertainty of the Re–Os isotope data from the S1 core compared to the uncertainties of the S2 core is caused by significant disturbance of the Re–Os systematics (1105 ± 37 Ma; 1107 ± 12 Ma and 1109 ± 22 Ma, respectively). Two studies provide evidence that the Re–Os systematics in ORS can be disturbed and/or reset (Kendall et al., 2009b; Yang et al., 2009). Work focusing on Mesoproterozoic shales from the McArthur basin, Australia reported an imprecise age, a large MSWD (86) and highly radiogenic Os_i (3.5 ± 1.5; Kendall et al., 2009b). These factors were attributed to disturbance of the Re–Os systematics in this example, by hydrothermal fluid flow associated with ore deposition. Kendall et al. (2009b) also reported an increase in the $^{187}Os/^{188}Os$ composition as an indication of disturbance, either by mobilisation of Os relative to Re or addition of Re relative to Os.

In addition, a Re–Os data set for Archean carbonaceous slates generated a meaningful Re–Os age, but produced negative Os_i (Yang et al., 2009). These authors concluded that the Re–Os systematics had been affected by the recent addition of ^{187}Re from weathering of adjacent mafic rocks, and that the addition of ^{187}Re was proportional to the ^{187}Os concentration of each sample.

However, another explanation for the Re–Os data of the Archean carbonaceous slates may relate to the small amount of material prepared (<1 g) for the Re–Os analyses. As a result, these small aliquots do not minimize the Re–Os heterogeneity known to occur in ORS (Kendall et al., 2009a).

The $^{187}Re/^{188}Os$ values for the S1 core are slightly lower than those from the two S2 core analyses (Table 3; Fig. 3; 431 to 696 compared with 594 to 865 and 683 to 1041, respectively). In addition, the $^{187}Os/^{188}Os$ values for the S1 core are also less radiogenic (8.4 to 13.3) than those from the S2 core analyses (11.3 to 16.4 and 13.0 to 19.7; Table 3; Fig. 3). However, both cores are significantly enriched in Re and Os, particularly in comparison to average continental crust. Although the Re–Os age for the S1 core is nominally identical for those determined for the S2 core (Fig. 3), it possesses a larger uncertainty (±37 Ma). This may relate to the cluster of points between 520 and 580 on the S1 isochron and not disturbance of the Re–Os systematics by hydrothermal fluid flow and/or hydrocarbon maturation and migration. Evaluation of the Re and Os isotope data can reveal whether or not Re–Os systematics have been disturbed. The scattered relationship between present day $^{187}Os/^{188}Os$ and $1/^{188}Os$ indicate that the Re–Os systematics has not been disturbed (Fig. 3 insets).

As noted above, the Os_i of the S1 and S2 cores are identical within uncertainty (0.31 ± 0.34; 0.28 ± 0.13 and 0.31 ± 0.28, respectively) and are interpreted to record the Os isotope composition of seawater at the time of deposition (Fig. 3). Any disturbance of Re and/or Os isotope values would result in large variations and radiogenic Os_i as seen in the Mesoproterozoic Velkerri Formation (Kendall et al., 2009b).

Together, enriched levels of Re and Os; the broadly similar $^{187}Re/^{188}Os$ and $^{187}Os/^{188}Os$ values and the identical Os_i values indicate that the Re–Os geochronology data of the S1 core is recording the depositional age of ORS from the Touirist Formation.

The $^{40}Ar/^{39}Ar$ dating of the dolerite sill that intersects the ORS of the S1 core yields an age of ~230 Ma indicating that the intrusion occurred nearly 900 Ma after deposition of the Atar Group (Fig. 4). The age of the intrusion suggests that it is related to the opening of the North Atlantic during the late Triassic/early Jurassic.

The ORS of S1 are baked black 20 m above and 5 m below the contact between the S1 shales and the intrusion. Quantifying the grade of metamorphism is restricted by a lack of index minerals present in the S1 shales. Thin section and XRD analysis of the overmature S1 shales reveal compositions similar to the immature S2 shales, but with minor amounts of pyrrhotite. Pyrrhotite is a common mineral in metamorphosed graphitic rocks and generally forms under reducing conditions at temperatures >200 °C (Lambert, 1973; Hall, 1986; Gillett, 2003; Pattison, 2006). The absence of extensive metamorphism can be explained by a low geothermal gradient, burial limited to ~3 km, a low country rock temperature (<100 °C) and a short duration of heat transfer due to a rapid cooling of the intrusion (Delaney and Pollard, 1982; Delaney, 1987; Raymond and Murchison, 1988; Galushkin, 1997). The overmature shales (S1) and borderline mature shales (S2) of this study both have elevated TOC (0.8 to 22.6%; Table 1). The TOC of overmature shales consists of a carbon-rich hydrogen-poor residue. In contrast, TOC of borderline mature shales consist of 'extractable organic matter carbon' and 'convertible carbon' (Jarvie, 1991).

Gaining a precise intrusion temperature of the sill and the extent of heating of the surrounding ORS is beyond the scope of this research. However, previous studies have modelled palaeotemperatures that sedimentary rocks experienced during intrusion of igneous bodies (Galushkin, 1997; Barker et al., 1998; Kalsbeek and Frei, 2006). From the mineralogy and petrology of the sill it can be estimated that the temperature of intrusion was between 1000 and 1200 °C and the shales of S1 were buried to depths of less than 3 km with corresponding burial temperatures less than 100 °C (Girard et al., 1989; Deynoux et al., 2006). Using the equation ($T_{contact} = (T_{magma} + T_{host})/2$), where T = temperature (Carslaw and Jaeger, 1959), the ORS experienced temperatures between ~550 and 650 °C at the sill/ORS contact.

Mean vitrinite reflectance data can be used to estimate the maximum peak temperature experienced by the ORS. However, because of the absence of vitrinite in Proterozoic ORS, bitumen reflectance data (BRo) has been converted into vitrinite reflectance data (Ro) using Ro = 0.618BRo + 0.4 (Jacob, 1989). Two values of BRo, taken from above and below the sill, were provided by TOTAL and yield a mean vitrinite reflectance value (Rv−r) of 2.91. The mean vitrinite reflectance data is then used to estimate the maximum peak temperature (T_{peak}) experienced by the ORS by $T_{peak} = (\ln (Rv-r) + 1.19/0.00782$; Barker and Pawlewicz, 1994). This gives a peak temperature of ~288 °C experienced by the altered S1 shales. Convective and/or conductive cooling would have lowered the temperature from ~550 to 650 °C at the contact to ~288 °C through the rest of the altered shales (Barker et al., 1998). Together the occurrence of pyrrhotite, T_{max} data, HI data and the estimated peak temperatures provide strong evidence that the shales from the S1 core have experienced maturation and expulsion of hydrocarbons as a result of flash pyrolysis. The Re–Os ORS geochronology data presented here indicates that flash pyrolysis has not significantly affected the Re–Os ORS systematics.

5.4. Implications for basin correlation, craton–craton correlation and Rodinia reconstructions

The current age for the Char Group which unconformably underlies the Atar Group is from Rb–Sr illite and glauconite geochronology and gives an age of 998 ± 34 Ma (Clauer, 1981). The Atar Group Mid-Stenian Re–Os ORS ages (~1100 Ma) strongly suggest that the Char Group is also much older than previously thought. As the unconformity between the Char and Atar Groups is basin-wide in scale it is impossible to extrapolate an age for the Char Group from the depositional age of the Atar Group. However, based upon the increased age (older by 24%) the Re–Os geochronology for the Atar Group suggests that the Char Group may also be ~200 Ma older than the Rb–Sr derived age of 998 ± 34 Ma. The new geochronology data for the Atar Group enables us to provide improved models of sedimentation for the West African craton and enhance existing models of sequence stratigraphy as presented by Bertrand-Sarfati and Moussine-Pouchkine (1988).

Previous correlations of the Atar Group ORS from drill core and outcrop were based on matching high TOC horizons and using distinct stromatolite morphology as marker horizons (Bertrand-Sarfati and Moussine-Pouchkine, 1985, 1988). These methods are unsuitable for the large distances involved in basin-wide hydrocarbon exploration because the large range in TOC levels (0.8 to 22.6%; Table 1) within individual formations of the Atar Group. The Atar Group biostromes consist of juxtaposed stromatolites which record growth at different times in distinct environmental settings (Bertrand-Sarfati and Moussine-Pouchkine, 1988; Kah et al., 2008). As a consequence, the biostrome horizons cannot be used as marker horizons for correlation on a basin or craton-wide scale.

The two cores were drilled in regions separated by >200 km and the results advocate that Re–Os ORS geochronology can provide precise depositional ages for hydrocarbon source rocks and permits correlations between source rocks on a basin-wide scale.

The new Re–Os ORS geochronology provides precise absolute age data that supports chemostratigraphy evidence that the West African craton has a depositional history that predates 1100 Ma (Teal and Kah, 2005). From this, we can infer that sedimentation onto the cratonic

platform began ~1.2 Ga rather than at 1 Ga which is implied by the Rb–Sr geochronology. The new geochronology data has implications for the development of sedimentation histories and basin modelling used for hydrocarbon exploration in cratonic settings.

It has been suggested that the Taoudeni basin is a vast 'super basin' consisting of a number of sub-basins (Villeneuve and Cornée, 1994; Lottaroli et al., 2009). The Re–Os geochronology is recording deposition of the Touirist Formation possibly in separate sub-basins of the Taoudeni 'super basin.' The identical Os_i values of the S1 and S2 cores are suggested to be recording the osmium isotope composition of local seawater at the time of deposition (Ravizza and Turekian, 1989; Cohen et al., 1999; Selby and Creaser, 2003). Therefore, the identical Os_i values for this 'super basin' may be used as a proxy for global seawater Os isotope composition at 1100 Ma.

The Re–Os geochronology presented here for the Atar Group provides a depositional age that is consistent with sedimentation histories of other cratons involved in the formation, and subsequent break up, of the supercontinent Rodinia. However, because of the lack of available palaeomagnetic data for the West African craton its palaeogeography is poorly constrained (Li et al., 2008). Despite this, work on the West African, Amazon and Rio de la Plata cratons proposed the existence of a mega-craton that existed during the Meso- and Neoproterozoic (Onstott and Hargraves, 1981; Trompette, 1994; Zhao et al., 2006). There is strong evidence to suggest that the West Africa craton was linked with the São Francisco craton of South America during the Mesoproterozoic (Onstott et al., 1984; D'Agrella-Filho et al., 1990, 2004; Zhao et al., 2006; Li et al., 2008). The new Re–Os geochronology data require a reassessment of the drift histories of the West African craton as discussed by Tohver et al. (2006).

The Re–Os ORS geochronology suggests that the Atar Group sedimentary rocks of the Taoudeni basin are approximately equivalent to Mesoproterozoic sedimentary rocks found on the São Francisco craton (Fairchild et al., 1996; Geboy, 2006; Zhao et al., 2006; Azmy et al., 2008; Li et al., 2008). The Vazante Group of the São Francisco craton has two Re–Os data sets that yield ages of 1126 ± 47 Ma and 1100 ± 77 Ma for the Serra do Poço Verde and Lapa formations, respectively (Geboy, 2006; Azmy et al., 2008). These two formations are separated by an unconformity of unknown duration. Both of the Re–Os ages from the Vazante Group are identical, within uncertainty, to the Re–Os ages of the Atar Group (this study) and suggest that these successions were deposited coevally onto the passive margins of the São Francisco and West African cratons. The São Francisco, Amazon, Congo and West African cratons are speculated to have been separated by the Brasiliano Ocean at ~1100 Ma and were not involved in the formation of Rodinia at this time (Kröner and Cordani, 2003; D'Agrella-Filho et al., 2004). The Atar Group of the Taoudeni basin provides a rare record of exceptionally well-preserved sedimentary rocks that were possibly deposited in basins that existed between the West African, São Francisco and Amazon cratons during the Mesoproterozoic.

6. Conclusions

1. The Re–Os ORS geochronology of the Atar Group suggests that sedimentation of the Taoudeni basin began prior to 1100 Ma. This age is >200 Ma older than previous ages based upon Rb–Sr illite and glauconite geochronology (Clauer, 1976, 1981).
2. The Re–Os ages from both immature and overmature ORS strongly suggest that the Re–Os ORS systematics are not significantly affected by flash pyrolysis associated with contact metamorphism of mafic intrusions.
3. The new Re–Os ages highlight implications for supercontinent reconstructions involving the West African craton. The Re–Os data records the onset of sedimentation on the passive margin of the West African craton prior to 1100 Ma. We suggest that a reassessment of the role of the West African craton in the Rodinia supercontinent configuration is required.

Acknowledgements

This research was funded by a Total CEREES PhD scholarship and an American Association of Petroleum Geologists grants-in-Aid awarded to AR. Francoise Champion, Valerie Aout and Jean-Bernard Berrut are thanked for their technical assistance. Kath Liddell is also thanked for her assistance with the XRD work. This paper has benefited from constructive criticism from Linda Kah and Greg Ravizza. The Total laboratory for source rock geochronology and geochemistry at NCIET is partly funded by Total.

References

Ahmed Benan, C.A., Deynoux, M., 1998. Facies analysis and sequence stratigraphy of Neoproterozoic platform deposits in Adrar of Mauritania, Taoudeni basin, West Africa. Geol. Rundsch. 87, 283–302.
Anbar, A.D., Duan, Y., Lyons, T.W., Arnold, G.L., Kendall, B., Creaser, R.A., Kaufman, A.J., Gordon, G.W., Scott, C., Garvin, J., Buick, R., 2007. A whiff of oxygen before the great oxidation event? Geochim. Cosmochim. Acta 71, A24-A24.
Awwiller, D.N., 1994. Geochronology and mass-transfer in Gulf-Coast Mudrocks (South-Central Texas, USA) — Rb–Sr, Sm–Nd and Ree systematics. Chem. Geol. 116, 61–84.
Azmy, K., Kendall, B., Creaser, R.A., Heaman, L., de Oliveira, T.F., 2008. Global correlation of the Vazante Group, Sao Francisco Basin, Brazil: Re–Os and U–Pb radiometric age constraints. Precambrian Res. 164, 160–172.
Bailey, S.W., 1966. The Status of Clay Mineral Structures. Proceedings of the 14th National Conference on Clays and Clay minerals. Pergamon, New York.
Barker, C.E., Pawlewicz, M.J., 1994. Calculation of vitrinite-reflectance from thermal histories and peak temperature: a comparison of methods. In: Mukhopadhyay, P.K., Dow, W.G. (Eds.), Vitrinite-Reflectance as a Maturity Parameter: Applications and Limitations, ACS Symposium Series No. 570, pp. 216–229.
Barker, C.E., Bone, Y., Lewan, M.D., 1998. Fluid inclusion and vitrinite-reflectance geothermometry compared to heat-flow models of maximum paleotemperature next to dikes, western onshore Gippsland Basin, Australia. Int. J. Coal Geol. 37, 73–111.
Bartley, J.K., Semikhatov, M.A., Kaufman, A.J., Knoll, A.H., Pope, M.C., Jacobsen, S.B., 2001. Global events across the Mesoproterozoic-Neoproterozoic boundary: C and Sr isotopic evidence from Siberia. Precambrian Res. 111, 165–202.
Behar, F., Beaumont, V., Penteado, H.L., De, B., 2001. Rock-Eval 6 technology: performances and developments. Oil Gas Sci. Technol. 56, 111–134.
Bertrand-Sarfati, J., Moussine-Pouchkine, A., 1985. Evolution and environmental-conditions of Conophyton–Jacutophyton associations in the Atar dolomite (Upper Proterozoic, Mauritania). Precambrian Res. 29, 207–234.
Bertrand-Sarfati, J., Moussine-Pouchkine, A., 1988. Is cratonic sedimentation consistent with available models — an example from the Upper Proterozoic of the West-African Craton. Sed. Geol. 58, 255–276.
Bertrand-Sarfati, J., Trompette, R., Walter, M.R., 1976. Chapter 10.1 Use of Stromatolites for Intrabasinal Correlation: Example from the Late Proterozoic of the North-Western Margin of the Taoudenni Basin. Developments in Sedimentology. Elsevier.
Bronner, G., Roussel, J., Trompette, R., Clauer, N., 1980. Genesis and geodynamic evolution of the Taoudeni Cratonic Basin (Upper Precambrian and Paleozoic), western Africa. In: Bally, A.W. (Ed.), Dynamics of Plate Interiors. Geodyn. Series, vol. 1. AGU-GSA, pp. 81–90.
Carslaw, H.S., Jaeger, J.C., 1959. Conduction of Heat in Solids. Oxford University Press, New York, p. 510.
Cassata, W.S., Renne, P.R., Shuster, D.L., 2009. Argon diffusion in plagioclase and implications for thermochronometry: a case study from the Bushveld Complex. South Africa Geochim. Cosmochim. Acta 73, 6600–6612.
Clauer, N., 1976. Chimie isotopique du strontium des milieux sédimentaires. Application a la géochronologie de la couverture du craton ouest africain. Mem. Sci. Geol. 45, 1–256.
Clauer, N., 1981. Rb–Sr and K–Ar dating of Precambrian clays and glauconies. Precambrian Res. 15, 331–352.
Clauer, N., Caby, R., Jeannette, D., Trompette, R., 1982. Geochronology of sedimentary and meta-sedimentary Precambrian rocks of the West-African craton. Precambrian Res. 18, 53–71.
Cohen, A.S., 2004. The rhenium–osmium isotope system: applications to geochronological and palaeoenvironmental problems. J. Geol. Soc. 161, 729–734.
Cohen, A.S., Coe, A.L., Bartlett, J.M., Hawkesworth, C.J., 1999. Precise Re–Os ages of organic-rich mudrocks and the Os isotope composition of Jurassic seawater. Earth Planet. Sci. Lett. 167, 159–173.
Colodner, D., Sachs, J., Ravizza, G., Turekian, K., Edmond, J., Boyle, E., 1993. The geochemical cycles of rhenium: a reconnaissance. Earth Planet. Sci. Lett. 117, 205–221.
Creaser, R.A., Sannigrahi, P., Chacko, T., Selby, D., 2002. Further evaluation of the Re–Os geochronometer in organic-rich sedimentary rocks: a test of hydrocarbon maturation effects in the Exshaw Formation, Western Canada Sedimentary Basin. Geochim. Cosmochim. Acta 66, 3441–3452.
Crusius, J., Thomson, J., 2000. Comparative behavior of authigenic Re, U, and Mo during reoxidation and subsequent long-term burial in marine sediments. Geochim. Cosmochim. 64, 2233–2242.

Crusius, J., Calvert, S., Pedersen, T., Sage, D., 1996. Rhenium and molybdenum enrichments in sediments as indicators of oxic, suboxic and sulfidic conditions of deposition. Earth Planet. Sci. Lett. 145, 65–78.

D'Agrella-Filho, M.S., Pacca, I.G., Teixeira, W., Onstott, T.C., Renne, P.R., 1990. Paleomagnetic evidence for the evolution of Meso- to Neo-Proterozoic glaciogenic rocks in central-eastern Brazil. Palaeogeogr. Palaeoclimatol. Palaeoecol. 80, 255–265.

D'Agrella-Filho, M.S., Pacca, I.I.G., Trindade, R.I.F., Teixeira, W., Raposo, M.I.B., Onstott, T.C., 2004. Paleomagnetism and 40Ar/39Ar ages of mafic dikes from Salvador (Brazil): new constraints on the São Francisco craton APW path between 1080 and 1010 Ma. Precambrian Res. 132, 55–77.

Delaney, P.T., 1987. Heat transfer theory applied to mafic dike intrusions. In: Halls, H.L., Fahrig, W.F. (Eds.), Mafic Dike Swarms: Geological Association of Canada special paper, p. 34.

Delaney, P.T., Pollard, D.D., 1982. Solidification of basaltic magma during flow in a dike. Am. J. Sci. 282 (6), 856–885.

Dempster, T.J., Rogers, G., Tanner, P.W.G., Bluck, B.J., Muir, R.J., Redwood, S.D., Ireland, T.R., Paterson, B.A., 2002. Timing of deposition, orogenesis and glaciation within the Dalradian rocks of Scotland: constraints from U–Pb zircon ages. J. Geol. Soc. 159, 83–94.

Deynoux, M., Affaton, P., Trompette, R., Villeneuve, M., 2006. Pan-African tectonic evolution and glacial events registered in Neoproterozoic to Cambrian cratonic and foreland basins of West Africa. J. Afr. Earth Sci. 46, 397–426.

Esser, B.K., Turekian, K.K., 1993. The osmium isotopic composition of the continental crust. Geochim. Cosmochim. Acta 57, 3093–3104.

Evans, J.A., 1996. Dating the transition of smectite to illite in Palaeozoic mudrocks using the Rb–Sr whole-rock technique. J. Geol. Soc. London 153, 101–108.

Fairchild, T.R., Schopf, J.W., Shen-Miller, J., Guimarães, E.M., Edwards, M.D., Lagstein, A., Li, X., Pabst, M., de Melo-Filho, L.S., 1996. Recent discoveries of Proterozoic microfossils in south-central Brazil. Precambrian Res. 80, 125–152.

Frank, T.D., Kah, L.C., Lyons, T.W., 2003. Changes in organic matter production and accumulation as a mechanism for isotopic evolution in the Mesoproterozoic ocean. Geol. Mag. 140, 397–420.

Galushkin, Y.I., 1997. Thermal effects of igneous intrusions on maturity of organic matter: a possible mechanism of intrusion. Org. Geochem. 26, 645–658.

Geboy, N.J., 2006. Rhenium–Osmium Age Determinations of Glaciogenic Shales from the Mesoproterozoic Vazante Formation, Brazil, Masters Thesis, University of Maryland.

Gillett, S.L., 2003. Paleomagnetism of the Notch Peak contact metamorphic aureole, revisited: pyrrhotite from magnetite plus pyrite under sub metamorphic conditions. J. Geophys. Res. Solid Earth 108.

Girard, J.P., Deynoux, M., Nahon, D., 1989. Diagenesis of the Upper proterozoic siliciclastic sediments of the Taoudeni Basin (West-Africa) and relation to diabase emplacement. J. Sed. Petrol. 59, 233–248.

Gorokhov, I.M., Siedlecka, A., Roberts, D., Melnikov, N.N., Turchenko, T.L., 2001. Rb–Sr dating of diagenetic illite in Neoproterozoic shales, Varanger Peninsula, northern Norway. Geol. Mag. 138, 541–562.

Grathoff, G.H., D.M., 1996. Illite polytype quantification using WILDFIRE calculated X-ray diffraction patterns. Clays Clay Minerals 44, 835–842.

Hall, A.J., 1986. Pyrite pyrrhotite redox reactions in nature. Mineral. Mag. 50, 223–229.

Halliday, A.N., Graham, C.M., Aftalion, M., Dymoke, P., 1989. The depositional age of the Dalradian Supergroup — U–Pb and Sm–Nd isotopic studies of the Tayvallich Volcanics, Scotland. J. Geol. Soc. 146, 3–6.

Halverson, G.P., Hoffman, P.F., Schrag, D.P., Maloof, A.C., Rice, A.H.N., 2005. Toward a Neoproterozoic composite carbon-isotope record. Geol. Soc. Amer. Bull. 117, 1181–1207.

Hattori, Y., Suzuki, K., Honda, M., Shimizu, H., 2003. Re–Os isotope systematics of the Taklimakan Desert sands, moraines and river sediments around the Taklimakan Desert, and of Tibetan soils. Geochim. Cosmochim. Acta 67, 1203–1213.

Heaman, L.M., LeCheminant, A.N., Rainbird, R.H., 1990. A U–Pb Baddeleyite Study of Franklin Igneous Events. Geological Association of Canada, Programs with Abstracts.

Heaman, L.M., LeCheminant, A.N., Rainbird, R.H., 1992. Nature and timing of Franklin Igneous Events, Canada — implications for a Late Proterozoic mantle plume and the break-up of Laurentia. Earth Planet. Sci. Lett. 109, 117–131.

Hunt, J.M., 1961. Distribution of hydrocarbons in sedimentary rocks. Geochim. Cosmochim. Acta 22, 37–49.

Jacob, H., 1989. Classification, structure, genesis and practical importance of natural solid oil bitumen ("migrabitumen"). Int. J. Coal Geol. 11, 65–79.

Jarvie, D.M., 1991. Total organic carbon (TOC) analysis. In: Merril, R.K. (Ed.), Source and Migration Processes and Evaluation Techniques: The American Association of Petroleum Geologists, pp. 113–118.

Kah, L.C., Bartley, J.K., 2004. Effect of Marine Carbon Reservoir Size on the Duration of Carbon Isotope Excursions: Interpreting the Mesoproterozoic Carbon Isotope Record. Geological Society of America Abstracts with Programs.

Kah, L.C., Sherman, A.G., Narbonne, G.M., Knoll, A.H., Kaufman, A.J., 1999. delta C-13 stratigraphy of the Proterozoic Bylot Supergroup, Baffin Island, Canada: implications for regional lithostratigraphic correlations. Can. J. Earth Sci. 36, 313–332.

Kah, L.C., Bartley, J.K., Stagner, A.F., 2008. Reinterpreting a Proterozoic enigma: *Conophyton–Jacutophyton* stromatolites of the Mesoproterozoic Atar Group, Mauritania. Spec. Publ.-Int. Assoc. Sed. 41, 277–295.

Kalsbeek, F., Frei, R., 2006. The Mesoproterozoic Midsommersø dolerites and associated high-silica intrusions, North Greenland: crustal melting, contamination and hydrothermal alteration. Contrib. Mineral. Petrol. 152, 89–110.

Kendall, B.S., Creaser, R.A., Ross, G.M., Selby, D., 2004. Constraints on the timing of Marinoan 'Snowball Earth' glaciation by 187Re–187Os dating of a Neoproterozoic post-glacial black shale in Western Canada. Earth Planet. Sci. Lett. 222, 729–740.

Kendall, B., Creaser, R.A., Selby, D., 2006. Re–Os geochronology of postglacial black shales in Australia: constraints on the timing of "Sturtian" glaciation. Geology 34, 729–732.

Kendall, B., Creaser, R.A., Selby, D., 2009a. 187Re–187Os geochronology of Precambrian organic-rich sedimentary rocks. Spec. Publ.-Geol. Soc. Lond. 326, 85–107.

Kendall, B., Creaser, R.A., Gordon, G.W., Anbar, A.D., 2009b. Re–Os and Mo isotope systematics of black shales from the Middle Proterozoic Velkerri and Wollogorang Formations, McArthur Basin, northern Australia. Geochim. Cosmochim. Acta 73, 2534–2558.

Koide, M., Goldberg, E.D., Niemeyer, S., Gerlach, D., Hodge, V., Bertine, K.K., Padova, A., 1991. Osmium in marine sediments. Geochim. Cosmochim. Acta 55, 1641–1648.

Kröner, A., Cordani, U., 2003. African, southern Indian and South American cratons were not part of the Rodinia supercontinent: evidence from field relationships and geochronology. Tectonophysics 375, 325–352.

Lahondère, D., Thieblemont, D., Goujou, J.C., Roger, J., Moussine-Pouchkine, A., Le Metour, J., Cocherie, A., Guerrot, C., 2003. Notice explicative des cartes géologiques et gîtologiques à 1/200 000 et 1/500 000 du Nord de la Mauritanie, Vol. 1. DMG, Ministère des Mines et de l'Industrie, Nouakchott.

Lambert, I.B., 1973. Post-depositional availability of sulphur and metals and formation of secondary textures and structures in stratiform sedimentary sulphide deposits. Austr. J. Earth Sci. Int. Geosci. J. Geol. Soc. Australia 20, 205–215.

LeCheminant, A.N., Heaman, L.M., 1989. Mackenzie igneous events, Canada — Middle Proterozoic hotspot magmatism associated with ocean opening. Earth Planet. Sci. Lett. 96, 38–48.

Levasseur, S., Birck, J., J A. C., 1998. Direct measurement of femtomoles of osmium and the 187Os/186Os ratio in seawater. Science 282, 272–274.

Lewan, M.D., Maynard, J.B., 1982. Factors controlling enrichment of vanadium and nickel in the bitumen of organic sedimentary rocks. Geochim. Cosmochim. Acta 46, 2547–2560.

Li, Z.X., Bogdanova, S.V., Collins, A.S., Davidson, A., De Waele, B., Ernst, R.E., Fitzsimons, I.C.W., Fuck, R.A., Gladkochub, D.P., Jacobs, J., Karlstrom, K.E., Lu, S., Natapov, L.M., Pease, V., Pisarevsky, S.A., Thrane, K., Vernikovsky, V., 2008. Assembly, configuration, and break-up history of Rodinia: a synthesis. Precambrian Res. 160, 179–210.

Lottaroli, F., Craig, J., Thusu, B., 2009. Neoproterozoic–Early Cambrian (Infracambrian) hydrocarbon prospectivity of North Africa: a synthesis. In: Craig, J., Thurow, J., Thusu, B., Whitham, A., Abutarruma, Y. (Eds.), Global Neoproterozoic Petroleum Systems: The Emerging Potential in North Africa, vol. 326. Geological Society of London, London, pp. 137–156.

Ludwig, K.R., 1980. Calculation of uncertainties of U–Pb isotope data. Earth Planet. Sci. Lett. 46, 212–220.

Ludwig, K., 2003. Isoplot/Ex, Version 3: A Geochronological Toolkit for Microsoft Excel. Geochronology Center Berkeley.

Morton, J.P., Long, L.E., 1982. Rb–Sr dating of illite diagenesis. AAPG Bull. Am. Assoc. Petrol. Geol. 66, 610-610.

Noble, S.R., Hyslop, E.K., Highton, A.J., 1996. High-precision U–Pb monazite geochronology of the c.806 Ma Grampian shear zone and the implications for the evolution of the central highlands of Scotland. J. Geol. Soc. 153, 511–514.

Nowell, G.M., Luguet, A., Pearson, D.G., Horstwood, M.S.A., 2008. Precise and accurate 186Os/188Os and 187Os/188Os measurements by multi-collector plasma ionisation mass spectrometry (MC-ICP-MS) part I: Solution analyses. Chem. Geol. 248, 363–393.

Odin, G.S., Hunziker, J.C., 1982. Radiometric dating of the Albian-Cenomanian. In: Odin, G.S. (Ed.), Numerical Dating in Stratigraphy Part 1. John Wiley & Sons, pp. 537–557.

Ogg, J.G., Ogg, G., Gradstein, F.M., 2008. The Concise Geologic Time Scale. Cambridge University Press, Cambridge.

Ohr, M., Halliday, A.N., Peacor, D.R., 1991. Sr and Nd isotopic evidence for punctuated clay diagenesis, Texas Gulf-Coast. Earth Planet. Sci. Lett. 105, 110–126.

Onstott, T.C., Hargraves, R.B., 1981. Proterozoic transcurrent tectonics — paleomagnetic evidence from Venezuela and Africa. Nature 289, 131–136.

Onstott, T.C., Hargraves, R.B., York, D., Hall, C., 1984. Constraints on the motions of South American and African Shields during the Proterozoic: I. 40Ar/39Ar and paleomagnetic correlations between Venezuela and Liberia. Geol. Soc. Amer. Bull. 95, 1045–1054.

Oxbugh, R., 1998. Variations in the osmium isotope composition of seawater over the past 200000 years. Earth Planet. Sci. Lett. 159, 183–191.

Pattison, D.R.M., 2006. The fate of graphite in prograde metamorphism of pelites: an example from the Ballachulish aureole, Scotland. Lithos 88, 85–99.

Peters, K.E., 1986. Guidelines for evaluating programmed pyrolysis. AAPG Bull. 70, 318–329.

Peucker-Ehrenbrink, B., Jahn, B.-m., 2001. Rhenium–osmium isotope systematics and platinum group element concentrations: loess and the upper continental crust. Geochem. Geophys. Geosyst. 2.

Rainbird, R.H., McNicoll, V.J., Heaman, L.M., 1994. Detrital Zircon Studies of Neoproterozoic Quartzarenites from North-western Canada: Additional Support for an Extensive River System Originating from Grenville Orogen. Eighth International Conference on Geochronology. U.S. Geological Survey Circular, Berkeley, California, p. 258.

Ravizza, G., Peucker-Ehrenbrink, B., 2003. Chemostratigraphic evidence of Deccan volcanism from the marine osmium isotope record. Science 302, 1392–1395.

Ravizza, G., Turekian, K.K., 1989. Application of the 187Re–187Os system to black shale geochronometry. Geochim. Cosmochim. Acta 53, 3257–3262.

Raymond, A.C., Murchison, D.G., 1988. Development of organic maturation in the thermal aureoles of sills and its relation to sediment compaction. Fuel 67, 1599–1608.

Renne, P.R., Swisher, C.C., Deino, A.L., Karner, D.B., Owens, T.L., DePaolo, D.J., 1998. Intercalibration of standards, absolute ages and uncertainties in 40Ar/39Ar dating. Chem. Geol. 145, 117–152.

Renne, P.R., Knight, K.B., Nomade, S., Leung, K.-N., Lou, T.-P., 2005. Application of deuteron–deuteron (D–D) fusion neutrons to 40Ar/39Ar geochronology. Appl. Radiat. Isotopes 62, 25–32.

Renne, P.R., Sharp, Z.D., Heizler, M.T., 2008. Cl-derived argon isotope production in the CLICIT facility of OSTR reactor and the effects of the Cl-correction in 40Ar/39Ar geochronology. Chem. Geol. 255, 463–466.
Renne, P.R., Cassata, W.S., Morgan, L.E., 2009. The isotopic composition of atmospheric argon and 40Ar/39Ar geochronology: Time for a change? Quat. Geochronol. 4, 288–298.
Schofield, D.I., Gillespie, M.R., 2007. A tectonic interpretation of "Eburnean terrane" outliers in the Reguibat Shield, Mauritania. J. Afr. Earth Sci. 49, 179–186.
Schofield, D.I., Horstwood, M.S.A., Pitfield, P.E.J., Crowley, Q.G., Wilkinson, A.F., Sidaty, H.C.O., 2006. Timing and kinematics of Eburnean tectonics in the central Reguibat Shield, Mauritania. J. Geol. Soc. 163, 549–560.
Selby, D., 2007. Direct rhenium–osmium age of the Oxfordian–Kimmeridgian boundary, Staffin bay, Isle of Skye, U.K., and the Late Jurassic time scale. Norw. J. Geol. 87, 9.
Selby, D., 2009. U–Pb zircon geochronology of the Aptian/Albian boundary implies that the GL-O international glauconite standard is anomalously young. Cretaceous Res. 30, 1263–1267.
Selby, D., Creaser, R.A., 2003. Re–Os geochronology of organic rich sediments: an evaluation of organic matter analysis methods. Chem. Geol. 200, 225–240.
Selby, D., Creaser, R.A., 2005. Direct radiometric dating of the Devonian–Mississippian time-scale boundary using the Re–Os black shale geochronometer. Geology 33, 545–548.
Selby, D., Mutterlose, J., Condon, D.J., 2009. U–Pb and Re–Os geochronology of the Aptian/Albian and Cenomanian/Turonian stage boundaries: implications for timescale calibration, osmium isotope seawater composition and Re–Os systematics in organic-rich sediments. Chem. Geol. 265, 394–409.
Smith, P.E., Evensen, N.M., York, D., Odin, G.S., 1998. Single-grain 40Ar–39Ar ages of glauconies: implications for the geologic time scale and global sea level variations. Science 279, 1517–1519.
Smoliar, M.I., Walker, R.J., Morgan, J.W., 1996. Re–Os isotope constraints on the age of Group IIA, IIIA, IVA, and IVB iron meteorites. Science 271, 1099–1102.
Steiger, R.H., Jager, E., 1977. Subcommission on geochronology — convention on use of decay constants in geochronology and cosmochronology. Earth Planet. Sci. Lett. 36, 359–362.
Sun, W., Arculus, R.J., Bennett, V.C., Eggins, S.M., Binns, R.A., 2003. Evidence for rhenium enrichment in the mantle wedge from submarine arc-like volcanic glasses (Papua New Guinea). Geology 31, 845–848.
Teal, D.A.J., Kah, L.C., 2005. Using C-Isotopes to Constrain Intrabasinal Stratigraphic Correlations: Mesoproterozoic Atar Group, Mauritania. Geological Society of America Abstracts with Programs, vol. 37, p. 45.
Tohver, E., D'Agrella-Filho, M.S., Trindade, R.I.F., 2006. Paleomagnetic record of Africa and South America for the 1200–500 Ma interval, and evaluation of Rodinia and Gondwana assemblies. Precambrian Res. 147, 193–222.
Trompette, R., 1973. Le Précambrien supérieur et le Paléozoïque inferieur de l'Adrar de Mauritanie (bordure occidentale de Bassin de Taoudeni, Afrique de l'Oust). Un exemple de sédimentation de craton. Etude stratigraphique et sédimentologique.
Trompette, R., 1994. Geology of Western Gondwana (2000–500 Ma). Balkema, Rotterdam. pp. 350.
Turgeon, S.C., Creaser, R.A., Algeo, T.J., 2007. Re–Os depositional ages and seawater Os estimates for the Frasnian–Famennian boundary: implications for weathering rates, land plant evolution, and extinction mechanisms. Earth Planet. Sci. Lett. 261, 649–661.
Verati, C., Bertrand, H., Féraud, G., 2005. The farthest record of the Central Atlantic Magmatic Province into West Africa craton: precise 40Ar/39Ar dating and geochemistry of Taoudenni basin intrusives (northern Mali). Earth Planet. Sci. Lett. 235, 391–407.
Villeneuve, M., Cornée, J.J., 1994. Structure, evolution and paleogeography of the West African craton and bordering belts during the Neoproterozoic. Precambrian Res. 69, 307–326.
Vogel, N., Renne, P.R., 2008. Ar-40–Ar-39 dating of plagioclase grain size separates from silicate inclusions in IAB iron meteorites and implications for the thermochronological evolution of the IAB parent body. Geochim. Cosmochim. Acta 72, 1231–1255.
Yang, G., Hannah, J.L., Zimmerman, A., Stein, H.J., Bekker, A., 2009. Re–Os depositional age for Archean carbonaceous slates from the south-western Superior Province: challenges and insights. Earth Planet. Sci. Lett. 280, 83–92.
Zhao, G., Sun, M., Wilde, S.A., Li, S., Zhang, J., 2006. Some key issues in reconstructions of Proterozoic supercontinents. J. Asian Earth Sci. 28, 3–19.

Precambrian Research 185 (2011) 202–214

Contents lists available at ScienceDirect

Precambrian Research

journal homepage: www.elsevier.com/locate/precamres

Re–Os geochronology of the Neoproterozoic–Cambrian Dalradian Supergroup of Scotland and Ireland: Implications for Neoproterozoic stratigraphy, glaciations and Re–Os systematics

Alan D. Rooney[a,*], David M. Chew[b], David Selby[a]

[a] Department of Earth Sciences, University of Durham, Durham DH1 3LE, UK
[b] Department of Geology, Trinity College Dublin, Dublin 2, Ireland

ARTICLE INFO

Article history:
Received 13 July 2010
Received in revised form
10 December 2010
Accepted 7 January 2011
Available online 18 January 2011

Keywords:
Re–Os
Dalradian
Neoproterozoic
Sturtian
Rodinia
Laurentia

ABSTRACT

New Re–Os geochronology for the Ballachulish Slate Formation of the Dalradian Supergroup, Scotland yields a depositional age of 659.6 ± 9.6 Ma. This age represents the first successful application of the Re–Os system to rocks that have extremely low Re and Os abundances (<1 ppb and < 50 ppt, respectively). The Re–Os age represents a maximum age for the glaciogenic Port Askaig Formation and refutes previous chemostratigraphic and lithostratigraphic studies which correlated the Port Askaig Formation with a series of middle Cryogenian (ca. 715 Ma) glacials. Additionally, the Re–Os age strongly suggests that the Port Askaig Formation may be correlative with the ~650 Ma end-Sturtian glaciations of Australia. As a consequence, the correlation of the Ballachulish Limestone Formation with the ca. 800 Ma Bitter Springs anomaly is not tenable. Initial Os isotope data from the Ballachulish Slate Formation coupled with data from Australia reveals a radiogenic $^{187}Os/^{188}Os$ isotope composition (~0.8–1.0) for seawater during the Neoproterozoic, which is similar to that of modern seawater (1.06).

We also report a young, highly imprecise Re–Os age (310 ± 110 Ma) for the Early Cambrian Leny Limestone Formation which is constrained biostratigraphically by a polymerid and miomerid trilobite fauna. We suggest, based on the mineralogy of the Leny Limestone, (kaolinite, muscovite and a serpentine group mineral, berthierine), that the Re–Os systematics have been disturbed by post-depositional fluid flow associated with Palaeozoic igneous intrusions. However, it is evident from the Ballachulish Slate Formation results that anhydrous metamorphism does not disturb the Re–Os geochronometer.

1. Introduction

Neoproterozoic strata record a number of significant events such as the transition from stratified Proterozoic oceans with oxic surface waters and anoxic deep waters to a more-or-less fully oxygenated ocean (Anbar and Knoll, 2002; Knoll, 2003; Fike et al., 2006; Halverson and Hurtgen, 2007; Canfield et al., 2008). Major changes in biological systems and evolutionary developments occurred towards the end of the Proterozoic including the evolution of metazoans (Logan et al., 1995, 1997; Vidal and Moczydlowska-Vidal, 1997; Jensen et al., 2000; Martin et al., 2000; Narbonne and Gehling, 2003; Knoll et al., 2006; Macdonald et al., 2010a,b). Additionally, the Neoproterozoic was a time of major climatic fluctuation with a number of extreme glacial events recorded in the rock record (e.g. the "Snowball Earth" of Kirschvink, 1992; Hoffman et al., 1998; Hoffman and Schrag, 2002 or the "Slushball Earth" of Hyde et al., 2000). However, there is, at present, no consensus as to the cause, extent, duration or number of these glacial events (Kennedy et al., 1998; Evans, 2000; Fairchild and Kennedy, 2007). The lack of precise and accurate geochronological data has severely hindered attempts to develop a chronological framework for the Neoproterozoic. In particular, understanding and constraining the extent and duration of these glacial events has relied upon lithostratigraphy and chemostratigraphy with only a few glaciogenic successions constrained by robust geochronological data (Hoffmann et al., 2004; Zhou et al., 2004; Kendall et al., 2004, 2006, 2009a; Condon et al., 2005; Bowring et al., 2007; Macdonald et al., 2010a).

During the Neoproterozoic, the continental masses of Laurentia, Baltica and Amazonia were juxtaposed as a result of various orogenic events to form the supercontinent Rodinia (e.g. Li et al., 2008 and references therein). During the break-up of Rodinia which commenced at ca. 750 Ma there was a period of intracontinental extension and basin genesis along the eastern margin of Laurentia (Harris et al., 1994; Soper, 1994; Cawood et al., 2007). Scotland occupied a unique position within the Rodinia supercontinent lying close to the junction of the Laurentian, Baltica and Amazonian

* Corresponding author. Tel.: +44 0191 334 2300; fax: +44 0191 334 2301.
E-mail address: alan.rooney@durham.ac.uk (A.D. Rooney).

0301-9268/$ – see front matter.
doi:10.1016/j.precamres.2011.01.009

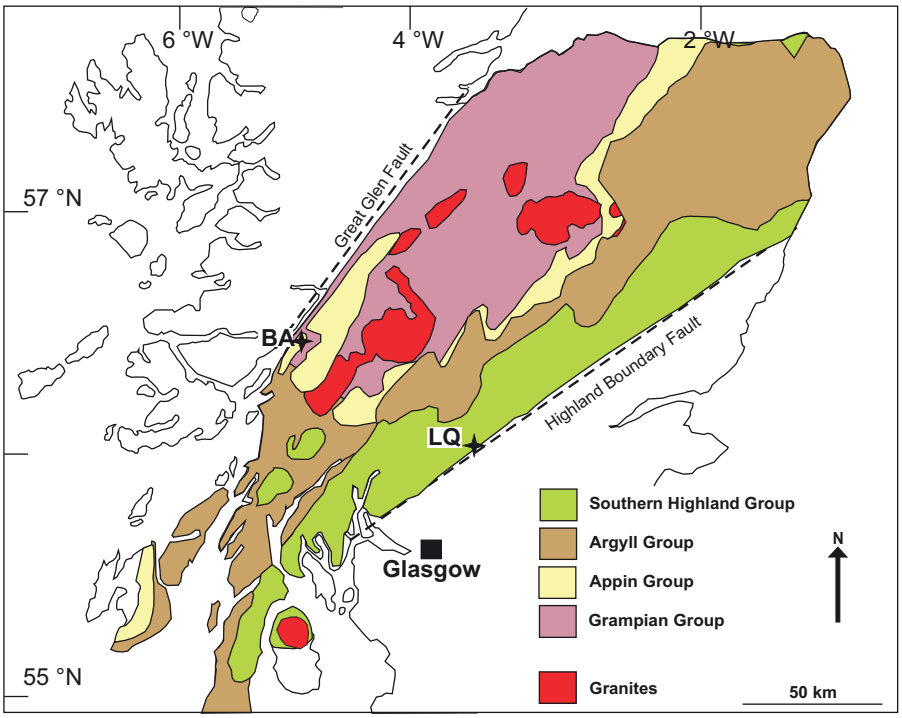

Fig. 1. Simplified geological and location map highlighting the fourfold division of the Dalradian Supergroup of the Grampian Terrane Abbreviations of sampling locations: BA – Ballachulish Slate quarry; LQ - Leny Limestone quarry.
Modified from Harris et al. (1994) and Thomas et al. (2004).

continental blocks (Dalziel, 1994). The sedimentary basins that formed during the formation and breakup of Rodinia are preserved in Scotland as the Torridonian, Moine and Dalradian Supergroups (Anderton, 1982, 1985; Rainbird et al., 2001; Strachan et al., 2002; Cawood et al., 2003, 2004, 2007).

The Dalradian Supergroup of Scotland and Ireland is a metasedimentary succession that was deposited on the eastern margin of Laurentia during the late Neoproterozoic and Early Cambrian. Existing constraints imply the base is younger than 800 Ma and it extends to at least 510 Ma (Harris et al., 1994; Smith et al., 1999; Prave et al., 2009a). Despite its importance in regional and global studies of the Proterozoic, our understanding of the Dalradian sequence suffers from a lack of radiometric ages (Halliday et al., 1989; Dempster et al., 2002). In an attempt to improve the chronostratigraphy of the Dalradian, several workers have applied lithostratigraphic and chemostratigraphic tools with varying levels of success (Prave, 1999; Brasier and Shields, 2000; Condon and Prave, 2000; Thomas et al., 2004; McCay et al., 2006; Prave et al., 2009a; Sawaki et al., 2010). These studies have improved our knowledge of the Proterozoic ocean chemistry and the environmental conditions of deposition within the Dalradian sedimentary basin. However, chemostratigraphic tools cannot provide absolute ages and ultimately rely upon correlation with sequences which have robust radiometric and/or biostratigraphic age constraints (Melezhik et al., 2001, 2008; Fairchild and Kennedy, 2007; Jiang et al., 2007; Meert, 2007; Giddings and Wallace, 2009; Frimmel, 2010). As a result, obtaining precise and accurate radiometric ages remain a priority for resolving many of the issues regarding global correlations.

The rhenium–osmium (Re–Os) geochronometer has been shown to provide robust depositional ages even for sedimentary rocks that have experienced hydrocarbon maturation, greenschist metamorphism and flash pyrolysis associated with igneous intrusions (Creaser et al., 2002; Kendall et al., 2004, 2006, 2009a,b; Selby and Creaser, 2005; Rooney et al., 2010). Thus, the Re–Os system represents an accurate, precise and reliable geochronometer for providing depositional age data for the Dalradian metasediments and constructing a chronostratigraphic framework for the chemostratigraphic, tectonostratigraphic and lithostratigraphic datasets.

Here, we present new Re–Os age that constrain the depositional age of a sedimentary unit from the Dalradian Supergroup. The Re–Os data also provide an estimate for the osmium isotope composition of seawater in the Dalradian basin during the Neoproterozoic and ultimately provide a maximum depositional age for a key Neoproterozoic glacial horizon. A further aspect of this study involves the application of Re–Os geochronology to sedimentary units with low Re and Os abundances (<1 ppb Re and <50 ppt Os) to provide accurate and precise geochronology. Additionally, this work presents results from a sedimentary unit (Leny Limestone Formation) in which the Re–Os geochronometer has been disturbed as a result of post-depositional fluid flow. The results from this study provide us with new insights into the robustness of the Re–Os geochronometer.

2. Geological setting

2.1. The Dalradian Supergroup

The Dalradian Supergroup of Scotland and Ireland consists of a thick (~25 km) metasedimentary succession and a minor amount of mafic volcanics deposited on the eastern margin of the Laurentian craton during the Neoproterozoic to Early Cambrian (Fig. 1; Harris et al., 1994 and references therein). This quoted thickness of the Dalradian Supergroup is a cumulative thickness from all subgroups and is not a true reflection of sediment thickness. Many aspects of basin genesis have proved controversial, with little consensus apparent even after more than a century of studies. Most models for Dalradian deposition invoke a long, shallow-marine, ensialic basin which underwent prolonged extension during the late Neoprotero-

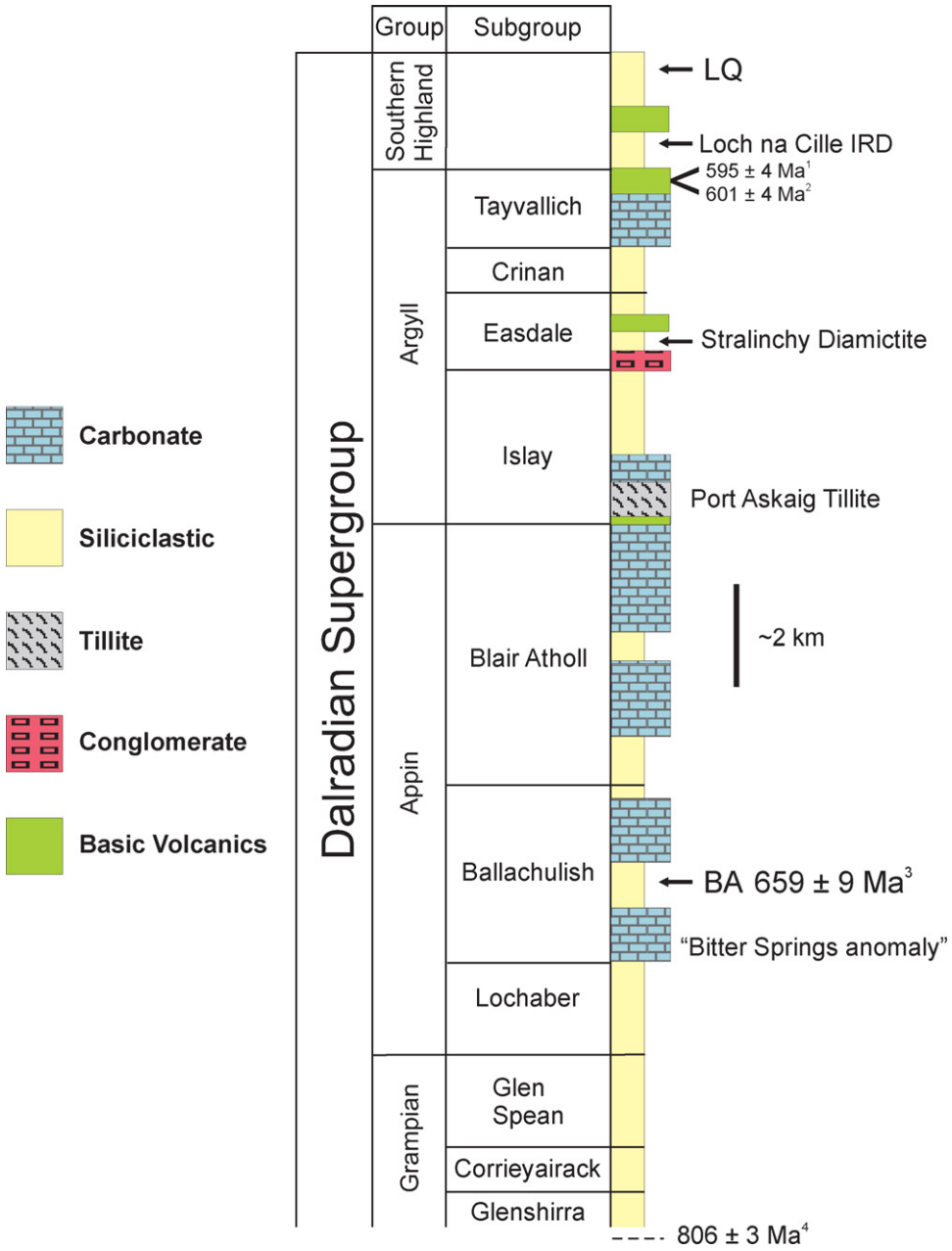

Fig. 2. Generalised stratigraphic column of the Dalradian Supergroup with glaciogenic horizons and the purported Bitter Springs anomaly suggested by (Prave et al., 2009a,b) but refuted by the new Re–Os geochronology data. See text for details. BA – Ballachulish Slate Formation; LQ – Leny Limestone Formation. (1. Halliday et al., 1989; 2. Dempster et al., 2002; 3. This study; 4. Noble et al., 1996).
Modified from Prave et al. (2009a).

zoic, resulting in the eventual separation of Laurentia from western Gondwana at ca. 550 Ma (Hoffman, 1991; Soper, 1994; Dalziel and Soper, 2001). An alternative model proposes that the lower portions of the Dalradian represented a rapidly formed foredeep basin associated with the mid-Neoproterozoic (840–730 Ma) Knoydartian Orogeny (Prave, 1999). In both models extensional tectonics played a major role in the genesis of the upper portions of the Dalradian basin during the latest Neoproterozoic to Early Cambrian.

Lithostratigraphic correlation of the Dalradian Supergroup is hampered by the paucity of volcanic horizons suitable for U–Pb geochronology and the lack of biostratigraphically diagnostic fossils (Fig. 2). Additionally, many portions of the Dalradian sequence exhibit extreme facies variability along strike having experienced complex polyphase deformation and metamorphism (Harris et al., 1994; Strachan et al., 2002 and references therein). Despite these issues, a coherent lithostratigraphy has been established from western Ireland to the Shetland Islands, 200 km north of mainland Scotland (Harris et al., 1994).

The Dalradian Supergroup consists of four groups which are from oldest to youngest; the Grampian, Appin, Argyll and Southern Highland groups (Figs. 1 and 2).

The basal Grampian Group crops out primarily in the Central Highlands although possible correlatives exist on the north Grampian coast and on the Shetland Islands (Strachan et al., 2002). The Grampian Group consists of up to 7 km of predominantly marine, quartzo-feldspathic psammites and semi-pelites (Glover and Winchester, 1989; Harris et al., 1994). The Grampian Group sedimentary succession displays sharp lateral variations typical of a syn-rift origin (Soper and England, 1995; Banks et al., 2007). The overlying Appin Group is exposed in a broad zone throughout Scot-

land and Ireland as far north as the Shetland Islands. The Appin Group consists of up to 4 km of quartzite, semi-pelites and phyllites deposited as a post-rift, thermal subsidence sequence (Litherland, 1980; Glover et al., 1995; Soper and England, 1995; Glover and McKie, 1996). The overlying Argyll Group records rapid deepening of the basin following the shallow marine conditions of the Appin Group (Anderton, 1985). The Argyll Group comprises of a thick heterogeneous succession of shelf sediments up to 9 km thick which passes upwards into deep water turbidite and basinal facies and associated mafic volcanics (Anderton, 1982). The marked change from a shelf setting to deep water sedimentation is widely ascribed to the onset of syn-depositional rifting. The basal subgroup (Islay Subgroup) of the Argyll Group is marked by a distinctive and persistent tillite horizon; the Port Askaig Formation, correlatives of which are traceable from Connemara in western Ireland to Banffshire in NE Scotland (Anderton, 1985; Harris et al., 1994). The Southern Highland Group (along with the newly defined Trossachs Group of Tanner and Sutherland, 2007) marks the top of the Dalradian succession and consists of ca. 4 km of coarse-grained turbiditic clastics and volcaniclastic strata (Anderton, 1985; Soper and England, 1995). The Southern Highland Group is considered to represent the change from a period of continental rifting and rupture to that of a thermally subsiding margin (Anderton, 1985).

2.1.1. Glaciogenic horizons within the Dalradian and possible global correlations

The Port Askaig Formation of the Argyll Group is a thick (~900 m) succession of diamictites interbedded with sandstone, conglomerate and mudstone (Kilburn et al., 1965; Spencer, 1971; Eyles, 1988; Arnaud and Eyles, 2002). The formation represents the most persistent and distinctive glaciogenic horizon within the Dalradian Supergroup (Fig. 2). A glaciogenic origin was first recognised in the late nineteenth century (Thomson, 1871, 1877), and is described in detail in the classic memoir of (Spencer, 1971). The most extensive outcrops of the Port Askaig Formation consists of ~400 m of coarse-grained and poorly sorted diamictite interbedded with sandstone, mudstone and conglomerate with some megaclasts in the diamictite exceeding 100 m in size (Spencer, 1971; Arnaud, 2004). Recent studies identified enriched $\delta^{13}C$ (+11.7‰) and unradiogenic $^{87}Sr/^{86}Sr$ (0.7067) in carbonate formations above and below the Port Askaig Formation (Brasier and Shields, 2000; Sawaki et al., 2010). These data have been used to correlate the glaciogenic horizon with the ca. 750–690 Ma global Sturtian glaciation (Brasier and Shields, 2000; Fanning and Link, 2004; McCay et al., 2006; Macdonald et al., 2010a). Two more stratigraphically limited glaciogenic units within the Dalradian Supergroup have also been identified; the Stralinchy "Boulder Bed" Formation and the Inishowen – Loch na Cille Ice Rafted Debris (IRD) Formations (Fig. 2; Condon and Prave, 2000; McCay et al., 2006). The Stralinchy Formation occurs in the Easdale Subgroup in Donegal in NW Ireland and has been correlated with the ~635 Ma global Marinoan glaciation (Hoffmann et al., 2004; Condon et al., 2005; McCay et al., 2006). The Loch na Cille and Inishowen glaciogenic formations occur within the uppermost Argyll Group and basal Southern Highland Group respectively, and have been correlated with the 580 Ma Laurentian Gaskiers glacial event (Condon and Prave, 2000; Bowring et al., 2003).

2.2. Current chronological constraints for the Dalradian Supergroup

With the exception of *Bonnia-Ollenellus* Zone Early Cambrian trilobites and inarticulate brachiopods of the upper Southern Highland Group, the Dalradian Supergroup is almost entirely devoid of fossils (Pringle, 1939; Fletcher and Rushton, 2007). In addition, absolute chronological constraints on the age of Dalradian sedimentation are also very sparse (Fig. 2). The oldest phase of volcanic activity in the Dalradian Supergroup occurs within correlatives of the Port Askaig Formation in NE Scotland (Chew et al., 2010). However, this thin tholeiitic pillow basalt has not been dated thus far. The lower part of the Southern Highland Group in SW Scotland is characterised by ca. 2 km of tholeiitic mafic volcanic rocks and sills (Tayvallich Volcanic Formation). The Tayvallich Formation is cross cut by a 595 ± 4 Ma (U–Pb SHIRIMP) keratophyre intrusion and a felsic tuff from this formation has yielded a U–Pb zircon age of 601 ± 4 Ma (Halliday et al., 1989; Dempster et al., 2002). Pegmatites from the Central Scottish Highlands has yielded a U–Pb monazite age of 806 ± 3 Ma although the stratigraphic position of these pegmatites remains controversial (Noble et al., 1996). These pegmatites have been suggested to intrude into Grampian Group rocks thus providing a minimum age for these sediments (Noble et al., 1996; Highton et al., 1999). However, other studies (e.g. Smith et al., 1999) propose that the pegmatites intrude into the Dava and Glen Banchor successions which lie unconformably below the Grampian Group and that therefore the Grampian Group is younger than 806 Ma (Smith et al., 1999; Strachan et al., 2002).

Numerous studies have utilised $\delta^{13}C$, $\delta^{18}O$ and $^{87}Sr/^{86}Sr$ data from several different carbonate units of the Dalradian Supergroup with the aim of correlation with global chemostratigraphic curves (Brasier and Shields, 2000; Thomas et al., 2004; McCay et al., 2006; Halverson et al., 2007a; Prave et al., 2009a; Sawaki et al., 2010). A composite $\delta^{13}C$ profile for the Dalradian Supergroup has been used to tentatively correlate the Ballachulish Limestone of the Appin Group with the ca. 800 Ma Bitter Springs anomaly (Prave et al., 2009a; Fig. 2). Additional correlations include the pre-Marinoan Trezona anomaly and ca. 635 Ma Marinoan-equivalent cap carbonate sequence with units of the middle Easdale Subgroup and the terminal Proterozoic (ca. 600–551 Ma) Shuram-Wonoka anomaly in the Girlsta Limestone on Shetland (Melezhik et al., 2008; Prave et al., 2009a,b).

2.3. Metamorphism and deformation of the Dalradian Supergroup

The Dalradian Supergroup of Scotland is one of the classic areas for the study of regional and contact metamorphism (e.g., Barrow, 1893; Tilley, 1925; Baker, 1985; Voll et al., 1991; Dempster, 1992; Pattison and Harte, 1997). The main phases of regional metamorphism took place during the Grampian Orogeny. The Grampian Orogeny is understood to be related to the collision of Laurentia with an oceanic arc during the Early Ordovician and can be considered broadly equivalent to the Taconic Orogeny of the Appalachians (Dewey and Mange, 1999; Soper et al., 1999). Geochronological constraints for the Grampian Orogeny include U–Pb zircon ages from syn-tectonic intrusives of 475–468 Ma and Sm–Nd metamorphic garnet crystallisation ages of 473–465 Ma which date peak metamorphism (Friedrich et al., 1999; Baxter et al., 2002).

The Dalradian sedimentary succession also experienced contact metamorphism associated with the intrusion of numerous Late Caledonian (ca. 430–390 Ma; Oliver, 2001) granites throughout the Grampian Terrane of Scotland (Fig. 1). In addition to the granites there are also a number of minor Late Palaeozoic intrusive suites recorded in the Dalradian (Neilson et al., 2009 and references therein).

3. Samples for this study

Two localities were chosen for Re–Os geochronology analyses; the Ballachulish Slate Formation from the Ballachulish Subgroup of the Appin Group and the Leny Limestone Formation of the Southern Highland Group (Figs. 1 and 2). The Ballachulish Slate was chosen

to provide a maximum age constraint on the depositional age of the Port Askaig Formation (Fig. 2). The Leny Limestone Formation was chosen as it contains the only biostratigraphically diagnostic fauna found in the Dalradian Supergroup (Pringle, 1939; Fletcher and Rushton, 2007). Additionally, the metasedimentary rocks of the Dalradian Supergroup represent an opportunity to further our understanding of the effects of regional and contact metamorphism on the Re–Os geochronometer.

3.1. Appin Group – Ballachulish Slate Formation

The Appin Group is made up of three subgroups, the Lochaber, Ballachulish and Blair Atholl (Fig. 2). The Ballachulish Slate Formation consists of ca. 400 m of pyritiferous black slates and graphitic phyllites. Samples were collected on the eastern foreshore of Loch Linnhe at the entrance to Loch Leven (56°42.1′N, 5°11.6′W; Fig. 1). In this area, the top of the Ballachulish Slate Formation is estimated to be ca. 1 km below the equivalent of the Port Askaig Formation (Litherland, 1980; Harris et al., 1994). Regional metamorphic grade associated with the Grampian Orogeny varies from chlorite grade in the NW to garnet grade in the SE. Estimates of P-T conditions range from ca. 450 to 550 °C from NW to SE, at ca. 6 kbar (Pattison and Voll, 1991). In addition to Grampian regional metamorphism, the Ballachulish Slates also experienced Late Caledonian (ca. 430 Ma) igneous activity and contact metamorphism primarily associated with the well-characterised Ballachulish Igneous Complex (Pattison and Harte, 1997; Pattison, 2006). The metamorphic aureole varies in width from ca. 400 to 1700 m, based upon the first appearance of cordierite in metapelites (Pattison, 2006). Regional P-T conditions at the time of intrusion are estimated at ca. 250–300 °C at ca. 3 kbar. The age of the Ballachulish Igneous Complex is constrained by Re–Os molybdenite and U–Pb zircon ages of 433.5 ± 1.8 Ma and 428 ± 9.8 Ma, respectively (Conliffe et al., 2010; Rogers and Dunning, 1991, recalculated by Neilson et al., 2009). Fluid flow between the intrusion and the aureole was limited and there is no evidence for a large-scale hydrothermal circulation system or associated mineralogical changes connected to the intrusion (Harte et al., 1991; Pattison, 2006).

The slates analysed in this study were sampled ca. 2 km NNW of the NW contact of the Ballachulish Igneous complex and are hence outside the aureole. The slates sampled are black and massive with bedding occasionally still discernible and predominantly orientated parallel to cleavage. X-ray diffractometry (XRD) studies indicate that the Ballachulish Slates have a composition of quartz, mica, chlorite and feldspars (albite and occasionally orthoclase), typical of an argillaceous slate. The samples of Ballachulish slate used in this study are similar in composition to those described in greater detail by Walsh (2007).

3.2. Southern Highland Group – Leny Limestone

The Leny Limestone forms part of the Keltie Water Grit Formation of the Southern Highland Group. The formation consists of pale grey to white, siliceous grits, black graphitic slates and rare locally fossiliferous limestones (Tanner and Pringle, 1999). The limestones of this formation yield a fauna including polymerid and miomerid trilobites, brachiopods, sponges, hyoliths and bradoriids (Fletcher and Rushton, 2007). The miomerid trilobites indicate a stratigraphical age equivalent to the base of the paradoxidid Amgan Stage of Siberia traditionally regarded as Middle Cambrian (511–506 Ma, Ogg et al., 2008). However, the polymerid trilobites e.g., *Pagetides*, are forms from the *Bonnia-Olenellus* Zone and are thus regarded as Lower Cambrian (516.5–512 Ma; Ogg et al., 2008). An age of ca. 512 Ma has been adopted here as the age of the Leny Limestone Formation (Fletcher and Rushton, 2007).

Black graphitic slates of the Leny Limestone Formation were sampled on the south-easterly face of the Western Quarry (56°15.5′N, 4°13.1W; Fig. 1). The metamorphic grade during the Grampian Orogeny was low, with an estimated peak metamorphic temperature of 270 °C (Tanner and Pringle, 1999). Detrital biotite is preserved, albeit commonly partially altered to chlorite. The locality is also the locus of several phases of igneous activity such as intrusions of Devonian quartz-felsite dykes and Permo-Carboniferous quartz dolerite dykes (British Geological Survey, 2005; Fletcher and Rushton, 2007). The Devonian intrusion exhibits a 70 m fault offset, though this faulting is not seen in the Permo-Carboniferous dyke suggesting faulting occurred prior to this younger intrusive episode. XRD analysis of the Leny Limestone Formation slates reveal a composition of quartz, micas (mainly muscovite), kaolinite and a serpentine-group mineral with the chemical formula of $Fe_3Si_2O_5(OH)_4$ suggested to represent berthierine (Brindley, 1982).

4. Sampling and analytical methods

Sampling of the Ballachulish Slate and Leny Limestone Formations was limited to a vertical interval of ca. 50 cm of stratigraphy across a lateral interval of several tens of metres. Weathered material was removed from the outcrop prior to sampling of fresh surfaces. Large (~100 g) samples were selected to ensure homogenisation of Re–Os abundances in the samples (Kendall et al., 2009b). All samples were polished to remove cutting and drilling marks to eliminate any potential contamination. The samples were dried at 60 °C for ~12 h and then crushed to a fine powder of ~30 μm. The samples were broken into chips with no metal contact and powdered in a ceramic dish using a shatterbox.

Rhenium–osmium isotope analysis was carried out at Durham University's TOTAL laboratory for source rock geochronology and geochemistry at the Northern Centre for Isotopic and Elemental Tracing (NCIET). Sample digestion using a CrO_3–H_2SO_4 solution is the preferred method for Re–Os geochronology as it has been shown to preferentially liberate hydrogenous Re and Os, ultimately providing more precise ages (Selby and Creaser, 2003; Kendall et al., 2004). An inverse *aqua-regia* solution was also employed in an attempt to evaluate the contribution of detrital Re and Os in these samples. Previous work has shown that *aqua-regia* digestion liberates both non-hydrogenous (detrital and meteoritic) and hydrogenous Re and Os. This detrital Os component has been shown to represent a source of geological scatter that results in determination of imprecise and/or inaccurate depositional ages (Ravizza et al., 1991; Selby and Creaser, 2003; Kendall et al., 2004).

Approximately 1 g of sample powder was digested together with a mixed tracer (spike) solution of ^{190}Os and ^{185}Re in a Cr^{VI}–H_2SO_4 solution in a sealed carius tube at 220 °C for ~48 h (Selby and Creaser, 2003; Kendall et al., 2004). Through the use of the Cr^{VI}–H_2SO_4 digestion media it is possible to preferentially liberate the hydrogenous Re and Os components from the samples thus limiting any detrital component (Selby and Creaser, 2003; Kendall et al., 2004). For the inverse *aqua-regia* digestions approximately 1 g of sample powder was dissolved together with a spike solution of ^{190}Os and ^{185}Re in a 1:2 acid mixture of 3 ml 12 N HCl and 6 ml of 16 N HNO_3 in a sealed carius tube at 220 °C for ~48 h (Selby and Creaser, 2003).

Rhenium and Os were purified from the acid solution using solvent extraction ($CHCl_3$), micro-distillation and anion chromatography methods and analysed by negative thermal ionisation mass spectrometry as outlined by (Selby and Creaser, 2003), and (Selby, 2007). The purified Re and Os fractions were loaded onto Ni and Pt filaments, respectively (Selby et al., 2007), with the isotopic measurements conducted using a ThermoElectron TRITON mass spectrometer via static Faraday collection for Re and ion-counting

Table 1
Re–Os isotope data for the Ballachulish Slate and Leny Limestone Formations.

Sample[a]	Re (ppb)	±	Os (ppt)	±	^{192}Os (ppt)	±	^{187}Re/^{188}Os	±	^{187}Os/^{188}Os	±	rho[b]	Os$_i$[c]
Ballachulish Slate samples												
Balla 2B	1.20	0.01	46.0	0.5	13.9	0.2	172.6	2.3	2.944	0.044	0.731	1.04
Balla 2B ar	1.08	0.00*	43.8	0.4	13.3	0.2	161.3	1.9	2.876	0.042	0.763	1.09
Balla 2C	1.85	0.01	52.2	0.5	14.5	0.2	253.8	3.2	3.841	0.055	0.758	1.04
Balla 2C ar	1.77	0.01	53.5	0.5	15.3	0.2	230.8	2.6	3.564	0.050	0.745	1.01
Balla 3	1.69	0.01	40.9	0.5	10.8	0.2	311.7	4.6	4.478	0.072	0.813	1.04
Balla 3 ar	1.68	0.01	40.9	0.5	10.9	0.1	308.2	4.1	4.364	0.067	0.805	0.96
Balla 5B	0.29	0.01	29.2	0.3	10.1	0.2	56.5	1.4	1.660	0.029	0.482	1.04
Balla 5B ar	0.30	0.00*	30.6	0.3	10.6	0.1	55.6	0.8	1.593	0.026	0.767	0.98
Balla 6	0.39	0.02	25.5	0.7	8.4	0.5	93.3	6.4	2.060	0.142	0.645	1.03
Balla 6 ar	0.30	0.01	41.4	0.6	16.7	0.6	41.4	1.3	1.472	0.050	0.511	1.01
Leny Slate samples												
L1	55.8	0.2	487.7	3.1	107.1	0.5	1036.8	5.6	6.874	0.033	0.716	−1.97
L2	55.4	0.2	431.0	3.0	89.8	0.4	1228.0	7.2	7.649	0.041	0.756	−2.83
L3	49.4	0.2	430.6	3.0	92.2	0.5	1065.8	6.2	7.239	0.038	0.759	−1.85
L4	50.9	0.2	419.2	3.0	85.0	0.4	1192.4	7.2	8.075	0.045	0.778	−2.10
L5	49.6	0.2	424.1	3.0	88.4	0.5	1117.0	6.7	7.642	0.042	0.771	−1.89
L6	51.2	0.2	443.0	3.0	92.1	0.4	1107.2	6.3	7.691	0.039	0.755	−1.76
L7	66.1	0.2	633.1	4.1	146.3	0.6	898.4	4.5	6.162	0.031	0.583	−1.50
L8	46.2	0.2	447.0	3.2	99.7	0.5	921.5	5.4	6.650	0.040	0.682	−1.21
L9	57.7	0.2	515.9	3.3	114.5	0.5	1001.9	5.2	6.716	0.031	0.680	−1.83

* Uncertainty is less than 0.01.
[a] "ar" denotes inverse aqua regia digestion.
[b] Rho is the associated error correlation (Ludwig, 1980).
[c] Os$_i$ = initial ^{187}Os/^{188}Os isotope ratio calculated at 659 Ma for the Ballachulish Slate samples and at 512 Ma for the Leny Slate samples.

using a secondary electron multiplier in peak-hopping mode for Os. Average procedural blanks for the Cr^{VI}–H_2SO_4 method during this study were 16.8 ± 0.06 pg and 0.43 ± 0.06 pg (1σ S.D., n = 3) for Re and Os respectively, with an average ^{187}Os/^{188}Os value of ∼0.25 ± 0.11 (n = 3). For the inverse *aqua-regia* method procedural blanks for Re and Os were 1.9 ± 0.01 pg and 0.12 ± 0.06 pg, respectively (1σ S.D. n = 2) with an average ^{187}Os/^{188}Os value of ∼0.4 ± 0.5 (1σ S.D., n = 2).

Uncertainties for ^{187}Re/^{188}Os and ^{187}Os/^{188}Os are determined by error propagation of uncertainties in Re and Os mass spectrometer measurements, blank abundances and isotopic compositions, spike calibrations and reproducibility of standard Re and Os isotopic values using methods identical to previous studies (e.g., Kendall et al., 2004; Selby and Creaser, 2005). The Re–Os isotopic data, 2σ calculated uncertainties for ^{187}Re/^{188}Os and ^{187}Os/^{188}Os and the associated error correlation function (rho) are regressed to yield a Re–Os date using *Isoplot V. 3.0* with a λ ^{187}Re constant of 1.666×10^{-11} a^{-1} (Ludwig, 1980, 2003; Smoliar et al., 1996).

To ensure and monitor long-term mass spectrometry reproducibility, in-house standard solutions of Re and Os (Durham Romil Osmium Standard [DROsS]) are repeatedly analysed at NCIET. The Re standard analysed during the course of this study is made from 99.999% zone-refined Re ribbon and is considered to have an identical Re isotopic composition to that of the AB-1 Re standard (Creaser et al., 2002; Selby and Creaser, 2003; Kendall et al., 2004). The NCIET Re standard yields an average ^{185}Re/^{187}Re ratio of 0.59772 ± 0.00172 (1 S.D., n = 114). This is in excellent agreement with the value reported for the AB-1 standard (Creaser et al., 2002). The Os isotope reference material (DROsS) yields an ^{187}Os/^{188}Os ratio of 0.106093 ± 0.00015 (1 S.D., n = 36). The isotopic compositions of these solutions are identical within uncertainty to those reported by Rooney et al. (2010) and references therein.

5. Results

5.1. Ballachulish Slate Formation samples

The Ballachulish Slate samples have Re (0.3–1.9 ppb) and Os (25.5–52.2 ppt) abundances that are close to or less than that of average continental crustal values of ∼1 ppb and 50 ppt, respectively (Table 1; Esser and Turekian, 1993; Peucker-Ehrenbrink and Jahn, 2001; Hattori et al., 2003; Sun et al., 2003). The ^{187}Re/^{188}Os ratios range from 56.5 to 311.7 and the ^{187}Os/^{188}Os ratios range from 1.660 to 4.478 (Table 1). Regression of the Re–Os isotope data yield a Re–Os age of 659.6 ± 9.6 Ma (2σ, n = 5, Model 1, Mean Square of Weighted Deviates [MSWD] = 0.01, initial ^{187}Os/^{188}Os = 1.04 ± 0.03; Fig. 3a).

Digestion of the Ballachulish samples using inverse *aqua-regia* yields elemental abundances of 0.3–1.8 ppb and 30.6–53.5 ppt for Re and Os, respectively, which are identical within uncertainty to the values from the samples digested using CrO_3–H_2SO_4 (Table 1). The ^{187}Re/^{188}Os ratios range from 41.4 to 308.2 and the ^{187}Os/^{188}Os ratios range from 1.472 to 4.364 (Table 1). Regression of the *aqua-regia* derived Re–Os isotope data yield a Model 3 age of 655 ± 49 Ma (2σ, n = 5, MSWD = 16) with an initial Os isotope composition of 1.03 ± 0.16 (Fig. 3b).

5.2. Leny Limestone slate samples

The Leny Limestone slates are enriched in Re (46.2–66.1 ppb) and Os (419–633 ppt) in comparison to average continental crustal values of ∼1 ppb and 50 ppt, respectively (Table 1). The ^{187}Re/^{188}Os ratios range from 898.4 to 1228.0 and the ^{187}Os/^{188}Os ratios range from 6.162 to 8.075 (Table 1). Regression of the Re–Os isotope data yield a Re–Os age of 310 ± 110 Ma (2σ, n = 9, Model 3, MSWD = 388, initial ^{187}Os/^{188}Os = 1.7 ± 2.0; Fig. 4).

6. Discussion

6.1. Effect of non-hydrogenous Re and Os in low abundance samples

The CrO_3–H_2SO_4 method has been shown to yield precise and accurate depositional age determinations for both Phanerozoic and Proterozoic sedimentary successions (Kendall et al., 2004, 2006, 2009a,c; Selby and Creaser, 2005; Anbar et al., 2007; Selby, 2007; Yang et al., 2009; Rooney et al., 2010). Data from the Ballachulish samples using the CrO_3–H_2SO_4 digestion method yields a Model 1 age with a low uncertainty (1.5%) and a low degree of scatter about the isochron (MSWD < 1). However, as these samples have

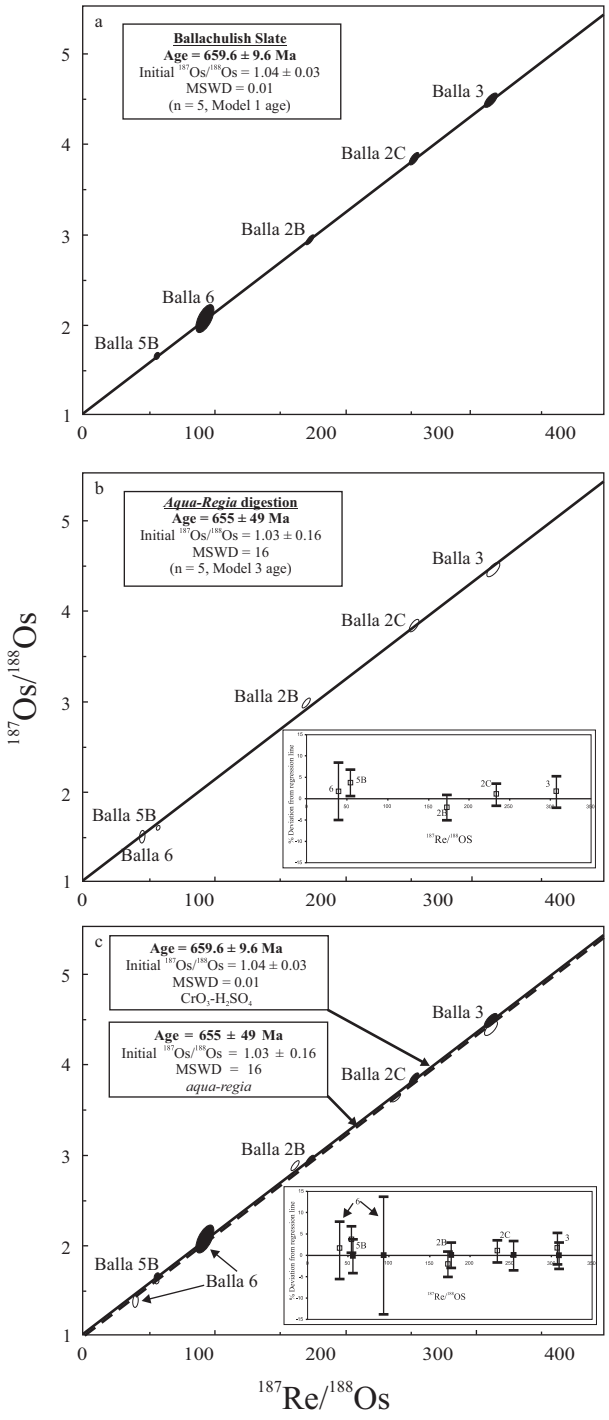

Fig. 3. Re–Os isochron diagram for the Ballachulish Slate Formation using various digestion mediums (a) the CrO_3–H_2SO_4 digestion method, (b) inverse *aqua-regia* digestion, (c) both digestion analyses (CrO_3–H_2SO_4 solid line, inverse *aqua-regia* dashed line). Inset diagrams show the deviation of each point from the CrO_3–H_2SO_4 best-fit regression. A Model 1 isochron is accomplished by assuming scatter along the regression line is derived only from the input 2σ uncertainties for $^{187}Re/^{188}Os$ and $^{187}Os/^{188}Os$, and ρ (rho).

Re and Os abundances comparable to that of average continental crust it is important to assess the effects of a detrital Re and Os component on the geochronology data. It has been shown that the incorporation of a detrital Os component could lead to a younger or older age depending on the isotopic composition of the detrital Os (Ravizza et al., 1991). The effects of a detrital Os component on Re–Os depositional ages have been assessed previously during the

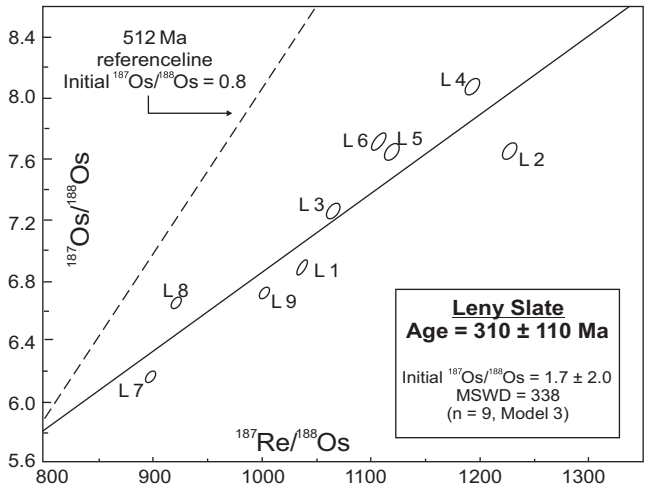

Fig. 4. Re–Os isochron diagram for the Leny Slate Member. The dashed line represents a 512 Ma reference line with the Os_i value of 0.8 representing Cambrian seawater (Mao et al., 2002). The 512 Ma age assigned for the Leny Limestone is based on a trilobite fauna (Fletcher and Rushton, 2007). See text for discussion.

development of the CrO_3–H_2SO_4 method (Selby and Creaser, 2003; Kendall et al., 2004).

The results from the inverse *aqua-regia* digestion show Re and Os abundances that are comparable with the samples digested using CrO_3–H_2SO_4 (Table 1). The isotopic composition data highlights the impact of detrital Re and Os on the determination of depositional ages. All of the $^{187}Re/^{188}Os$ and $^{187}Os/^{188}Os$ values for the *aqua-regia* samples are lower than those of the samples digested using CrO_3–H_2SO_4 (15% and 9% lower, respectively; Table 1). This suggests that the *aqua-regia* digestion has liberated an unradiogenic detrital Os component. Both ages for the Ballachulish Slate Formation are very similar however, the *aqua-regia* Re–Os data have a much larger degree of scatter (MSWD = 16) and yield a less precise age (9% uncertainty; Fig. 3b and c). The samples digested using the CrO_3–H_2SO_4 method yield a much more precise age with a lower degree of scatter (MSWD = 0.01; Fig. 3a). These variations in precision and geological scatter are very similar to those identified by previous studies which undertook digestion of samples in *aqua-regia* (Selby and Creaser, 2003; Kendall et al., 2004). Additionally, digesting samples in the CrO_3–H_2SO_4 solution at 80 °C instead of 220 °C has been shown to yield identical data, supporting the notion that this method does not liberate non-hydrogenous Re and Os even at high temperatures (Kendall et al., 2009a).

The $^{187}Os/^{188}Os$ initial ratio (Os_i) data from the samples digested using the CrO_3–H_2SO_4 method are all very similar with a coefficient of variation of 0.3% in contrast to the Os_i data from the samples digested in *aqua-regia* which have a coefficient of variation of 5% (coefficient of variation = (S.D./mean) × 100; Table 1). This suggests that there were variations in Os isotope composition and/or magnitude of the detrital Os flux into the Ballachulish Slate during deposition. Again, this is identical to the findings of Kendall et al. (2004) on the Old Fort Point Formation of Canada.

The low degree of scatter coupled with the precise age of 659.6 ± 9.6 Ma represents a depositional age for the Ballachulish Slate Formation and the initial $^{187}Os/^{188}Os$ isotope composition of 1.04 represents that of seawater at the time of deposition.

6.2. Implications for low Re and Os abundance geochronology

The Re–Os age for the Ballachulish Slate Formation indicate that samples with low Re and Os abundances (<1 ppb Re and <50 ppt Os) can be used to provide precise geochronological data (Fig. 3a; Table 1). These values are similar to abundances in aver-

age continental crust which range from 0.2 to 2 ppb and 30–50 ppt, respectively (Esser and Turekian, 1993; Peucker-Ehrenbrink and Jahn, 2001; Hattori et al., 2003; Sun et al., 2003).

Previous work on Re–Os geochronology has focused on sedimentary units greatly enriched in Re and Os with abundances >20 ppb and 500 ppt, respectively (Ravizza and Turekian, 1989; Cohen et al., 1999; Creaser et al., 2002; Selby and Creaser, 2005; Selby, 2007; Rooney et al., 2010). However, some recent studies have successfully applied the Re–Os geochronometer to sedimentary rocks with low to moderate enrichments of Re and Os (1.7–50 ppb and 82–250 ppt, respectively; Kendall et al., 2004, 2006, 2009a,b; Yang et al., 2009). The Re–Os geochronology data for the Ballachulish Slate Formation represent successful application of the system to samples with very low Re and Os abundances provided that the system has not been disturbed as discussed below.

The low Re and Os abundances do not appear to impair the robustness of the system as the Ballachulish samples all have similar $^{187}Os/^{188}Os$ (Os_i) values, yield a large spread in present-day $^{187}Re/^{188}Os$ values (~260 units) and display positively correlated, radiogenic $^{187}Os/^{188}Os$ values indicative of a closed system (Table 1). This positive correlation indicates that the 659.6 ± 9.6 Ma age for the Ballachulish Slate Formation does not represent a mixing line. Additionally, if the systematics had been disturbed, any detrital Os component in these samples would represent a significant cause of geological uncertainty, resulting in an imprecise and geologically meaningless age. The highly precise age coupled with the low degree of scatter in the data, (659.6 ± 9.6 Ma and MSWD = 0.01), suggests that this is a depositional age and the Os_i value of 1.04 represents the Os isotope composition of local seawater at the time of deposition. The results from the Ballachulish Slate Formation strongly suggest that the system can be applied to sedimentary units that have low Re and Os abundances. From this we can also propose that the system is robust enough to provide depositional ages for strata that have experienced complex and polyphase metamorphic histories.

6.3. Age of the Ballachulish Slate Formation

The Re–Os isotope data from the Ballachulish slates yield an age of 659.6 ± 9.6 Ma which represents the depositional age of the Ballachulish Slate Formation (Fig. 3a). Accordingly, this Re–Os age defines a maximum age constraint for the glaciogenic Port Askaig Formation (Fig. 2). Taken in the context of the previous geochronological constraints for the Dalradian, the Re–Os age for the Ballachulish Slate Formation strongly suggests that the Argyll Group was deposited within ~60 Ma, prior to the eruption of the Tayvallich volcanics at ca. 600 Ma. From these two geochronological constraints, combined with the possibility that correlatives of the ca. 635 Ma Marinoan cap carbonate sequence are found within units of the Easdale Subgroup (McCay et al., 2006) we suggest that the Port Askaig Formation records a low-latitude glacial event that occurred at ca. 650 Ma.

Much of the recent work relating to the Dalradian Supergroup has focused on $\delta^{13}C$ carbonate and $^{87}Sr/^{86}Sr$ chemostratigraphy of the various carbonate units (Prave et al., 2009a and references therein; Sawaki et al., 2010). This focus on chemostratigraphy coupled with the lack of reliable geochronology data has resulted in several attempts at correlation of the Dalradian Supergroup with better constrained Neoproterozoic sequences (McCay et al., 2006; Prave et al., 2009a; Sawaki et al., 2010). The Ballachulish Limestone is ca. 200 m in thickness and passes upwards into the Ballachulish Slate (Anderton, 1982; Prave et al., 2009a). Work by Prave et al. (2009a) suggested that the Ballachulish Limestone possess $\delta^{13}C_{carbonate}$ values as low as −7‰ and was tentatively correlated with the ca. 800 Ma Bitter Springs anomaly of central Australia (Hill and Walter, 2000; Halverson et al., 2007b). However, the Re–Os data of 659.6 ± 9.6 Ma for the Ballachulish Slate Formation negates the possibility of this correlation (Fig. 2).

A 60 Ma duration for Argyll Group deposition suggested by the Re–Os data presented here contrasts with a duration of ca. 120 Ma required by chemostratigraphic and lithostratigraphic correlations of the Port Askaig Formation with a ca. 715 Ma "Sturtian" glacial (Prave, 1999; Brasier and Shields, 2000; Prave et al., 2009a). A short duration for Argyll Group deposition is geologically more probable given that the Argyll Group represents a time of increased tectonic activity and syn-depositional faulting with rapid deposition taking place in subsiding fault-bounded sub-basins (Anderton, 1982, 1985). A short duration for Argyll Group deposition also negates the need for any putative regional-scale unconformity within the Argyll Group, which remains contentious (see Hutton and Alsop, 2004; Tanner et al., 2005 for a review).

The new Re–Os geochronology data provide a more precise chronostratigraphic framework for understanding the tectonic evolution of the Dalradian basin and the onset of sedimentation within the basin. Furthermore, the Re–Os geochronology helps refine Neoproterozoic palaeogeographies related to the formation and breakup of the Rodinia supercontinent (e.g., Li et al., 2008; Li and Evans, 2010). Deposition of the Dalradian Supergroup occurred along the eastern margin of Laurentia, close to the triple junction of Baltica, Laurentia and Amazonia (Soper, 1994; Dalziel, 1994).

6.4. Implications for global correlations involving the glacial Port Askaig Formation

At present, global correlation schemes for Neoproterozoic glaciogenic deposits are dependent on correlation of two distinctive types of diamictite cap-carbonate pairs. These have been designated as "Sturtian" and "Marinoan" events after the type localities in southern Australia (Kennedy et al., 1998; Hoffman and Schrag, 2002; Halverson et al., 2005; Corsetti and Lorentz, 2006). The Sturtian glaciation however, is also used to define much older glacial events than the Sturtian *sensu stricto* of the Adelaide Rift Complex which has geochronological constraints of ca. 640–660 Ma (Preiss, 2000; Kendall et al., 2009a and references therein). These earlier glacial events assigned to the "Sturtian" have geochronological constraints which indicate low-latitude global glaciation at ca. 715 Ma based on U–Pb zircon ages (Bowring et al., 2007; Macdonald et al., 2010a). In this summary, they are referred to as middle Cryogenian (ca. 715 Ma) deposits to distinguish them from younger Sturtian (*sensu stricto*) glacial deposits on the Australian craton at ca. 640–660 Ma.

Early work on correlation of the Port Askaig Formation (Fig. 2) suggested a possible correlation with North Atlantic Varangerian tillite sequences which were originally constrained by a Rb–Sr diagenetic illite age of ca. 630 Ma (Hambrey, 1983; Fairchild and Hambrey, 1995; Gorokhov et al., 2001). Correlation of the Port Askaig Formation with the Varangerian tillite was also suggested by $^{87}Sr/^{86}Sr$ chemostratigraphy of Dalradian limestones that indicate that the base of the Dalradian Supergroup is younger than ca. 800 Ma and may be as young as ca. 700 Ma (Thomas et al., 2004). This correlation is difficult to support as the geochronological constraints for the Varangerian glaciation are based upon Rb–Sr illite geochronology, which is unlikely to represent a depositional age (Morton and Long, 1982; Ohr et al., 1991; Awwiller, 1994; Evans, 1996; Gorokhov et al., 2001; Selby, 2009).

Recent work has rejected the correlation of the Port Askaig Formation and the Varangerian glaciation. Instead, $\delta^{13}C$ and $^{87}Sr/^{86}Sr$ profiles from the underlying Islay Limestone and overlying Bonahaven Formation have been used to suggest a middle Cryogenian (ca. 715 Ma) age for the Port Askaig Formation (Brasier and Shields, 2000; Prave et al., 2009a). Further 'evidence' for a 715 Ma middle Cryogenian age for the Port Askaig Formation is the presence of

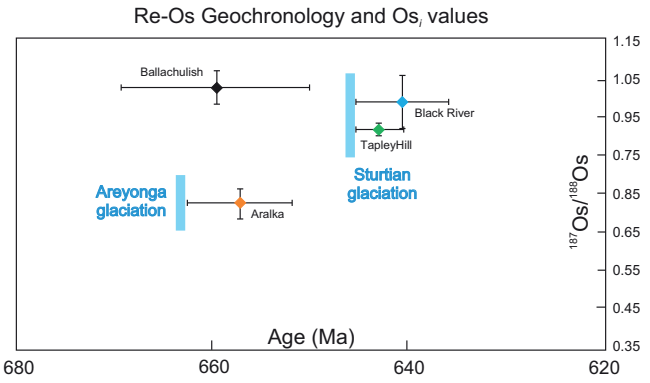

Fig. 5. Graphic illustration of Re–Os geochronology data and Os_i values for Cryogenian and Sturtian (*sensu stricto*) pre- and post-glacial horizons. See text for discussion. Data from Ballachulish Slate Formation (this study); Aralka Formation (Kendall et al., 2006); Tapley Hill Formation (Kendall et al., 2006); Black River Dolomite (Kendall et al., 2009a).

younger glaciogenic units in the Dalradian, namely the Stralinchy-Reelan (a possible Marinoan correlative) and the Inishowen-Loch na Cille Formations (a possible Gaskiers correlative; Condon and Prave, 2000; McCay et al., 2006). However, the Re–Os age of 659.6 ± 9.6 Ma for the Ballachulish Slate Formation refutes the notion that the Port Askaig Formation is a component of a middle Cryogenian (ca. 715 Ma) glaciation. As reported above, the Re–Os age, coupled with existing geochronology constraints on the Tayvallich volcanics strongly suggest that the Port Askaig Formation records a glacial event on the eastern margin of Laurentia at ~650 Ma.

Palaeomagnetic constraints from Laurentia during the Neoproterozoic indicate that Laurentia (and hence the Port Askaig Formation) was at low latitudes from 723 to 614 Ma (see Trindade and Macouin, 2007 and references therein). Similarly, the Sturtian (*sensu stricto*) glaciations on the Australian craton were also at low latitude and Re–Os geochronology of post-glacial rocks indicates an age of ~650 Ma for these glacial deposits. The Ballachulish Slate Formation Re–Os geochronology implies that the Port Askaig Formation could be correlated with the ~650 Ma Sturtian (*sensu stricto*) deposits of the Adelaide Rift Complex (Preiss, 2000; Kendall et al., 2006, 2009a). This suggestion is also supported by the Os_i data for the Ballachulish Slate, Upper Black River Dolomite and Tapley Hill formations as discussed below (Fig. 5; Kendall et al., 2006, 2009a; This study).

6.5. Os isotopic composition of seawater at 660 Ma

The initial Os_i values determined from the regression of the Re–Os isotope data (Table 1; Figs. 3 and 4) are interpreted to reflect the Os isotope composition of seawater at the time of deposition (Ravizza and Turekian, 1989; Cohen et al., 1999; Selby and Creaser, 2003). The Os isotope composition for seawater at the time of deposition of the Ballachulish Slate (1.04 ± 0.03) is identical, within uncertainty, to that of the present day Os isotopic composition of seawater (~1.06; Peucker-Ehrenbrink and Ravizza, 2000 and references therein; Rooney et al., unpublished data). The radiogenic Os_i value from the Ballachulish Slate Formation suggests that the contribution of radiogenic Os from riverine inputs and weathering of upper continental crustal material (present-day riverine inputs of $^{187}Os/^{188}Os$ ~1.5; Levasseur et al., 1999) dominated over the influx of unradiogenic Os from cosmic dust and hydrothermal alteration of oceanic crust and peridotites (present-day $^{187}Os/^{188}Os$ ~ 0.13; Walker et al., 2002a,b).

The radiogenic values for the Os_i of the Ballachulish Slate Formation closely match values for the post-glacial Upper Black River Dolomite, Aralka and Tapley Hill Formations of southern Australia (1.04; 1.00; 0.82; 0.95, respectively; Kendall et al., 2006, 2009a). Although there are many contrasting palaeomagnetic reconstructions of the Laurentian and Australian cratons, most models indicate that during the Neoproterozoic these two cratons were both located at low latitudes and were separated by oceanic basins that formed as a result of rifting associated with the breakup of Rodinia (Li et al., 2008 and references therein; Li and Evans, 2010). We postulate that the very similar Os_i values reported from the pre-glacial Ballachulish and post-glacial Upper Black River Dolomite, Aralka and Tapley Hill Formations represent a possibly global Os isotope composition for the 660–640 Ma time interval (Kendall et al., 2006, 2009a). Additionally, this 'global' isotope composition for this interval is significantly more radiogenic than values for Mesoproterozoic seawater Os isotope composition (1.04 compared to 0.33 and 0.29; Rooney et al., 2010; Kendall et al., 2009c). One possibility is that falling sea levels and the exposure of rifted margins associated with the breakup of Rodinia would expose older, more radiogenic continental crust to weathering. A further explanation for the increase in $^{187}Os/^{188}Os$ isotope composition for the Neoproterozoic is the increased oxygenation of deep waters during the late Neoproterozoic (Canfield and Teske, 1996; Anbar and Knoll, 2002; Canfield et al., 2007, 2008; Scott et al., 2008). This oxygenation of the oceans and atmosphere would result in increased chemical weathering of continental crust which, coupled with the breakup of Rodinia may result in an increase in seawater Os as seen for the Sr isotope composition of Neoproterozoic seawater (Jacobsen and Kaufman, 1999; Halverson et al., 2007a).

6.6. Systematics of Re–Os in Leny Limestone Formation

Although the Ballachulish Slate Formation experienced complex and polyphase metamorphism, these samples yield a precise depositional age with a low degree of scatter about the linear regression of the Re–Os data (659.6 ± 9.6 Ma, MSWD = 0.01). The results for the Ballachulish Slate samples imply that anhydrous metamorphism and dehydration reactions do not adversely affect Re–Os systematics. In contrast, the Leny Limestone Formation which has also experienced regional Grampian metamorphic events has been disturbed. We suggest that this Re–Os isotope disturbance is probably related to hydration and fluid-flow events associated with Carboniferous/Permian contact metamorphism as discussed below.

The Re–Os isotope data for the Leny Limestone Formation yield a highly imprecise age of 310 ± 110 Ma (MSWD = 338) that is significantly younger than the accepted age of ca. 512 Ma based upon the trilobite fauna found in the Leny Limestone (Fletcher and Rushton, 2007). In addition, the Os_i value of 1.7 ± 2.0 is much more radiogenic than known values for Cambrian seawater (~0.8; Mao et al., 2002) and all of the Phanerozoic. The Re–Os geochronometer has been shown to be robust following hydrocarbon maturation events, greenschist-facies metamorphism and flash pyrolysis thus suggesting the system is robust even after temperatures as high as 650 °C and pressures as high as 3 kbar (Creaser et al., 2002; Kendall et al., 2004, 2006, 2009a,b,c; Rooney et al., 2010). Disturbance of the Re–Os systematics by chemical weathering has been identified from outcrop studies on the Ohio Shale (Jaffe et al., 2002). The Leny Limestone Formation outcrop is not significantly weathered and the samples were taken in such a way as to avoid the effects of recent chemical weathering on the outcrop. The measures undertaken to ensure that fresh samples were used for Re–Os geochronology include; removal of surficial weathering prior to sampling of large (~200 g) samples extracted from the outcrop prior to cutting which meant that any evidence of weathering e.g., iron-staining or leaching and features such as quartz veins could be scrupulously avoided. Thus we do not consider these factors to

have played a role in the Re–Os analysis of the Leny Limestone Formation.

Recent work has shown that the Re–Os geochronometer is susceptible to disturbance caused by hydrothermal fluid interaction with sedimentary units associated with the formation of a SEDEX deposit (Kendall et al., 2009c). The proximity of the Leny Limestone exposures to the Devonian and Permo-Carboniferous intrusions and associated interactions with hydrothermal fluids are likely causes of disturbance of the Re–Os systematics. In agreement with work by (Kendall et al., 2009c) we suggest that the Re–Os age for the Leny Limestone represents a disturbed dataset. The negative Os_i values calculated at 512 Ma and the anomalously young age can be best explained by post-depositional mobilization of Re and Os resulting from hydrothermal fluid flow driven by the igneous intrusions found within the Leny Quarry. Possibly oxidising fluids generated by the intrusions may have leached Re and/or Os from the Leny Slate samples. The Leny Limestone slate samples all have $^{187}Re/^{188}Os$ values that plot to the right of the 512 Ma reference line suggestive of either Re gain or Os loss (Fig. 5). The occurrence of kaolinite, muscovite and berthierine from XRD analysis of the Leny Limestone Formation slates suggests that these minerals are the products of retrograde reactions involving chlorite, muscovite and an Fe-rich phase such as cordierite that was driven by reactions with hydrothermal fluids (Slack et al., 1992; Abad et al., 2010).

The lack of documented mineralisation (small [<1 cm thick] dolomite veins in the limestones notwithstanding) and identifiable accessory or index minerals renders it extremely challenging to gain a full understanding of the P-T conditions of contact metamorphism in the Leny Limestone Formation. However, given that the Grampian Orogeny would have generated local greenschist-facies conditions it is likely that hydrothermal fluid flow driven by the Palaeozoic igneous intrusions hydrated the Leny Limestone slates resulting in retrograde reactions and the disturbance of the Re–Os geochronometer.

7. Conclusions

New Re–Os geochronology for the Ballachulish Slate Formation yields a depositional age of 659.6 ± 9.6 Ma providing a maximum age constraint for the overlying glaciogenic Port Askaig Formation. The precise age coupled with the excellent linear fit of the Re–Os isotope data for the Ballachulish Slate Formation represents the first successful application of the Re–Os system in samples with Re and Os abundances comparable with, or lower than, average continental crustal values. Additionally, these results strongly suggest that meaningful Re–Os geochronology data can be obtained from sedimentary successions that have experienced polyphase contact and regional metamorphism provided that thermal alteration was anhydrous.

The Re–Os geochronology presented here indicates that the Port Askaig Formation is much younger than the middle Cryogenian glacial horizons bracketed at ca. 750–690 Ma, with which it was previously correlated. The new geochronology data for the Ballachulish Slate Formation also refutes a correlation of the underlying Ballachulish Limestone Formation with the ca. 800 Ma Bitter Springs anomaly of Australia (Hill and Walter, 2000; Halverson et al., 2007b; Prave et al., 2009a). The Re–Os geochronology provides a chronostratigraphic framework that indicates deposition of the Argyll Group occurred within a ~60 Ma interval prior to eruption of the Tayvallich Volcanics. The Re–Os data provide further support for the argument that Re–Os and U–Pb zircon geochronology are fundamental if we are to use chemostratigraphy to evaluate Neoproterozoic environments.

The Os_i value for seawater at the time of deposition of the Ballachulish Slate Formation is similar to that of the present-day value indicating that the dominant input of Os to seawater was radiogenic input from the weathering of the continental crust. Additionally, the close similarity of Os_i values from the Ballachulish Slate Formation with Sturtian (*sensu stricto*) deposits from the Australian craton indicates that the dominant source of Os to the oceans was from weathering of an evolved upper continental crust.

Disturbance of Re–Os systematics in the Leny Limestone Formation is evident by a very imprecise and inaccurate age along with a negative value for the Os_i value (calculated at 512 Ma) for seawater in this biostratigraphically constrained Cambrian unit. These factors strongly suggest that the Re–Os system was disturbed in response to hydrothermal fluid flow associated with the intrusion of a number of igneous bodies during the Palaeozoic. The circulation of fluids through the Leny Limestone Formation is suggested to be the cause for the gain of Re and/or the loss of Os thus generating an imprecise age younger than the known depositional age.

Acknowledgements

This research was funded by a TOTAL CeREES PhD scholarship awarded to ADR. Maggie White is thanked for her assistance with the XRD work. We would like to thank Rob Strachan, Tony Prave, and Alex Finlay for discussions on Dalradian geology and Re–Os systematics. Constructive criticism from Graham Shields and an anonymous reviewer also further improved this manuscript. The TOTAL laboratory for source rock geochronology and geochemistry at NCIET is partly funded by TOTAL.

References

Abad, I., Murphy, B., Nieto, F., Guiterrez-Alonso, G., 2010. Diagenesis to metamorphism transition in an episutural basin: the late Paleozoic St. Mary's Basin, Nova Scotia Canada. Canadian Journal of Earth Sciences 47, 121–135.

Anbar, A.D., Knoll, A.H., 2002. Proterozoic ocean chemistry and evolution: a bioinorganic bridge? Science 297, 1137–1142.

Anbar, A.D., Duan, Y., Lyons, T.W., Arnold, G.L., Kendall, B., Creaser, R.A., Kaufman, A.J., Gordon, G.W., Scott, C., Garvin, J., Buick, R., 2007. A whiff of oxygen before the Great Oxidation Event? Science 317, 1903–1906.

Anderton, R., 1982. Dalradian deposition and the late Precambrian–Cambrian history of the N Atlantic region: a review of the early evolution of the Iapetus Ocean. Journal of the Geological Society 139, 421–431.

Anderton, R., 1985. Sedimentation and tectonics in the Scottish Dalradian. Scottish Journal of Geology 21, 407–436.

Arnaud, E., Eyles, C.H., 2002. Catastrophic mass failure of a Neoproterozoic glacially influenced continental margin, the Great Breccia Port Askaig Formation, Scotland. Sedimentary Geology 151, 313–333.

Arnaud, E., 2004. Giant cross-beds in the Neoproterozoic Port Askaig Formation Scotland: implications for snowball Earth. Sedimentary Geology 165, 155–174.

Awwiller, D.N., 1994. Geochronology and mass-transfer in Gulf-Coast Mudrocks (South-Central Texas, USA) – Rb–Sr, Sm–Nd and Ree systematics. Chemical Geology 116, 61–84.

Baker, A.J., 1985. Pressures and temperatures of metamorphism in the eastern Dalradian. Journal of the Geological Society 142, 137–148.

Banks, C.J., Smith, M., Winchester, J.A., Horstwood, M.S.A., Noble, S.R., Ottley, C.J., 2007. Provenance of intra-Rodinian basin-fills: the Lower Dalradian Supergroup Scotland. Precambrian Research 153, 46–64.

Barrow, G., 1893. On an intrusion of muscovite–biotite gneiss in the southeast Highlands of Scotland and its accompanying metamorphism. Quarterly Journal of the Geological Society of London 19, 330–358.

Baxter, E.F., Ague, J.J., Depaolo, D.J., 2002. Prograde temperature-time evolution in the Barrovian type-locality constrained by Sm/Nd garnet ages from Glen Clova, Scotland. Journal of the Geological Society 159, 71–82.

Bowring, S., Myrow, P., Landing, E., Ramezani, J., Grotzinger, J., 2003. Geochronological constraints on terminal Neoproterozoic events and the rise of metazoans. Geophysical Research Abstracts 5, 13219.

Bowring, S.A., Grotzinger, J.P., Condon, D.J., Ramezani, J., Newall, M.J., Allen, P.A., 2007. Geochronologic constraints on the chronostratigraphic framework of the Neoproterozoic Huqf Supergroup Sultanate of Oman. American Journal of Science 307, 1097–1145.

Brasier, M.D., Shields, G., 2000. Neoproterozoic chemostratigraphy and correlation of the Port Askaig glaciation, Dalradian Supergroup of Scotland. Journal of the Geological Society 157, 909–914.

British Geological Survey, 2005. Aberfoyle. Scotland Sheet 38E. Bedrock and Superficial geology. 1:50 000. Geology Series. British Geological Survey, Keyworth, Nottingham.

Brindley, G.W., 1982. Chemical compositions of berthierines, a review. Clays and Clay Minerals 30, 153–155.

Canfield, D.E., Teske, A., 1996. Late Proterozoic rise in atmospheric oxygen concentration inferred from phylogenetic and sulphur-isotope studies. Nature 382, 127–132.
Canfield, D.E., Poulton, S.W., Narbonne, G.M., 2007. Late-Neoproterozoic deep-ocean oxygenation and the rise of animal life. Science 315, 92–95.
Canfield, D.E., Poulton, S.W., Knoll, A.H., Narbonne, G.M., Ross, G., Goldberg, T., Strauss, H., 2008. Ferruginous conditions dominated later Neoproterozoic deep-water chemistry. Science 321, 949–952.
Cawood, P.A., Nemchin, A.A., Smith, M., Loewy, S., 2003. Source of the Dalradian Supergroup constrained by U–Pb dating of detrital zircon and implications for the East Laurentian margin. Journal of the Geological Society 160, 231–246.
Cawood, P.A., Nemchin, A.A., Strachan, R., Prave, T., Krabbendam, M., 2007. Sedimentary basin and detrital zircon record along East Laurentia and Baltica during assembly and breakup of Rodinia. Journal of the Geological Society 164, 257–275.
Cawood, P.A., Nemchin, A.A., Strachan, R.A., Kinny, P.D., Loewy, S., 2004. Laurentian provenance and an intracratonic tectonic setting for the Moine Supergroup, Scotland, constrained by detrital zircons from the Loch Eil and Glen Urquhart successions. Journal of the Geological Society 161, 861–874.
Chew, D.M, Fallon, N., Kennelly, C., Crowley, Q., Pointon, M., 2010. Basic volcanism contemporaneous with the Sturtian glacial episode in NE Scotland. Transactions of the Royal Society of Edinburgh-Earth Sciences.
Cohen, A.S., Coe, A.L., Bartlett, J.M., Hawkesworth, C.J., 1999. Precise Re–Os ages of organic-rich mudrocks and the Os isotope composition of Jurassic seawater. Earth and Planetary Science Letters 167, 159–173.
Condon, D.J., Prave, A.R., 2000. Two from Donegal: Neoproterozoic glacial episodes on the northeast margin of Laurentia. Geology 28, 951–954.
Condon, D., Zhu, M., Bowring, S., Wang, W., Yang, A., Jin, Y., 2005. U–Pb Ages from the Neoproterozoic Doushantuo Formation, China. Science 308, 95–98.
Conliffe, J., Selby, D., Porter, S.J., Feely, M., 2010. Re–Os molybdenite dates from the Ballachulish and Kilmelford Igneous Complexes (Scottish Highlands): age constraints for late Caledonian magmatism. Journal of the Geological Society 167, 297–302.
Corsetti, F.A., Lorentz, N.J., 2006. On Neoproterozoic cap carbonates as chronostratigraphic markers. In: Xiao, S., Kaufman, A.J. (Eds.), Neoproterozoic Geobiology and Paleobiology. Springer, New York, pp. 273–294.
Creaser, R.A., Sannigrahi, P., Chacko, T., Selby, D., 2002. Further evaluation of the Re–Os geochronometer in organic-rich sedimentary rocks: a test of hydrocarbon maturation effects in the Exshaw Formation Western Canada Sedimentary Basin. Geochimica et Cosmochimica Acta 66, 3441–3452.
Dalziel, I.W.D., 1994. Precambrian Scotland as a Laurentia-Gondwana link – origin and significance of Cratonic Promontories. Geology 22, 589–592.
Dalziel, I.W.D., Soper, N.J., 2001. Neoproterozoic extension on the Scottish Promontory of Laurentia: Paleogeographic and tectonic implications. The Journal of Geology 109, 299–317.
Dempster, T.J., 1992. Zoning and recrystallization of phengitic micas: implications for metamorphic equilibration. Contributions to Mineralogy and Petrology 109, 526–537.
Dempster, T.J., Rogers, G., Tanner, P.W.G., Bluck, B.J., Muir, R.J., Redwood, S.D., Ireland, T.R., Paterson, B.A., 2002. Timing of deposition, orogenesis and glaciation within the Dalradian rocks of Scotland: constraints from U–Pb zircon ages. Journal of the Geological Society 159, 83–94.
Dewey, J, Mange, M., 1999. Petrography of Ordovician and Silurian sediments in the western Irish Caledonides: tracers of a short-lived Ordovician continent-arc collision orogeny and the evolution of the Laurentian Appalachian-Caledonian margin. Geological Society, London, Special Publications 164, 55–107.
Esser, B.K., Turekian, K.K., 1993. The osmium isotopic composition of the continental crust. Geochimica et Cosmochimica Acta 57, 3093–3104.
Evans, J.A., 1996. Dating the transition of smectite to illite in Palaeozoic mudrocks using the Rb–Sr whole-rock technique. Journal of the Geological Society 153, 101–108.
Evans, D.A.D., 2000. Stratigraphic, geochronological, and paleomagnetic constraints upon the Neoproterozoic climatic paradox. American Journal of Science 300, 347–433.
Eyles, C.H., 1988. Glacially-influenced and tidally-influenced shallow marine sedimentation of the late Precambrian Port Askaig Formation Scotland. Palaeogeography Palaeoclimatology Palaeoecology 68, 1–25.
Fairchild, I.J., Hambrey, M.J., 1995. Vendian basin evolution in East Greenland and NE Svalbard. Precambrian Research 73, 217–233.
Fairchild, I.J., Kennedy, M.J., 2007. Neoproterozoic glaciation in the Earth System. Journal of the Geological Society 164, 895–921.
Fanning, C.M., Link, P.K., 2004. U–Pb SHRIMP ages of Neoproterozoic (Sturtian) glaciogenic Pocatello Formation, southeastern Idaho. Geology 32, 881–884.
Fike, D.A., Grotzinger, J.P., Pratt, L.M., Summons, R.E., 2006. Oxidation of the Ediacaran Ocean. Nature 444, 744–747.
Fletcher, T.P., Rushton, A.W.A., 2007. The Cambrian Fauna of the Leny Limestone, Perthshire Scotland. Earth and Environmental Science: Transactions of the Royal Society of Edinburgh 98, 199–218.
Friedrich, A.M., Hodges, K.V., Bowring, S.A., Martin, M.W., 1999. Geochronological constraints on the magmatic, metamorphic and thermal evolution of the Connemara Caledonides, western Ireland. Journal of the Geological Society 156, 1217–1230.
Frimmel, H.E, 2010. On the reliability of stable carbon isotopes for Neoproterozoic chemostratigraphic correlation. Precambrian Research 182, 239–253.
Giddings, J.A., Wallace, M.W., 2009. Facies-dependent [delta]13C variation from a Cryogenian platform margin, South Australia: evidence for stratified Neoproterozoic oceans? Palaeogeography, Palaeoclimatology Palaeoecology 271, 196–214.
Glover, B.W., Key, R.M., May, F., Clark, G.G., Phillips, E.R., Chacksfield, B.C., 1995. A Neoproterozoic multi-phase rift sequence: the Grampian and Appin groups of the southwestern Monadhliath Mountains of Scotland. Journal of the Geological Society 152, 391–406.
Glover, B.W., McKie, T., 1996. A sequence stratigraphical approach to the understanding of basin history in orogenic Neoproterozoic successions: an example from the central Highlands of Scotland. Geological Society, London Special Publications 103, 257–269.
Glover, B.W., Winchester, J.A., 1989. The Grampian Group: a major Late Proterozoic clastic sequence in the Central Highlands of Scotland. Journal of the Geological Society 146, 85–96.
Gorokhov, I.M., Semikhatov, M.A., Mel'nikov, N.N., Turchenko, T.L., Konstantinova, G.V., Kutyavin, E.P., 2001. Rb–Sr geochronology of middle Riphean shales, the Yusmastakh Formation of the Anabar Massif, northern Siberia. Stratigraphy and Geological Correlation 9, 213–231.
Halliday, A.N., Graham, C.M., Aftalion, M., Dymoke, P., 1989. The depositional age of the Dalradian Supergroup – U–Pb and Sm–Nd isotopic studies of the Tayvallich Volcanics, Scotland. Journal of the Geological Society 146, 3–6.
Halverson, G.P., Hoffman, P.F., Schrag, D.P., Maloof, A.C., Rice, A.H.N., 2005. Toward a Neoproterozoic composite carbon-isotope record. Geological Society of America Bulletin 117, 1181–1207.
Halverson, G.P., Hurtgen, M.T., 2007. Ediacaran growth of the marine sulfate reservoir. Earth and Planetary Science Letters 263, 32–44.
Halverson, G.P., Dudás, F.Ö., Maloof, A.C., Bowring, S.A., 2007a. Evolution of the $^{87}Sr/^{86}Sr$ composition of Neoproterozoic seawater. Palaeogeography, Palaeoclimatology, Palaeoecology 256, 103–129.
Halverson, G.P., Maloof, A.C., Schrag, D.P., Dudás, F.Ö., Hurtgen, M., 2007b. Stratigraphy and geochemistry of a ca 800 Ma negative carbon isotope interval in northeastern Svalbard. Chemical Geology 237, 5–27.
Hambrey, M.J., 1983. Correlation of Late Proterozoic tillites in the North Atlantic region and Europe. Geological Magazine 120, 209–232.
Harris, A.L., Haselock, P.J., Kennedy, M.J., Mendum, J.R., Long, C.B., Winchester, J.A., Tanner, P.W.G., 1994. The Dalradian Supergroup in Scotland and Ireland. In: Gibbons, W., Harris, A.L. (Eds.), A Revised Correlation of Precambrian Rocks in the British Isles. Geological Society, London.
Harte, B., Pattison, D.R.M., Heuss-Assbichler, S., Hoernes, S., Masch, L., Strong, D.F., 1991. Evidence of fluid phase behaviour and controls in the intrusive complex and its aureole. In: Voll, G., Topel, J., Pattison, D.R.M., Seifert, F. (Eds.), Equilibrium and Kinetics in Contact Metamorphism: The Ballachulish Igneous Complex and its Thermal Aureole. Springer Verlag, Heidelberg.
Hattori, Y., Suzuki, K., Honda, M., Shimizu, H., 2003. Re–Os isotope systematics of the Taklimakan Desert sands, moraines and river sediments around the taklimakan desert, and of Tibetan soils. Geochimica et Cosmochimica Acta 67, 1203–1213.
Highton, A.J., Hyslop, E.K., Noble, S.R., 1999. U–Pb zircon geochronology of migmatization in the northern Central Highlands: evidence for pre-Caledonian (Neoproterozoic) tectonometamorphism in the Grampian block, Scotland. Journal of the Geological Society 156, 1195–1204.
Hill, A.C., Walter, M.R., 2000. Mid-Neoproterozoic (~830–750 Ma) isotope stratigraphy of Australia and global correlation. Precambrian Research 100, 181–211.
Hoffman, P.F., 1991. Did the breakout of Laurentia Turn Gondwanaland inside-out? Science 252, 1409–1412.
Hoffman, P.F., Kaufman, A.J., Halverson, G.P., Schrag, D.P., 1998. A Neoproterozoic snowball earth. Science 281, 1342–1346.
Hoffman, P.F., Schrag, D.P., 2002. The snowball Earth hypothesis: testing the limits of global change. Terra Nova 14, 129–155.
Hoffmann, K.H., Condon, D.J., Bowring, S.A., Crowley, J.L., 2004. U–Pb zircon date from the Neoproterozoic Ghaub Formation Namibia Constraints on Marinoan glaciation. Geology 32, 817–820.
Hutton, D.H.W., Alsop, G.I., 2004. Evidence for a major Neoproterozoic orogenic unconformity within the Dalradian Supergroup of NW Ireland. Journal of the Geological Society 161, 629–640.
Hyde, W.T., Crowley, T.J., Baum, S.K., Peltier, W.R., 2000. Neoproterozoic/snowball Earth/simulations with a coupled climate/ice-sheet model. Nature 405, 425–429.
Jacobsen, S.B., Kaufman, A.J., 1999. The Sr, C and O isotopic evolution of Neoproterozoic seawater. Chemical Geology 161, 37–57.
Jaffe, L.A., Peucker-Ehrenbrink, B., Petsch, S.T., 2002. Mobility of rhenium, platinum group elements and organic carbon during black shale weathering. Earth and Planetary Science Letters 198, 339–353.
Jensen, S., Saylor, B.Z., Gehling, J.G., Germs, G.J.B., 2000. Complex trace fossils from the terminal Proterozoic of Namibia. Geology 28, 143–146.
Jiang, G., Kaufman, A.J., Christie-Blick, N., Zhang, S., Wu, H., 2007. Carbon isotope variability across the Ediacaran Yangtze platform in South China: implications for a large surface-to-deep ocean [delta]13C gradient. Earth and Planetary Science Letters 261, 303–320.
Kendall, B., Creaser, R.A., Calver, C.R., Raub, T.D., Evans, D.A.D., 2009a. Correlation of Sturtian diamictite successions in southern Australia and northwestern Tasmania by Re–Os black shale geochronology and the ambiguity of "Sturtian"-type diamictite-cap carbonate pairs as chronostratigraphic marker horizons. Precambrian Research 172, 301–310.

Kendall, B., Creaser, R.A., Selby, D., 2009b. ^{187}Re–^{187}Os geochronology of Precambrian organic-rich sedimentary rocks. Geological Society, London, Special Publications 326, 85–107.
Kendall, B., Creaser, R.A., Gordon, G.W., Anbar, A.D., 2009c. Re–Os and Mo isotope systematics of black shales from the Middle Proterozoic Velkerri and Wollogorang Formations McArthur Basin, northern Australia. Geochimica et Cosmochimica Acta 73, 2534–2558.
Kendall, B., Creaser, R.A., Selby, D., 2006. Re–Os geochronology of postglacial black shales in Australia: constraints on the timing of "Sturtian" glaciation. Geology 34, 729–732.
Kendall, B.S., Creaser, R.A., Ross, G.M., Selby, D., 2004. Constraints on the timing of Marinoan 'Snowball Earth' glaciation by ^{187}Re–^{187}Os dating of a Neoproterozoic post-glacial black shale in Western Canada. Earth and Planetary Science Letters 222, 729–740.
Kennedy, M.J., Runnegar, B., Prave, A.R., Hoffmann, K.H., Arthur, M.A., 1998. Two or four Neoproterozoic glaciations? Geology 26, 1059–1063.
Kilburn, C., Shackleton, R.M., Pitcher, W.S., 1965. The stratigraphy and origin of the Port Askaig boulder bed series (Dalradian). Geological Journal 4, 343–360.
Kirschvink, J.L., 1992. Late Proterozoic low-latitude global glaciation: the snow ball earth. In: Schopf, J.W.a.K.C. (Ed.), The Proterozoic Biosphere. Cambridge University Press, Cambridge.
Knoll, A.H., 2003. The geological consequences of evolution. Geobiology 1, 3–14.
Knoll, A.H., Javaux, E.J., Hewitt, D., Cohen, P., 2006. Eukaryotic organisms in Proterozoic oceans. Philosophical Transactions of the Royal Society B: Biological Sciences 361, 1023–1038.
Levasseur, S., Birck, J., Allègre, C.J., 1999. The osmium riverine flux and oceanic mass balance of osmium. Earth and Planetary Science Letters 174, 7–23.
Li, Z.X., Bogdanova, S.V., Collins, A.S., Davidson, A., De Waele, B., Ernst, R.E., Fitzsimons, I.C.W., Fuck, R.A., Gladkochub, D.P., Jacobs, J., Karlstrom, K.E., Lu, S., Natapov, L.M., Pease, V., Pisarevsky, S.A., Thrane, K., Vernikovsky, V., 2008. Assembly, configuration, and break-up history of Rodinia: a synthesis. Precambrian Research 160, 179–210.
Li, Z.-X., Evans, D.A.D., 2010. Late Neoproterozoic 40° intraplate rotation within Australia allows for a tighter-fitting and longer-lasting Rodinia. Geology 39, 39–42.
Litherland, M., 1980. The stratigraphy of the Dalradian rocks around Loch Creran, Argyll. Scottish Journal of Geology 16, 105–123.
Logan, G.A., Hayes, J.M., Hieshima, G.B., Summons, R.E., 1995. Terminal Proterozoic reorganization of biogeochemical cycles. Nature 376, 53–56.
Logan, G.A., Summons, R.E., Hayes, J.M., 1997. An isotopic biogeochemical study of Neoproterozoic and Early Cambrian sediments from the Centralian Superbasin Australia. Geochimica et Cosmochimica Acta 61, 5391–5409.
Ludwig, K., 2003. Isoplot/Ex, Version 3: A Geochronological Toolkit for Microsoft Excel. Geochronology Center Berkeley.
Ludwig, K.R., 1980. Calculation of uncertainties of U–Pb isotope data. Earth and Planetary Science Letters 46, 212–220.
Macdonald, F.A., Schmitz, M.D., Crowley, J.L., Roots, C.F., Jones, D.S., Maloof, A.C., Strauss, J.V., Cohen, P.A., Johnston, D.T., Schrag, D.P., 2010a. Calibrating the Cryogenian. Science 327, 1241–1243.
Macdonald, F.A., Cohen, P.A., Dudas, F.O., Schrag, D.P., 2010b. Early Neoproterozoic scale microfossils in the Lower Tindir Group of Alaska and the Yukon Territory. Geology 38, 143–146.
Mao, J., Lehmann, B., Du, A., Zhang, G., Ma, D., Wang, Y., Zeng, M., Kerrich, R., 2002. Re–Os dating of polymetallic Ni–Mo–PGE–Au mineralization in lower Cambrian Black Shales of South China and its geological significance. Economic Geology 97, 1051–1061.
Martin, M.W., Grazhdankin, D.V., Bowring, S.A., Evans, D.A.D., Fedonkin, M.A., Kirschvink, J.L., 2000. Age of Neoproterozoic Bilatarian body and trace fossils, White Sea, Russia: implications for Metazoan Evolution. Science 288, 841–845.
McCay, G.A., Prave, A.R., Alsop, G.I., Fallick, A.E., 2006. Glacial trinity: Neoproterozoic Earth history within the British-Irish Caledonides. Geology 34, 909–912.
Meert, J.G., 2007. Testing the Neoproterozoic glacial models. Gondwana Research 11, 573–574.
Melezhik, V.A., Gorokhov, I.M., Kuznetsov, A.B., Fallick, A.E., 2001. Chemostratigraphy of Neoproterozoic carbonates: implications for 'blind dating'. Terra Nova 13, 1–11.
Melezhik, V.A., Roberts, D., Fallick, A.E., Gorokhov, I.M., 2008. The Shuram-Wonoka event recorded in a high-grade metamorphic terrane: insight from the Scandinavian Caledonides. Geological Magazine 145, 161–172.
Morton, J.P., Long, L.E., 1982. Rb–Sr ages of Precambrian sedimentary-rocks in the USA. Precambrian Research 18 (1–2), 133–138.
Narbonne, G.M., Gehling, J.G., 2003. Life after snowball: the oldest complex Ediacaran fossils. Geology 31, 27–30.
Neilson, J.C., Kokelaar, B.P., Crowley, Q.G., 2009. Timing, relations and cause of plutonic and volcanic activity of the Siluro-Devonian post-collision magmatic episode in the Grampian Terrane, Scotland. Journal of the Geological Society 166, 545–561.
Noble, S.R., Hyslop, E.K., Highton, A.J., 1996. High precision U–Pb monazite geochronology of the *c.* 806 Ma Grampian Shear Zone and the implications for the evolution of the Central Highlands of Scotland. Journal of the Geological Society 153, 511–514.
Ogg, J.G., Ogg, G., Gradstein, F.M., 2008. The Concise Geologic Time Scale. Cambridge University Press, Cambridge.
Ohr, M., Halliday, A.N., Peacor, D.R., 1991. Sr and Nd isotopic evidence for punctuated clay diagenesis, Texas Gulf-Coast. Earth and Planetary Science Letters 105, 110–126.
Oliver, G.J.H., 2001. Reconstruction of the Grampian episode in Scotland: its place in the Caledonian Orogeny. Tectonophysics 332, 23–49.
Pattison, D.R.M., 2006. The fate of graphite in prograde metamorphism of pelites: an example from the Ballachulish aureole, Scotland. Lithos 88, 85–99.
Pattison, D.R.M., Voll, G., 1991. Regional geology of the Ballachulish area. In: Voll, G., Töpel, J., Pattison, D.R.M., Seifert, F. (Eds.), Equilibrium and Kinetics in contact metamorphism: the Ballachulish Igneous Complex and its Thermal Aureole. Springer Verlag, Heidelberg, pp. 19–38.
Pattison, D.R.M., Harte, B., 1997. The geology and evolution of the Ballachulish Igneous Complex and Aureole. Scottish Journal of Geology 33, 1–29.
Peucker-Ehrenbrink, B., Jahn, B.-m., 2001. Rhenium–osmium isotope systematics and platinum group element concentrations: Loess and the upper continental crust. Geochemistry Geophysics Geosystems, 2.
Peucker-Ehrenbrink, B., Ravizza, G., 2000. The marine osmium isotope record. Terra Nova 12, 205–219.
Prave, A.R., 1999. The Neoproterozoic Dalradian Supergroup of Scotland: an alternative hypothesis. Geological Magazine 136, 609–617.
Prave, A.R., Fallick, A.E., Thomas, C.W., Graham, C.M., 2009a. A composite C-isotope profile for the Neoproterozoic Dalradian Supergroup of Scotland and Ireland. Journal of the Geological Society 166, 845–857.
Prave, A.R., Strachan, R.A., Fallick, A.E., 2009b. Global C cycle perturbations recorded in marbles: a record of Neoproterozoic Earth history within the Dalradian succession of the Shetland Islands, Scotland. Journal of the Geological Society 166, 129–135.
Preiss, W.V., 2000. The Adelaide Geosyncline of South Australia and its significance in Neoproterozoic continental reconstruction. Precambrian Research 100, 21–63.
Pringle, J., 1939. The Discovery of Cambrian Trilobites in the Highland Border Rocks Near Callander Perthshire. Report of the British Association for the Advancement of Science, p. 252.
Rainbird, R.H., Hamilton, M.A., Young, G.M., 2001. Detrital zircon geochronology and provenance of the Torridonian, NW, Scotland. Journal of the Geological Society 158, 15–27.
Ravizza, G., Turekian, K.K., 1989. Application of the ^{187}Re–^{187}Os system to black shale geochronometry. Geochimica et Cosmochimica Acta 53, 3257–3262.
Ravizza, G., Turekian, K.K., Hay, B.J., 1991. The geochemistry of rhenium and osmium in recent sediments from the Black Sea. Geochimica et Cosmochimica Acta 55, 3741–3752.
Rogers, G., Dunning, G.R., 1991. Geochronology of appinitic and related granitic magmatism in the W Highlands of Scotland: constraints on the timing of transcurrent fault movement. Journal of the Geological Society 148, 17–27.
Rooney, A.D., Selby, D., Houzay, J.-P., Renne, P.R., 2010. Re–Os geochronology of a Mesoproterozoic sedimentary succession, Taoudeni basin Mauritania: implications for basin-wide correlations and Re–Os organic-rich sediments systematics. Earth and Planetary Science Letters 289, 486–496.
Sawaki, Y., Kawai, T., Shibuya, T., Tahata, M., Omori, S., Komiya, T., Yoshida, N., Hirata, T., Ohno, T., Windley, B.F., Maruyama, S., 2010. $^{87}Sr/^{86}Sr$ chemostratigraphy of Neoproterozoic Dalradian carbonates below the Port Askaig Glaciogenic Formation, Scotland. Precambrian Research 179, 150–164.
Scott, C., Lyons, T.W., Bekker, A., Shen, Y., Poulton, S.W., Chu, X., Anbar, A.D., 2008. Tracing the stepwise oxygenation of the Proterozoic ocean. Nature 452, 456–460.
Selby, D., 2007. Direct rhenium–osmium age of the Oxfordian-Kimmeridgian boundary, Staffin bay, Isle of Skye, U. K., and the Late Jurassic time scale. Norwegian Journal of Geology 87, 9.
Selby, D., 2009. U–Pb zircon geochronology of the Aptian/Albian boundary implies that the GL-O international glauconite standard is anomalously young. Cretaceous Research 30, 1263–1267.
Selby, D., Creaser, R.A., 2003. Re–Os geochronology of organic rich sediments: an evaluation of organic matter analysis methods. Chemical Geology 200, 225–240.
Selby, D., Creaser, R.A., 2005. Direct radiometric dating of the Devonian-Mississippian time-scale boundary using the Re–Os black shale geochronometer. Geology 33, 545–548.
Selby, D., Creaser, R.A., Stein, H.J., Markey, R.J., Hannah, J.L., 2007. Assessment of the Re-^{187} decay constant by cross calibration of Re–Os molybdenite and U–Pb zircon chronometers in magmatic ore systems. Geochimica et Cosmochimica Acta 71, 1999–2013.
Slack, J.F., Jiang, W.T., Peacor, D.R., Okita, P.M., 1992. Hydrothermal and metamorphic berthierine from the Kidd Creek Volcanogenic Massive Sulfide Deposit, Timmins, Ontario. Canadian Mineralogist 30, 1127–1142.
Smith, M., Robertson, S., Rollin, K.E., 1999. Rift basin architecture and stratigraphical implications for basement-cover relationships in the Neoproterozoic Grampian Group of the Scottish Caledonides. Journal of the Geological Society 156, 1163–1173.
Smoliar, M.I., Walker, R.J., Morgan, J.W., 1996. Re–Os isotope constraints on the age of Group IIA, IIIA, IVA, and IVB iron meteorites. Science 271, 1099–1102.
Soper, N.J., 1994. Was Scotland a Vendian RRR junction? Journal of the Geological Society 151, 579–582.
Soper, N.J., England, R.W., 1995. Vendian and Riphean rifting in NW Scotland. Journal of the Geological Society 152, 11–14.
Soper, N.J., Ryan, P.D., Dewey, J.F., 1999. Age of the Grampian orogeny in Scotland and Ireland. Journal of the Geological Society 156, 1231–1236.
Spencer, A.M., 1971. Late Precambrian glaciation in Scotland. Memoirs of the Geological Society of London 6, 1–100.

Strachan, R.A., Smith, M., Harris, A.L., Fettes, D.J., 2002. The Northern Highland and Grampian terranes. In: Trewin, N.H. (Ed.), The Geology of Scotland. The Geological Society, London.

Sun, W., Arculus, R.J., Bennett, V.C., Eggins, S.M., Binns, R.A., 2003. Evidence for rhenium enrichment in the mantle wedge from submarine arc-like volcanic glasses (Papua New Guinea). Geology 31, 845–848.

Tanner, P.W.G., Alsop, G.I., Hutton, D.H.W., 2005. Discussion on evidence for a major Neoproterozoic orogenic unconformity within the Dalradian Supergroup of NW Ireland. Journal of the Geological Society 162, 221–224.

Tanner, P.W.G., Pringle, M.S., 1999. Testing for the presence of a terrane boundary within Neoproterozoic (Dalradian) to Cambrian siliceous turbidites at Callander, Perthshire, Scotland. Journal of the Geological Society 156, 1205–1216.

Tanner, P.W.G., Sutherland, S., 2007. The Highland Border Complex, Scotland: a paradox resolved. Journal of the Geological Society 164, 111–116.

Thomas, C., Graham, C., Ellam, R., Fallick, A., 2004. $^{87}Sr/^{86}Sr$ chemostratigraphy of Neoproterozoic Dalradian limestones of Scotland and Ireland: constraints on depositional ages and time scales. Journal of the Geological Society 161, 229–242.

Thomson, J., 1871. On the occurrence of pebbles and boulders of granite in schistose rocks on Islay, Scotland. Report of the 40th Meeting of the British Association for the Advancement of Science, Liverpool.

Thomson, J., 1877. On the geology of the island of Islay. Transactions of the Geological Society of Glasgow 5, 200–222.

Tilley, C.E., 1925. A preliminary survey of metamorphic zones in the southern Highlands of Scotland. Quarterly Journal of the Geological Society of London, 81.

Trindade, R.I.F., Macouin, M., 2007. Palaeolatitude of glacial deposits and palaeogeography of Neoproterozoic ice ages. Comptes Rendus Geosciences 339, 200–211.

Vidal, G., Moczydlowska-Vidal, M., 1997. Biodiversity, speciation, and extinction trends of Proterozoic and Cambrian Phytoplankton. Paleobiology 23, 230–246.

Voll, G., Topel, J., Pattison, D.R.M., Seifert, F., 1991. Equilibrium and Kinetics in Contact Metamorphism: The Ballachulish Igneous Complex and its Aureole. Springer Verlag, Heidelberg.

Walker, R.J., Horan, M.F., Morgan, J.W., Becker, H., Grossman, J.N., Rubin, A.E., 2002a. Comparative ^{187}Re–^{187}Os systematics of chondrites: implications regarding early solar system processes. Geochimica et Cosmochimica Acta 66, 4187–4201.

Walker, R.J., Prichard, H.M., Ishiwatari, A., Pimentel, M., 2002b. The osmium isotopic composition of convecting upper mantle deduced from ophiolite chromites. Geochimica et Cosmochimica Acta 66, 329–345.

Walsh, J.A., 2007. The use of the scanning electron microscope in the determination of the mineral composition of Ballachulish slate. Materials Characterization 58, 1095–1103.

Yang, G., Hannah, J.L., Zimmerman, A., Stein, H.J., Bekker, A., 2009. Re–Os depositional age for Archean carbonaceous slates from the southwestern Superior Province: challenges and insights. Earth and Planetary Science Letters 280, 83–92.

Zhou, C., Tucker, R., Xiao, S., Peng, Z., Yuan, X., Chen, Z., 2004. New constraints on the ages of Neoproterozoic glaciations in south China. Geology 32, 437–440.